4

E7.6-10201

LARS Information Note 121275

NASA CR 147473

Computer-Aided Analysis of SKYLAB Multispectral Scanner Data in Mountainous Terrain for Land Use, Forestry, Water Resource, and Geologic Applications

by Roger M. Hoffer and Staff

The Laboratory for Applications of Remote Sensing

Purdue University, West Lafayette, Indiana

1975

COMPUTER-AIDED ANALYSIS OF SKYLAB MULTISPECTRAL SCANNER DATA IN MOUNTAINOUS TERRAIN FOR LAND USE, FORESTRY, WATER RESOURCE, AND GEOLOGIC APPLICATIONS

by

Roger M. Hoffer and Staff
Laboratory for Applications of Remote Sensing
Purdue University
West Lafayette, Indiana 47907

Final Report on Contract No. NAS 9-13380, SKYLAB EREP Project 398.
Prepared for the National Aeronautics and Space Administration, Lyndon B. Johnson Space Center, Houston, Texas; Rigdon B. Joosten, Technical Monitor.

1 Report No.	2. Government Accession No.	3. Recipient's Catalog No.

4. Title and Subtitle	5. Report Date
COMPUTER-AIDED ANALYSIS OF SKYLAB MULTISPECTRAL SCANNER DATA IN MOUNTAINOUS TERRAIN FOR LAND USE, FORESTRY, WATER RESOURCE, AND GEOLOGIC APPLICATIONS	December 12, 1975
	6. Performing Organization Code

7. Author(s)	8. Performing Organization Report No.
Roger M. Hoffer and Staff	121275
	10. Work Unit No.

9. Performing Organization Name and Address	11. Contract or Grant No.
Laboratory for Applications of Remote Sensing (LARS) Purdue University W. Lafayette, IN 47906	NAS9-13380
	13. Type of Report and Period Covered Type III-Final Report 1 April, 1973-31 Dec.1975
12. Sponsoring Agency Name and Address	14. Sponsoring Agency Code
National Aeronautics and Space Administration Lyndon B. Johnson Space Center Houston, TX	EREP 398

15. Supplementary Notes

Sub-contract to the Institute of Arctic and Alpine Research, University of Colorado

16. Abstract This report describes the results of an interdisciplinary research project involving the analysis of SKYLAB data obtained over the San Juan Mountains in SW Colorado. Computer-aided analysis techniques were applied to the S-192 MSS data for purposes of mapping land use, forest cover types, hydrologic and geologic features of significance. In spite of the vegetative and topographic complexity of the test site, computer classification accuracies of 85% and 71% were obtained for Level II Land Use maps and Forest Cover maps, respectively. Accurate acreage estimates of forest cover were obtained by computer analysis of SKYLAB S-192 data. A detailed wavelength band study clearly indicated the importance of the near infrared wavelengths for vegetation mapping. The value of the improved spectral resolution of the SKYLAB MSS, as compared to LANDSAT, was also shown. Another result of particular significance involved the use of digital computer techniques to geometrically correct and overlay multiple data sets, including SKYLAB, LANDSAT, and topographic (elevation, slope and aspect) data.

SKYLAB MSS data clearly showed for the first time that the middle infrared wavelengths are essential for reliably separating snow from clouds on the basis of spectral response. Forest density and snow melt differences within the snowpack area could be mapped through use of the near infrared wavelengths. Calibration of the thermal infrared band allowed the surface temperature of a high elevation reservoir to be accurately determined from space. Geologic mapping, involving a variety of ratioing and classification techniques, indicated the need for additional study to better define the theoretical basis for use of these analysis procedures, in order to obtain reliable, predictable results. A number of additional significant results and recommendations are included in this report.

17. Key Words (Suggested by Author(s))	18. Distribution Statement
Remote Sensing, SKYLAB, Land use mapping, Forestry, Geology, Water resources, Snow mapping, Digital registration techniques, Computer analysis techniques.	

19. Security Classif. (of this report)	20. Security Classif. (of this page)	21. No. of Pages	22. Price*
Unclassified	Unclassified	381	

*For sale by the National Technical Information Service, Springfield, Virginia 22161

ACKNOWLEDGEMENTS

As principal investigator, I would like to thank many individuals in various agencies who have been involved in the successful completion of this SKYLAB research project. First, I would point out that this work was supported by NASA Contract NAS 9-13380 from NASA's Johnson Space Center, Houston, Texas. Mr. Roger Hicks and Mr. Rigdon Joosten served as Technical Monitors on this contract, and I would like to thank them for their extremely effective coordination at the time of the SKYLAB missions and their continued support and advice throughout the project.

Among the many people at the Laboratory for Applications of Remote Sensing (LARS), Purdue University, who were involved in this research,particular recognition should be given to Mr. Luis Bartolucci and Mr. Michael Fleming. These two men did an outstanding job in the analysis of the SKYLAB S-192 data and the preparation of this final report, and I take this opportunity to praise them for their work and extend my deepest appreciation. I also want to thank Mr. Stephen Luther for his work as project coordinator, and particularly for his effective handling of the various progress reports. Dr. Donald Levandowski, Mr. Robert Borger, and Mr. Terry Lehman are acknowledged for their work on the geology phase of the project. Mr. Paul Anuta and Mr. David Freeman did an excellent job on the geometric correction and overlay of SKYLAB, LANDSAT, and topographic data. Mr. Richard Mroczynski and Mrs. Donna Scholz should also be

acknowledged for their technical support. I would particularly like to thank Mrs. Debby Shafer, Mrs. Donna Dasaro, Mrs. Beverly Edgell, Mrs. Marta Dziubinskyj, and other members of the LARS secretarial staff for their outstanding support throughout the various phases of this project, especially in the typing of this final report. Many other personnel too numerous to mention by name were also involved in various other phases of this project, but I would like to acknowledge their efforts and say thank you for their excellent help.

Dr. Paula Krebs, of the Institute of Artic and Alpine Research (INSTAAR), University of Colorado should receive special recognition for her work in the coordination of the photointerpretation aspects of the Ecological Inventory phase of this project, and in the supporting field work that was involved in this research. Both Dr. Krebs and Miss Page Spencer should receive a great deal of credit for their efforts in developing and preparing the permanent SKYLAB display that has been established in the Headquarters at Mesa Verde National Park. Other INSTAAR personnel who primarily contributed to the field work and photointerpretation activities in this project (as reported in Section 3.2) include Mr. David Goeneveld, Mrs. Debbie Keammerer, and Mr. Steve Loranger. Mr. Jack Ives was responsible for the subcontract to INSTAAR under which this work was conducted. Special thanks is also extended to many personnel of the U. S. Forest Service and National Park Service for their valuable comments and assistance in the evaluation of the results obtained from this SKYLAB data.

TABLE OF CONTENTS

CHAPTER I -- INTRODUCTION

CHAPTER II -- DATA CHARACTERISTICS AND OVERLAY OF TOPOGRAPHIC DATA

CHAPTER III -- ECOLOGICAL INVENTORY

LIST OF FIGURES

CHAPTER I

CHAPTER II

CHAPTER III

CHAPTER IV

CHAPTER V

LIST OF TABLES

CHAPTER II

CHAPTER III

CHAPTER IV

CHAPTER 1 -- OVERVIEW OF SKYLAB PROJECT

by

Roger M. Hoffer

1.1 INTRODUCTION

This report discusses the results of an interdisciplinary study having an overall objective of testing the value and applicability of digital computer-aided analysis techniques for identifying, mapping, and tabulating areas of important cover types in a region of mountainous terrain, using SKYLAB multispectral scanner data. This study was comprised of four major tasks including:

1) a Data Handling and Analysis Techniques Study, involving the geometric correction and overlay of both SKYLAB and LANDSAT -1 MSS data onto topographic data, data quality evaluation, and testing various data analysis and evaluation techniques;
2) an Ecological Inventory, involving general land use mapping, forest cover type mapping, and a spectral wavelength band analysis;
3) a Hydrological Features Survey, with particular emphasis on spectral differentiation between clouds and snow, snow cover mapping, and thermal data evaluation;
4) a Geological Analysis, involving rock alteration study, structural lineaments mapping, lithologic units mapping

and land form mapping.

The specific objectives of these research tasks will be discussed in the individual chapters dealing with that particular subject.

1.2 BACKGROUND

The San Juan Mountains and surrounding areas of southwestern Colorado are a particularly important region within the Rocky Mountains from the standpoint of timber, water, mineral, and other natural resources. Therefore, this area provided a nearly ideal test site for purposes of an interdisciplinary study. The combination of spectacular mountain scenery, forests, snow and water has also produced an excellent recreation potential for this area. Consequently, there is much pressure and conflict for use of the land. Various governmental agencies, private firms, conservation groups and individuals are extremely interested in obtaining accurate, up-to-date maps with acreage tabulations of the various resources.

The ability to collect data from satellites far surpasses existing capabilities to interpret and analyze even a small portion of the data in a timely manner. This fact has been evident to many researchers working with MSS data collected from LANDSAT-1 when only four wavelength bands of data were being obtained. Since the SKYLAB S-192 MSS could

collect data in thirteen discreet wavelength bands throughout the optical portion of the spectrum and, when the spectral, spatial and temporal characteristics of future satellite systems (e.g., the Thematic Mapper proposed for LANDSAT-D) are considered, there is little question about the need for effective, efficient techniques to convert such data into useful information in a timely manner.

During the last nine years, research involving MSS data and computer-aided analysis techniques (CAAT) has clearly shown the potential for such a combination of data and analysis technique. Studies involving aircraft MSS data collected in 12 or more wavelength bands throughout the optical portion of the spectrum have indicated the value of various wavelength regions for correctly identifying many earth surface features. More recent work with LANDSAT-1 data has indicated the value of the synoptic view obtained from satellite altitudes. However, the combination of synoptic view and multispectral data throughout the optical portion of the spectrum had not been available until the SKYLAB S-192 data were obtained. Only then did it become possible to study the value of the various wavelength bands (particularly the middle and thermal infrared bands) for correctly identifying earth surface features from satellite altitudes. Thus, a major thrust of this research project was to determine the value of the various wavelength bands for effectively mapping earth surface features from satellite altitudes, using computer-aided analysis techniques.

Until the launch of LANDSAT-1, nearly all of the analysis of MSS data had involved areas of relatively flat terrain. It was thought that the effects of slope, aspect, and elevation would probably have a significant influence on the spectral response recorded by a scanner system, and work with the LANDSAT-1 data has shown that topographic effects do indeed influence the spectral response measured by the scanner system. If MSS data are to be analyzed by CAAT on an operational basis, it is important to determine the accuracy, reliability and level of detail of the information that can be obtained with such techniques for all conditions of terrain. For this reason, and because of the importance of the San Juan Mountains for their forest, water, mineral, and other resources, this mountainous region, with its complex association of cover types and topography, was selected as the test site.

1.3 GENERAL TEST SITE DESCRIPTION

The San Juan Mountains of southwestern Colorado (Figure 1.1) contain a complex mixture of forest types, rangeland, alpine tundra, agricultural areas, water bodies, geological features, and various man-made features. The topography of the test site area is rugged, ranging from elevation from less than 2000 meters to over 4200 meters. Within this range of elevation, a distinct distribution of cover types occurs according to altitude. Figure 1.2 indicates the impact of elevation on some of the major forest types found in the test site. Timberline in the region is approximately 3600 meters, and extensive areas of tundra are found above this elevation. A more complete listing of forest cover types in the test area would include Spruce-Fir, Douglas and White Fir, Ponderosa Pine, Aspen, Oak-Mahogany, and Pinyon-Juniper.

Many commercially important areas of timber are present in this region. Therefore, the forest resources of this area comprise an important part of the economy of the area, not only for wood fiber production but also for wildlife and recreation. Additionally, the forests are a key factor in watershed management since the forests provide control over the water runoff and protect the soil in these upland mountain watersheds. Production of water for irrigation, industry, and public consumption in much of the southwestern United States is centered around the water runoff of the upper mountain watersheds of the

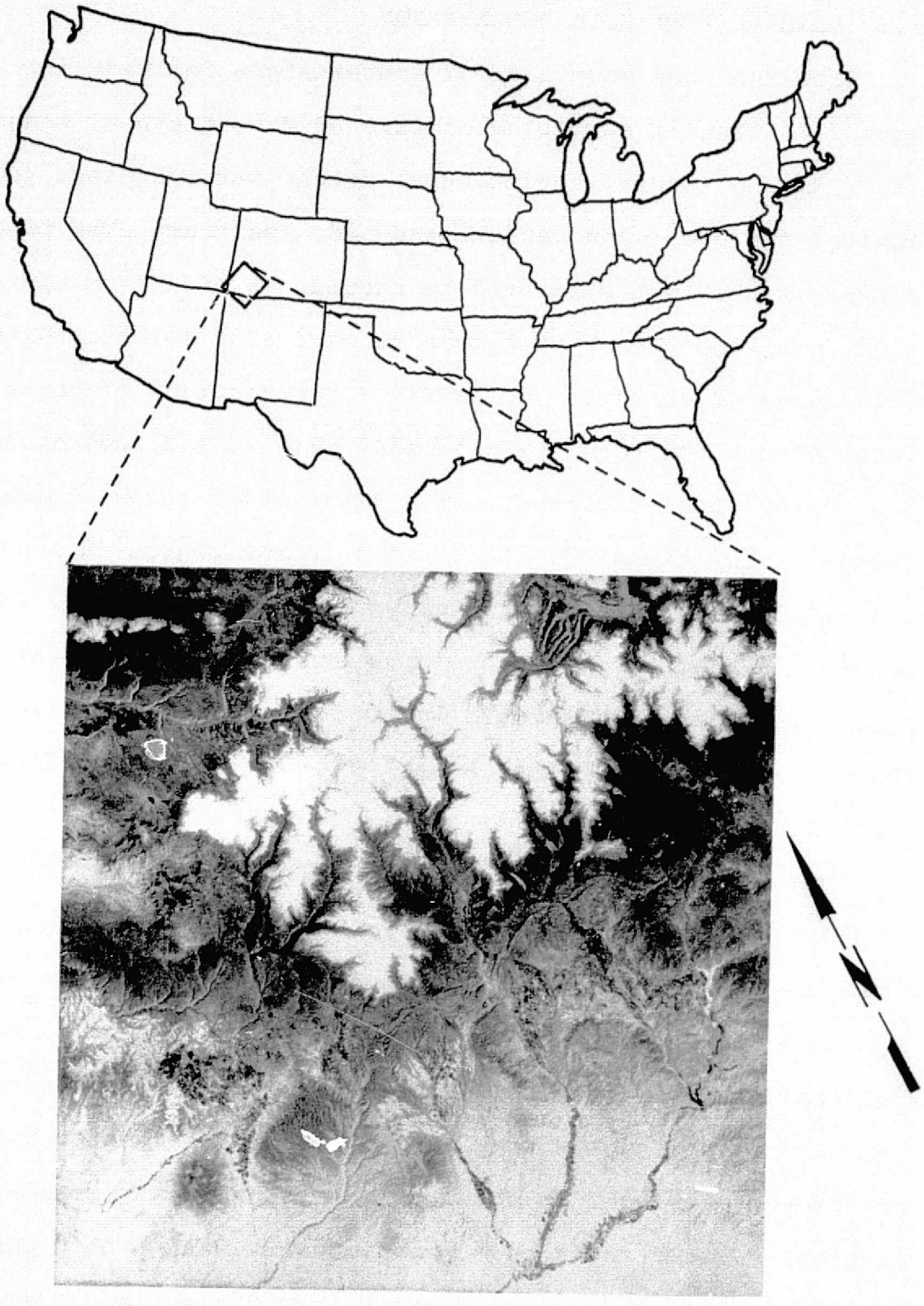

Figure 1.1 -- SKYLAB test site in the San Juan Mountains of Colorado

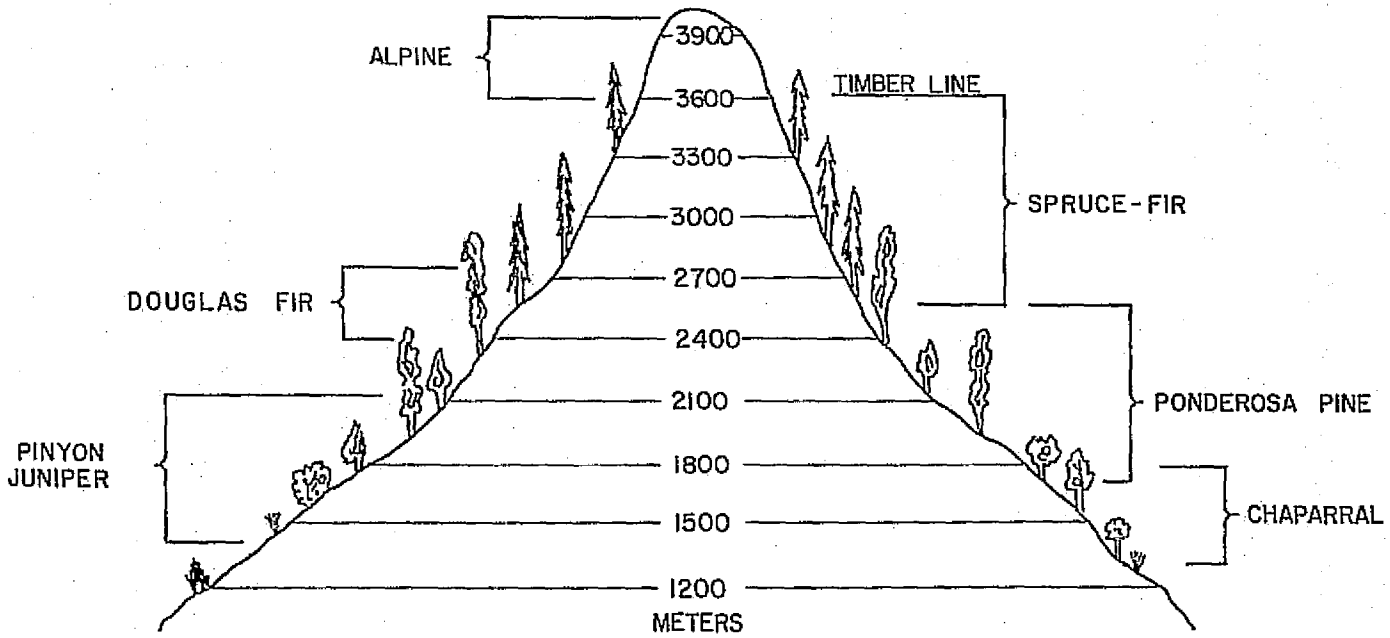

Figure 1.2 -- Relationship between elevation and vegetative cover type in the San Juan Mountains, Colorado

Rocky Mountains. The San Juan test site is in the center of this important water production region.

Farming is minimal within the San Juan study area and is limited primarily to hay crops in the valleys at lower altitudes. Grazing is common, and has a considerable effect upon the ecosystem. Those grasses and herbs which cattle and sheep find most palatable are gradually being eradicated in the grazing range. As a result, erosional problems are present in heavily grazed areas, especially where flock management is poor.

From a geological standpoint, the test site consists primarily of Tertiary volcanics with the topographic expression of a maturely dissected plateau which has been further modified by extensive valley glaciation. The area is characterized by numerous landslides, avalanches, rock glaciers, and glacial lakes. Many areas of mine tailings indicate its former prominence as a mineral, particularly silver, producing area. The direct effects of mining are severe, but quite localized. Mine tailings have a low organic content and usually have a low pH due to the mineral content; because of these factors the tailings tend to remain sterile and non-vegetated.

In areas where human influence has not caused major changes, the vegetative cover is determined by complex interactions of edaphic topographic and climatic influences. For example, as elevation increases, precipitation generally in-

creases and mean annual air temperatures decrease. A complex relationship also exists between elevation and quantity and quality of solar radiation. At high altitudes increased cloud cover occurs, but the solar radiation present at other times is intense due to minimal atmospheric attenuation. The aspect and angle of the slope also significantly influence microclimatic conditions, resulting in distinct vegetative effects. For example, during the summer an exposed site with a high angle of solar incidence tends to dry quickly, and vegetation in these sites must adapt to water stress during the growing season. The integration of the topographic characteristics of the area, the climatic influences, and the soils found in various areas produces a distribution of vegetative cover types that are closely related to elevation and aspect.

Thus, there are many complex interactions between the topographic, vegetative, geologic, edaphic, and hydrologic characteristics of the area. These interactions must be understood to obtain meaningful information to use in effective management of these natural resources. They must also be understood to effectively interpret the significance of the reflectance and emittance values measured by multispectral scanner systems.

More detailed descriptions of the vegetative, hydrologic, and geologic characteristics of the test site which are pertinent to the various portions of this SKYLAB research are contained in the appropriate sections of this report.

1.4 SIGNIFICANT ASPECTS OF THIS SKYLAB PROJECT

This SKYLAB research involved several different discipline areas. For this reason, and because of unique characteristics of the SKYLAB data and the activities involving user agency contacts, it seems appropriate to briefly summarize some of the more significant aspects of this SKYLAB project.

As discussed in Chapter 2, data from both the SL-2 and SL-3 SKYLAB missions were obtained and analyzed. The SL-2 data set was of particular importance because both SKYLAB and LANDSAT data were obtained under cloud-free conditions on the same day, June 5, 1973, and underflight aircraft data were obtained by NASA's WB-57 and NC-130 on the following day.

One of the most significant results of this SKYLAB research involved the geometric correction and overlay of the SKYLAB multispectral scanner data with the LANDSAT multispectral scanner data, and also with a set of topographic data, including elevation, slope, and aspect. This multiple data set allowed a detailed comparison of classification results obtained using the SKYLAB data and the LANDSAT data. Because of the interaction between elevation and forest cover types, the overlaying of topographic data onto the spectral data set enabled preliminary studies to be conducted into the value of such multiple data sets. It is believed that this work represents the first time that such a data set, contain-

ing multispectral scanner data from different scanner systems as well as topographic data, has been developed for a large geographic area. Both the SL-2 and SL-3 data were geometrically corrected and overlayed with LANDSAT data and topographic data.

The SKYLAB S-192 multispectral scanner data had distinct differences in noise level of the data in the various wavelength bands. One of the major activities in the Ecological Inventory research involved the assessment of the value of the different wavelength bands for vegetation mapping using computer-aided analysis techniques. Therefore, it was important to evaluate the quality of the data in each wavelength band. A detailed data quality evaluation study is reported in Chapter 2, Section 2.3. This study involved both qualitative and quantitative evaluation techniques, and provided a basis for the wavelength band studies that followed.

The Ecological Inventory portion of this report includes a number of major research activities and several significant results. The first phase of this work involved interpretation of the S-190 photography. The results of the temporal evaluation of the SL-2 and SL-3 photography were found to be particularly important for proper interpretation of the computer-aided analysis of the SL-2 and SL-3 multispectral scanner data. Although the photointerpretation results indicated that the SL-3 data would be better for vegetation mapping because of differences in vegetative condition in August as compared to June,

the computer analysis for SL-3 S-192 data produced relatively poor results. It was determined that this was due to a data quality problem involving a "ringing" effect. This "ringing" had been introduced by the digital filtering process which had been applied to the SL-3 data. Therefore, the majority of the Ecological Inventory study was conducted using only the SL-2 multispectral scanner data set, which had not been digitally filtered.

An analysis technique identified as "Modified Clustering" had initially been developed at LARS during the LANDSAT-1 investigation. Application of this technique to the SKYLAB data which contained many more wavelength bands than had previously been involved, provided an effective evaluation of the reliability of this technique. The results indicated that this technique is particularly valuable when working with multispectral scanner data involving many wavelength bands and covering large geographic areas. Therefore, a detailed description of the technique is included in Section 3.3.2.

Evaluation of the computer classification results of the S-192 data involved several different techniques, including both qualitative and quantitative evaluations. The underflight aircraft photography proved particularly valuable for the qualitative evaluation phase of the study. The quantitative evaluation techniques utilized are described in Section 3.3.3. These included both a statistical grid of test samples, and a comparison of acreage estimates utilizing photointerpretation techniques, as compared to results of the computer-aided analysis of SKYLAB scanner data.

Analysis of the SL-2 multispectral scanner data involved classification of major cover types (corresponding to USGS Circular 671 Level 2 land use classes) and also classification of forest cover types. The results indicated that the major cover types could be mapped with approximately 85% accuracy and forest cover types with approximately 71% accuracy. When acreages of the major cover types obtained from photointerpretation techniques were compared to the acreage summary based upon computer-aided analysis of SKYLAB data, a correlation coefficient of 0.929 resulted. We believe this is particularly significant since it indicates that reliable acreage estimates can be obtained using computer-aided analysis of satellite data even in areas of rugged mountainous terrain.

Comparison of the results obtained with SKYLAB MSS data and LANDSAT MSS data (Section 3.4.4) indicated that the improved spectral resolution of the SKYLAB scanner system (as compared to LANDSAT) enabled a higher classification accuracy to be obtained for forest cover types, although the classification performance for major cover types was not significantly different. It is believed that the classification results with the SKYLAB data would have been significantly improved had the data quality of the SKYLAB data been as good as that of the LANDSAT data. The results also indicated that the increased spectral range of the SKYLAB scanner system enabled a better combination of four wavelength bands to be defined for computer analysis than are present in the LANDSAT data.

This wavelength band evaluation study was one of the major activities in the Ecological Inventory study. Several different approaches and techniques were utilized in evaluating the various wavelength bands available in the SKYLAB S-192 data set. The results indicated that a number of different wavelength bands were particularly important for effective classification of various cover types. A preliminary study involved the number of wavelength bands required for effective classification of the SKYLAB MSS data. The results indicated that classification performance was not significantly improved when more than four wavelength bands were utilized. However, the combination of four wavelength bands which were of most value for classifying various cover types varied considerably. The near infrared portion of the spectrum - especially the 1.09-1.19 mm wavelength band - was shown to be of particular value for effective vegetation mapping. Additional wavelengths in the visible, near infrared, middle infrared, and thermal infrared wavelengths were also shown to be of importance. These results offer significant insight into the evaluation of the wavelength bands proposed for the Thematic Mapper to be carried on LANDSAT-D.

The topographic data was utilized in a preliminary study to improve classification performance. The results indicate the value of the combination of spectral data and topographic data, but also indicate that different analysis techniques need to be developed for effective analysis of combinations

of data from multiple data sources.

One of the last phases of the Ecological Inventory study involved utilization of a newly developed analysis technique referred to as "ECHO", which allows a much more map-like classification output to be obtained. The results of this analysis received very positive reactions from both U. S. Forest Service and National Park Service personnel.

One of the more significant user agency contacts involved the National Park Service personnel from Mesa Verde National Park. The results of a photointerpretation effort using the SKYLAB S-190 data and a computer-aided analysis of Mesa Verde using LANDSAT data, were enthusiastically received by the Park Service personnel. These results proved to be of considerable value in many phases of their activities. As a results of several discussions with N. P. S. personnel concerning the utility of satellite data, a permanent display featuring SKYLAB data over Mesa Verde National Park has been developed and opened to the public. It is anticipated that over 600,000 visitors will see this display during the next year.

The hydrologic features survey activities involved three major studies, including snow/cloud differentiation, snow-cover mapping, and thermal data calibration.

The snow/cloud differentiation analysis clearly showed the value and the necessity of the middle infrared portion of the spectrum (1.55-1.75 or 2.10-2.35 μm) for spectrally separating snow and clouds. Such snow/cloud differentiation

cannot be effectively accomplished with LANDSAT data. A detailed quantitative comparison of the spectral response for snow and clouds from both SKYLAB and LANDSAT scanner systems is shown.

The snow cover mapping activity showed that the multiple wavelength bands of SKYLAB data could be effectively utilized to map differences in spectral response within the snow pack area. Previous work with LANDSAT data had shown that one could effectively map area extent of snow cover utilizing the satellite data and computer-aided analysis techniques, but differences in spectral response within the snow pack could not be mapped. The near infrared portion of the spectrum proved particularly useful for mapping the different spectral response groupings in the snow pack area. Application of the topographic overlay data subsequently allowed for acreage estimates to be obtained for each of the spectral classes of snow at each 100 meter elevation increment. Such an ability to define differences in spectral characteristics of the snow cover, and to summarize this in terms of acreage for various elevation zones, should prove of particular value for more effective prediction of water runoff from mountain snow packs.

Thermal data calibration involved a two-point non-linear calibration of the SKYLAB S-192 Channel 13 data. The calibrated data were compared with water temperature measurements made at the time of the SKYLAB overpass on Vallecito Reser-

voir. The two results were in close agreement (less than 1^{o} C. difference) indicating that for areas with little atmospheric attenuation, reasonable calibration of the thermal data can be achieved.

The geology portion of the project attempted to demonstrate the value of satellite data as a supplement to mineral exploration reconnaissance techniques. It involved a comparison of the mapping of linear and lineament features on both SKYLAB photography and LANDSAT imagery, drainage anomalies which appear to reflect the basic caldera structures of the area, and spectral analysis of mineralized areas. The most significant result of the geological investigations was the definition of computer techniques to utilize in enhancement and mapping of oxidized areas of hydrothermal alteration associated with ore mineralization. The iron oxides developed in these areas display a characteristic decrease in reflection below approximately 0.55 - 0.60 μm and a distinct absorption band centered near 0.85 μm. Such spectral characteristics allowed the use of channels 2, 4, 8 and 12 of the NC-130 scanner data and channels 3, 7, 8, 9, 10 and 11 of the SKYLAB-3 S-192 data to be used for LARSYS classifications using the modified clustering technique. The classification results clearly delineated the areas of altered rock and also indicated the presence of a previously undetected and unmapped feature which may represent a mineralized pipe.

Another computer technique used to detect and map hydrothermally altered areas involved ratios of various channels of data including both single channel pairs (A/B) and various combinations of channels (A+B/C+D). The results indicated that although selected ratios may produce good results in one area or with one data set (aircraft, SKYLAB, or LANDSAT), they may not produce similar results in another area or data set.

CHAPTER II -- DATA CHARACTERISTICS AND OVERLAY OF TOPOGRAPHIC DATA

by

P.E. Anuta, L.A. Bartolucci,
S.G. Luther, and R.M. Hoffer

2.1 INTRODUCTION

This chapter of the report is divided into three primary sections. The first describes the location and characteristics of the SKYLAB data that were obtained and analyzed in this research. The LANDSAT and aircraft data that were utilized in conjunction with the SKYLAB data are also described.

Section 2.3 describes the results of a detailed data quality evaluation study. As has already been indicated, the emphasis of the research involved analysis of the S-192 Multispectral scanner data. When the data were first obtained and displayed, it became obvious that there were marked differences in quality of data among the various wavelength bands. Preliminary analysis showed that a visual indication of data quality did not always correspond to a more quantitative data quality assessment. Therefore, a detailed study to define a method for evaluating data quality of the individual wavelength bands of S-192 data was carried out. The results of this study were particularly critical in the wavelength band evaluation phase of the ecological inventory study.

The last portion of this chapter discusses one of the most significant results of this investigation. This involved the geometric correction, scaling and overlaying of SKYLAB S-192

data, LANDSAT data and topographic data. To the best of our knowledge, this is the first time that such a combination of scanner and topographic data has ever been geometrically corrected, scaled, and overlayed. Some preliminary tests indicating the importance of the ability to combine multispectral scanner data and topographic data are reported in both the ecological inventory and hydrological features chapters.

2.2 LOCATION AND CHARACTERISTICS OF DATA UTILIZED

The data utilized in this SKYLAB research consisted of multispectral scanner data and photographic data collected from several altitudes and with different sensor systems, including the SKYLAB Earth Resources Experiment Package, LANDSAT-1, NASA's WB-57F and NC-130 aircraft, small observation aircraft, and ground observations. SKYLAB data of useable quality were obtained during both the SL-2 and SL-3 missions. During SL-4, the test site was almost completely snowcovered and the data could not be utilized.

Figure 2.1 shows the location and date of collection for both the SKYLAB and LANDSAT scanner data that were collected during the summer of 1973 and utilized in this research. The area around Vallecito Reservoir, particularly the area where the SL-2 and SL-3 S-192 data were overlapping, was designated as the "Granite Peaks Test Site". This was the primary area utilized in the Ecological Inventory analysis. However, in that area the data utilized consisted primarily of SKYLAB S-190A and S-190B photography and LANDSAT MSS data, because the S-192 data did not cover most of the area of interest to the National Park Service. S-192 data around the LaSal Mountains in Utah was utilized for the snow/cloud differentiation phase of the Hydrologic Features study. SL-2 S-192 data from the area including the Lemon Reservoir (just west of Vallecito Reservoir) was used extensively in the other phases of the Hydrologic Features research.

Although the area around Rio Grande Reservoir had been designated as the primary test site for all phases of this investigation, the SL-2 S-192 data did not cover this area, and many geologic

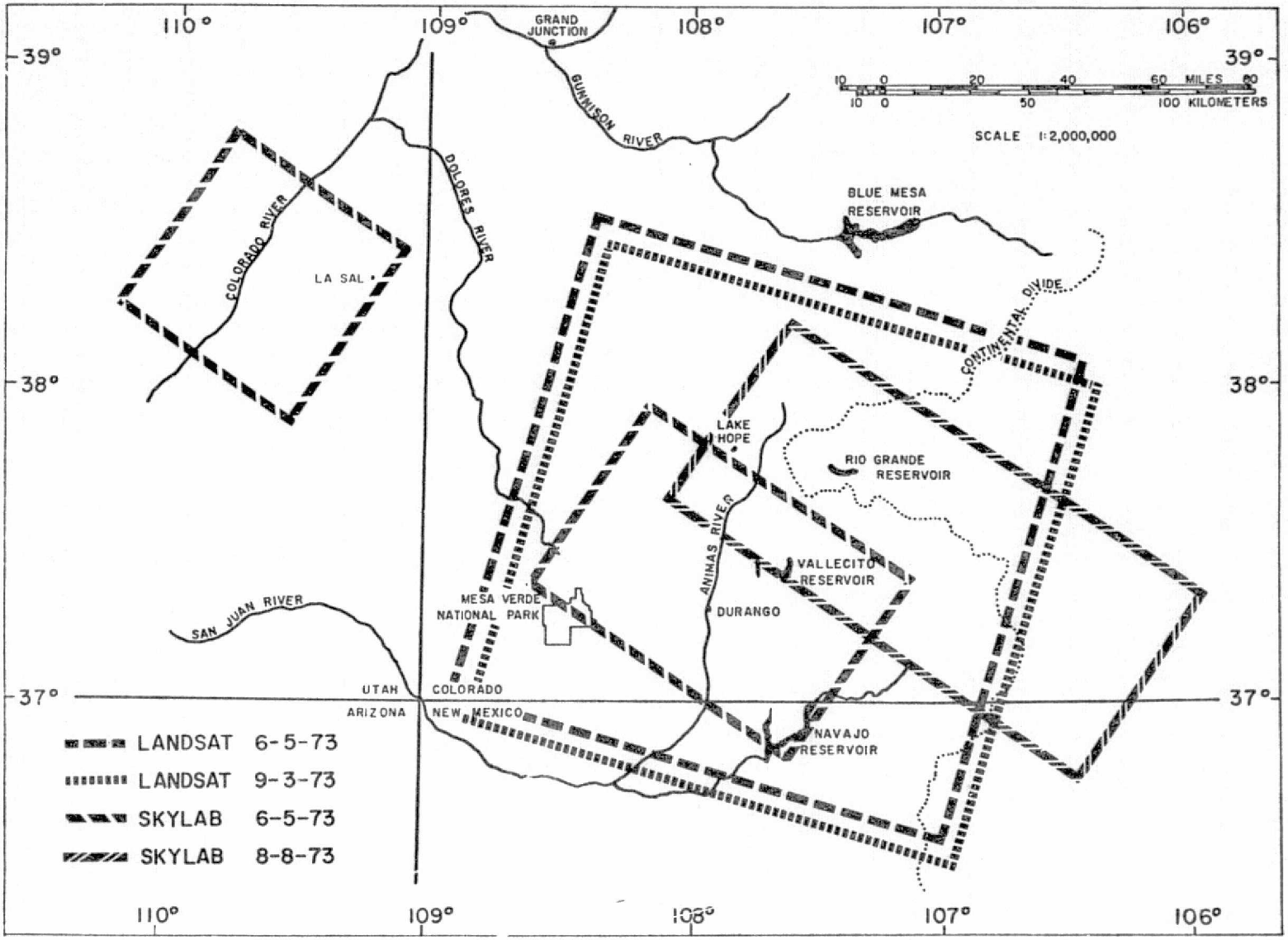

Figure 2.1 -- SKYLAB and LANDSAT multispectral scanner coverage of the test site collected during the SL-2 and SL-3 missions

features of interest were at the higher elevations that were still snow covered at the time of the SL-2 data collection. Consequently, the Geological Assessment study primarily utilized data from SL-3 collected on August 8. Even then, they had to shift the area of emphasis away from Rio Grande Reservoir because of cloud cover problems in that area. Cloud cover immediately over the reservoir at the time of the SL-3 data collection also precluded use of the S-191 data which was obtained using Rio Grande Reservoir as a target.

We were extremely fortunate in obtaining both SKYLAB and LANDSAT data over the test site under cloud free conditions on June 5. The following day both NC-130 and WB-57 data were obtained under equally cloud free conditions. Thus, the SL-2 data set consisted of a combination of data from different altitudes and sensor systems, all obtained within a thirty-one hour period, as outlined in Table 2.1. Reference data included photographs and descriptive information obtained from an observation aircraft as well as water temperature and water quality data obtained from Vallecito Reservoir, and other ground observation and reference data obtained throughout the test site area.

During SL-3, an attempt was made to obtain SKYLAB data on August 3, but at the time of the overpass (12:01 p.m.) the test site area was nearly obscured by cloud cover. The mission was rescheduled and data were obtained on August 8, 1973. Excellent aircraft support were provided by NASA, and NC-130 data were obtained on August 4 over the test site under nearly cloud free conditions, and WB-57 photography were obtained on August 3. Since the WB-57 photography were largely obtained early in the morning before the

Table 2.1 Data Collected For the SKYLAB SL-2 Mission

Platform	Altitude (MSL)	Date	Time	Sensors Utilized
LANDSAT	914 km	June 5	9:20 a.m.	4-Channel Multispectral Scanner
SKYLAB	435 km	June 5	11:59 a.m.	S-190A Multiband Camera S-190B Mapping Camera, and S-192 Multispectral Scanner
WB-57	18,300 m	June 6	≈10:00 a.m.	Mapping Camera, Color IR Film
NC-130	11,200 m	June 6	≈4:20 p.m.	Cameras and 24 Channel Multispectral Scanner
Observation Aircraft	3,400 m	June 5	≈11:30 a.m.	Cameras, PRT-10 Observations
Reference Data ("Ground Truth")	2,400 m	June 5-6	All Day	Cameras, Thermometers, Observations

attempted SKYLAB pass, cloud cover conditions on most of this data are within tolerable limits.

The location and dates of coverage obtained by both the WB-57 and the NC-130 aircraft during the SL-2 mission are shown in Figure 2.2. Figure 2.3 shows the location and dates of coverage obtained during SL-3, again involving both the WB-57 and the NC-130 aircraft. It should be pointed out here that the aircraft data were used extensively as reference data (ground truth) throughout this investigation. The analysis of the SKYLAB S-192 data could not have been effectively completed without the supporting aircraft data. Both the WB-57 and NC-130 photographic data and also the NC-130 scanner data proved useful in many phases of the investigation. The photographic data from the WB-57 and the NC-130 were of particular value in mapping the forest cover types in the Granite Peaks Test Site area, which was a requirement for effectively completing the Ecological Inventory phase of this investigation. The WB-57 photography also proved particularly valuable in interpreting the results of the snow cover mapping using the SKYLAB S-192 data. The multispectral scanner data obtained from the NC-130 aircraft was extensively utilized in the Geological Assessment study. Thus, good quality photographic and scanner data from aircraft altitudes proved essential for effective interpretation of the SKYLAB MSS data.

For reference purposes, Table 2.2 gives the wavelength bands of the multispectral scanners that were involved in this investigation, as well as the bands of the S-190A photographic system, which was part of the SKYLAB EREP sensor package.

The SKYLAB S-192 scanner system utilized a conical scan-line configuration. However, NASA developed a program to reformat the

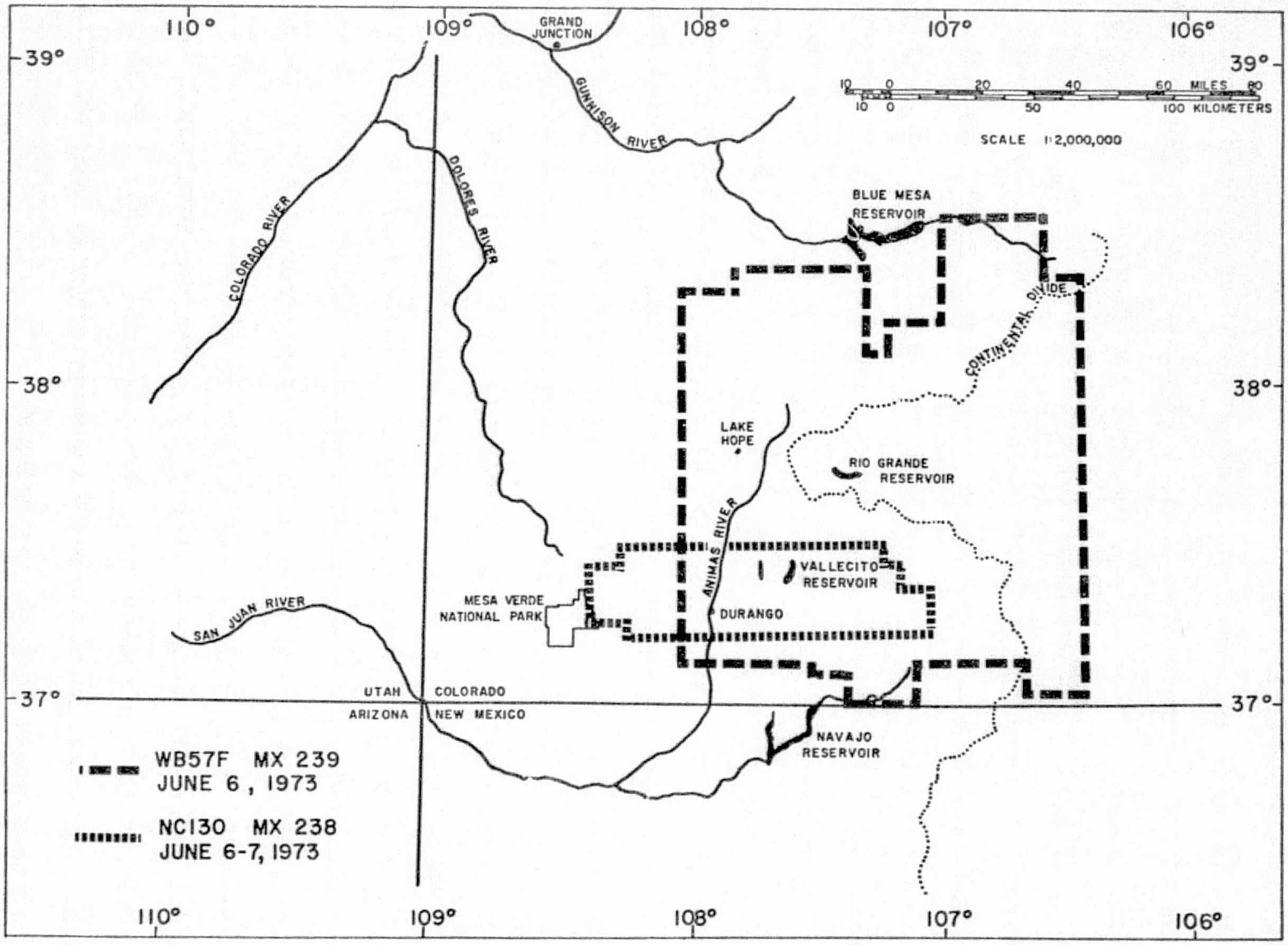

Figure 2.2 -- Aircraft data support coverage during SL-2

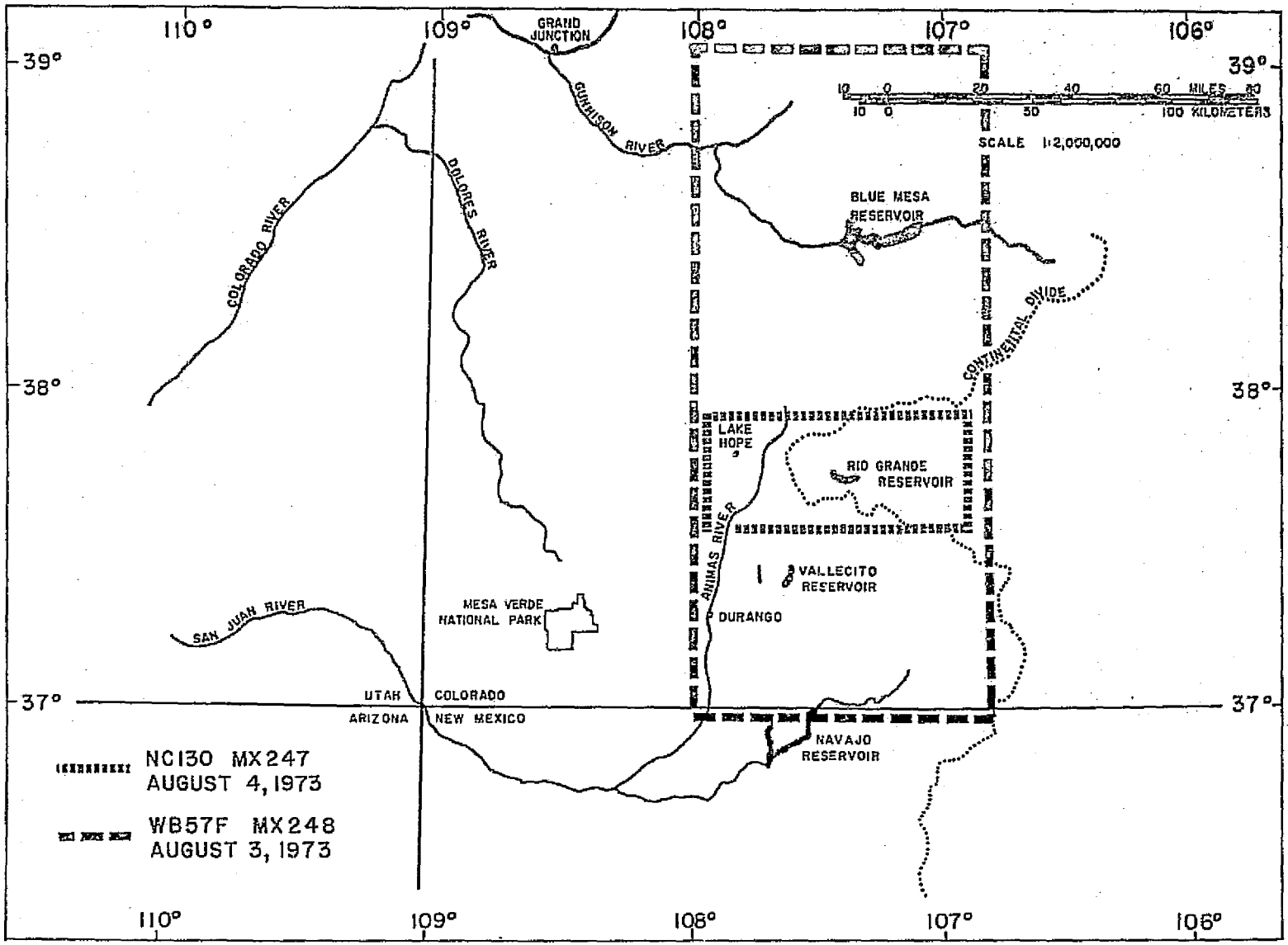

Figure 2.3 -- Aircraft data support coverage during SL-3

Table 2.2 Wavelength Bands of Photographic and Multispectral Scanner Systems Utilized

	S-192 MSS Alt: 435 km	S-190A Photographic Data Alt: 435 km	LANDSAT-1 MSS Alt: 914 km	NC-130 MSS Alt: 11.2 km
				(1) 0.38-0.40
Visible	(1)[1] 0.41-0.46	0.40-0.70 (color)		(2) 0.40-0.44
Visible	(2) 0.46-0.51	0.50-0.60 (B&W)		(3) 0.47-0.49
Visible	(3) 0.52-0.56		(4) 0.50-0.60	(4) 0.53-0.58
Visible	(4) 0.56-0.61	0.60-0.70 (B&W)		(5) 0.59-0.64
Visible	(5) 0.62-0.67	0.52-0.88 (CIR)	(5) 0.60-0.70	(6) 0.65-0.69
Visible	(6) 0.68-0.76	0.70-0.80 (CIR)	(6) 0.70-0.80	(7) 0.72-0.76
Visible	(7) 0.78-0.88	0.80-0.90 (B&W)		(8) 0.77-0.81
Near IR	(8) 0.98-1.08		(7) 0.80-1.10	(10) 0.82-0.88
Near IR		0.50-0.60 (color)		(24) 1.06-1.09
Near IR	(9) 1.09-1.19			(23) 1.13-1.17
Near IR	(10) 1.20-1.30			(11) 1.20-1.30
Middle IR	(11) 1.55-1.75			(12) 1.53-1.62
Middle IR	(12) 2.10-2.35			(13) 2.30-2.43
Thermal IR				(14) 3.78-4.04
Thermal IR				(15) 4.05-4.46
Thermal IR				(16) 6.00-7.00
Thermal IR				(17) 8.27-8.70
Thermal IR				(18) 8.80-9.30
Thermal IR				(19) 9.38-9.88
Thermal IR				(20) 10.10-11.00
Thermal IR	(13) 10.20-12.50			(21) 11.00-12.00
Thermal IR				(22) 12.00-13.00

[1] Numbers in parenthesis represent wavelength band designations

data, resulting in a data tape containing the S-192 data in a line straightened format. The data tapes provided to LARS from both the SL-2 and SL-3 missions contained the S-192 data in this line-straightened format. NASA also developed a digital filtering process designed to improve the data quality of the S-192 data. The SL-2 data utilized throughout this investigation had not been digitally filtered with this technique, but the SL-3 data had been put through NASA's digital filtering process. Thus, the SL-2 data utilized had been line-straightened, but not digitally filtered. The SL-3 data utilized in this investigation had been both line-straightened and digitally filtered. Unfortunately, there were a number of clouds in the test site area at the time the SL-3 data were obtained. It was found that the digital filtering process caused a "ringing effect" in the data whenever a very high reflecting object such as a cloud was encountered. An illustration of this effect is shown in Chapter 3, Section 3.43 which discusses the results of the analysis of the SL-3 data. The effect of the ringing due to the digital filtering caused enough abnormal variation in the data characteristics that the S-192 data from the SL-3 mission was found to be unusable for effective mapping of vegetative cover types using computer-aided analysis techniques.

The topographic data utilized in this study was obtained from the United States Army Defense Mapping Agency. The format was a digital data tape containing elevation data in an X-Y grid. This data had been obtained through the digitization of 1:250,000 scale USGS topographic maps. The area covered by the data tape included a 1^{o} x 1^{o} block, as indicated in Figure 2.4. Further details concerning the characteristics of this data set are discussed in Section 2.4 of this chapter.

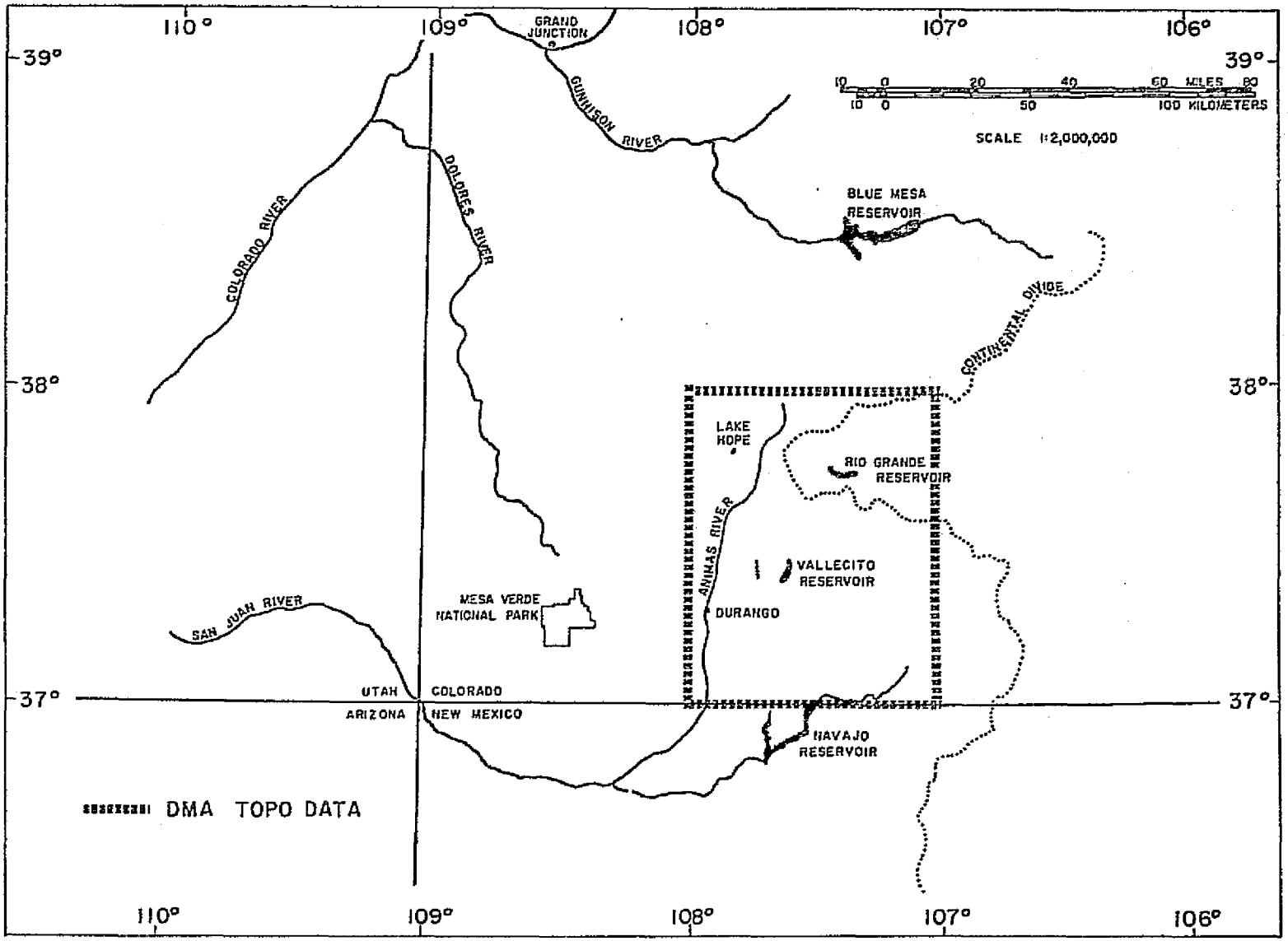

Figure 2.4 -- Location of DMA topographic data utilized

2.3 S-192 DATA QUALITY EVALUATION

2.3.1 Introduction

Since the performance of a multispectral classification is closely related to the quality of the data (signal to noise ratio), the quality of the data in the various spectral bands should be determined. If an image in a certain band appears to be of poor quality from a conventional photointerpretation point of view, it does not necessarily follow that it is a bad set of data for quantitative computer analysis (Ready et al., 1971). Because the data was to be analyzed by computer-aided analysis techniques, a quantitative evaluation of the noise level in each spectral band was essential. Such a quantitative data quality analysis was particularly necessary in order to determine the value of the various wavelength bands, based upon their spectral information content. For example, the feature selection processor of LARSYS indicates to the analyst which combination of the available wavelength bands will produce the highest classification accuracy. If the S/N ratio is equal for all wavelength bands, then the assumption can be made that the bands selected by the feature selection algorithm have the highest information content based upon the spectral characteristics of the materials involved. On the other hand, if two S/N ratios were different and the spectral information contained in the two wavelength bands were the same, then the wavelength band selected would be the one with the highest signal to noise ratio.

The set of data to be evaluated was gathered by the SKYLAB-2 crew during EREP Pass #5 on June 5, 1973 between 17:59:04 and 17:59:19 GMT. At that particular time, the Primary Y-3 detector

array was used and the attenuators had not been installed. This data set had not been digitally filtered. The data were first evaluated qualitatively and then several different quantitative techniques were utilized, including the variance in signal from a homogeneous cover type, variance of the calibration signal and a fourier analysis of the calibration signal.

2.3.2 Qualitative Evaluation

The imagery used in this qualitative evaluation was obtained from a computer compatible tape (CCT) containing straightened SKYLAB-2 S-192 data. The data were displayed on the LARS Digital Display Unit and photographed. Figures 2.5 through 2.17 show the imagery in the 13 bands of the SKYLAB-2 S-192 scanner system. Also shown in Figures 2.5 through 2.17 are the graphs of the calibration signals for the various wavelength bands. These graphs provide some indication of the noise level in the data, and are discussed in Section 2 as part of the quantitative data evaluation.

From a qualitative (pictorial) point of view, the imagery (Figures 2.5 - 2.17) shows two types of noise: one is along the scan line and the other is a banding effect. The severity of the noise problem varies significantly among the different spectral wavelength bands. The noise along the scan line is most apparent in bands 1, 2, 4, 5, and 13 (see Figures 2.5, 2.6, 2.8, 2.9, and 2.17). This is a structured-type noise of relatively high frequency ($\approx$ 44 Kc), i.e., approximately 144 cycles per scan line. The banding effect is most pronounced in bands 1, 2, 4, 13, and to a lesser extent in bands 5, 6, and 12 (see Figures 2.5, 2.6, 2.8, 2.17, 2.8, 2.9, and 2.16). This is also a structured-type noise and consists of a relatively low frequency. The spectral data of bands 3, 7, 8, 9, 10 and particularly of band 11 appear to be good quality throughout the entire image, with the exception of a few bad scan lines in band 7 and a bad portion of one scan line in band 11. Fortunately, the bad scan lines in band 7 are outside the test site area.

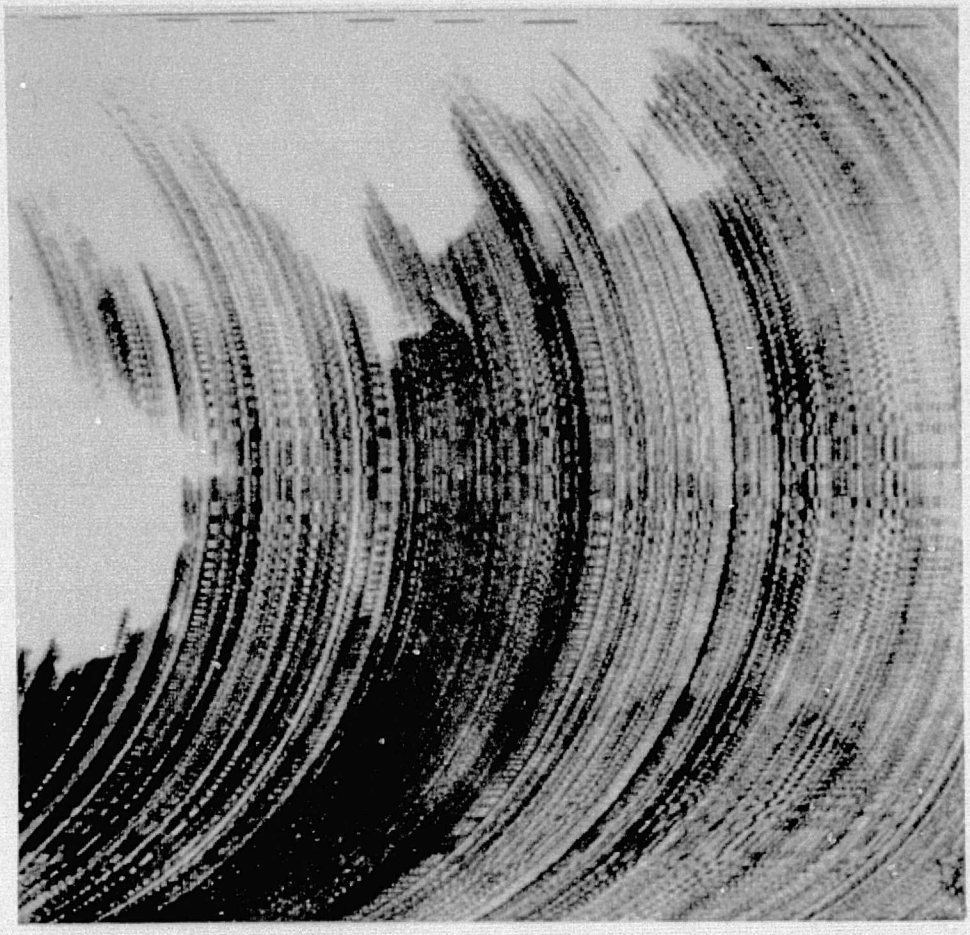

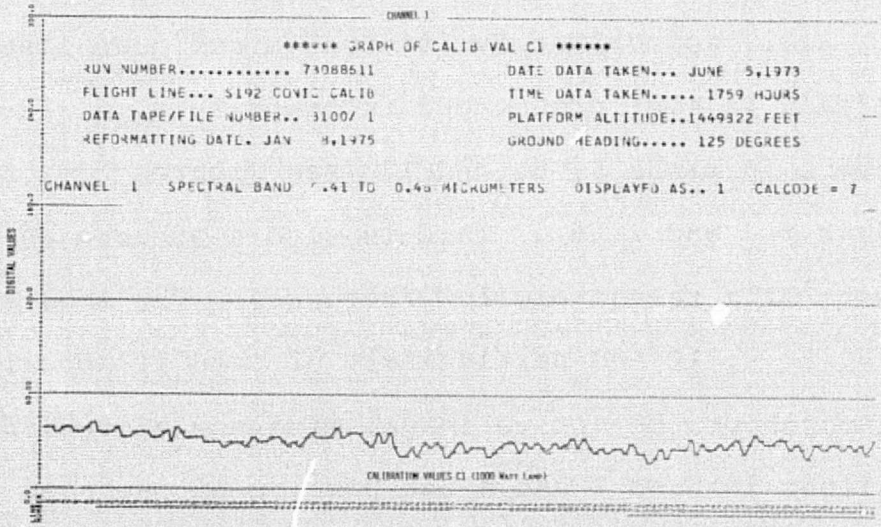

Figure 2.5 -- SKYLAB-2 S-192 multispectral scanner data - Band 1

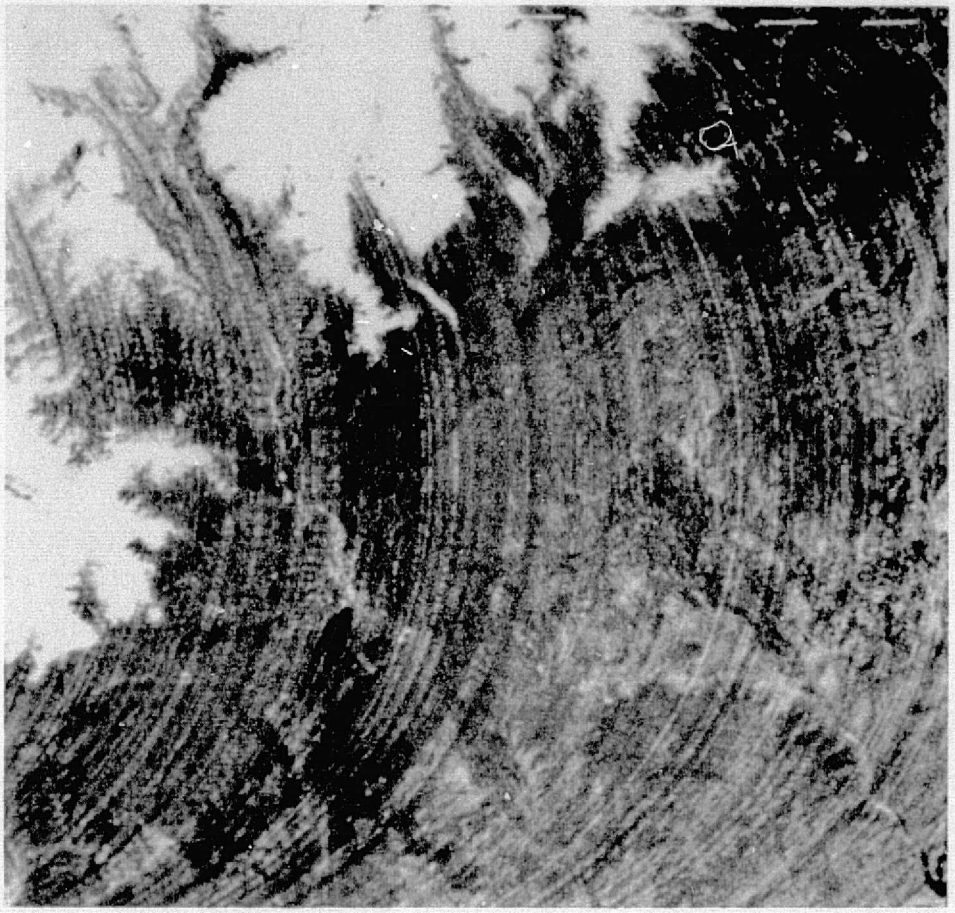

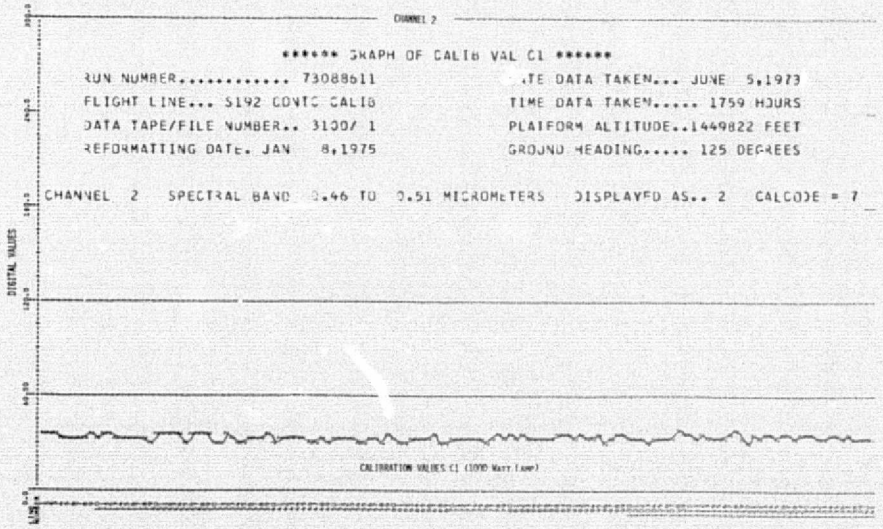

Figure 2.6 -- SKYLAB-2 S-192 multispectral scanner data - Band 2

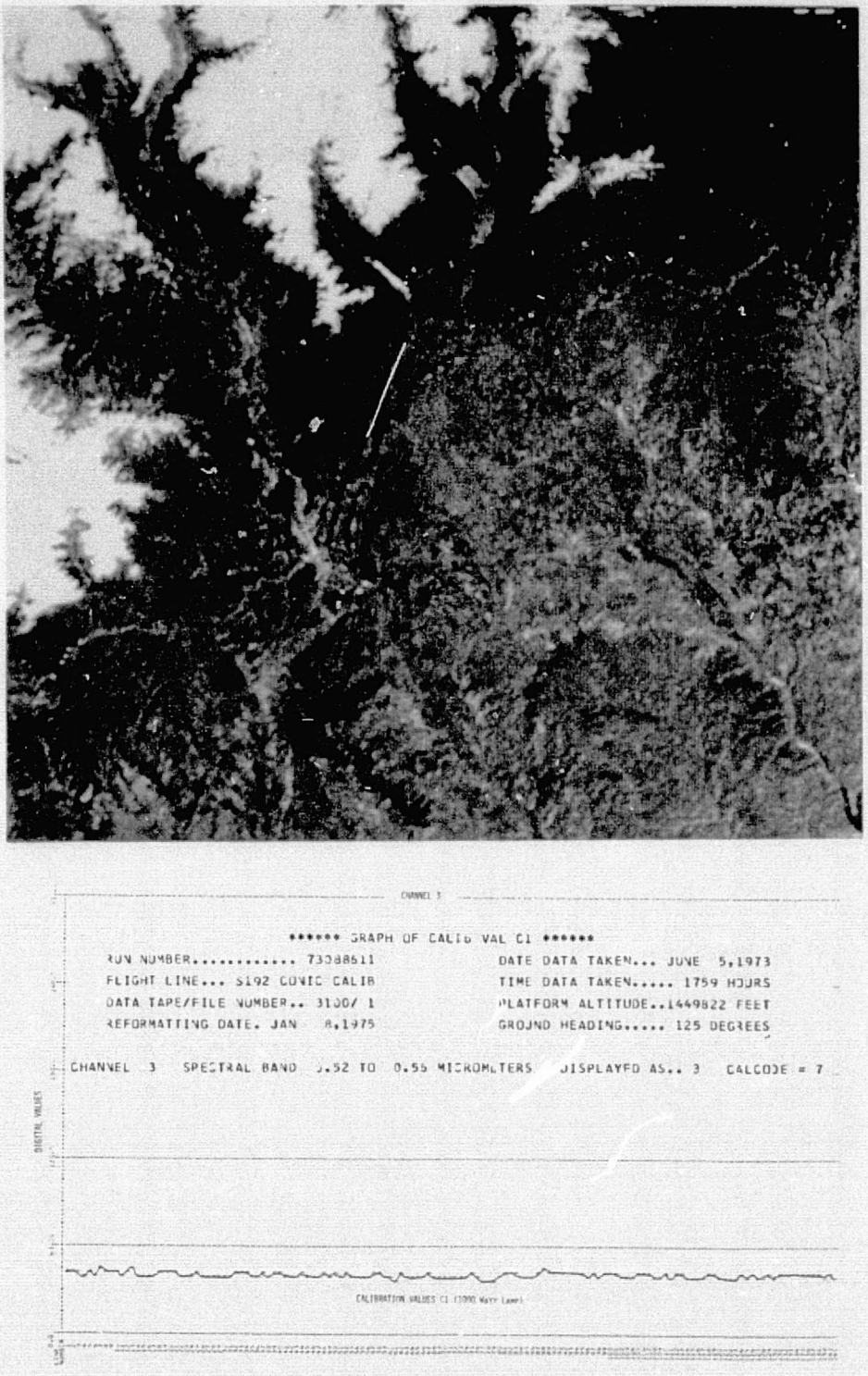

Figure 2.7 -- SKYLAB-2 S-192 multispectral scanner data - Band 3

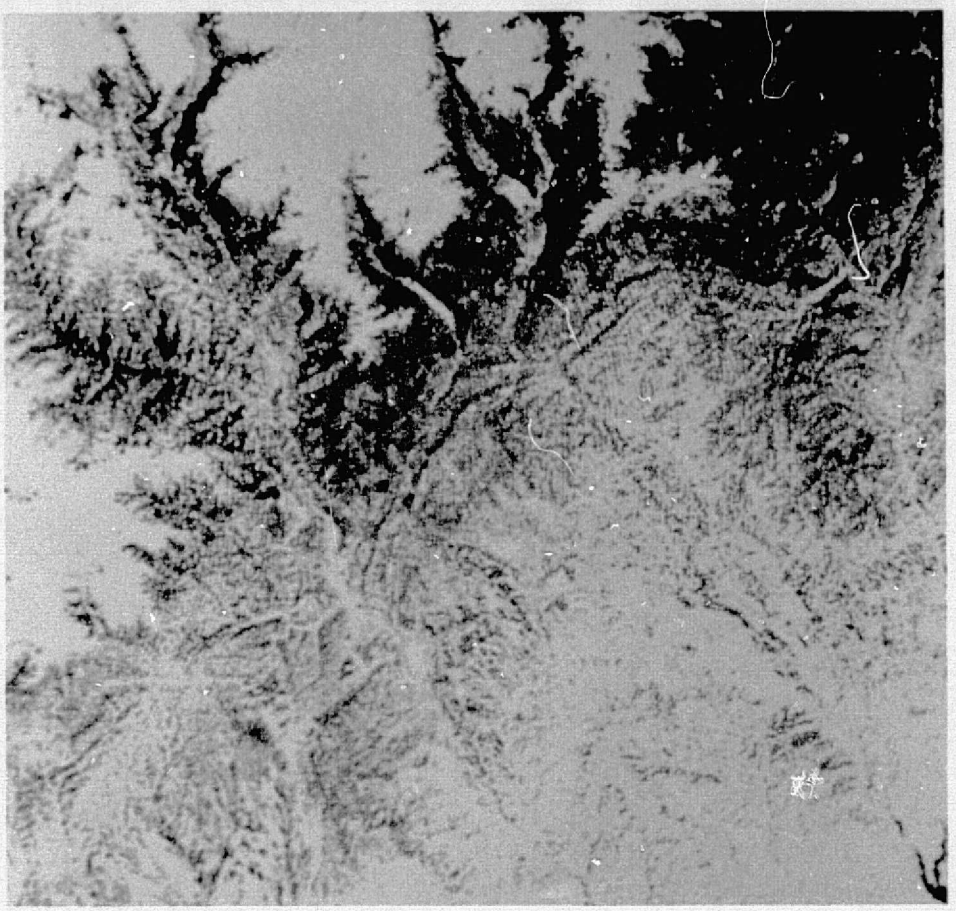

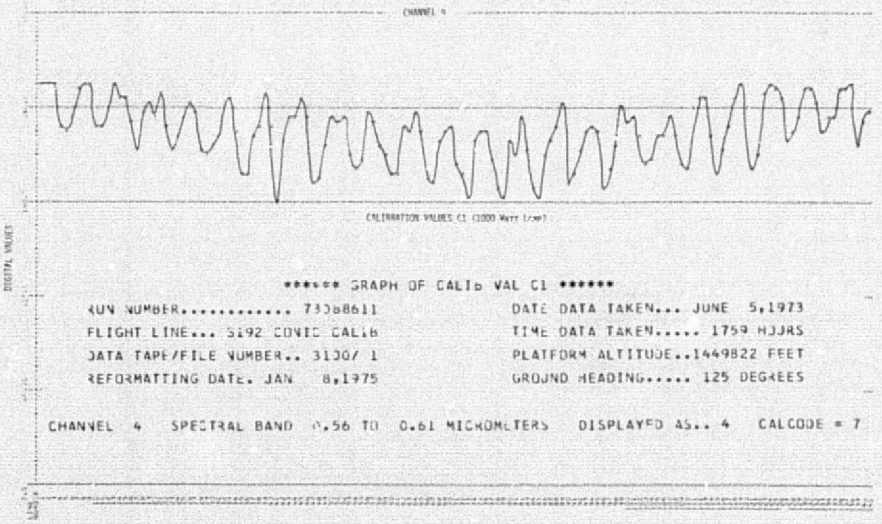

Figure 2.8 -- SKYLAB-2 S-192 multispectral scanner data - Band 4

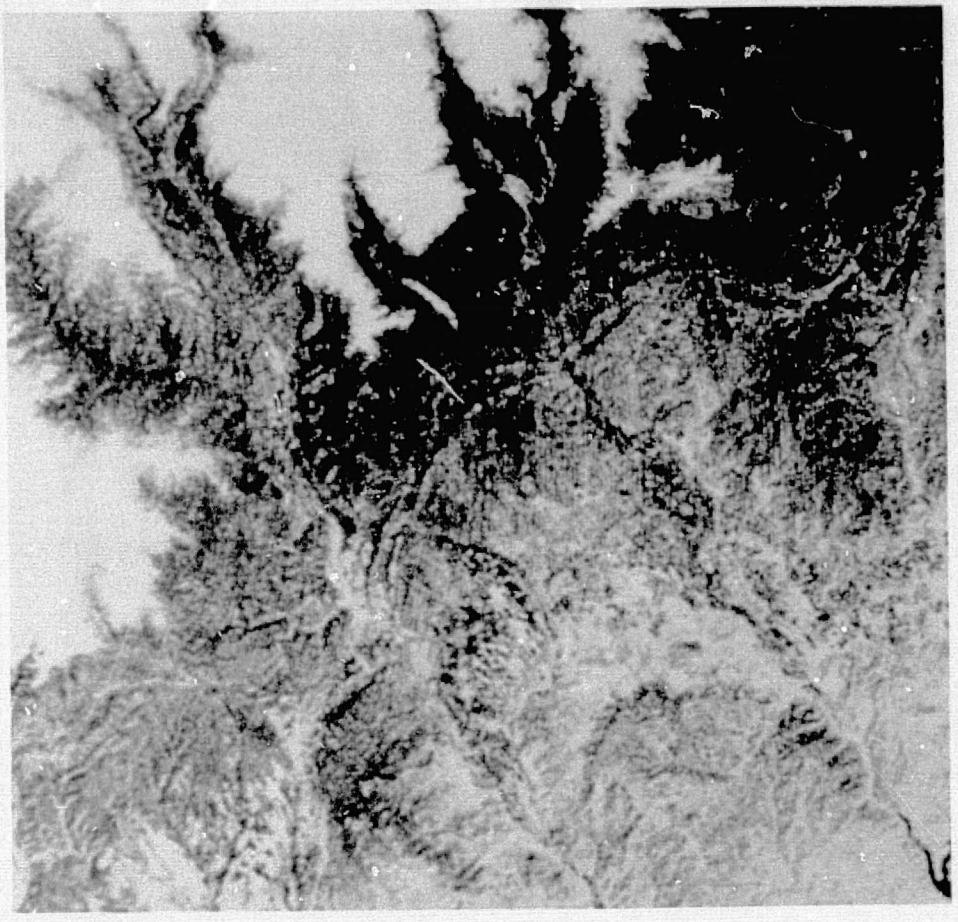

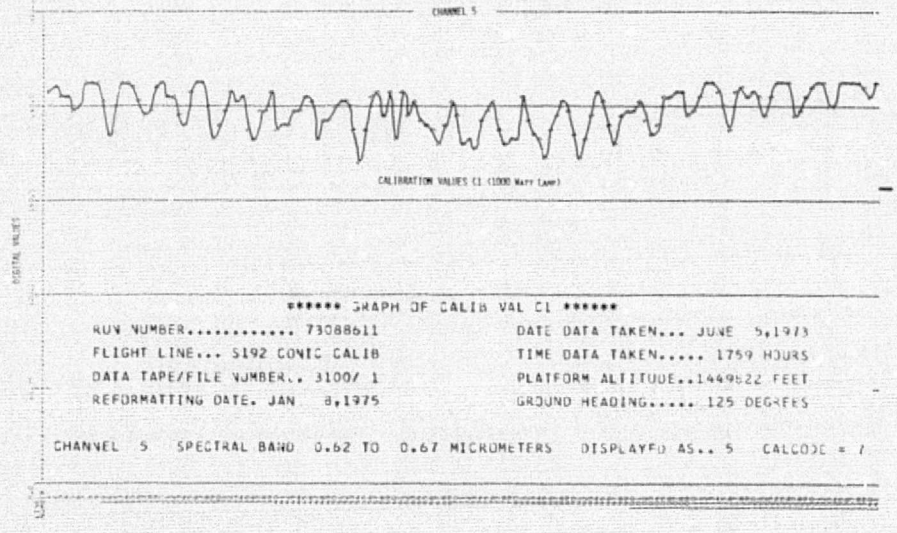

Figure 2.9 -- SKYLAB-2 S-192 multispectral scanner data - Band 5

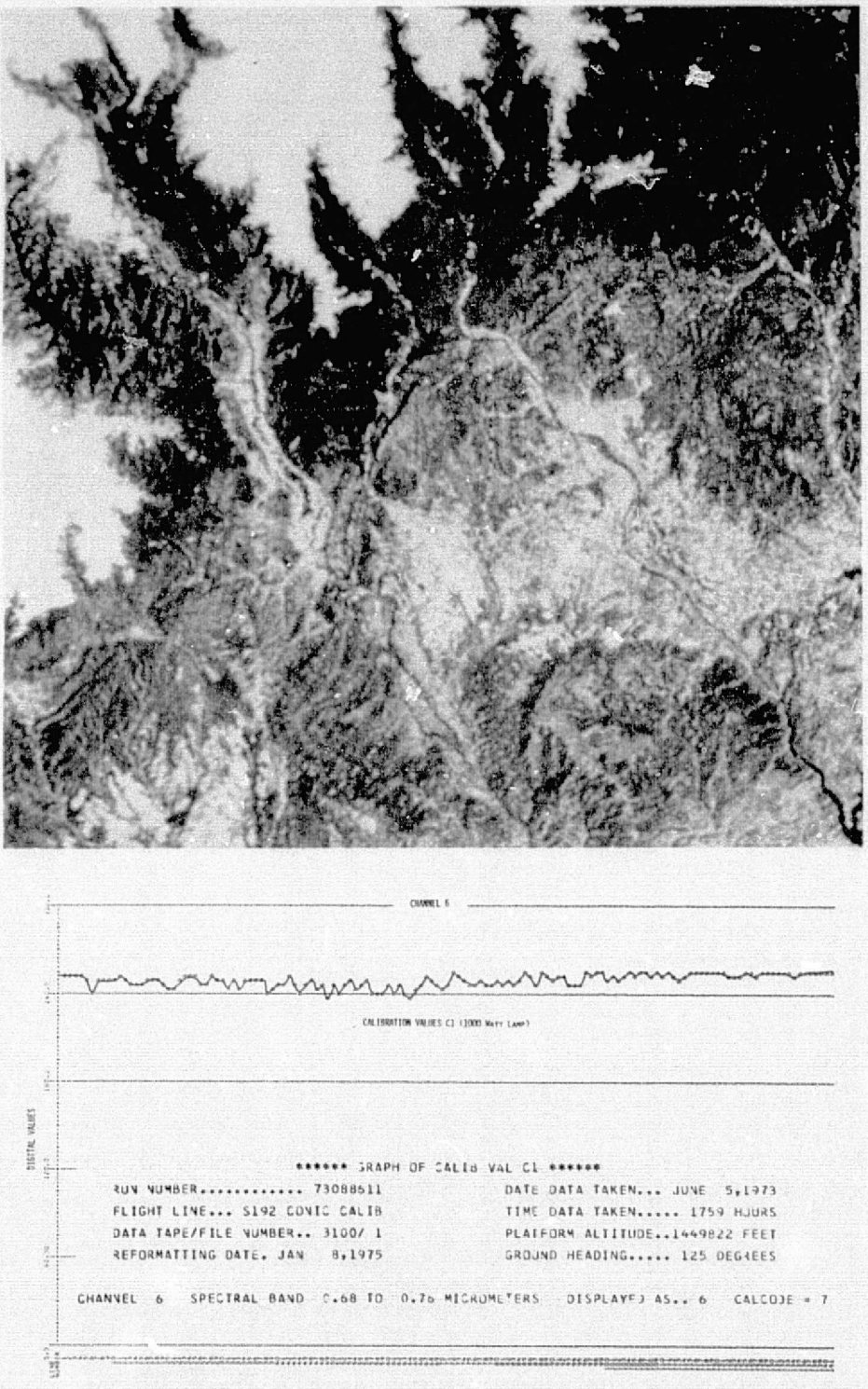

Figure 2.10 -- SKYLAB-2 S-192 multispectral scanner data - Band 6

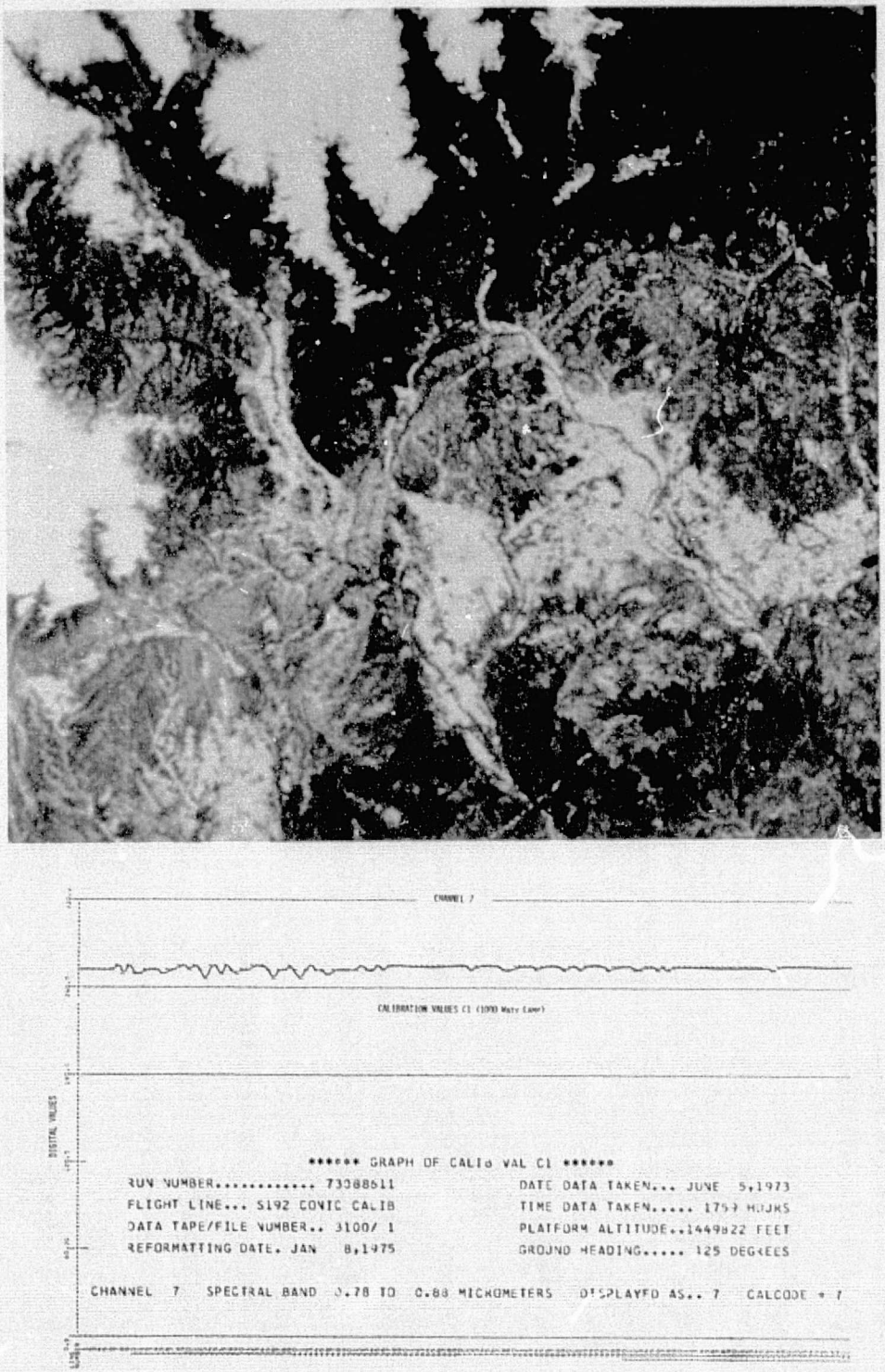

Figure 2.11 -- SKYLAB-2 S-192 multispectral scanner data - Band 7

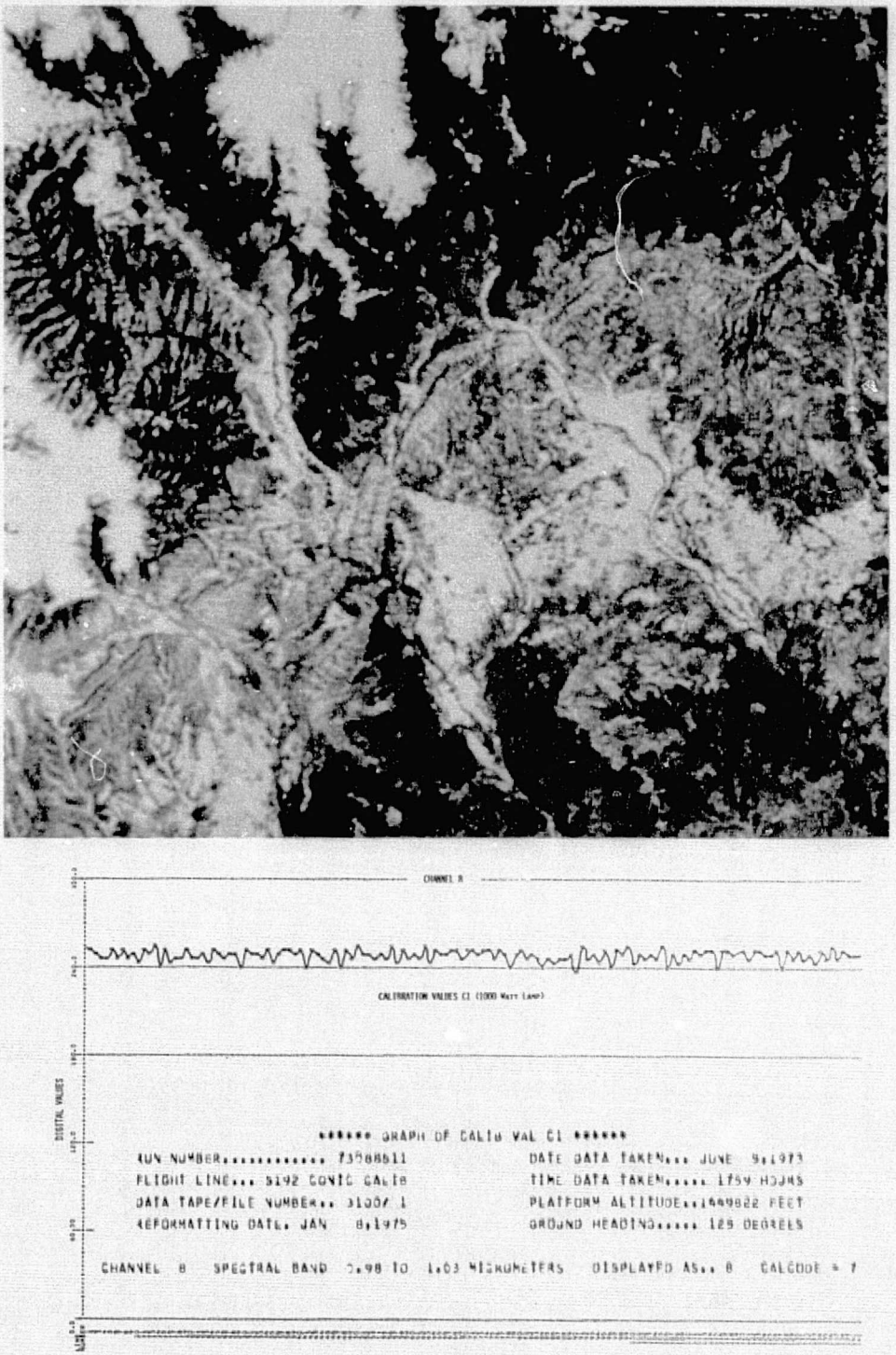

Figure 2.12 -- SKYLAB-2 S-192 multispectral scanner data - Band 8

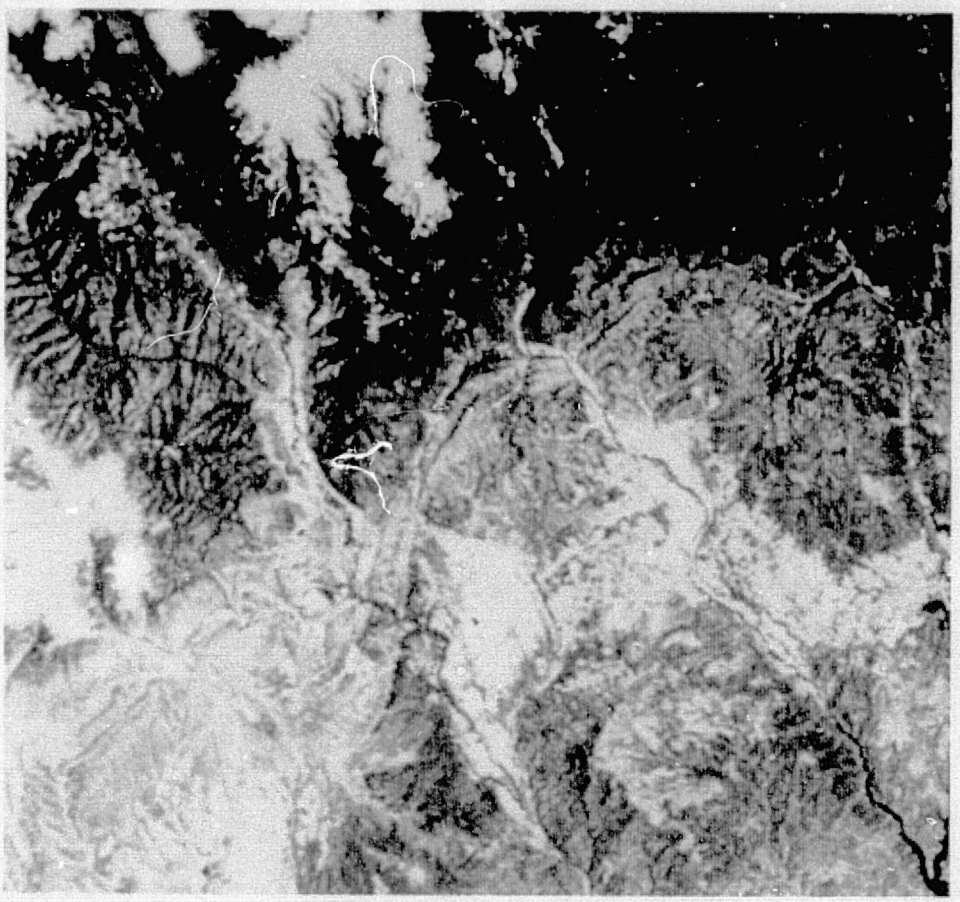

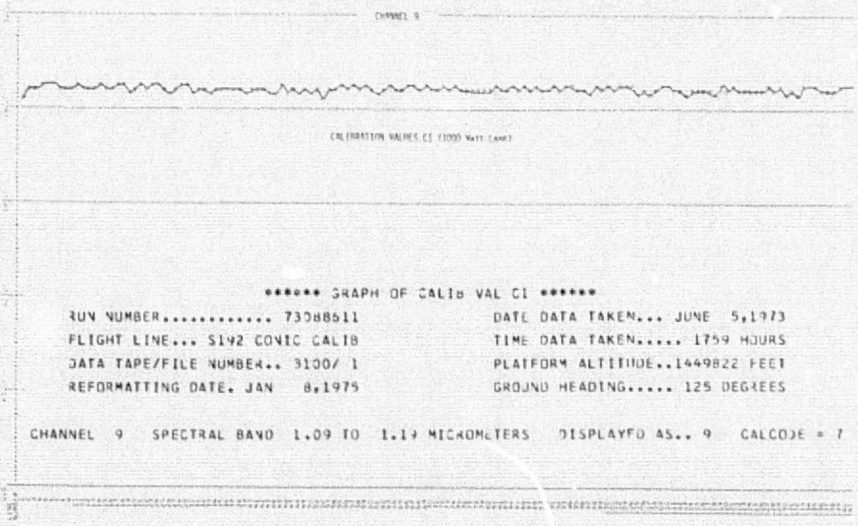

Figure 2.13 -- SKYLAB-2 S-192 multispectral scanner data - Band 9

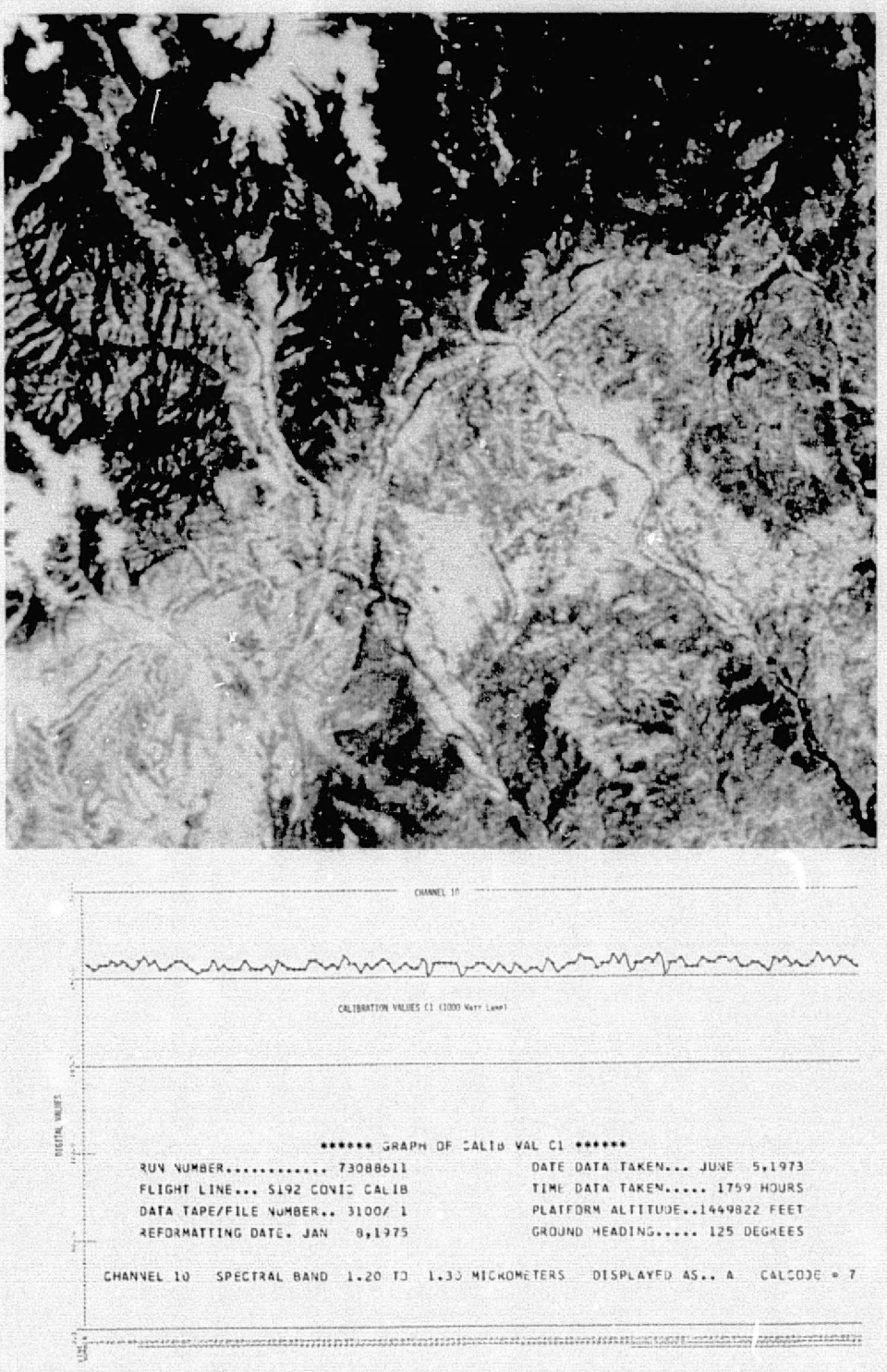

Figure 2.14 -- SKYLAB-2 S-192 multispectral scanner data - Band 10

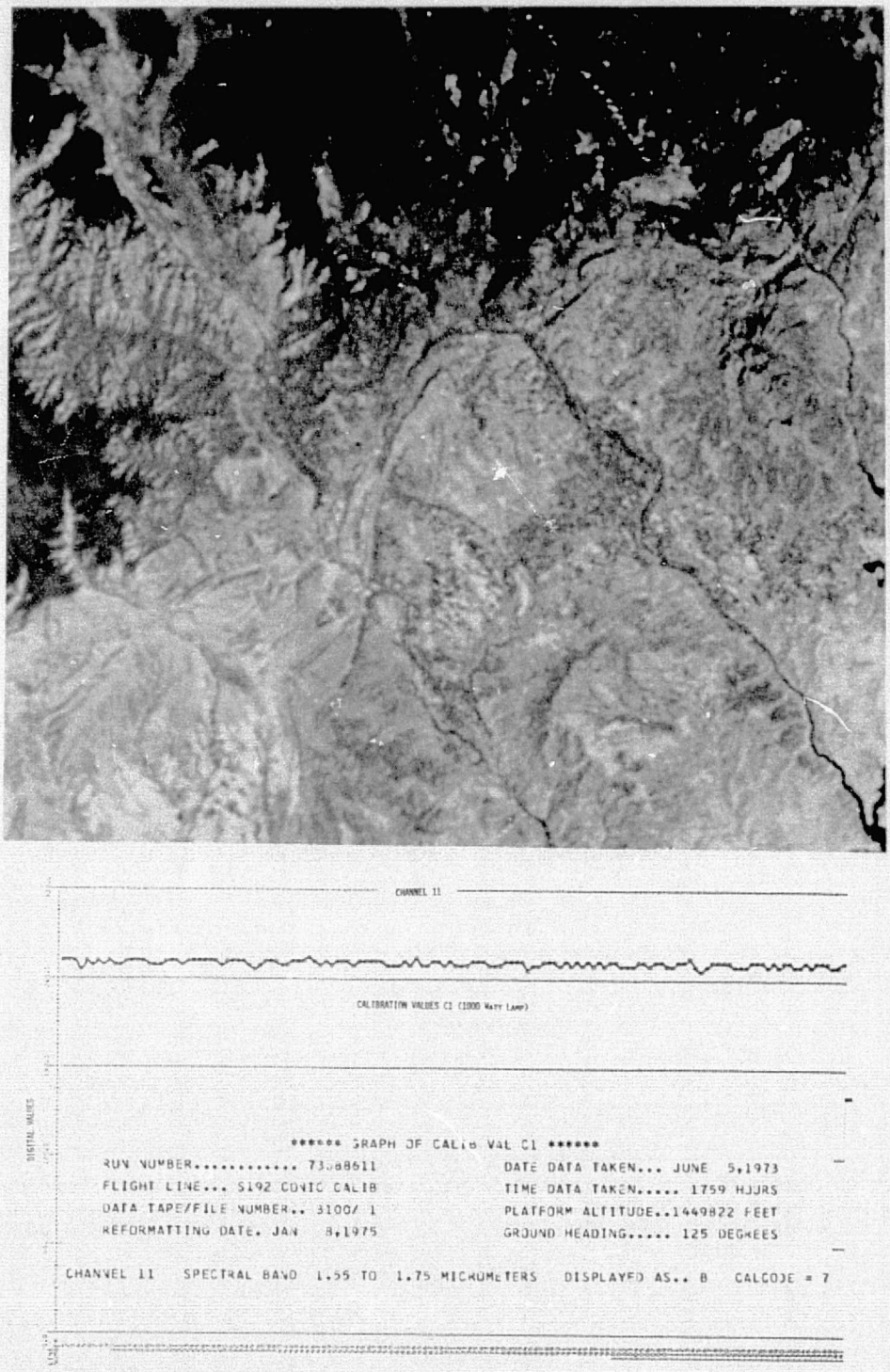

Figure 2.15 -- SKYLAB-2 S192 multispectral scanner data - Band 11

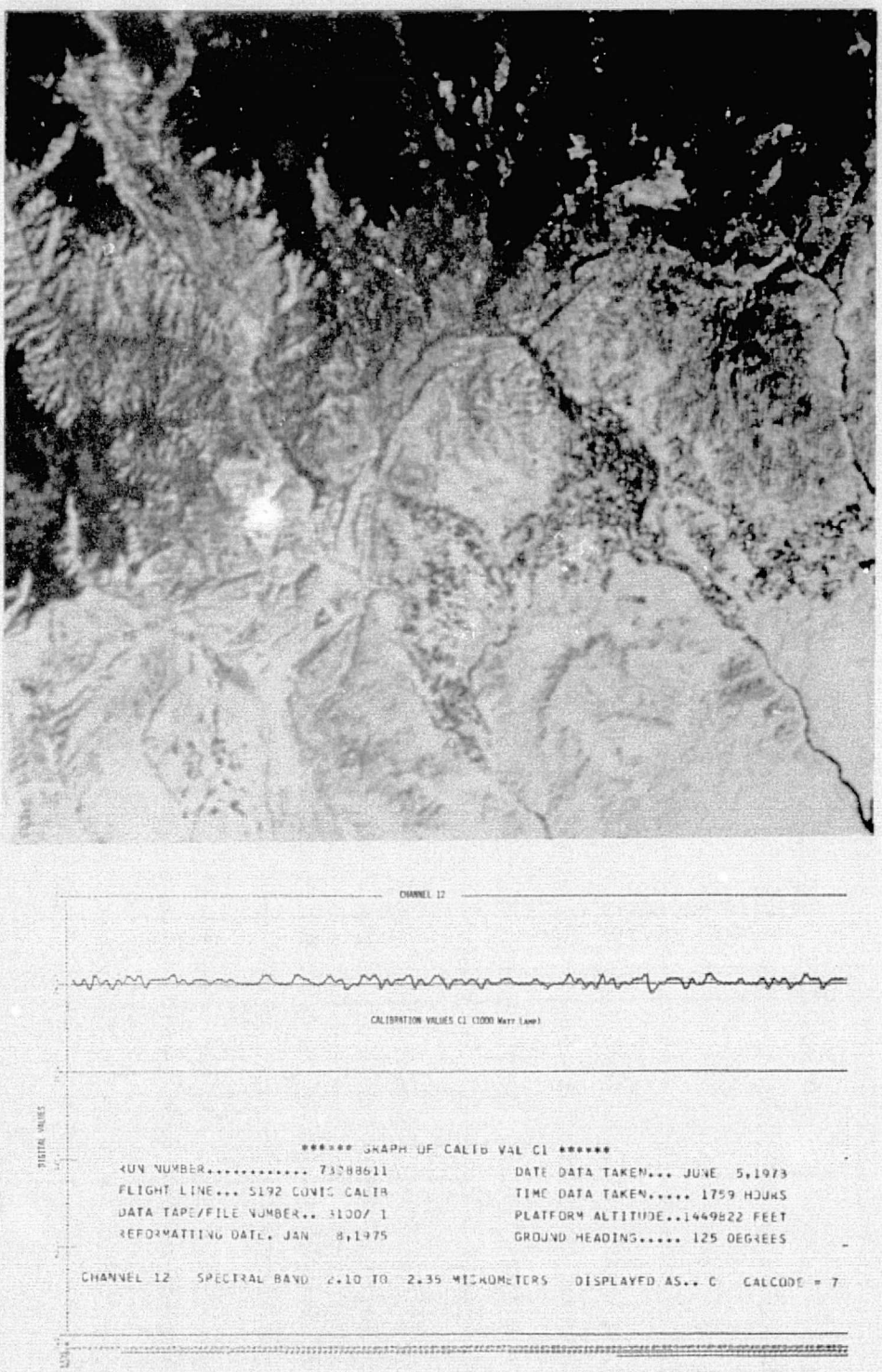

Figure 2.16 -- SKYLAB-2 S-192 multispectral scanner data - Band 12

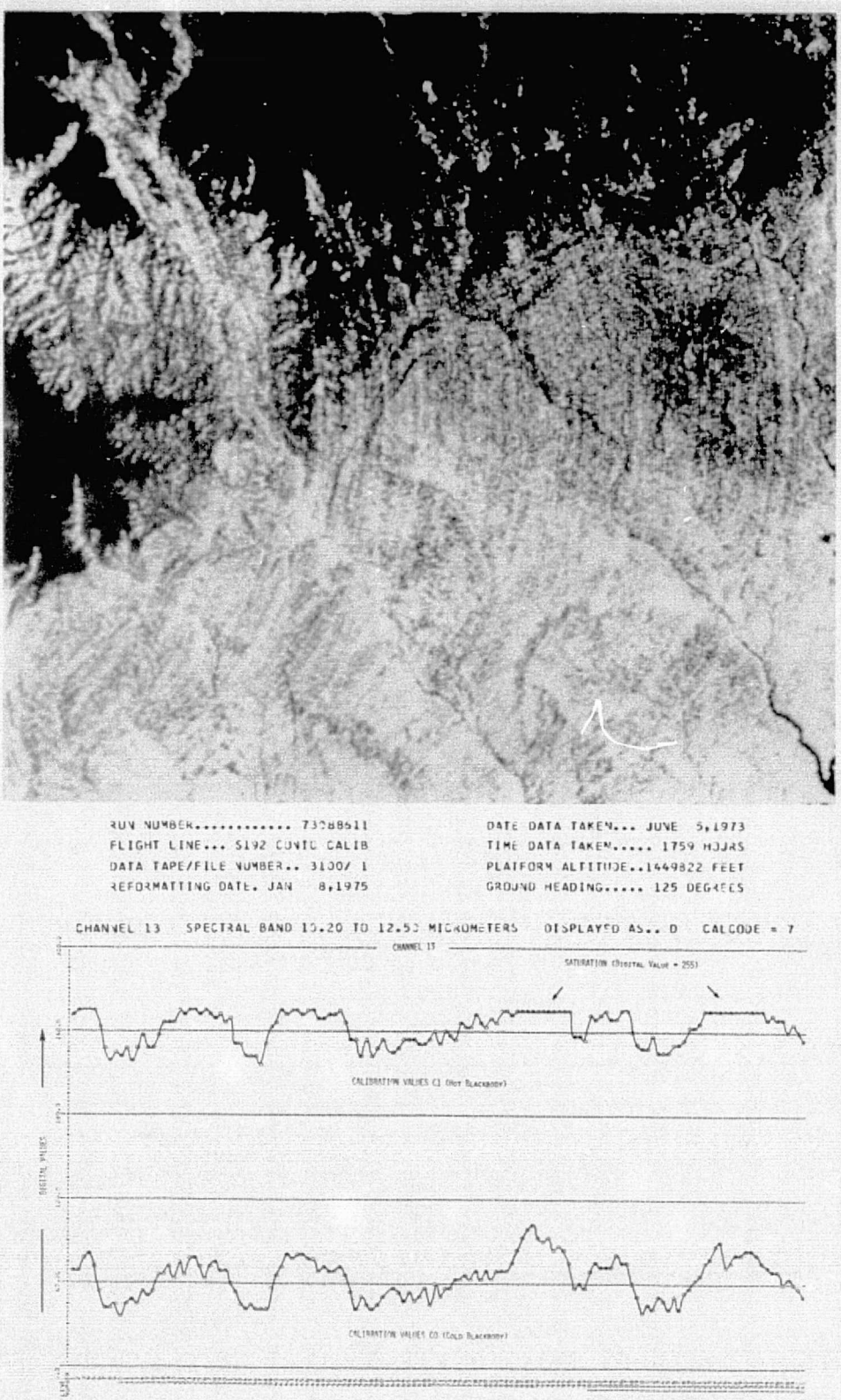

Figure 2.17 -- SKYLAB-2 S-192 multispectral scanner data - Band 13

In summary, the qualitative data evaluation strongly suggests that the best bands are 11 (1.55-1.75 μm), 3 (0.52-0.56 μm), 7 (0.78-0.88 μm), 9 (1.09-1.19 μm), and 8 (0.98-1.08 μm). The worst seem to be bands 1 (0.41-0.46 μm), 4 (0.56-0.61 μm), 2 (0.46-0.51 μm), 13 (10.2-12.5 μm), and to a lesser extent bands 5 (0.62-0.67 μm) and 6 (0.68-0.76 μm). The lack of contrast between different features on the ground in band 1 is, as expected, due to the strong atmospheric scattering effect in the violet portion of the spectrum and consequent detector saturation. Table 2.3 summarizes the results of the qualitative data evaluation, showing the ranking of bands from best to worst.

Table 2.3 SKYLAB-2 S-192 data quality evaluation, qualitative approach

Data Quality	Rank	Band Number	Spectral Range (μm)
Very Good	1	11	1.55-1.75
	2	3	0.52-0.56
	3	7	0.78-0.88
	4	9	1.09-1.19
	5	8	0.98-1.08
Good	6	10	1.20-1.30
	7	12	2.10-2.35
Fair	8	6	0.68-0.76
	9	5	0.62-0.67
Poor	10	13	10.2-12.5
	11	2	0.46-0.51
	12	4	0.56-0.61
Very Poor	13	1	0.41-0.46

2.3.3 Quantitative Evaluation

2.3.3.1 Natural Cover-Type Approach

The next phase of the data quality evaluation involved a quantitative technique utilizing data in the scene having a uniform reflectance. In this case, two homogeneous cover types present in the scene were studied. One was a portion of Vallecito Reservoir (near the dam to avoid spectral variations in the water due to specular reflection or differences in turbidity levels) and a uniform forested area southeast of the reservoir. The mean relative response (from 0 to 255 counts) and the standard deviation of the two selected cover types were computed for each of the 13 S-192 MSS bands (Table 2.4).

To obtain a measure of the noise level in each individual wavelength band, two different measures were used as suggested by Biehl and Silva (1975). These required computation of (1) the standard deviation and (2) the coefficient of variation (the ratio of the standard deviation divided by the mean). Table 2.4 shows the resulting statistics for both cover types.

Table 2.4 Mean Standard Deviations, and Coefficient of Variations for 286 Samples of Water and Forest

Channel Numbers	Mean		Standard Deviation		Coefficient of Variation ($\times 10^{-2}$)	
	Water	Forest	Water	Forest	Water	Forest
1	214.4	205.1	15.1	18.5	7.0	11.0
2	136.6	110.1	6.6	5.3	4.8	4.8
3	69.4	56.6	3.8	2.5	5.5	4.3
4	200.4	131.3	31.8	19.6	15.8	15.0
5	103.7	72.8	13.9	13.4	13.4	18.4
6	65.4	89.5	5.7	6.0	8.7	6.7
7	72.7	113.5	3.6	7.2	4.9	6.3
8	51.1	102.5	4.4	6.8	8.6	6.7
9	48.2	92.3	3.7	5.5	7.8	6.0
10	42.2	83.6	5.2	15.6	12.1	18.7
11	58.9	72.0	1.9	3.0	3.2	4.1
12	15.5	21.6	2.3	2.7	15.0	12.6
13	117.3	124.3	5.1	8.0	4.3	6.5

Note in Table 2.4 that the lowest coefficient of variation for both cover types is found in band 11. The variation in the data, however, is due to both the noise inherent in the scanner system, and to actual variations in the spectral response of the water and forest cover. Table 2.5 shows the ranking of the 13 bands of SL-2 S-192 data from best (lowest standard deviation) to worst (highest standard deviation) for both the water and forest cover-type measures. One sees that there are many differences in this ranking sequence between the two cover types. Therefore, it was decided to examine a different technique for a better quantitative data quality evaluation.

Table 2.5 Ranking of SKYLAB-2 S-192 bands as a function of data quality (magnitude of standard deviation for water and forest).

	Water		Forest	
Rank	Channel Number	Standard Deviation	Channel Number	Standard Deviation
1	11	1.9	3	2.5
2	12	2.3	12	2.7
3	7	3.6	11	3.0
4	9	3.7	2	5.3
5	3	3.8	9	5.5
6	8	4.4	6	6.0
7	13	5.1	8	6.8
8	10	5.2	7	7.2
9	6	5.7	13	8.0
10	2	6.6	5	13.4
11	5	13.9	10	15.6
12	1	15.1	1	18.5
13	4	31.8	4	19.6

2.3.3.2 Calibration Signal Approach

Ideally, in order to accurately assess the quality of the data, one would need a large and perfectly homogeneous cover on the ground, whereby the variation in response from one resolution element to another would be solely due to variations (noise) of the system. This type of an area was not found in the set of data available over the Granite Peaks Test Site (Colorado), since even the surface across the reservoir showed variation in spectral response caused by specular reflection. Therefore, the only sources of constant radiance over the entire data set were (1) the low calibration reference (cold blackbody), (2) the high calibration lamp (1000 watt A117A lamp), and (3) the hot blackbody for the thermal channel. Therefore, this next phase in the quantitative evaluation of data quality utilized the calibration signals present on the data tape. The mean and standard deviation of the signals from the internal reference sources were calculated and the resulting statistics are shown in Table 2.6.

Table 2.6 Data quality measure - internal reference sources (1300 samples)

Channel Number	Source	Mean	Standard Deviation
1	High Calib. Lamp	36.76	7.13
2	"	32.91	1.99
3	"	39.19	1.79
4	"	244.65	14.76
5	"	246.18	11.99
6	"	247.78	3.74
7	"	251.43	1.23
8	"	245.96	5.33
9	"	250.42	0.24
10	"	246.11	5.99
11	"	248.98	0.60
12	"	239.41	2.47
13	Cold B.B.[1]	60.70	13.06
13	Hot B.S.[2]	241.88	10.57

[1]The cold blackbody was set at 260.4°K.

[2]The hot blackbody was set at 321.3°K.

Table 2.7 shows the ranking of the 13 SL-2 S-192 wavelength bands from lowest to highest standard deviation as calculated from the internal calibration signals. The means for the calibration signals closely agree with pre-launch tests conducted at Kennedy Space Center on 3/24/73. However, the standard deviations shown in Table 2.6 and 2.7 do not agree with the pre-launch tests.

Table 2.7 Ranking of SKYLAB 2 S-192 bands as a function of the standard deviation of the calibration signals.

Rank	Channel Number	Spectral Range (μm)	Standard Deviation	
1	9	1.09-1.19	0.24	
2	11	1.55-1.75	0.60	
3	7	0.78-0.88	1.23	
4	3	0.52-0.56	1.79	
5	2	0.46-0.51	1.99	
6	12	2.10-2.35	2.47	
7	6	0.63-0.76	3.74	
8	8	0.98-1.08	5.33	
9	10	1.20-1.30	5.99	
10	1	0.41-0.46	7.13	
11	5	0.62-0.67	11.99	
12	13	10.2-12.5	10.57	Hot B.B.
			13.06	Cold B.B.
13	4	0.56-0.61	14.76	

A series of graphs (see Figures 2.5 through 2.17) shows the structured noise of the calibration signals for the first 141 scan lines of data in all 13 bands. An observation of the spectral response of the calibration sources shown in Figures 2.5 through 2.17 can give a good qualitative indication of the noise present in the data set, its approximate frequency and magnitude. For example, comparing the calibration signals for bands 3 and 4 (Figures 2.7 and 2.8); indicates that band 4 is definitely more noisy than band 3. The most obvious and relatively strong structured noise can be observed in band 13 (Figure 2.17) for which both blackbody calibration signals (CØ=cold B.B., and CL=hot B.B.) are shown. Such observations are confirmed by the standard deviation values shown in Tables 2.6 and 2.7. One also could note that the ranking of channels shown in Table 2.7 is different in many respects from the rankings shown in Table 2.5. To further our

understanding of the noise characteristics of the data we therefore carried out a Fourier analysis of the data in each wavelength band.

2.3.3.3 Fourier Analysis

In order to analytically determine the frequencies and relative intensity of the various noise components present in the data set, an autocorrelation of the signals was performed and a power spectrum was obtained. An example of these results is shown in Figures 2.18 and 2.19 which show the autocorrelation function and its Fourier transform (power spectral density) for band 13. A discrete Fourier transform (FFT) was utilized for this task (Kettig, 1975). As these figures show there are several strong cyclic components present in the data. This accounts for the banding effects seen for the thermal data in Figure 2.17. Several other wavelength bands showed similar results.

The autocorrelation and power spectrum results are summarized for all wavelength bands in Table 2.8. In essence, most of the reflective bands (1-12) show a strong noise component at a very low frequency (long term drift), i.e., one cycle every 412 lines. Furthermore, all of these 12 bands have a weak noise high frequency component at a high frequency of approximately 47 Hertz (one variation every scan line). A relatively strong noise component at 15 Hertz (6.3 lines per cycle) was found in bands 4, 8 and 12. This 15 Hertz noise was also found in most of the other reflective bands but is weaker in magnitude. In the thermal band both of the calibration signals (CØ=cold B.B. and C1=hot B.B.) showed a large-magnitude low frequency structured noise component at 1.99 Hertz,

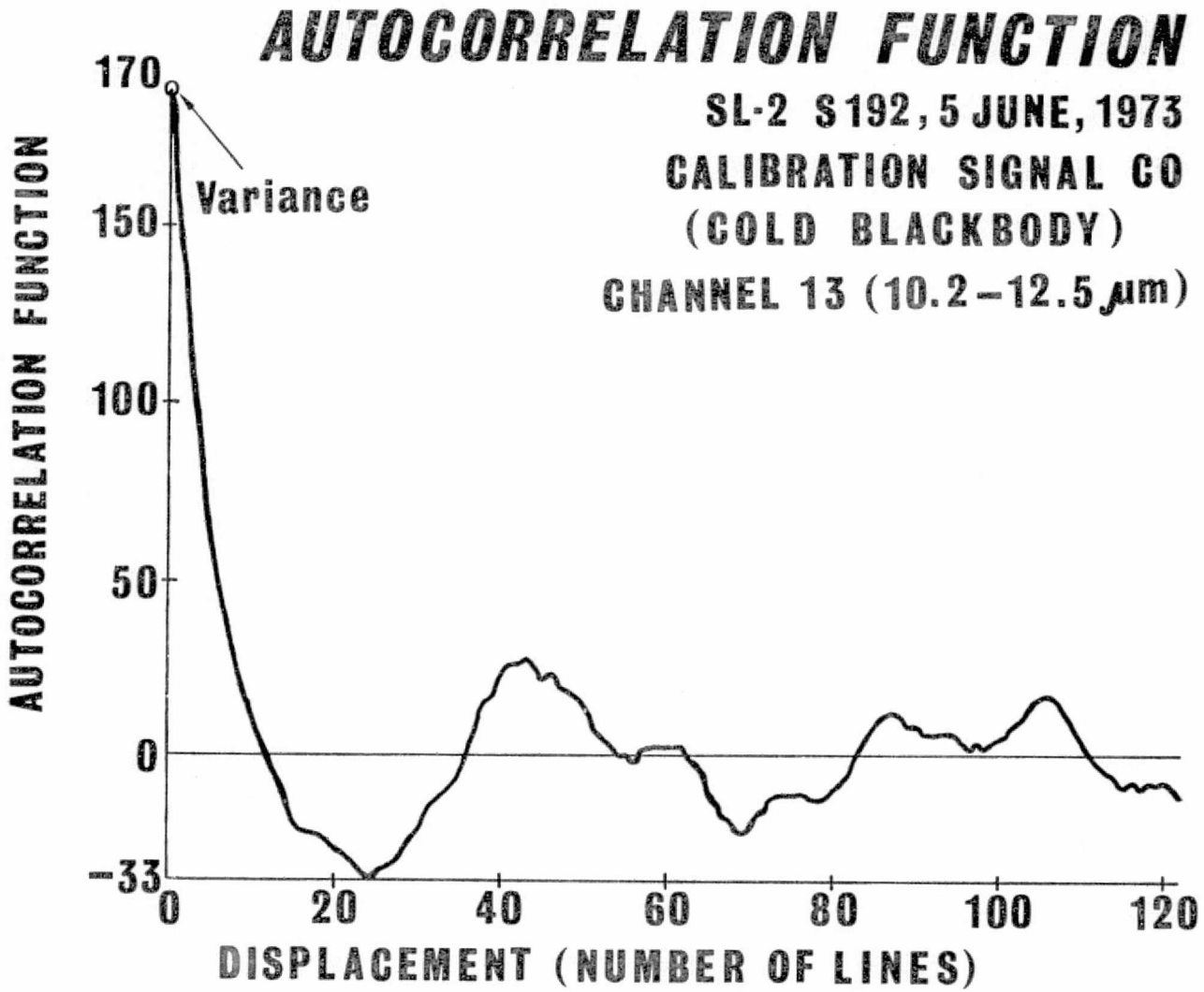

Figure 2.18 -- Autocorrelation function SL-2 S-192, June 5, 1973

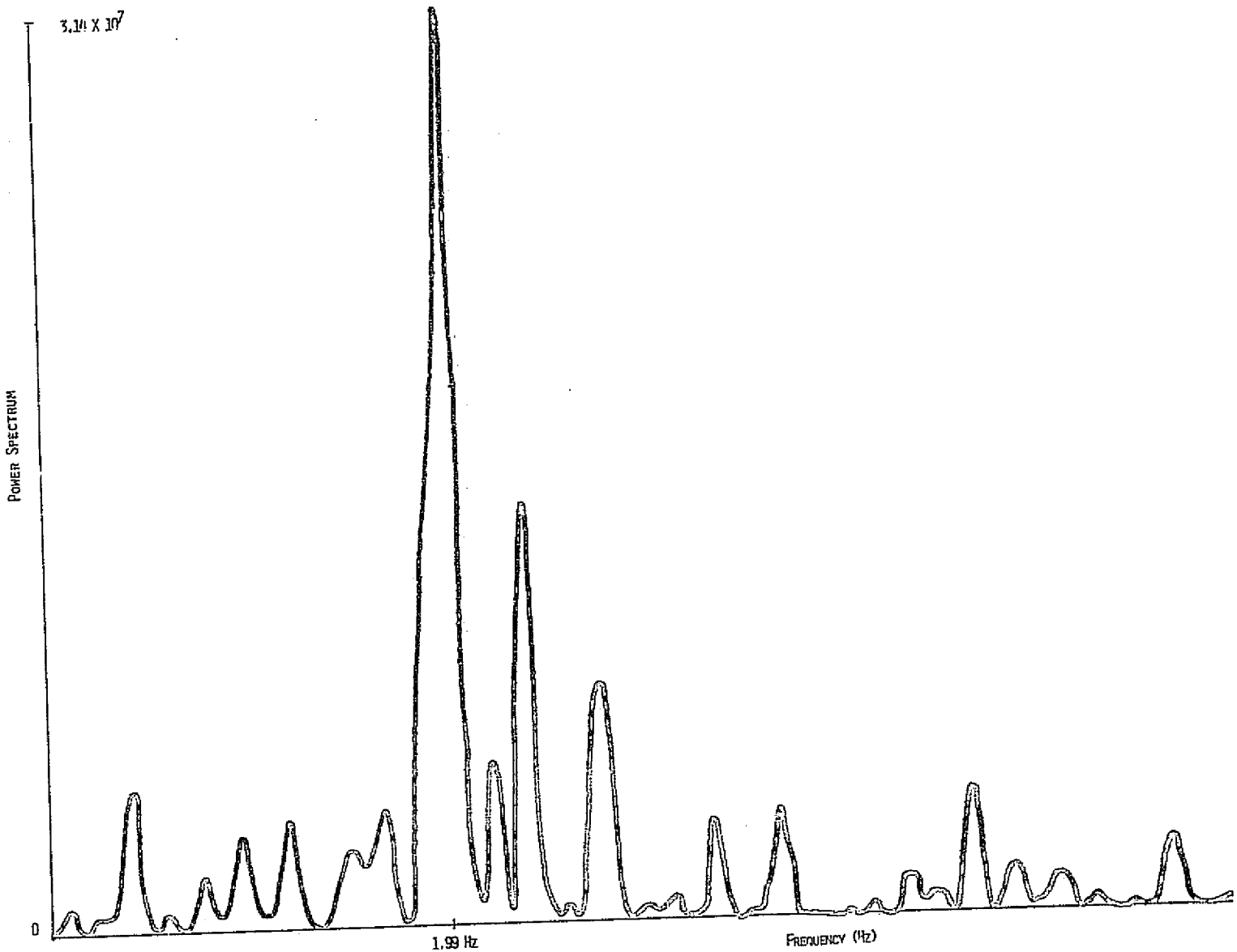

Figure 2.19 -- Fourier transform of the autocorrelation function shown above in Figure 2.18

Table 2.8 Autocorrelation and power spectrum for the SL-2 S-192 calibration signals

Band	Frequency (Hz)	P.S.D.[1] (relative units)	Lines/cycle	A.Z.S.[2]	$\sqrt{\text{A.Z.S.}(\sigma)}$
1	0.23	1.18×10^{8}	412	50.80	7.13
2	0.23	2.24×10^{4}	412	3.96	1.99
3	0.23	9.64×10^{3}	412	3.22	1.79
4	0.23 15	9.57×10^{8}	412 6.3	220.60	14.85
5	0.23	5.98×10^{8}	412	146.80	12.12
6	0.65 0.23	4.51×10^{5}	145 412	16.68	4.08
7	0.23	4.38×10^{4}	412	5.02	2.24
8	15 0.23	3.48×10^{4}	6.3 412	31.21	5.59
9	0.23	1.03×10^{3}	412	3.09	1.76
10	0.23	5.55×10^{4}	412	38.58	6.21
11	0.49	1.70×10^{3}	194	2.53	1.59
12	15	9.15×10^{3}	6.3	8.61	2.93
13 CØ	1.9	3.14×10^{7}	49.8	170	13.04
13 C1	1.9	1.95×10^{7}	49.8	114	10.67

[1] P.S.D. = power spectrum density

[2] A.Z.S. = autocorrelation for zero shift

or every 49 lines of data. In addition there was a weak, higher frequency component in band 13 at approximately 47 Hertz. Table 2.8 also shows that the square root of the autocorrelation values for zero shift are in agreement with the standard deviations computed in the previous section (Table 2.6), as would be expected. Table 2.9 shows the ranking of the 13 bands as a function of the square root of the autocorrelation function for zero displacement, i.e., the standard deviation of the calibration signals.

After evaluating the results shown in Table 2.8, it was concluded that the values of autocorrelation for zero displacement provided the best indication of the data quality based upon a quantitative evaluation approach. The smaller the autocorrelation values for zero displacement, the better the data quality. These results again show that channels 11, 9 and 3 contain relatively good quality data, and channel 4 again has the poorest quality data.

Table 2.9 Ranking of SKYLAB-2 S-192 bands as a function of the square root of the autocorrelation function for zero displacement

Rank	Band Number	Spectral Range (μm)	$\sqrt{A.Z.D.}$
1	11	1.55-1.75	1.59
2	9	1.09-1.19	1.76
3	3	0.52-0.56	1.79
4	2	0.46-0.51	1.99
5	7	0.78-0.88	2.24
6	12	2.10-2.35	2.93
7	6	0.68-0.76	4.08
8	8	0.98-1.08	5.59
9	10	1.20-1.30	6.21
10	1	0.41-0.46	7.13
11	5	0.62-0.67	12.12
12	13	10.2-12.5	13.04
13	4	0.56-0.61	14.85

2.3.4 Summary

Throughout the data quality evaluation study we found that certain wavelength bands tend to be evaluated as of very good quality, no matter which technique was utilized. Other wavelength bands were consistently poor. However, there was a considerable variation in the ranking sequence shown for the qualitative and the various quantitative data quality evaluations. Table 2.10 summarizes the results using a ranking of the various wavelength bands for all of the evaluation approaches attempted in this phase of the study. This table clearly shows a number of significant differences in the data quality evaluation between the qualitative and the quantitative techniques utilized. It is significant to note that the qualitative pictorial evaluation suggests that Channel 1 is the worst band (rated very poor), and the quantitative evaluation indicated that it is only fair data quality. However, in the subsequent analysis of this data we found many cases in which the feature selection processor selected Channel 1 as one of the desirable wavelength bands to be used for a multispectral classification of different earth cover types when a subset of 6 or more channels were requested. This indicated that there is valuable spectral information within this channel, in spite of the apparent poor data quality.

To provide a better comparison between a qualitative and quantitative evaluation results, Table 2.11 summarizes these results utilizing descriptive terminology as a basis for comparison. A qualitative evaluation designations were shown previously in Table 2.3. The quantitative indication of data quality are the square

Table 2.10 Ranking of SKYLAB-2 S-192 bands from best to worst for five data quality evaluation approaches

Rank	Qualitative	Water (S.D.)[1]	Forest (S.D.)	Calibration Signal (S.D.)[2]	Fourier Analysis ($\sqrt{A.Z.D.}$)
1	11	11	3	9	11
2	3	12	12	11	9
3	7	7	11	3	3
4	8	9	2	2	2
5	9	3	9	7	7
6	10	8	6	12	12
7	12	13	8	6	6
8	6	10	7	8	8
9	5	6	13	10	10
10	13	2	5	1	1
11	2	5	10	5	5
12	4	1	1	13	13
13	1	4	4	4	4

[1] S.D. = Standard Deviation

[2] Calculated from the autocorrelation function for zero displacement

Table 2.11 Data Quality Evaluation Results

Wavelength Region	Channel No.	Wavelength Band (μm)	Qualitative Evaluation Designation	Quantitative Data Quality Index	Quantitative Evaluation Designation
Visible	1	0.41-0.46	Very Poor	7.1	Fair
	2	0.46-0.51	Poor	2.0	Good
	3	0.52-0.56	Very Good	1.8	Very Good
	4	0.56-0.61	Poor	14.8	Poor
	5	0.62-0.67	Fair	12.1	Poor
Near IR	6	0.68-0.76	Fair	4.1	Fair
	7	0.78-0.88	Very Good	2.2	Good
	8	0.98-1.08	Very Good	5.6	Fair
	9	1.09-1.19	Very Good	1.8	Very Good
	10	1.20-1.30	Good	6.2	Fair
Middle IR	11	1.55-1.75	Very Good	1.6	Very Good
	12	2.10-2.35	Good	2.9	Good
Thermal IR	13	10.2-12.5	Poor	13.1	Poor

root of the autocorrelation for zero displacement values as given in Table 2.9. Because it is believed that these values provide the best quantitative indication of data quality, they will be used throughout the remainder of this report for that purpose and will be referred to as data quality index values. Quantitative evaluation designations are also shown in Table 2.11 as a method of comparing the qualitative and quantitative results. As can be seen, there are a number of places where the 2 techniques agree closely. However, there are also places where one sees that a qualitative assessment does not necessarily indicate the value of the data for computer-aided analysis. For example, Channel 1 was qualitatively very poor which seems reasonable in considering Figure 2.5. However, the quantitative assessment indicates that this wavelength band is at least of fair quality and as just indicated, this wavelength band was frequently selected for the multispectral calssification process. Channel 8 was qualitatively rated as very good but the quantitative evaluation was only fair. Thus, both channels 1 and 8 were of only fair quality from a quantitative standpoint, yet were distinctly different from a qualitative standpoint. It is therefore very clear that one cannot rely upon qualitative evaluations of data quality as being a good indication of the spectral information content when working with computer-aided analysis techniques. Quantitative data evaluations must be conducted. Our conclusion from this study is that the square root of the autocorrelation for zero displacement provides the best technique for quantitatively evaluating data quality and obtaining a data quality index.

2.4 TOPOGRAPHIC DATA OVERLAY

2.4.1 Introduction

The objective of this phase of the SKYLAB research was to develop a prototype system for relating topographic information to the S-192 multispectral scanner data. In particular, an elevation, slope and aspect channel was needed for each pixel of the MSS data. Such topographic data channels would enable machine analysis of spectral/topographic data to develop a better understanding of the impact of topographic effects on spectral response. Studies with LANDSAT-1 data had indicated that a combination of spectral/topographic data should allow more accurate forest cover type mapping than has been possible using only the spectral data.

A data set has been developed in which digitized topographic data has been overlayed onto SKYLAB S-192 and LANDSAT data for the San Juan Mountain area in Colorado. Software was developed and applied to the elevation data to produce additional slope and aspect data channels. Thus, the work has produced large-dimension, digital overlays in which two dates of multispectral scanner data, each including thirteen SKYLAB channels and four LANDSAT channels are registered with topographic data. These large coincident data sets are a first in the machine processing field at LARS. They have the potential of increasing classification accuracy of natural cover types and increasing the analysis productivity of remotely sensed data, in general. This section describes the details of the registration and topographic data processing which was carried out.

2.4.2 Data Set Description

Due to the extensive coverage and early availability of LANDSAT-1 data for the Colorado test area, this type of data was chosen as the reference data set for all the other data used in the project. LANDSAT Frame 1317-17204 obtained on June 5, 1973 formed the four reference channels and the topographic data was registered to this data. The SL-2 S-192 data set from June 5, 1973 was then overlayed on the LANDSAT data. This brought the three data types into registration. The SL-3 S-192 data from August 8, 1973 was later overlayed on the LANDSAT reference bringing it into registration with all the previous data. Finally LANDSAT data from frame 1407-17193 obtained on September 3, 1973 was overlayed on the reference for comparison with the August SL-3 S-192 data and June LANDSAT data.

The major problem in handling the various data sets was the great disparity in angular orientation of the frames and the lack of coincident data over large areas. Only a relatively small part of the test site near Durango contains data for all SKYLAB, LANDSAT and topographic channels. Figure 2.20 describes the orientation and extent of the data sets involved.

The topographic data is oriented north and covers the west half of the Durango 1:250,000 scale U.S.G.S. map quadrangle. The June 5, 1973 LANDSAT data covers a 185 kilometer square block encompassing the Durango west quadrangle. The June 5 SL-2 S-192 data set is rotated approximately 45^{o} west with respect to north, is approximately 83 kilometers square, and is centered around Durango. The September LANDSAT data coincides closely with the

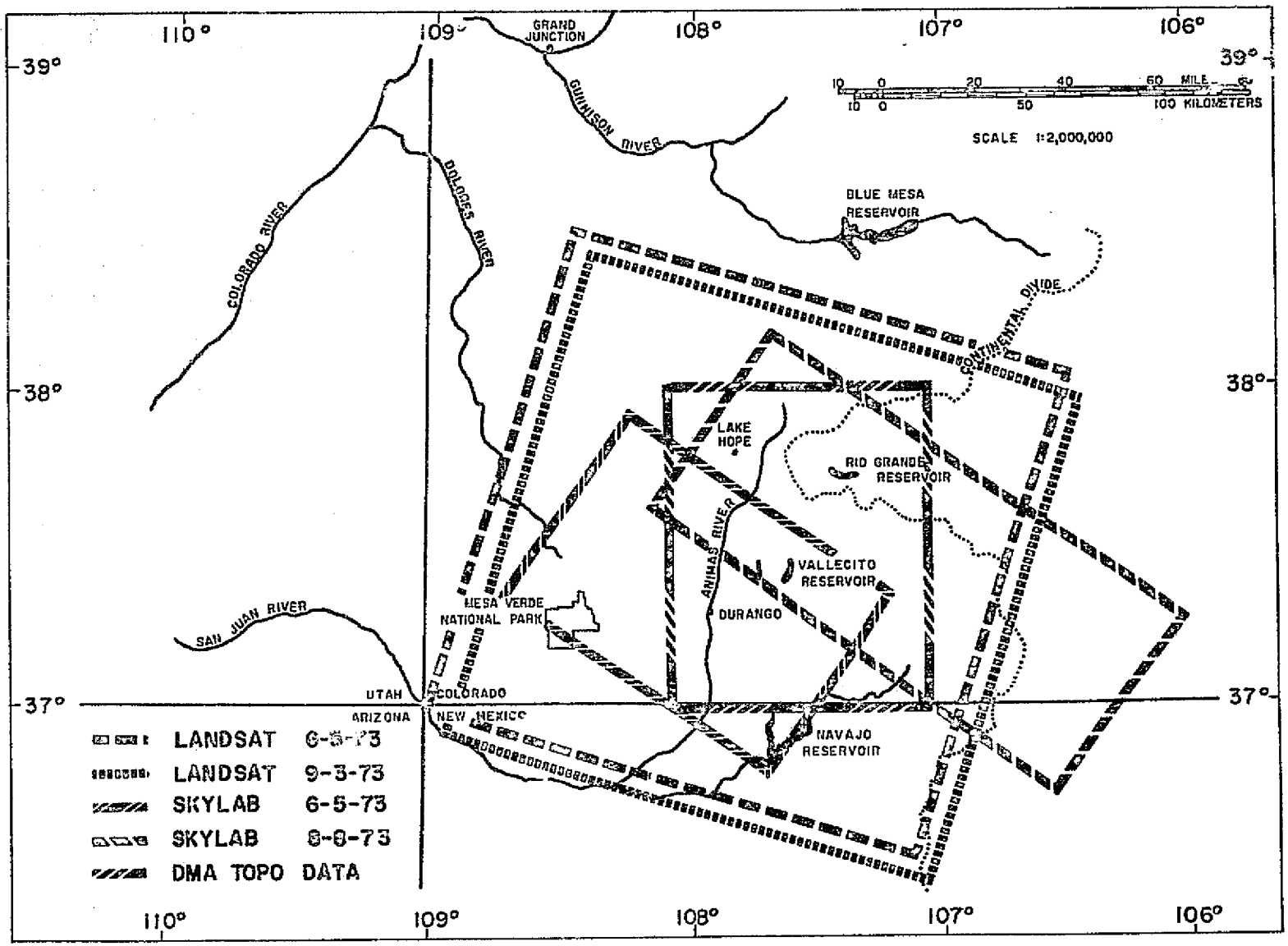

Figure 2.20 -- Data utilized in SKYLAB, LANDSAT, and topographic overlay

June 5 LANDSAT frame. The original LANDSAT data is rotated approximately 12^{o} east with respect to north. The SKYLAB SL-3 S-192 data from August 8, 1973 covers a 148 by 83 kilometer area centered on the San Juan Mountains.

2.4.3 Topographic Data

Digital topographic data was obtained from the U.S. Defense Mapping Agency (DMA) - Topographic Center, Washington, D.C. This data was obtained from the contour lines of 1:250,000 scale U.S.G.S. maps. The contour interval for the sheet used in this study (NJ13-7W Durango, Colorado) was 61 meters (200 feet) and the range of elevation in the study area was from 1805 meters to 4344 meters. The contours were digitized by hand on a table digitizer by the DMA and the resulting data points were interpolated using a "planar" algorithm which fits a plane to a triangle of three data points to define new points within the triangle (Noma, 1974). In this manner, a uniform grid of elevations values was obtained from the unequally spaced contour samples. The digitizing increment is .254 mm in the x and y directions. On a 1:250,000 map this corresponds to 64 meters. The output grid cell was thus made 64 meters square to coincide with this sampling resolution.

The topographic data is written in 16 bit words (15 bits plus sign, or 2^{15}=32768 levels) on tape and delivered to users. At LARS, the data was reformatted and placed in LARSYS format which utilizes 8 bit words. The quantization level of the original data is:

$$\frac{(4344-1805)\ \text{meters}}{32{,}768\ \text{discrete levels}} = .08\ \text{meters}$$

In order to fit this range into 8 bits (0-255), the data had to be rescaled resulting in a quantization of:

$$\frac{(4344-1805)\ \text{meters}}{256} = 9.9\ \text{meters}.$$

Thus a significant quantization is introduced with respect to the contour interval of 61 meters. However, on a percentage basis with respect to the 2539 meter range of elevation in the test site, it is only 0.4% which is reasonable. The accuracy of the original elevation points is not known, but since they were interpolated from contours having an interval of 61 meters it can be assumed that the 0.4% error is no worse than that obtained in the process of digitizing the elevations from the original map.

Another problem encountered was the designation of rows and columns on the DMA topographic data tape. The rows of the topographic data were oriented north-south on the DMA tapes and the row direction in the LARSYS and most other remote sensing systems in east-west or across the track of flight lines. Thus a transposition of the topographic data array on the tape was required. The final LARSYS topographic tape contained one channel of eight bit values on a grid of 64 meters for the west half of the Durango quadrangle, which covers a rectangle of one degree of latitude and longitude. In order to retrieve the true elevation values from the eight bit words, the lower and upper limits of elevation (1805 m and 4344 m in this case) are stored in full precision format on the tape identification record and used to rescale the eight bit data to the original range. Thus, true elevations can be printed out by LARSYS but are subject to the 0.4% quantization error. This DMA/LARSYS topographic data formed one of the several inputs to the registration process.

2.4.4 Registration Processing

The first step in the registration processing sequence involved rotation of each of the remote sensor data sets to an approximate north orientation. For LANDSAT data, this was approximately 12° counterclockwise and for SKYLAB S-192 data this was approximately 45° clockwise. Thus, because of the differences in orbital tracks, a total angular difference between the SKYLAB and LANDSAT data sets of about 57° had to be corrected. Also, the topographic data had to be transposed as previously mentioned. The normal procedure for image to image registration at LARS is to use a numerical correlation procedure to find control points in the images to be registered. Manual techniques were required for these registrations due to the dissimilar nature of the data involved. The topographic data, in general, will not correlate with the LANDSAT data and, although the SKYLAB data is similar in type, it was difficult to find low noise channels corresponding to LANDSAT channels which would correlate. Therefore, nominally, twelve matching points in each data set to be registered were visually defined using the LARS Digital Display images and computer line printer generated images. The coordinates of these points were punched on cards and processed by a least squares, bi-quadratic polynominal approximation program (Anuta and Bauer, 1973) to define coefficients for use by the registration program.

The registration algorithm uses a nearest neighbor rule to define output points which are required between existing input data points. Since the topographic grid spacing is 64 meters square and the LANDSAT reference grid is 79 meters square, the registered topographic data will have position errors which range from zero

to 32 meters. This is an error characteristic of the method used. Similarly the S-192 data has a sample spacing of approximately 66 meters. Therefore a comparable nearest neighbor error will result for overlay of this data.

The June and August S-192 data were registered onto the June LANDSAT reference, as was the topographic data and September LANDSAT data. The number of control points used and the curve fit errors for the various registrations are listed in Table 2.12.

Table 2.12 Statistical Summary of Overlay Errors

Data Registered to June LANDSAT	No. Control Points	Root Mean Square Error In Columns (E-W)	Square Root Mean Error In Rows (N-S)
Topographic	6	.54	1.20
June S-192	12	.97	.85
August S-192	8	.74	.81
Sept. LANDSAT	51	.48	.39

Numerical correlation was used for the September LANDSAT overlay since the data types matched. Hence a large number of points were obtained with a lower resulting error. All other points were obtained manually and since very few points could be determined the fit error is larger. Several data sets were generated with different combinations of channels of them; however, since all the data was registered to a common reference the coordinate system is the same for each channel and no problem results from combining any channel of any data type.

2.4.5 Topographic Slope and Aspect Derivation

The data analysis process could make good use of slope and direction of slope information if it could be made available on a pixel basis as additional registered channels on the data tape. This requirement was met by numerically differentiating the topographic data to produce an estimate of the gradient vector at each pixel location. The magnitude of the vector is then used to derive slope angle and the direction is used as the aspect angle. The approximate gradient at line i and column j is computed as:

$$\nabla\vec{Z} \approx \vec{I}(z_{i-1,j} - z_{i+1,j}) + \vec{J}(z_{i,j-1} - z_{i,j+1}) \qquad (2.1)$$

where: $\nabla\vec{Z}$ is the gradient vector,

z_{ij} is the topographic elevation value at i,j,

i,j are line and column coordinates and

$\vec{I}$ and $\vec{J}$ are line and column unit vectors.

The slope angle is computed from the magnitude of gradient. The $|\nabla\vec{Z}|$ value is the vertical change in elevation over one unit of pixel distance. Thus the slope is:

$$s_{ij} = \frac{\tan^{-1}\sqrt{(z_{i-1,j} - z_{i+1,j})^2 + (z_{i,j-1} - z_{i,j+1})^2}}{\Delta d} \qquad (2.2)$$

where s_{ij} is the slope angle at point i,j with $0 \leq S \leq 90$ degree.

Δd is the pixel spacing.

The aspect angle is derived from the vector direction of the gradient:

$$\alpha = \tan^{-1}\frac{(z_{i-1,j} - z_{i+1,j})}{(z_{i,j-1} - z_{i,j+1})} \qquad (2.3)$$

where α is the direction of slope measured clockwise from north.

Since only positive values from 0-255 can be represented on LARSYS format tapes, the aspect angle is recorded on a range of zero to 180 in one channel and an additional channel is used which has only the values zero or one. If the slope is uphill to the east the zero-one channel will have a value of zero and if the slope is uphill to the west the zero-one channel will have a value of one. Thus a pixel having a slope upward toward the east will have an angle value of 90^{o} and a flag value of zero. The resolution of the slope and aspect angles is one degree.

The slope and aspect angle derivation was implemented in a program (SLOPE) which adds the three angle channels to a data tape as three additional channels assuming the last channel on the input tape was the topographic elevation channel. Gray scale images were generated for an area centered near the Vallecito Reservoir to illustrate the topographic channels.

Figure 2.21 is an image of LANDSAT data (band 7, 0.80-1.10μm) from June 5, 1973 which was used as the reference base. Figure 2.22 is LANDSAT frame 1407-17193, band 7, 0.80-1.10μm, from September 3, 1973. Figure 2.23 is SL-2 S-192 band 8 data 0.98-1.08μm from June 5, 1973 and Figure 2.24 is SL-3 S-192 band 8, 0.98-1.08μm from August 8, 1973. Data was not available for the upper right corner because of the ground track of SKYLAB and swath width of the S-192.

Figure 2.25 is a gray scale reproduction of the topographic elevations for the same area in Figure 2.21. Lower elevations are darker and higher elevations are lighter. The gray resolution of the image is very limited to about 10 levels and the image cannot relate the information available very well. There are

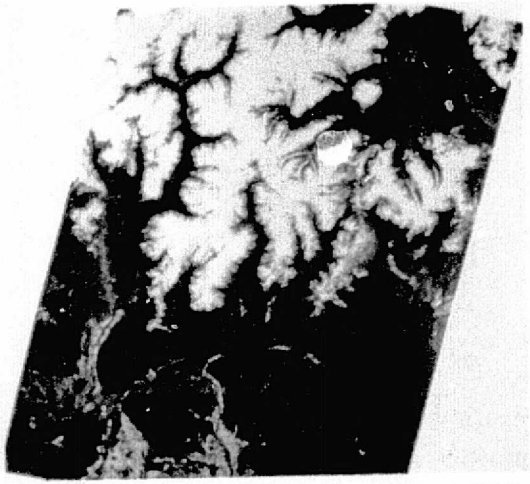

Figure 2.21 -- LANDSAT 1317- 17204
June 5, 1973

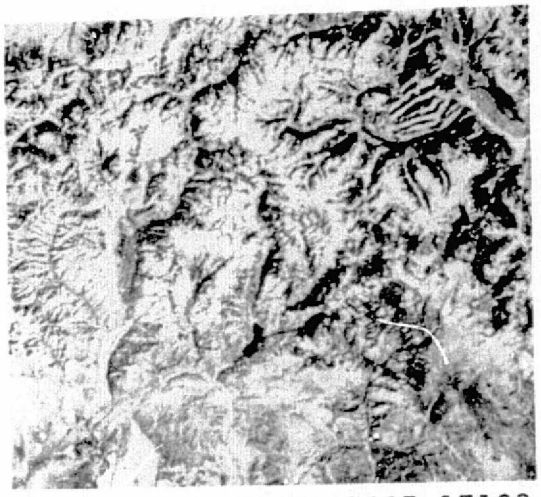

Figure 2.22 -- LANDSAT 1407-17193
September 3, 1973

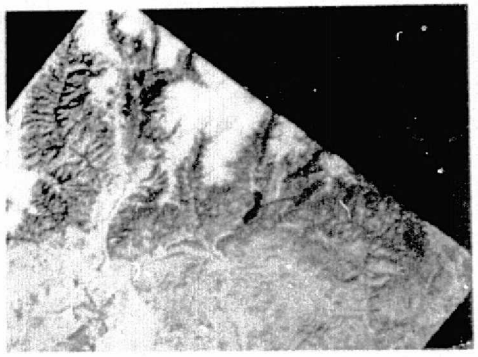

Figure 2.23 -- SKYLAB S-192
June 5, 1973

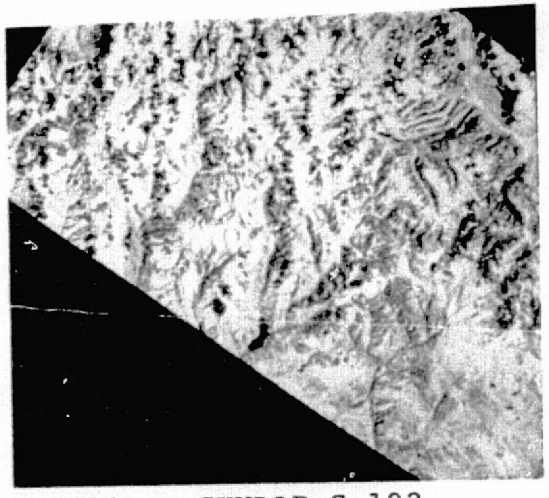

Figure 2.24 -- SKYLAB S-192
August 8, 1973

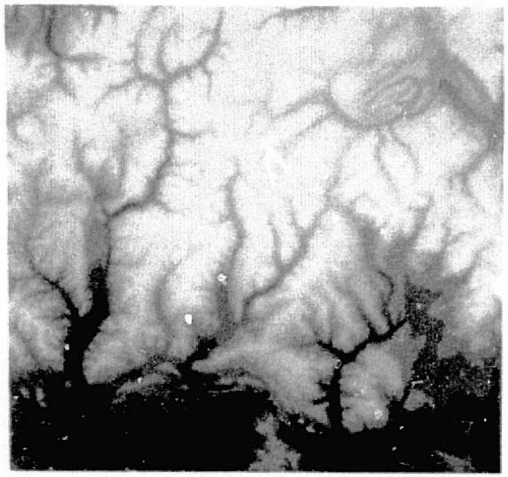

Figure 2.25 -- Gray scale reproduction of digital topographic elevations overlayed on LANDSAT reference

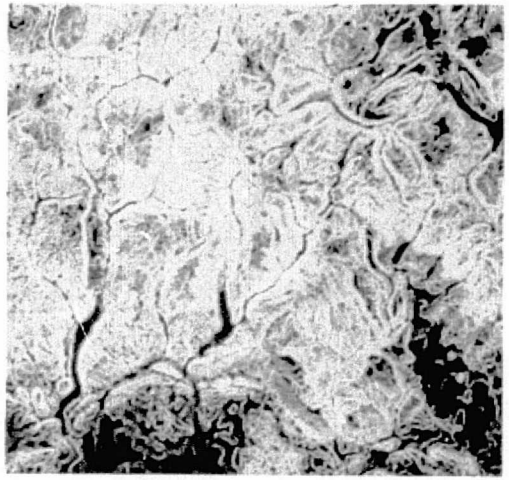

Figure 2.26 -- Gray scale reproduction of slope angle derived from topographic data

Figure 2.27 -- Gray scale reproduction of aspect angle derived from topographic data

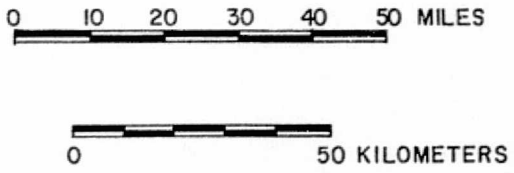

actually 256 discrete elevation levels available and these are compressed into the 10 gray levels seen in the image. Figure 2.26 contains a gray scale reproduction of the slope angle channel. Bright areas represent steep slopes and dark areas shallow slopes with black being flat areas. Figure 2.27 is a gray scale representation of the aspect angle for the same area. Darker areas represent southerly facing slopes and lighter areas represent northerly facing slopes. Black areas are level areas.

2.4.6 Summary

The level of effort involved in the topographic overlay activity was relatively modest and the work was therefore limited to the development of techniques for providing the topographic data in a digitally registered format on tape. The final results of this activity involved the development of the techniques, and also the production of a digital data tape containing 13 wavelength bands of S-192 SKYLAB data, 4 wavelength bands of LANDSAT MSS data and 3 channels containing topographic data (elevation, slope and aspect). These different data sets were all geometrically corrected and registered to a 1:24,000 scale data base. Table 2.13 summarizes this data set. Data tapes containing this multiple data set were developed for both the SL-2 and SL-3 SKYLAB missions using corresponding dates of LANDSAT data. Digital Display images in either a gray tone or color format and line printer outputs can be generated from the topographic channels, thereby allowing elevation, slope, or aspect to be indicated with different gray tones or colors on the digital display imagery or with different symbols on the line printer output. Utilization of the topographic data in combination with the SKYLAB multispectral scanner data for forestry and water resource applications are reported in Chapters 3 and 4 of this final report.

Table 2.13 Tape Format for Overlayed SKYLAB, LANDSAT, and Topographic Data for SL-2 or SL-3 Data Sets

Channel	Wavelength Band	Source
1	0.50- 0.60	LANDSAT
2	0.60- 0.70	LANDSAT
3	0.70- 0.80	LANDSAT
4	0.80- 1.10	LANDSAT
5	0.41- 0.46	SKYLAB
6	0.46- 0.51	SKYLAB
7	0.52- 0.56	SKYLAB
8	0.56- 0.61	SKYLAB
9	0.62- 0.67	SKYLAB
10	0.68- 0.76	SKYLAB
11	0.78- 0.88	SKYLAB
12	0.98- 1.03	SKYLAB
13	1.09- 1.19	SKYLAB
14	1.20- 1.30	SKYLAB
15	1.55- 1.75	SKYLAB
16	2.10- 2.35	SKYLAB
17	10.20-12.50	SKYLAB
18	Elevation, Feet or Meters	DMA
19	Slope, Degrees	DMA
20	Aspect, 0-360°	DMA

CHAPTER III -- ECOLOGICAL INVENTORY

by

Roger M. Hoffer and Michael D. Fleming

3.1 INTRODUCTION

3.1.1 Background

The San Juan Mountains and surrounding areas of southwestern Colorado are an important region from a forestry and land use standpoint. The region is dominated by areas of commercially important timber resources. Forests provide control over the water runoff and protect the soil in these upland mountain watersheds, as well as provide recreational opportunities. Increasing pressure for public use of the land for summer and permanent home developments in the area are causing a great deal of concern on the part of the U. S. Forest Service, Bureau of Reclamation, and other agencies who are charged with stewardship and proper management of these lands. High altitude tundra areas involve a particularly delicate ecological balance, and over-use by increasing numbers of people could produce disastrous effects on the ecology of such areas.

Conversations with personnel from the U. S. Forest Service, National Park Service, and other agencies have indicated a great deal of interest in the possibilities for obtaining reasonable accurate and up-to-date cover type maps derived from satellite data. The LANDSAT-1 investigation clearly showed that computer-aided analysis techniques and multispectral satellite data can be utilized to provide these agencies with useful maps and

tabular summaries. For example, major cover types (corresponding to USGS Circular 671, Level II land use categories) could be mapped with a reasonable degree of accuracy (85%) even in these areas of rugged mountainous terrain. However, the mapping of individual forest cover types could not be achieved with a satisfactory degree of reliability with the LANDSAT data. The unique spectral range of the SKYLAB S-192 multispectral scanner coupled with the knowledge and data processing capabilities developed during previous investigations offered an opportunity to further develop the capability to utilize computer-aided analysis techniques and multispectral scanner data obtained from satellite altitudes.

3.1.2 Objectives

The major objectives pursued under the Ecological Inventory section of this SKYLAB project are:

1. To determine the capability to utilize SKYLAB multispectral scanner data and computer-aided analysis techniques to identify and map major forest cover types in a mountainous test site, and to tabulate the areal extent of such cover types.
2. To determine the spectral regions and specific wavelength bands of greatest value in identifying and mapping various cover types, and to determine the significance of the spectral differences among major forest, alpine, and other cover types of ecological importance in order to better predict the spectral characteristics required on future satellite systems, and
3. To develop a prototype system for relating topographic information (in particular, the slope, aspect, and elevation) to the S-192 data. Analysis of this spectral/topographic data will enable a better understanding of the impact of topographic effects on spectral response and should allow more accurate forest cover type mapping than has been previously possible with multispectral scanner data.

As these objectives indicate, the major thrust of this study was placed upon the analysis of the S-192 data. As a

prelude to the scanner data analysis, a thorough evaluation of the S-190A data was pursued. The photographic data provided an opportunity to evaluate the capability for discriminating forest cover types from satellite altitudes and to compare this to the spectral discrimination achieved with the multispectral scanner data.

Several of these research objectives were defined as a result of previous work with LANDSAT-1 and aircraft data. Analysis of LANDSAT-1 data had indicated that four wavelength bands optimized the trade-off between classification performance and computer time. The use of the SKYLAB data offered an excellent opportunity to continue studying the interaction between the number of channels and the performance that could be achieved.

Aircraft data analysis had indicated the value of certain wavelengths, particularly the middle and thermal infrared portions of the spectrum for identifying various agricultural and land use cover types. The range of wavelengths available from the SKYLAB multispectral scanner offered an outstanding opportunity to evaluate the various wavelength bands for spectral differentiation among the various cover types. The SKYLAB S-192 data also provided an opportunity to evaluate the use of various wavelength bands and spectral regions for achieving an optimal classification performance for various cover types. Such results could have a significant impact in defining the optimal combination of wavelength bands on future satellite systems.

LANDSAT -1 data analysis had indicated an important interaction between spectral response measured by the LANDSAT-1

scanner and the topographic characteristics of the area. A statistically significant impact was determined to be caused by influences of elevation, slope, aspect, and stand density within each species. During this SKYLAB investigation we digitally overlayed topographic data onto the SKYLAB S-192 scanner data. This allowed us to carry out a preliminary study concerning the value of multiple source data sets and discover techniques for working with such data sets.

3.1.3 Vegetative Characteristics of Study Area

The primary study area utilized in the Ecological Inventory portion of this SKYLAB project was defined as the "Granite Peaks Study Area" (See Figure 3.1). This area is in the southern portion of the San Juan Mountains of southwestern Colorado. The area consists of six 7½' U.S.G.S. quadrangles totaling approximately 360 square miles of forest land. The Vallecito Reservoir, Ludwig Mountain, Granite Peaks, Baldy Mountain, Devil Mountain, and the Bear Mountain quadrangles are included in the area. However, part of the Bear Mountain quadrangle was not available on the S-192 data due to the orbital path of the SKYLAB station.

A brief, general description of the test site and its vegetative characteristics was included in Chapter 1. That description and Figure 1.2 in Chapter 1 showed the distinct distribution of forest cover types as a function of elevation. Figure 3.2 provides an indication of the impact of elevation and aspect on the various forest species in the San Juan Mountains. As this figure shows, the various forest species generally occur in defined elevation ranges. In some cases, only one or two species are dominant within a certain elevation zone. This figure also shows that for some species such as oak the range of occurance is about 400 meters higher in elevation on south facing slopes than north facing slopes.

Figure 3.3 shows the appearance and characteristics of the major forest cover types in this test site. The term

Figure 3.1 Granite Peaks test site as indicated on a S-190A color photo obtained on June 5, 1973

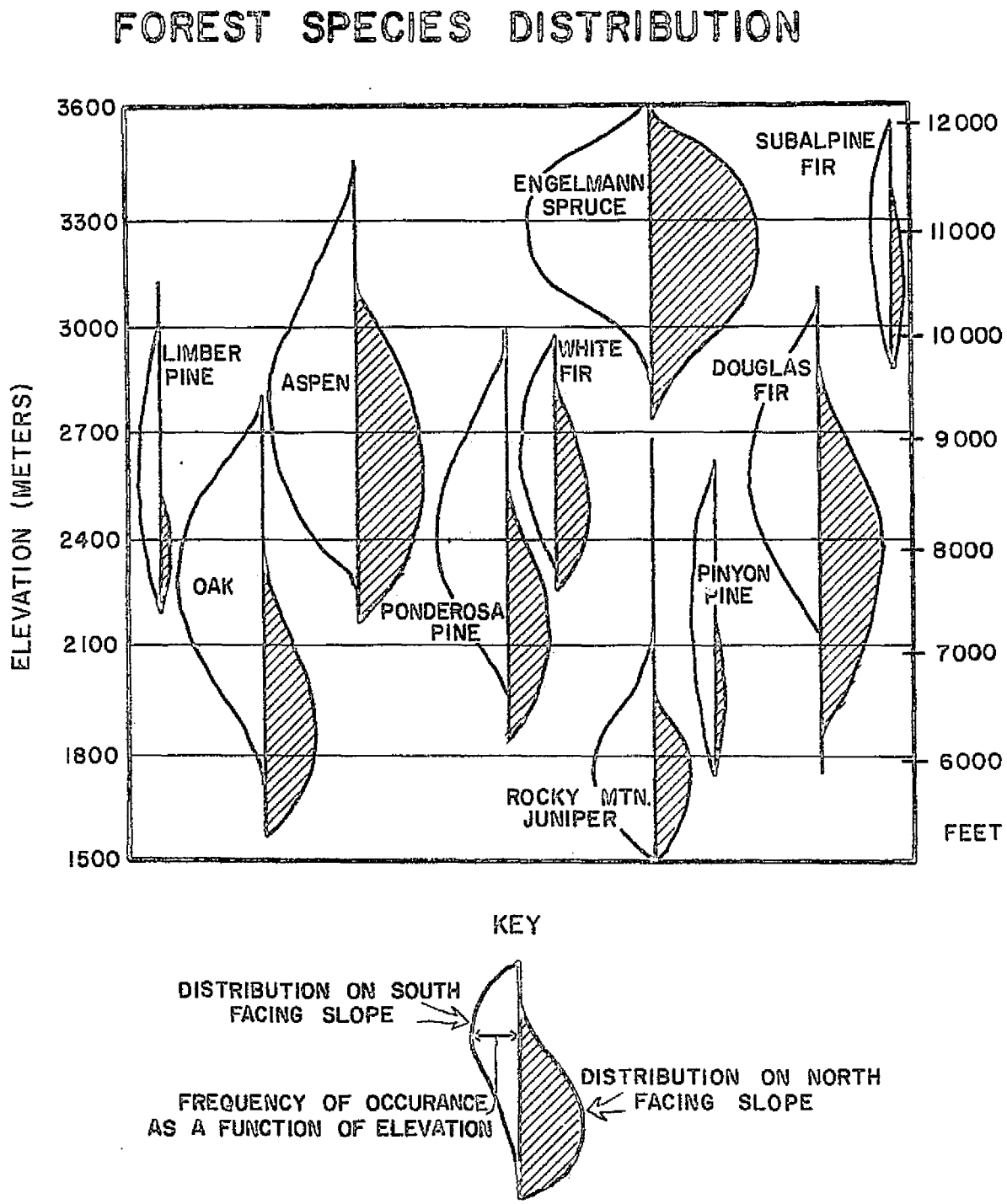

Figure 3.2 Forest species distribution as a function of elevation and aspect in the San Juan Mountains

Aspen

Oak

Pinyon Juniper

Ponderosa Pine

Spruce-Fir

Douglas Fir & White Fir

Figure 3.3 Appearance and characteristics of major forest cover types in the test site.

"forest cover type" is used frequently throughout this report and can be defined as follows: "A descriptive term used to group stands of similar character as regards composition and development due to given ecological factors, by which they may be differentiated from other groups of stands." The term suggests repitition of the same character under similar conditions (Society of American Foresters, 1967). Thus, a forest cover type consists of a mixture of one or more species that occur together. For example, Engelmann spruce and white fir are found in the same elevation range (Figure 3.2) and together, form an ecosystem; referred to in this report as the spruce-fir forest cover type.

A more detailed description of the various forest cover types and other vegetation zones involved in this study is as follows:

> Alpine tundra. The alpine area occurs above timber line, about 3650 meters in elevation. Because of the short frost-free growing season (frost may occur at anytime of the year) the vegetation is limited to short grasses and sedges, hardy forbs, alpine fir, subalpine willows, and other low shrubby plants. The principal plant species in this alpine zone include a number of species of sedges, alpine timothy, thurber fescue, arenaria, geraniums, bluebell, and a few species of alpine clovers.

Spruce-fir. The spruce-fir timber zone extends from about 2750 meters to timber line. The dominant tree species in this type include Engelmann spruce, alpine fir, white fir and cork bark fir. Other components of the type include aspen, limber pine, willow, alder, birches, and currents and gooseberries. Interspersed throughout this spruce-fir type are numerous subalpine and wet mountain meadows and grasslands. These meadows and grasslands characteristically are park-like openings between 2750 meters and timber line. The vegetation consists of lush growth of grasses and grasslike plants and forbs.

Ponderosa Pine and Douglas Fir. The ponderosa pine timber zone (or Montane Conifer Forest) extends from an elevation of about 1830 meters to 3000 meters with Douglas fir providing an important component of the timber zone between the elevations of 2400 meters and 3000 meters. Other woody components of this type include white fir, aspen, mountain maple, alder and Gambel oak. The grass and forb understory in the open and semi-open stands of ponderosa pine and associated species include Arizona fescue, mountain muhly, pine dropseed, and blue grama. The forbs include geranium, vetches, and clovers.

The lower part of the forest below about 2600 meters is warmer and drier and is primarily a forest of ponder-

osa pine, except on north-facing slopes. At midforest elevations, firs and ponderosa pine variously intermingle on all but north-facing slopes. Firs are dominant on north-facing slopes above 2290 meters, and at about 2600 meters they become increasingly more prevalent in the forbs on all slope exposures.

Pinyon Juniper. The pinyon-juniper type occurs at elevations above 1525 meters and generally occupies an area immediately below the ponderosa pine. The principal species in this type include on-seed juniper, Utah juniper, Rocky Mountain juniper, and pinyon pine, with an understory of Emory and Gambel oak, ceanothus, bitterbrush, and clift rose. Blue grama, galleta, sand dropseed and Arizona fescue make up the principal grass species.

Oak-Shrub Woodland. The oak-shrub woodland type extends from an elevation of about 1200 meters to 1600 meters. The principal species include Gambel oak, mountain mahogany, manzanita, ceanothus, cliff rose, Apache plume, and numerous species of cacti. Under normal conditions the oak-shrub type has a good stand of bluestem sideoats, black and blue grama, and sand dropseed.

3.2 INTERPRETATION OF SKYLAB PHOTOGRAPHY[1]

3.2.1 Introduction

Pressure of human growth and technological expansion on natural systems has been the subject of serious study in the last few years. Springing partly from this developing awareness, the SKYLAB experiments have produced data certain to be used by contemporary range managers, agriculturalists, foresters, ecologists, and land use planners as they examine present conditions to plan future actions. Even in the arid regions of the southwest, vegetation is an expression of the interrelationships of the physical and biological environment. With some training, man has learned to "read" the naturally occurring vegetation to determine the potential of a landscape for supporting his activities. Since the Apollo missions, space imagery has provided the type of small scale (<1:1,000,000) finely detailed photography and images of the earth's surface which make rapid vegetation mapping of broad categories and large areas a possibility.

This photointerpretation phase of the Ecological Inventory Study involved a series of mapping and evaluation sequences to determine the general value of small scale photography for vegetation mapping in areas of mountainous terrain, the comparative value of the different film/filter combinations available in the S-190A data, and the effect of seasonal variation on the accuracy of vegetative mapping.

---

[1] The work reported in Section 3.2 was carried out by personnel of the Institute of Artic and Alpine Research (INSTAAR), University of Colorado.

3.2.2 Initial Examination of S-190 Imagery

The available SL-2 and SL-3 frames of the test site were examined for resolution, contrast, and interpretability for varicus covertypes and feature selections. Using a light table, one could make an initial examination of the frames with the unaided eye or an 8x hand lens. For closer examination and for mapping purposes, a dissecting microscope with 15x eyepieces provided sufficient magnification. Although the SL-3 frames were too dense for viewing on the Bausch and Lomb Zoom Transfer Scope, the SL-2 imagery could be positioned on the transilluminator, enlarged and viewed in this manner. However, for direct comparisons of SL-2 and SL-3 imagery the use of a hand lens and microscope were preferred.

The resultant evaluations of imagery from both the S-190A and S-190B sensors proved to be beneficial and time saving in the manual image interpretations which followed. When discussing a cooperative involvement with representatives of numerous user agencies, the direct comparisons for particular feature selections emphasized the value of wavelength separability. Because the value of various individual wavelength bands is often not well understood by individuals who are not heavily involved in remote sensing technology, such examples showing the direct comparisons proved to be particularly valuable for effective communication with user agency personnel and also as an educational tool.

3.2.3 Interpretability of SKYLAB Photography

To define the wavelength bands of photographic data of most value to discriminate and map various earth surface features, a series of key features were identified. This set of features were used by a team of photo interpreters to summarize their impressions of the value of the various SKYLAB S-190 photographic products.

First, the interpreters indicated the overall contrast of all S-190A and S-190B photography and the color quality of the S-190A color, color infrared and S-190B color photography. Next, they indicated their ability to distinguish detail on the photography from each of the S-190A and S-190B stations. To provide an over-all synopsis of the utilization of the individual wavelength bands for various purposes, a group of earth surface features were defined and located on the imagery. Each interpreter then evaluated his or her ability to define and map the various features of interest. The results of this study are shown in Table 3.1 for the SL-2 photography and Table 3.2 for the SL-3 photography.

The ability to distinguish clear-cut areas on the August color infrared photography was encouraging from the standpoint of monitoring changes in cover type. However, only the larger avalanche tracks could be distinguished which was disappointing. The ability to define and monitor relatively small avalanche tracks would be of considerable value in many land-use monitoring and planning activities in these mountain regions. The tundra areas could not be evaluated due to snow cover during the SL-2 mission and cloud cover during the SL-3

Sensor & Wavelength Band	Color Quality	Overall Contrast	Ability to Distinguish Detail	← Ability to Separate →					← Ability to Discriminate →			
				Irrigated Fields from Arid Shrub and Grassland	Irrigated Fields from Forest	Deciduous Forest from Coniferous Forest	Land Form Classes	Land Use Classes	Avalanche Tracks	Clear-Cut Areas	Water Bodies	Snow Edge
S190A .5-.6μm	--	Good	Good, roads & streams visible	Good	Poor	Poor	Good	Fair	Large tracks visible	Visible due to more complete snow cover	Good	Excel.
S190A .6-.7μm	--	Excel.	Good, roads very clear	Excel.	Fair for sparse forest & poor for dense forest	Poor	Excel.	Good... in arid areas	Large tracks visible	Visible due to more complete snow cover	Fair	Excel.
S190A .7-.8μm	--	Generally fair;good on lakes & snow	Poor	Fair/good	Good/Excel. for sparse & dense forest	Poor	Fair/poor	Poor/fair	Largely indis-tinguish-able	Largely indis-tinguish-able	Excel.	Fair
S190A .8-.9μm	--	Generally good; Excel. on lakes & snow	Poor-very grainy -more like ERTS	Good/Excel.	Good/Excel.	Poor	Poor/fair	Fair	Largely indis-tinguish-able	Largely indis-tinguish-able	Excel.	Fair
S190A Color	Good	Good/ Excel.	Excel.	Good	Fair/good	Poor	Excel.	Good/Excel.	Large tracks visible	Visible	Good	Excel.
S190A CIR	Good	Excel.	Excel.	Excel.	Good/Excel.	Poor/fair	Excel.	Excel.	Large tracks visible	Visible	Excel.	Excel.
S190B Color	Good/ Excel.	Excel.	Excel. Many roads & some buildings appear to be visible on this larger scale	Excel.	Excel.	Some minor possible	Excel.	Excel.	Large & moderate size tracks visible	Very clear	Good/ Excel.	Excel.

1/ Tundra areas could not be evaluated because of snow cover

Table 3.1 Results of qualitative evaluation of SL-2 photography

Sensor & Wavelength Band	Color Quality	Overall Contrast	Ability to Distinguish Detail	Ability to Separate: Irrigated Fields from Arid Shrub and Grassland	Ability to Separate: Irrigated Fields from Forest	Ability to Separate: Deciduous Forest from Coniferous Forest	Ability to Separate: Land Form Classes	Ability to Separate: Land Use Classes	Ability to Discriminate: Avalanche Tracks	Ability to Discriminate: Clear-Cut Areas	Ability to Discriminate: Water Bodies	Ability to Discriminate: Snow Edge
S190A .5-.6um	--	Poor (appears under-exposed in some frames)	Excel.	Good/Excel. ...where exposure is adequate	Poor	Poor	Fair/good	Fair/good	Poor (exposure problem)	Poor (exposure problem)	Poor (exposure problem)	Some confusion due to similarity of cloud & snow
S190A .6-.7um	--	Good	Excel.	Fair/good	Poor	Poor	Good/ Excel.	Poor/ Good	Some large	Fair/Good	Fair/ Good	Excel.
S190A .7-.8um	--	Excel.	Fair/Good	Good	Good	Fair	Good/ Excel.	Good/ Excel.	Some large	Some visible	Excel.	Fair
S190A .8-.9um	--	Good	Good	Good/Excel.	Good/Excel.	Fair/good	Good/ Excel.	Good/ Excel.	Large	Some visible	Excel.	Poor
S190A Color	Fair in some places	Poor/ Good (appears under-exposed in some frames)	Excel.	Fair where exposure is adequate	Poor	Poor	Fair	Fair	Few due to poor exposure	Few due to poor exposure	Poor	Good but few recognizable land forms for easy location
S190A CIR	Fair/ Good	Fair/ Excel. (appears under-exposed in some frames)	Excel.	Excel.	Fair/Excel.	Fair	Good/ Excel.	Fair/ Excel.	Some large	Good/Excel.	Good/ Excel.	Good/Excel.
S190 B Color	Good	Good (appears under-exposed in some frames	Excel. some buildings & roads appear to be visible in this larger scale	Good/Excel.	Good	Poor	Good/ Excel.	Good/ Excel.	Large & moderate	Good visibility	Fair	Excel.

*Tundra areas could not be evaluated because of cloud cover

Table 3.2 Results of qualitative evaluation of SL-3 photography.

mission. Because of these snow and cloud conditions, the study of the ecologically sensitive tundra areas, which was one of the original objectives in this investigation, could not be pursued.

Tables 3.1 and 3.2 indicate that the general overall quality of the photographic data obtained during the SL-2 was somewhat better than that obtained during SL-3. However, in looking at Figures 3.4 and 3.5, which show the color infrared S-190A photos obtained during the SL-2 and SL-3 missions respectively, one sees that on June 5, 1973 (SL-2), the area is largely blue in tone instead of red. This indicates the lack of green vegetation and agrees with ground observations. The field team noted that the vegetation had not leafed out to any great extent at the time of the SL-2 mission. The color infrared photos obtained on August 8 have a different appearance to those obtained on June 5, due to the seasonal development of vegetation by the time of the SL-3 mission. This difference in vegetative condition was an important factor throughout many phases of this SKYLAB investigation. Thus, even though the overall quality of the SL-2 photos, primarily as indicated by exposure and contrast, were judged to be better than the SL-3 photos, seasonal effects dictated that the informational value of the data at the time of the SL-3 mission (August 8) was significantly greater, at least for vegetation mapping purposes. Because much of this Ecological Inventory phase of the investigation involved use of the multispectral scanner data to discrimin-

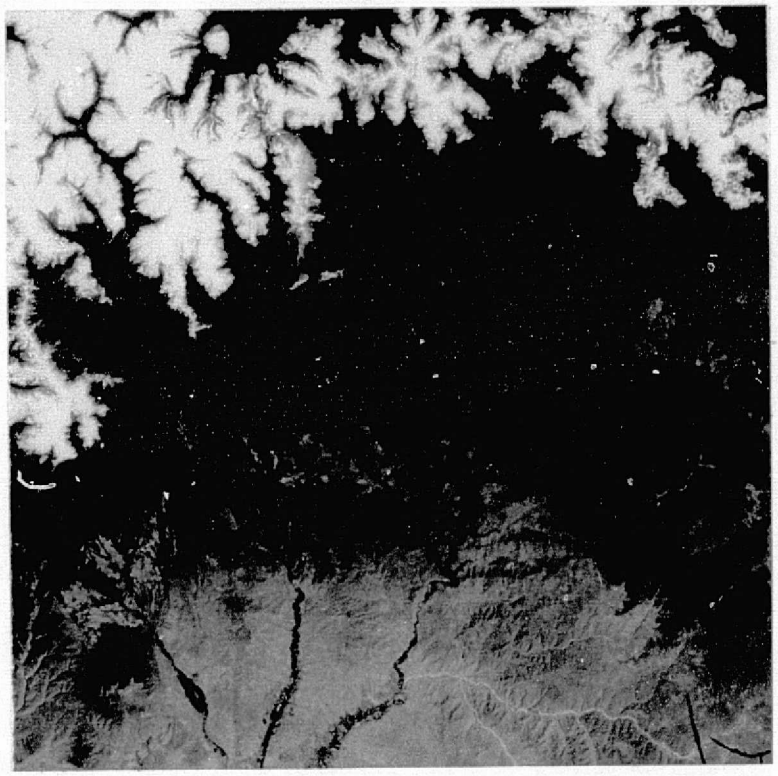

Figure 3.4 S-190A color infrared photo obtained during SL-2 on June 5, 1973

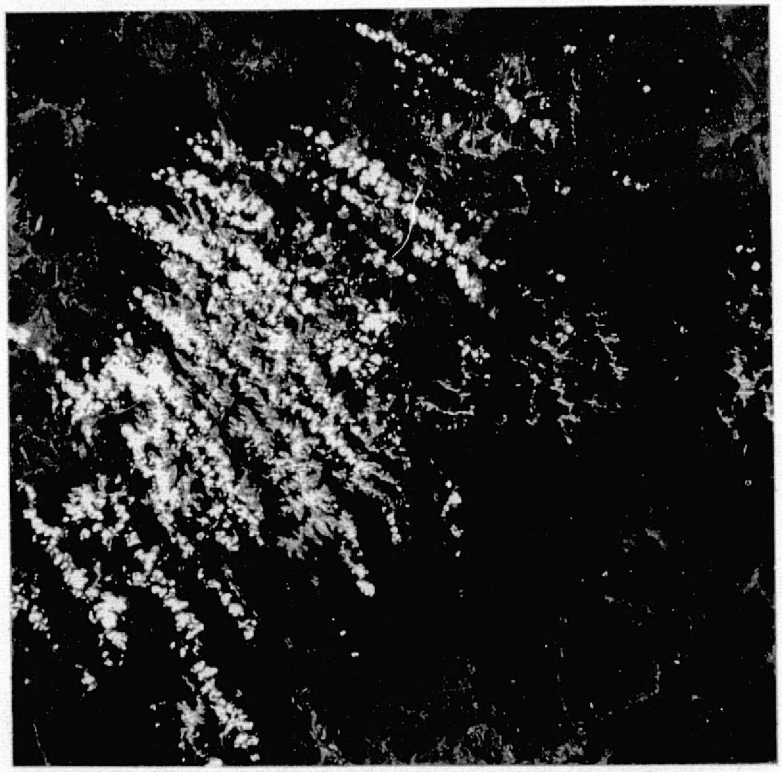

Figure 3.5 S-190A color infrared photo obtained during SL-3 on August 8, 1973

ate deciduous and coniferous forest cover and to map and identify various forest cover types, the difficulties experienced by the photo interpreters in effectively distinguishing between deciduous and coniferous forest cover on the SL-2 photos and to a lesser extent on the SL-3 photos, were important when evaluating the results of the computer-aided analysis.

In summary, the overall photographic quality for both the SL-2 and the SL-3 missions was generally good. However, many vegetative categories of interest could not be effectively mapped from the color IR obtained during SL-2 because of the immature stage of development of the vegetation. The utility of the SL-3 color infrared photos was much better because of advanced vegetative condition at this time of the year. None of the features evaluated could be seen better on black-and-white multi-band imagery than on the color or color infrared photos. Because of better exposure and scale, the S-190B color photos were generally more useful than the S-190A color photos. Also, many of the features which were difficult to distinguish on the color photos could be easily seen on the color infrared imagery and vice-versa. The results of this study of the photographic data proved valuable as a basis for evaluating some of the results obtained during the computer-aided analysis of the S-192 data.

3.2.4 Small Scale Mapping of Existing Vegetation

One of our earliest studies, involving the SKYLAB data, utilized the SKYLAB S-190A and S-190B photography from both SL-2 and SL-3 to produce a map of existing vegetation for portions of southern Colorado and northern New Mexico. This map was visually compared to other maps showing potential vegetation zones of the same area. This work allowed considerable insight to be obtained regarding the ability to generate useful vegetation maps using satellite photography, and to more clearly see the advantages of utilizing such synoptic small scale data (1:708,000).

A panchromatic 6" by 6" enlargement of the 70mm S-190B frame (ID 81-023, SL-2) was utilized as a mapping base. The natural vegetation zones, as they currently exist, were then mapped, utilizing the color and color infrared photos, and plotting all results on the panchromatic photo base (Figure 3.6). Two natural vegetation maps of the same area (Küchler, 1964: and U.S.D.A., 1972) were enlarged to the same scale (1:708,000) using the zoom transfer scope and were placed on mylar overlays for easy comparison with the results obtained from mapping the SKYLAB data. The Küchler and U.S.D.A. maps are shown in Figures 3.7 and 3.8 depicting the natural vegetation zones in this area.

There are two major sources of discrepancies between the U.S.D.A. map and the map by Küchler. One is the difference in mapping criteria. The U.S.D.A. mapped natural vegetation, while Küchler mapped potential natural vegetation. This,

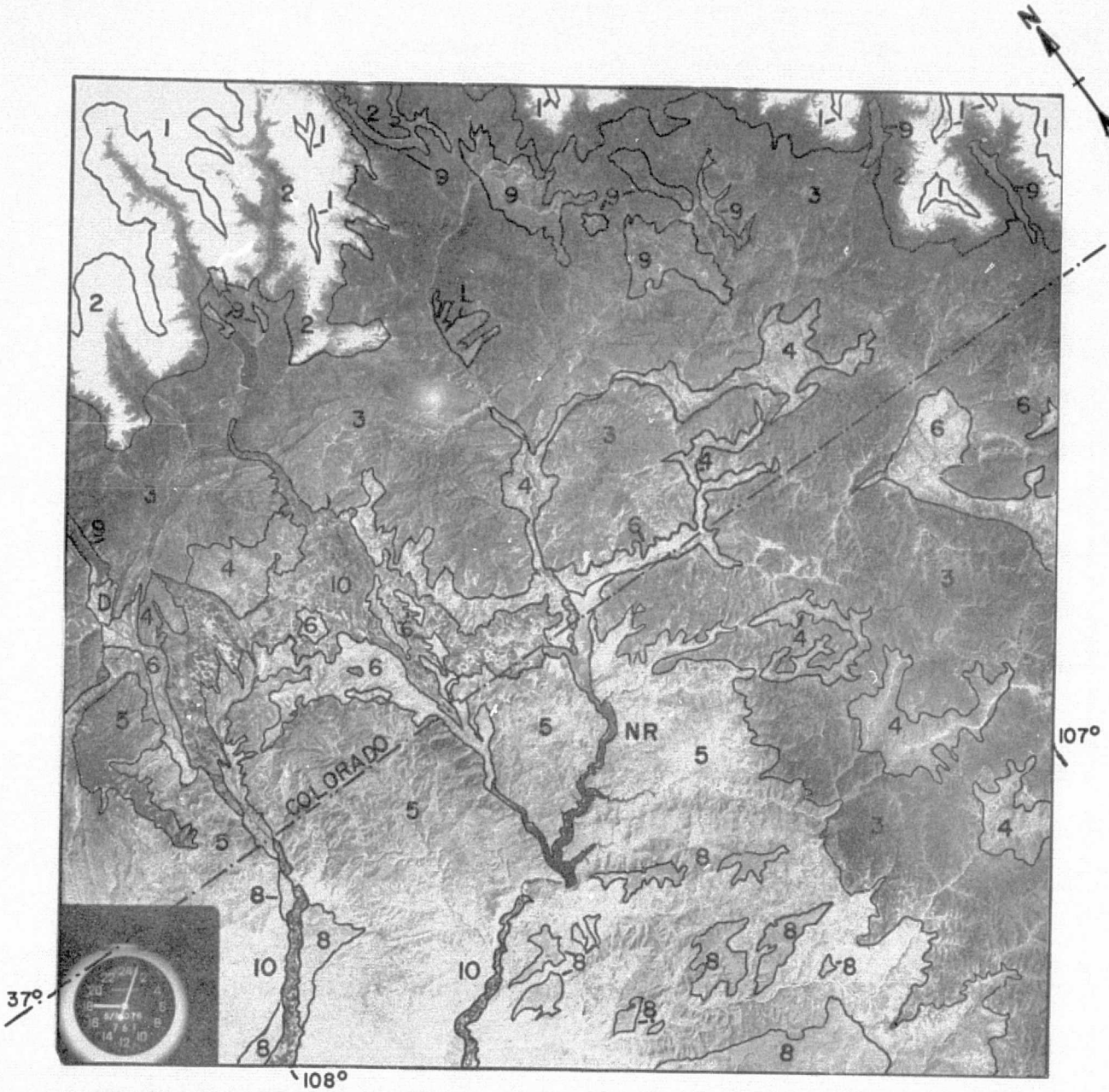

Key:
1. Alpine Meadow
2. Spruce-fir forest
3. Pine-Douglas fir forest
4. Mountain mahogany oak scrub
5. Juniper-pinon woodland
6. Sagebrush
8. Gramma-galleta steppe
9. Mountain grassland
10. Agricultural land
D Durango
NR Navajo Reservoir
L Logged area (many other such areas not indicated)

Figure 3.6 Existing vegetation map prepared from SKYLAB photographic data. The area mapped includes the Granite Peaks Test Site and a large area of southern Colorado and northern New Mexico.

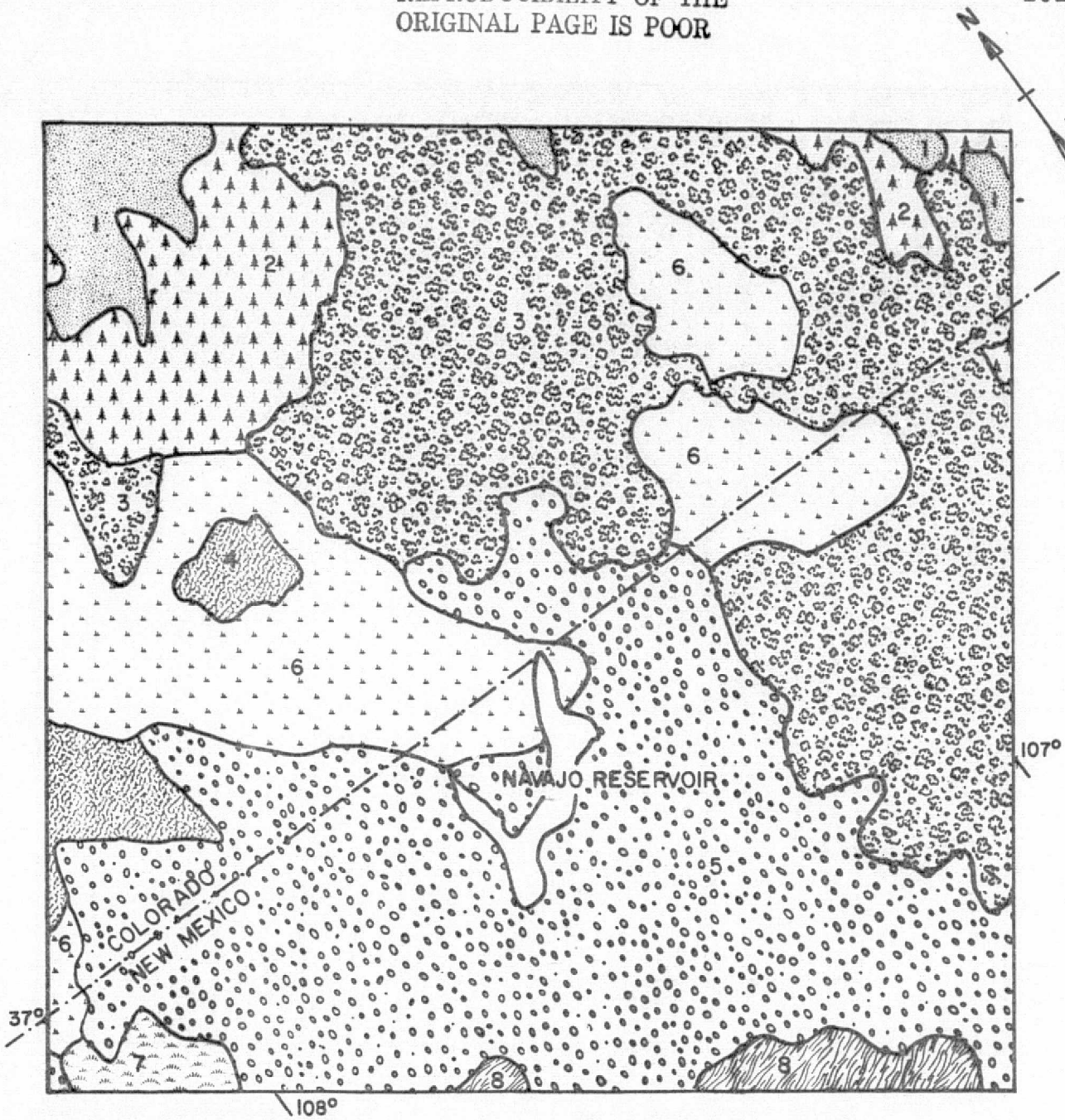

Key:
1. Alpine meadow
2. Spruce-fir forest
3. Pine-Douglas fir forest
4. Mountain mahogany-oak scrub
5. Juniper-pinon woodland
6. Sagebrush
7. Salt bush - grass wood
8. Gamma-galleta steppe

Scale approximately 1:708,000

Figure 3.7 Potential natural vegetation map for the same area shown in Figure 3.6 (from Kuchler, 1964).

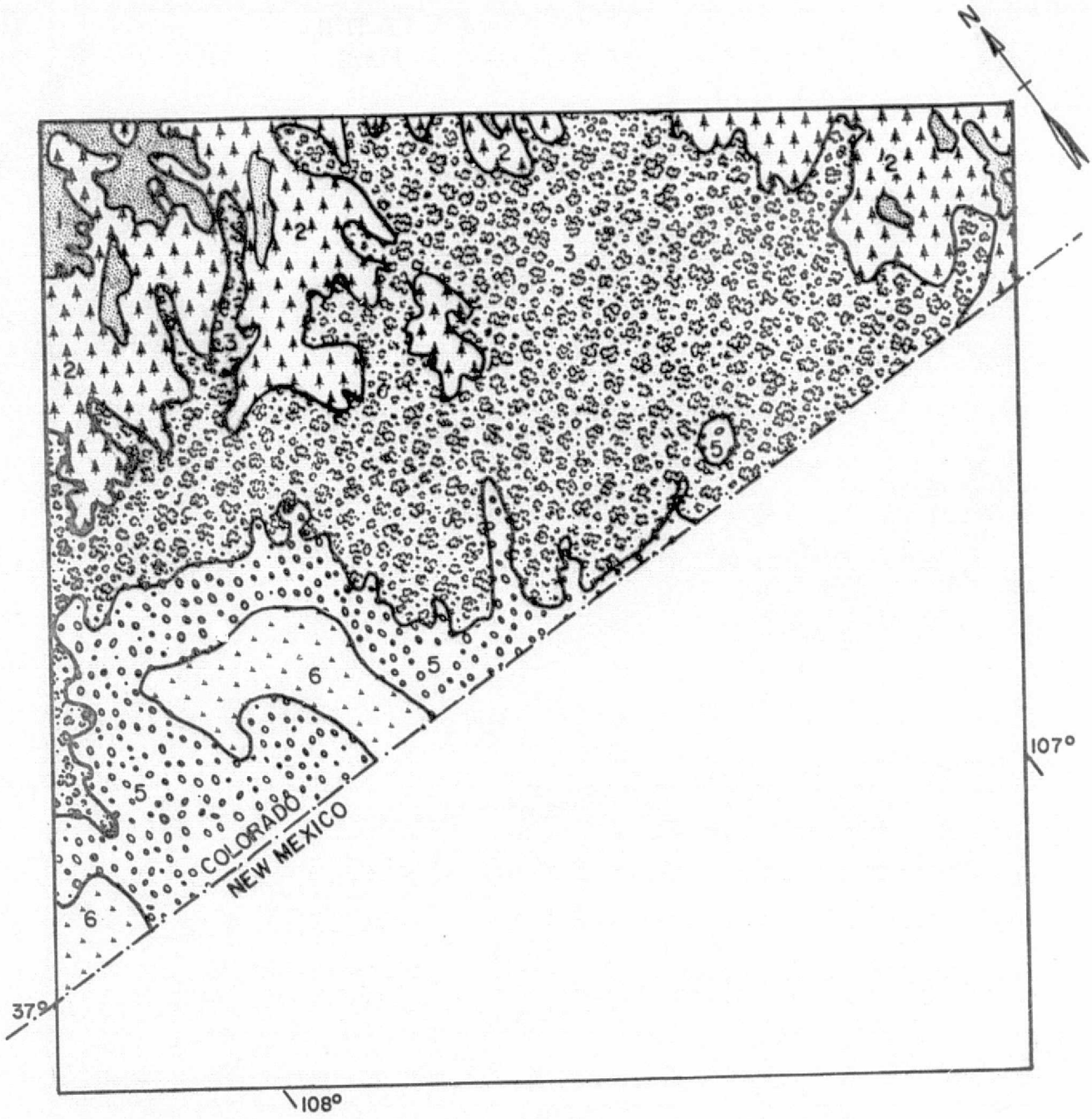

Key:
1. Alpine meadow
2. Spruce-fir forest
3. Pine-Douglas fir forest
5. Juniper-pinon woodland
6. Sagebrush

Scale approximately - 1:708,000

Figure 3.8 Natural vegetation of those portions of Colorado shown in Figure 3.6 (from U.S.D.A., 1972)

along with the slight differences in actual categories mapped account for the several discrepancies. The vegetation map prepared from the SKYLAB photography was of natural vegetation, but the categories varied from those of both the U.S.D.A. and Küchler maps.

The SL-2 S-190B color frames were used most frequently during the mapping, although the S-190A bands 0.7-0.8μm and 0.8-0.9μm were helpful during initial location of agricultural fields and mountain grasslands. These highly reflective areas were obvious in the near infrared, but the reference landmarks were clearer on the S-190B frames.

Mountain mahogany-oak scrub, sagebrush, and in some cases juniper-pinon woodland were the most difficult cover types to separate. As they form a natural mosaic on the ground, some confusion of types on the photographs was expected. However, ground observations in identified problematic areas could have helped to clarify such uncertainties generated during the mapping project. It is interesting to note that the greatest variation between Küchler's map (1964) and the U.S.D.A. (1972) occured in these categories. Apparently such interpretive difficulties are characteristic of photography other than SKYLAB.

The large agricultural area appearing on the existing vegetation map prepared from SKYLAB photographs (Figure 3.6) occurs in areas mapped by both Küchler and U.S.D.A. as sagebrush and juniper-pinon woodland. Irrigation must be practiced in order to support crops in lands which naturally

support such xerophytic vegetation.

The boundary between ponderosa pine (pine-Douglas fir) forest and juniper pinyon woodland (trending southward in the southern half of Figure 3.6) was much clearer than the boundary dividing the upper elevational limit of pine-Douglas fir and spruce-fir forest. This may be due to the dense stand growth of both Douglas fir and Engelmann spruce-subalpine fir forests. Some discrepancies between the same boundary can also be noted in Figures 3.6 and 3.7.

In summary, the availability of SKYLAB photography synoptically covering about 5000 square miles on one frame is of great value for broad-scale mapping. Not only does it reduce the cost involved in contracting for special aerial photographic coverage or acquisition of existing photography, but it eliminates the problems of dealing with such a bulk of photography for mapping purposes. Also, large scale photography obtained from lower altitudes does not necessarily insure more accurate mapping results when dealing with very small scale maps. The equipment necessary for preparation of a broad cover-type map from SKYLAB photographs requires only a modest capital investment. Field checking of problematic areas is still a valuable supplementary step in the mapping procedure. Comparisons with existing small scale maps clearly indicate the value of the satellite imagery for obtaining more accurate vegetation maps than have ever before been possible.

3.2.5 Temporal Evaluation of S-190 Data

In this phase of the photo interpretation effort, two different dates of SKYLAB S-190A photos were evaluated for use in vegetation mapping. A study area was selected which had coverage from both the June 5, 1973 (SL-2) and August 8, 1973 (SL-3) passes. The area is a transect on the western slope of the La Plata Mountains in southwestern Colorado. The area covered by both the SL-2 and SL-3 data involved an area of 855 km^2 (330 square miles), and includes portions of Dolores and Montezuma counties. Most of this transect lies within the San Juan National Forest. The range of elevation is from 1,950 m (6,400 feet) of the dry farming lands in the west to 4,035 m (13,232 feet) of Hesperus Peak at the eastern margin of the transect.

Because of the small scale of the S-190A transparencies (approximately 1:3,000,000), magnification was necessary for photo interpretation. The use of a binocular dissecting microscope over a light table yielded optimal magnification (10-20x). The film was put in glass slide mounts fitted with a flange to reduce glare from the light table. This enabled the interpreter to distinguish mapable units as small as one hectare. The map base used was the U.S.G.S. 1:250,000 scale, Cortez 2' map.

The primary thrust of the analysis involved the comparisom of the S-190A color infrared photos over the La Plata Mountains. Distinct differences in spectral response between the two data sets could be seen. These differences were pri-

marily due to vegetative phenology. Vegetation patterns were more clearly defined on the SL-3 pass in August because of the complete leafing out of the deciduous canopy. Table 3.3 lists the various cover types that were mapped using the August 8 color IR photos, along with the N.B.S. (National Bureau of Standards) color which corresponded to the various cover types on this particular photo set. In several cases, note that the photo interpreter could not distinguish different cover types on the basis of color alone, but had to rely on his knowledge of the elevation ranges of the various species and the topographic data available on the base map in order to differentiate various species.

To obtain a more quantitative evaluation of the vegetative differences observed on the color infrared photos obtained on June 5 and August 8, and to compare the color infrared and color positive photos obtained on August 8, each data set (SL-2 color infrared and SL-3 color infrared and color positive film) was used to generate a vegetation map of the study area. The resultant maps (Figure 3.9 a,b,c) were evaluated using a grid of 20 rectangles. Each rectangle unit of the map was evaluated separately with field check standards, 1971 Hurd photos, and NASA Mission 238, Roll 49 color infrared underflight photography of the study transect. The percentage of the rectangular grid area that had been correctly mapped from the SKYLAB photography was

Table 3.3 Cover types and their color characteristics on the SL-3 color infrared film

Symbol	Cover type	Characteristic N.B.S. Color	Comments
O	Oak	34. v.v.O.	Aspen may be differentiated from oak only on the basis of elevation.
A	Aspen	34. v.v.O.	
FP	Flood Plain	34. v.v.O.	Found only at canyon bottoms.
M	Aspen - Conifer	37. m.v.O.	Spacing of dark conifer clumps causes a graying appearance on the lighter red aspen background.
OP	Ponderosa pine - Oak	36. m.v.O.	None.
P	Ponderosa pine	38. d.v.O.	Douglasfir is distinguishable from Ponderosa only by topography.
D	Douglasfir	38. d.v.O.	
E	Englemann Spruce Subalpine fir	44. d.r.br.	None.
PJ	Pinyon pine - Juniper	90. gy. Y.	None.
C	Clearcut	57. l. br.	Found at higher elevations in the Spruce fir forest.
N	Meadow	93. y. Gray.	Found only in areas of deciduous cover.
DF	Dry farming	(main hue) 120. m.Y.G.	Signature highly variable found in fields discrete patches and only at lower elevations.
R	Bare rock	153 g.White	Distinguished from tundra by elevation- Bare rock is found from low elevations to timberline.
T	Tundra	153 g.White	Areas above timberline have very sparse vegetation cover and image as bare rock. Mapped all areas above timberline as tundra.

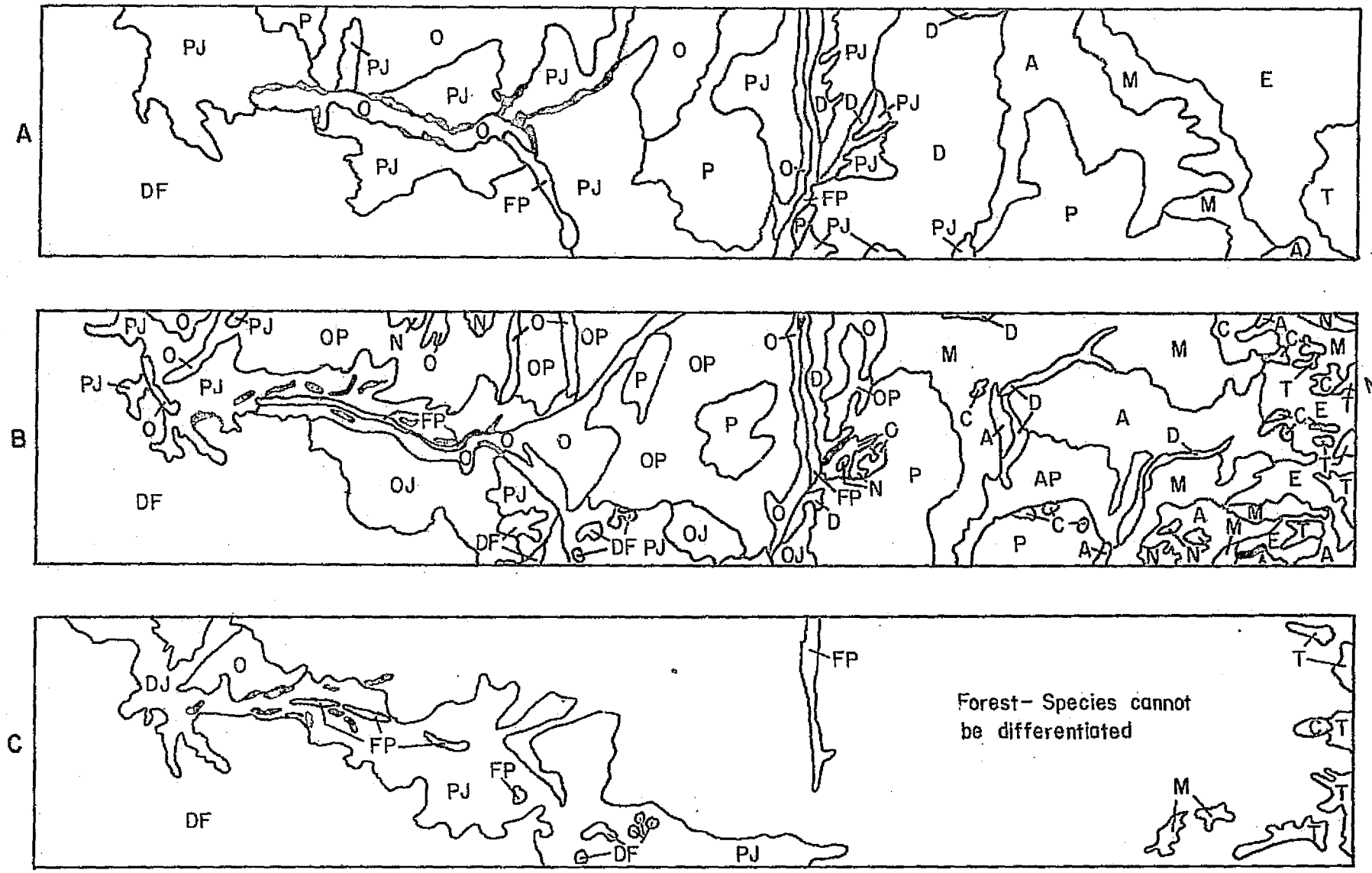

Figure 3.9 S190A photo interpretation comparison -- vegetation maps obtained from: (a) SL-2 color infrared, (b) SL-3 color infrared, and (c) SL-3 color positive film.

estimated and assigned an index value from one (20% accuracy) to five (100% accuracy). The sum of the index values for the 20 grid cells provided an index of the approximate overall map accuracy.

This evaluation procedure indicated that the map produced by photointerpretation of the SL-3 color infrared photos had an accuracy index of approximately 87 (out of 100 possible). Because the SL-2 coverage was collected early in the growing season, the deciduous canopy was not completely leafed out. The map produced from the SL-2 color infrared photos therefore had an accuracy index of only 40. The SL-3 color positive film was quite poor for vegetational analysis by photo interpretation because of the difficulty in distinguishing shades of green, due to underexposure of the film in the vegetated areas. The map that resulted from the interpretation of this color photography had an accuracy index of less than 20. These results clearly indicate the value of the August 8 data, as compared to the June 5 data, for vegetative mapping purposes.

3.2.6 Enhancement of S-190A Multi-Band Photography

The next phase of the vegetation mapping activity utilizing the S-190A multi-band photography involved an image enhancement study. In this study the SL-3 black and white multi-band photos were enhanced to evaluate the ability of the photo interpreter to effectively map vegetation using enhanced images. A Spatial Data Systems Model 703 microdensitometer and color enhancer unit was utilized to density-slice and color code each of the four black and white multi-band photos. A gray-scale wedge was used to adjust the color enhancer for the greatest tonal separation and contrast in each of the four bands. The color enhanced image was photographed and enlarged prints were obtained at a scale similar to that of the base map. These prints were then analyzed to determine the correlation between the enhanced color imagery and the vegetation type map.

Results of this activity indicated that the 0.5-0.6 micrometer band allowed some of the aspen in the eastern end of the transect to be discriminated and dryland farming in the southwestern region of the study area could be separated into two groups - corresponding first to wheatfields in non-irrigated grazing lands, and, secondly, to pinto bean fields. The 0.6-0.7 micrometer band seems to be superior to the other three bands for distinguishing highly reflective bodies such as snow, bare rock, and clouds. In several cases, however, the enhancement showed the same color for several different cover types, such as exposed rock and bare soil in agricultural lands, and, in some cases, even sparse deciduous

forest was shown as the same tone on the enhanced image. In other areas, tundra and bare rock were shown in the same color tones.

The 0.7-0.8 micrometer bands allowed topographic features, such as drainage patterns, slope, aspect, and ridging to be enhanced. Several situations were again noted where the same color on the enhanced image corresponded to several very different cover types. For example, dry farming areas, aspen and oak cover all had approximately the same density on the black and white image, and were therefore shown in the same color on the enhanced image. In other areas, Ponderosa pine and oak forest cover were displayed in the same color tones, although this was not true for all sections of the image. At higher elevations, bare rock, tundra, and clear-cut areas in the forest were enhanced in the same tone, indicating that these cover types could not be easily differentiated in this wavelength band. The evaluation of the 0.8-0.9 micrometer image resulted in essentially the same effects that had been seen on the 0.7-0.8 micrometer image.

In summary, the enhancement of S-190 multi-band photography enabled the photo interpreters to define boundaries fairly easily and quickly in many instances. However, such boundaries were not always consistent; they tended to vary, depending on the way in which the color enhancer unit was adjusted. In this particular study, the enhanced products that were used had some features clearly defined in one or more wavelength bands, but in many cases, different forest

cover types of interest were displayed in the same enhanced color tones, indicating that the photographic density was approximately the same for these different cover types in the individual wavelength bands. The overall results did not indicate enough substantial advantages for the photo interpreters, so enhanced single-band black-and-white photographic data were not utilized in the other phases of the photo interpretation efforts. When considering the results obtained by other investigators (Yost, et.al., 1972), it seems likely that if this effort had involved a system capable by combining several wavelength bands simultaneously into a single color enhanced image, the resultant product might have been substantially better and more useful.

3.2.7 Mapping of Mesa Verde National Park

During the course of the SKYLAB investigation, many talks, briefings, and discussions were held with personnel from various potential user agencies. One of the most positive expressions of interest in cooperative endeavors came from the personnel in the National Park Service at Mesa Verde National Park. Mesa Verde National Park is the only one in the United States that was established as a historical preserve. The other national parks are basically designed as wilderness areas or natural preserves. Because of this difference, some of the needs and management decisions in Mesa Verde are different than for many of the national parks in the National Park System. For example, the policy of Mesa Verde National Park is to fight forest fires, but in many National Parks, the policy is one of allowing the fire to burn itself out, since the parks are considered to be natural areas. However, because of the need to protect archeological sites, no fire is allowed to burn out of control in Mesa Verde. The heat generated by fires causes the mud plaster and mortar of the Anasazi structures to oxidize and disintegrate more rapidly than would normally be the case. (The Anasazi were the ancestors of the cliff dwellers.)

Preliminary discussions with the park service personnel indicated that they were in the process of updating the only available vegetation map of the park. This map had been

produced in 1938, largely on the basis of ground surveys. Since the entire area of Mesa Verde National Park was included on the S-190B SKYLAB photography and the LANDSAT data obtained on June 5, 1973 during the SL-2 mission, the Park Service was interested in the possibility of utilizing these data to assist in the vegetation mapping activity.

The importance of vegetation maps in properly managing the natural resources of Mesa Verde is found in several areas of activity, including the following:

Wildlife habitat - The types of wildlife and their available habitat in Mesa Verde National Park is part of the resource inventory. Habitat preferences are keyed to the vegetation and its distribution. For instance, the habitat of cottontail rabbit is shrub, sage, and grasslands. The predominant vegetation of the mesa top areas of Mesa Verde at the present time is pinyon pine-juniper. However, it is known that the Anasazi who lived in the mesa top areas (600 A.D. - 1000 A.D.) included large quantities of cottontail rabbits in their diet. Thus, it has been inferred that there was a climatic change which has resulted in a vegetation change in the mesa top area. Park personnel feel that such a change in vegetation in the mesa top might provide some clues in answering the question: "Why did the Anasazi leave the mesa tops and then eventually abandon their cliff dwellings?"

Vegetative change in condition - As mentioned above, the only available vegetation map of the park had been produced in 1938. Many changes in vegetation have occured since then, due mainly to fires. Large burns occurred in 1949 and 1969, and these are reflected in present vegetation. The pinyon pine-juniper forest of the mesa top areas of Mesa Verde National Park is of particular interest because this area is rather unique in that it has not been graded in over 50 years.

Fire control - As previously pointed out, because of the archeological characteristics of Mesa Verde, forest fires are not allowed to burn out of control in Mesa Verde. In fighting forest fires, knowledge of the vegetation type which is burning allows several important decisions to be made. For example, the fuel content characteristics for different cover types can be utilized in a computerized program to project the rate of fire spread. Knowledge of the vegetation of the area allows fire control personnel to define the extent of the potential burn area. Information such as this enables Park Service personnel to come to a decision on how quickly to mobilize and whether outside help will be needed in fighting forest fires in various portions of the park. Furthermore, vegetation maps along with the derived fire spread information, aid in the selection of geographical locations for fire breaks.

Search and rescue - Topography and vegetation are considered when planning a search and rescue mission. Several helipads are located throughout Mesa Verde National Park. The selection of a particular helipad location as a center for the operation is governed by the terrain and vegetation of the search area.

It is clear from the above comments that a reliable vegetation map of Mesa Verde would meet a variety of needs and have many applications in Mesa Verde National Park. Enlargements of the color photos obtained on June 5 were obtained, interpreted, and the photos and interpretation overlays were provided to the park personnel. These results were received enthusiastically. The synoptic view of the park and surrounding areas was of particular interest to the National Park Service personnel.

A prominant feature on the photography was the Moccasin Mesa Burn of 1972, which was on the border between the National Park and the adjacent Ute Indian Reservation. This fire had burned more than 2,000 acres in total, and the burn area could be effectively delineated on the SKYLAB S-190B photography (Figure 3.10). The area involved in the burn was of particular interest to Park Service personnel, since it is on the basis of area that fire suppression costs are normally assigned to the different agencies involved. In other words, if 60% of the burn area is within the National Park, then

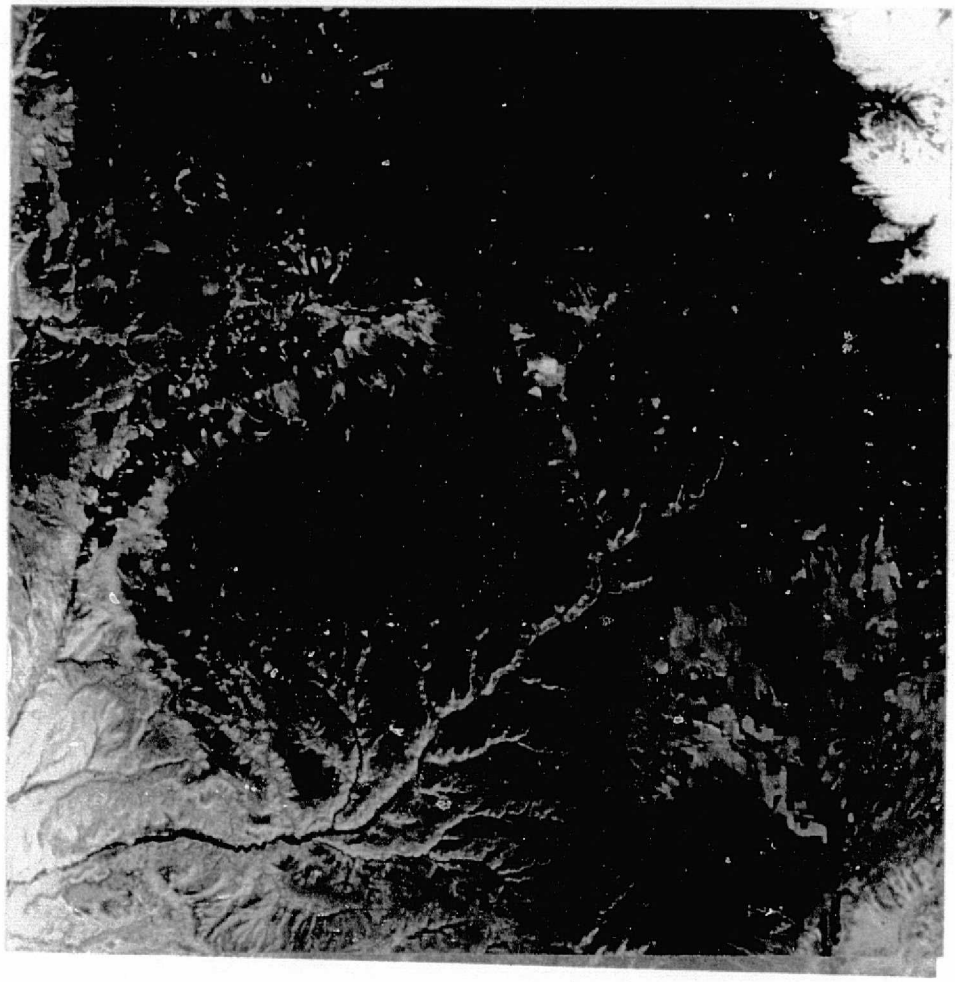

Figure 3.10 Enlargement of SKYLAB S-190B photography of Mesa Verde National Park

60% of costs for suppression of the fire are assigned to the National Park Service. In this case, interpretation of the imagery revealed that there were several unburned areas within the outside boundaries of the burn, indicating potential for effectively mapping forest burn areas with satellite data. The two older burn areas from fires in 1959, as well as in 1939, could also be defined on the SKYLAB S-190B photography.

Mesa Verde has a generally southern aspect, with the northern portion of the park being over 200 meters higher in elevation than the sourthern portion of the park. Generalized vegetation zones could be defined on the photography, and it was clear that these vegetation zones emphasized the elevational gradient in the park.

The enlargements of SKYLAB S-190B photos have been used by Park Service personnel to locate potential sites of helipads for future fire control needs. The photos have also been used by researchers affiliated with the park to make a preliminary survey of probable locations of archeological ruins that have not yet been surveyed. The S-190B color enlargement of the park and a color-coded computer classification of the vegetation of the park have also been used in a documentary film on the park as an example of recent research within Mesa Verde National Park. The photographic enlargement has also been shown to some park visitors. In general, they have been rather intrigued by what they could see -- The road system, parking lots, the Park

Headquarters, the Visitor Center, some of the ruins, ancient irrigation ditches, as well as the general vegetation patterns.

The vegetation map that was produced from the photo interpretation of the park area showed a good definition of the boundaries of the various vegetative cover types. However, it was believed that a more detailed class vegetation map could be obtained using the multispectral scanner data, since the scanner data would have resolution elements of approximately 1 acre in size. Unfortunately, the S-192 scanner data did not include the park area, but the LANDSAT imagery obtained on June 5 did contain the park area. Therefore, a classification using the LANDSAT imagery was carried out. The results of this classification were provided to park personnel in two formats; a 1:24,000 scale computer printout map and a color-coded map from the digital display unit (Figure 3.11). Both products were evaluated by park personnel. The vegetative classes which were defined in this classification were as follows: [1)]

ARID (BARE ROCK-BARE SOIL)

Vegetation is scarce or non-existant on the talus slopes, on the rim areas and on the easily eroded ridges near the park entrance.

---

1) These descriptions are also given on Panel 4 of the Remote Sensing Display in the museum of Mesa Verde National Park, which is described in the following section of this report.

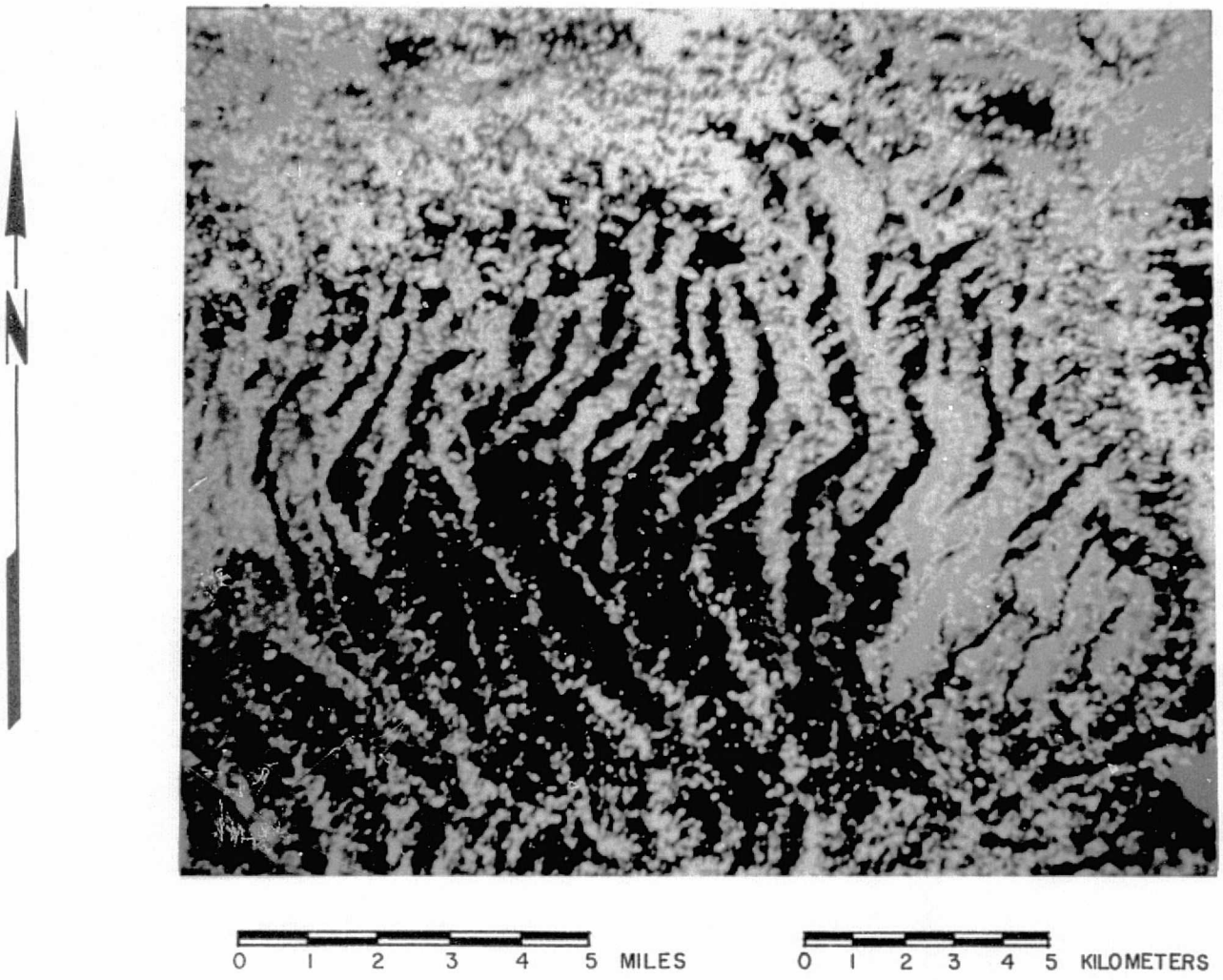

Figure 3.11 Map of major cover types in Mesa Verde National Park obtained by computer classification and LANDSAT MSS data. Yellow indicates grassland and low shrub, green is dense pinyon pine - juniper, brown is sparse juniper - pinyon pine, light blue is shrub, dark blue is shadow, white is rock and bare soil, and red is a recent burn area.

SHRUB

Gambel oak and Utah serviceberry are found in a mountain shrub zone along the higher parts of the mesas. This shrub zone is caused by recurring fires over many centuries.

DOUGLAS-FIR

The Douglas-fir stands grow in sheltered side canyons, steep areas, and the north-facing mesa escarpments.

PINYON-PINE JUNIPER (DENSE)

The dense forest of Pinyon Pine-Juniper grows on the mesa tops in a broad belt across the middle of the park. The Pinyon Pine and Juniper trees reach maximum heights of 10 meters (35 feet). Grass and yucca grow in forest openings.

JUNIPER-PINYON (SPARSE)

Areas of sparse Juniper-Pinyon Pine have small trees which are widely spaced. Such areas are relatively undisturbed over the last 400 years. Bitterbrush is a common shrub found in the forest openings and is a favorite browse plant of the mule deer.

SHADOW

When the satellite passed over the park at 10 A.M. the northeast-facing slopes were in shadow. The shadow areas emphasize the canyon topography of the park. Pinyon Pine, Juniper and shrubs grow on these slopes.

GRASS-LOW SHRUB

Meadows of grass and low shrub occur in valley bottoms in the northern part of the park. Where an area has been burned within the last 25 years grass and low shrub are conspicuous.

RECENT BURN

The most recent major forest fire in the park was on Mocassin Mesa in 1972. This burn was caused by lightening as are most of the fires in the park. Some fires were started by the Indians to increase game habitat. More game is found in the grass and shrub areas than in the forest.

The potential uses of these vegetation maps (obtained from satellite altitudes through computer-analysis procedures) were discussed with Park Service personnel. These discussions indicated the desirability of determining the areal extent of the various vegetative classes for the entire park, as well as sub-units within the park. Because of the usefulness of this type of information for the fire management program of the park, a request was made by Park Service personnel to give them information for the park of each cover type on a township grid basis (36 square mile areas). The tabulation of area estimates of the various cover types on a grid basis is also of value for wildlife management purposes within the park. This tabulation was obtained and provided to the National Park Service.

The initial reaction to these maps and tabular data was

one of general satisfaction. The detail on the computer print out maps is felt to be better than an existing map derived from field work. Part of the reason for this is felt to be the quantitative characteristics of the computer-aided analysis results, whereas other types of maps often contain opinions and biases of the interpreters involved. Their evaluation of the computer print-out map, in conjunction with a study in 1964, generally tends to support the classification results. Detailed evaluation of these materials is still in progress by various personnel of Mesa Verde National Park.

3.2.8 Mesa Verde National Park Museum Display

One of the most interesting aspects of our discussion with personnel of the Mesa Verde National Park was the idea of a museum display. Stemming from the many contacts with park personnel through correspondence, phone conversations, and meetings, the concept of a permanent display in the Mesa Verde National Park museum was formed. The visitors who had the opportunity to see the photographic enlargement of the SKYLAB data, as well as the color-coded classification maps, were intrigued and astonished by the detail that could be seen from space altitudes. Thus, the interest that these products generated led to the commitment of 25 feet of wall space in the park museum to be devoted to a display on remote sensing and how the products are derived. Relying on the expertise of the museum director and other park personnel, the format, scale plans and materials incorporated were decided upon. The text of the display was prepared and submitted for review for the appropriate park personnel. Suggested changes were then incorporated to meet with the approval of the museum director and park superintendent.

The display is basically composed of four panels and a free-standing central column. The central column has nine color photographs with captions on several aspects of the SKYLAB program. The four major panels are entitled respectively: 1) SKYLAB View From Space; 2) Remote Sensing: From Earth to Satellite to Map; 3) Objectives: Useful Products;

and 4) A Present-Day Vegetation Map From Space.

The display was completed and opened to the public in late October, 1975. It is estimated that this display will be viewed by over 600,000 visitors per year. The detail of the layout and wording for the displays are shown in Figures 3.12 - 3.15. It should be noted that Panel 2 describes, in non-technical terms, a remote sensing system more like LANDSAT than SKYLAB because the computer-derived maps shown in Panels 3 and 4 were generated with LANDSAT data. The reason for this was that LANDSAT data was available over Mesa Verde National Park but SKYLAB S-192 data had not been obtained over the park.

In summary, the SKYLAB photographic data and LANDSAT MSS data have proven of interest and of value in the number of applications to personnel from the Mesa Verde National Park. A computer-aided analysis of multispectral scanner data of the park has resulted in an update of the existing 1938 vegetation map of the park. The map and acreage tables derived from the classification are being carefully evaluated by several park personnel. A permanent display of SKYLAB photography and the updated vegetation maps have been prepared for display in the museum of Mesa Verde National Park. This exposure to large numbers of visitors should be of considerable value in explaining the application of the U. S. space program to user agencies such as the National Park Service.

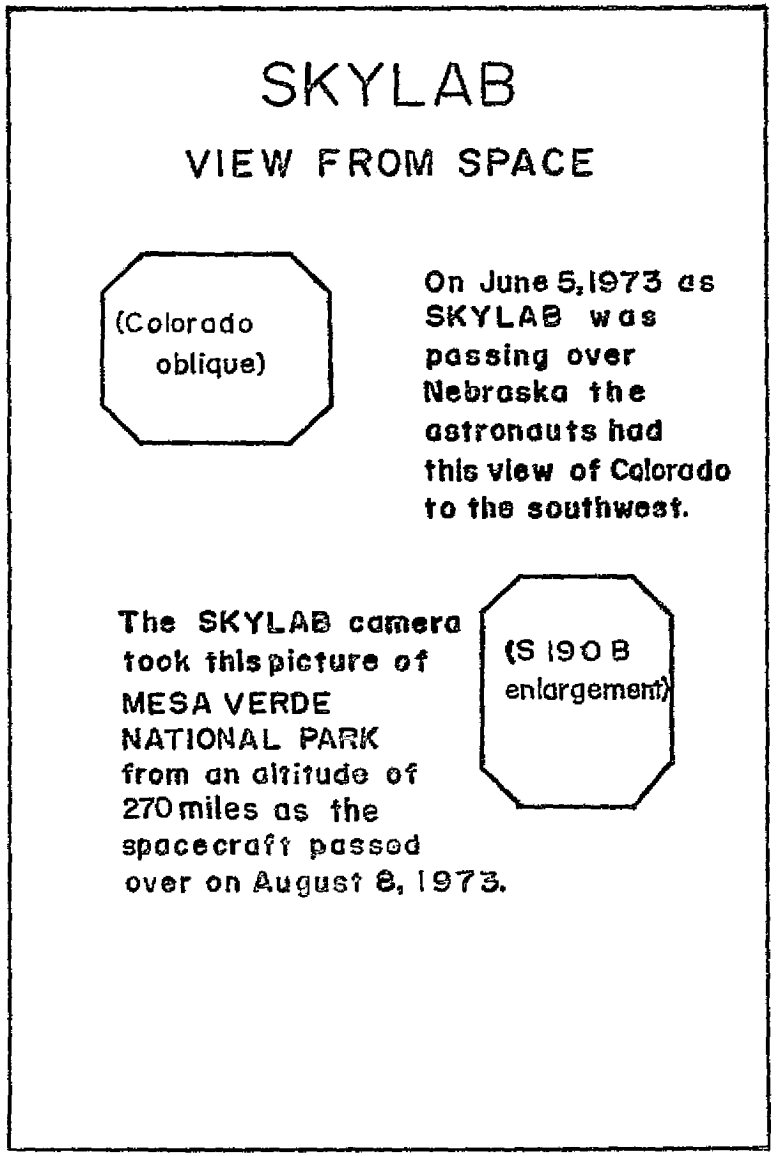

Figure 3.12 Panel 1 of the remote sensing displya in Mesa Verde National Park

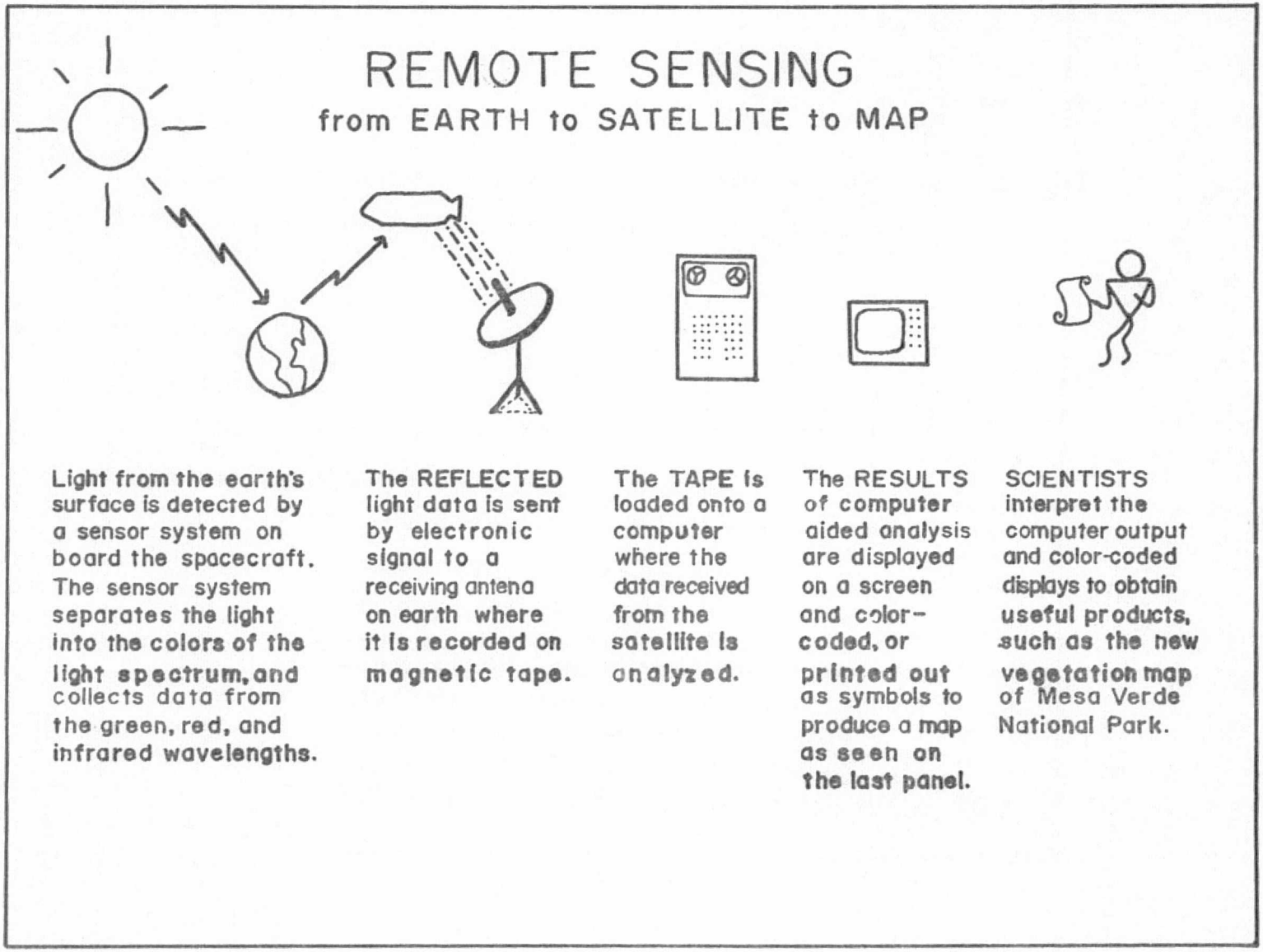

Figure 3.13 Panel 2 of the remote sensing display in Mesa Verde National Park

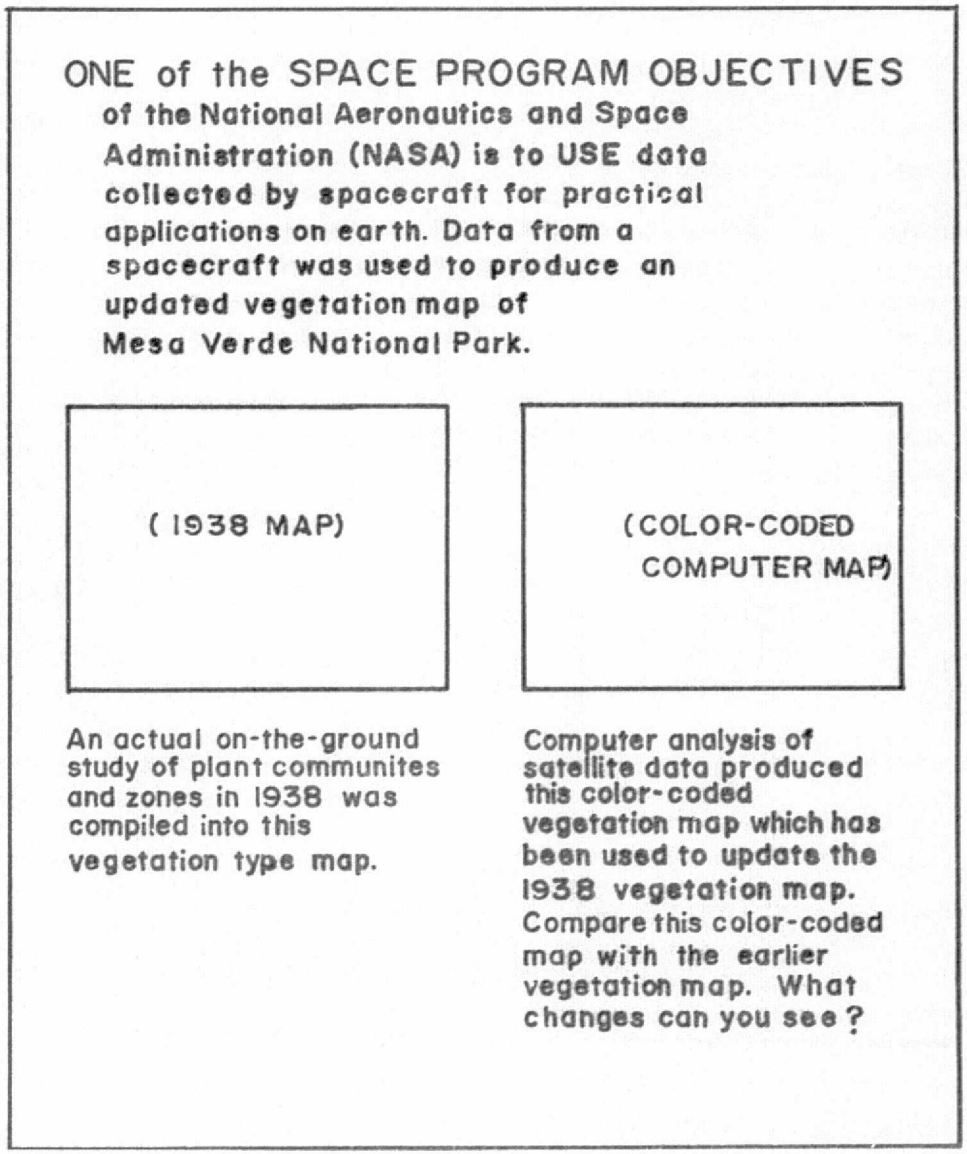

Figure 3.14 Panel 3 of the remote sensing display in Mesa Verde National Park

VEGETATION TYPES
MESA VERDE NATIONAL PARK

The types of present day vegetation probably closely resemble that which flourished before the prehistoric indians entered the area. The differences in vegetation now found in the park are due to subtle variations in slope, altitude, soil, the effects of fire, and the influences of prehistoric man.

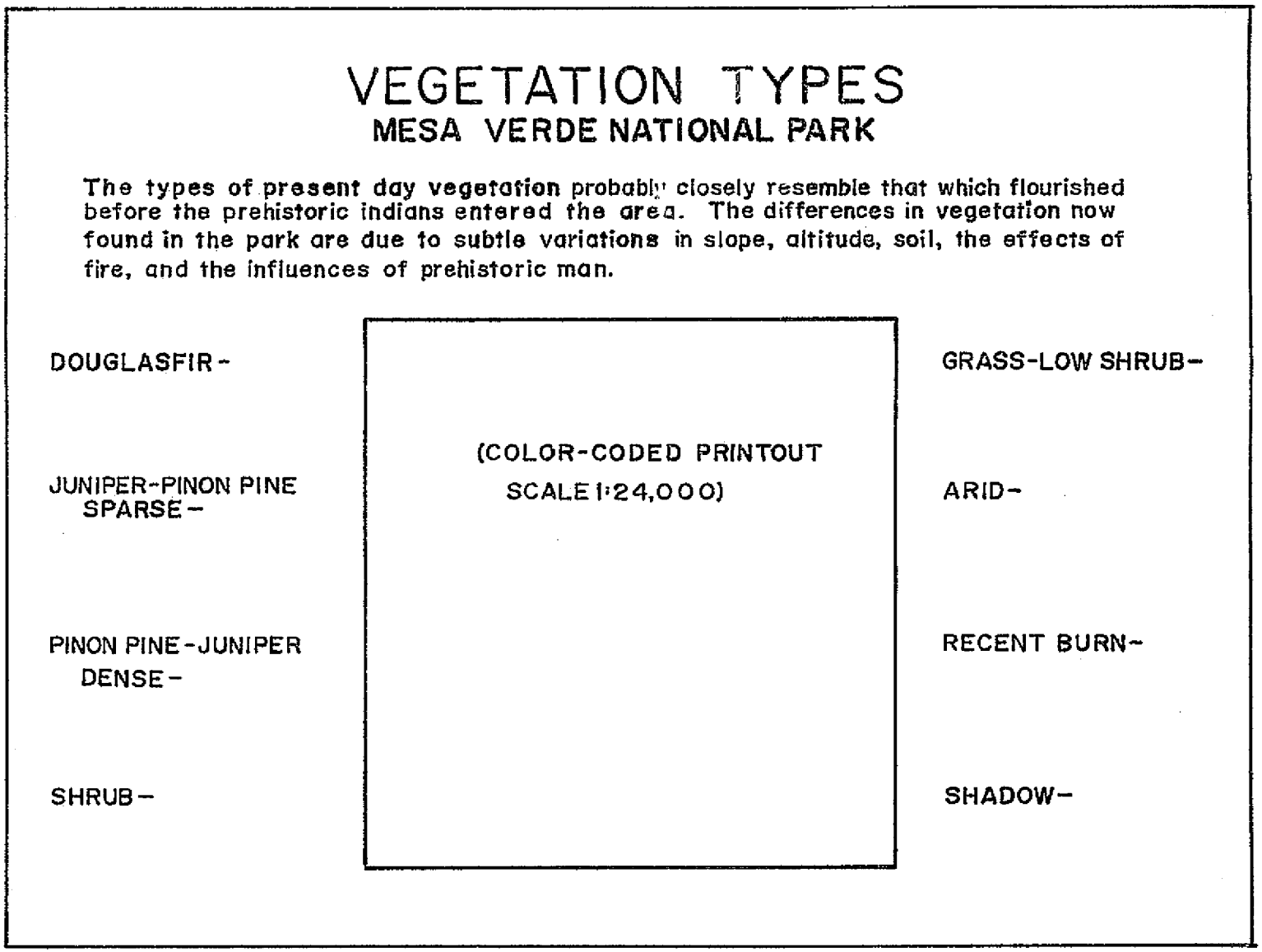

Figure 3.15 Panel 4 of the remote sensing display in Mesa Verde National Park

3.3 S-192 ANALYSIS TECHNIQUES

3.3.1 Introduction

Over the past decade, tremendous progress has been made in development of computer-aided analysis techniques (CAAT) involving the application of pattern recognition theory to multispectral scanner data. The basic procedure utilized for an analysis fo multispectral scanner data normally followed includes:

1. Defining a group of spectral classes (training classes);
2. Specifying the location of these training classes to a statistical algorithm which calculates defined statistical parameters;
3. Utilizing the calculated statistics to "train" a pattern recognition algorithm;
4. Classifying each data point or group of data points within the data set of interest (such as an entire LANDSAT frame) into one of the training classes.
5. Displaying the classification results in map and/or tabular format, according to the specifications of the analyst;
6. Evaluating the classification results.

During the past few years, experience at LARS has shown that there are many possible refinements in the methodology utilized by the analysts for obtaining the training classes

(step 1 above) and in the procedures for evaluating the results (step 6 above), whereas the rest of the procedure varies much less from one analysis task to another.

Over the past several years, both "supervised" analysis techniques, involving a training sample approach, and "non-supervised" or clustering techniques have been used with considerable success to define the training classes. In the "supervised" approach, the analyst selects areas of known cover types and specifies these to the computer as training fields, using a system of X-Y coordinates. The training field statistics are obtained for each cover type category. The entire data set is then classified, with these training statistics, and the results evaluated. These types of classification are referred to as "supervised" because the analyst must locate specific areas of known cover types to train the computer.

During the LANDSAT-1 investigations in the San Juan Mountain Test Site, we found that the "supervised" approach was extremely difficult to utilize in an area of such complex vegetation types and rugged terrain. This was because the supervised approach requires the analyst to select homogenous training samples which would be representative of all possible variations in spectral response for each cover type. In mountainous terrain, selection of such a training data set proved extremely difficult because of the spectral differences caused by variations in elevation,

slope, and aspect, as well as because of the many spectral differences in the cover types themselves.

In the "non-supervised" or clustering approach, an algorithm is utilized which divides a designated area into a number of spectrally distinct classes. The analyst must specify the number of spectral classes into which the data will be divided. The spectral classes defined by the clustering algorithm are then used to classify the data, but at this point the analyst does not know what cover type is defined by each of the spectral classes. Normally, after the classification is completed, the analyst will identify the cover type represented by each spectral class, using available support data such as cover type maps or aerial photographs. Because the analyst need not define particular portions of the data for use as training fields, but must only specify the number of spectral classes into which the data are to be divided, a classification using this procedure is called "non-supervised". Because of the difficulty in knowing how many spectral classes are included in a single species or cover type, previous work (Smeeds, 1970; Hoffer, 1974) had indicated that the non-supervised approach was usually more satisfactory when analyzing MSS data obtained over wildland areas.

Due to the vegetative and topographic complexity of the San Juan Mountain area, use of the supervised approach was not feasible in this study. Also, we found that utilization

of the non-supervised approach required defining such a high number of spectral classes that identification of each spectral class into a specific cover type (or category of interest) proved extremely difficult. Therefore, a more effective procedure had to be defined to accurately classify and map the forest cover types in an area of such complex spectral characteristics. A techniques defined here as the "modified cluster" technique was used during the LANDSAT-1 investigations, and this approach was further refined and tested throughout this SKYLAB experiment. Because we believe that this technique represents a major step forward in the effective utilization of MSS data and computer analysis software for areas that are spectrally complex, the following paragraphs describe the modified cluster technique in detail.

3.3.2 Detailed Description of the Modified Cluster Technique

Modified cluster is an effective and efficient technique for defining training statistics. It is essentially a hybrid of the supervised and non-supervised training approaches, and overcomes many of the disadvantages inherent in both of these other techniques. Supervised training is limited by the unknown relationship between categories of importance and spectral classes. Non-supervised training is suboptimal since the analyst must estimate and specify the number of spectral classes present in the data. Also, numerous spectral classes are usually required which makes proper interpretation of the results extremely difficult. This hybrid technique, modified cluster, overcomes these obstacles by allowing a more effective analyst/data interaction. We also found that the modified cluster technique required less computer time to develop training statistics and produced statistics which would yield a higher classification performance (Fleming, et al., 1975).

The modified cluster technique is comprised of four basic steps including:

* Step 1 - define training areas dispersed over the entire study site, with three to five cover types present in each training area;

* Step 2 - cluster each training area separately; compare map with the support data, and recluster if necessary.

*Step 3 - combine the results of all training areas, using the separability algorithm, and develop a single set of training statistics; and

*Step 4 - classify the training areas as a preliminary test of training statistics, modify statistics deck, if necessary; then classify the entire study site.

The following paragraphs will discuss each of these steps in detail.

The basic goal when selecting training areas is to obtain a representative sample of all spectral classes present in the study area. To do this, a representative sample of each cover type, including spectral subclasses caused by variations in slope, aspect, and crown density, must be included in at least one but preferably two training areas. Figure 3.16 shows a color infrared composite image derived from SKYLAB S-192 data, using the 0.52-0.56, 0.62-0.67, and 0.98-1.08μm wavelength bands. Several training areas to be utilized in the modified cluster techniques for developing training statistics have been delineated.

Selection of training areas throughout the entire study area provides a better sample of each cover type and lessens the problems encountered in extrapolating the training statistics to the entire data set. Since each cluster class must be accurately identified, informational support data of good quality (e.g., maps and aerial photography) must be available for all selected training areas. Classifica-

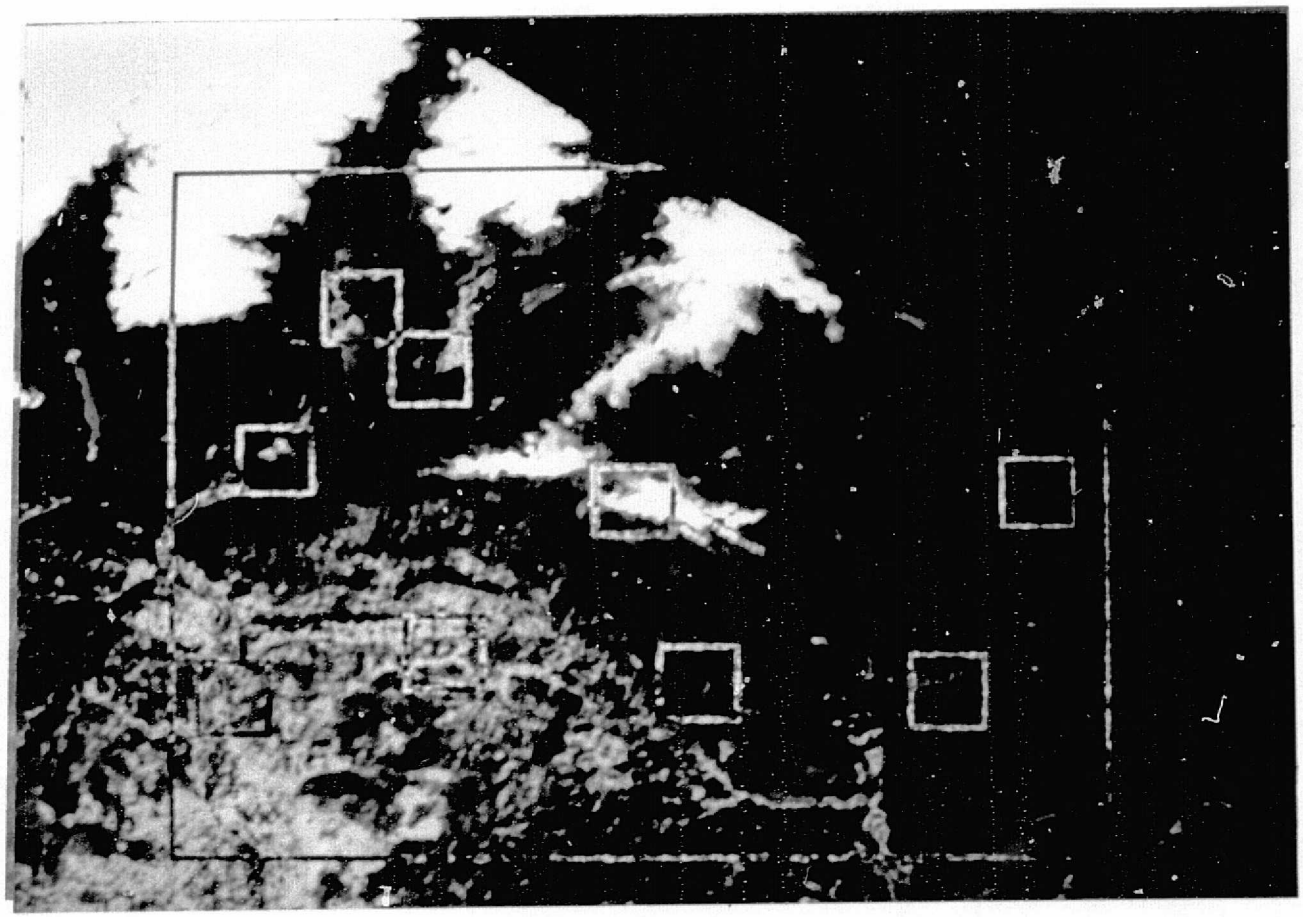

Figure 3.16 Color infrared composite image derived from SKYLAB S-192 data showing nine training areas to be utilized with the modified cluster technique to develop training statistics.

tion accuracy is heavily dependent upon the precision with which the cluster classes were identified and described. Thus, the more accurate the identification of the spectral cluster training classes, the more accurate the final classification. Selecting training areas that have a precisely locatable feature such as a lake, rock outcropping, etc., allows easier and more accurate correlation between the support data and cluster classes.

Experimentation with different LANDSAT-1 and SKYLAB data sets indicated that the optimum size for a training area is approximately 40 lines by 40 columns (1600 pixels or resolution elements). This size area was large enough to yield approximately 100 pixels per spectral class, yet was small enough to be clustered relatively quickly.

Experimentation also indicated that selecting and clustering a training area with three to five spectrally similar cover types optimized the spectral separability between these cover types. Additionally, this procedure indicated whether the various cover types of interest could be defined on the basis of their spectral reflectances. In other words, if a single spectral class was identified as representing several different cover types, a clear relationship did not exist between the spectral classes present and the cover types of interest.

The MSS data for each training area are clustered into a number of spectral classes, independent of all other training areas. In this manner a greater number of spec-

tral classes are obtained, and the amount of computer time required is greatly reduced as compared to clustering all training areas together.

Table 3.4 shows the comparison between clustering seven training areas separately and clustering all of them together. In this case, by separate clustering, the computer time was reduced by nearly 86%, and the number of spectral classes was increased from 30 to 76. Although there may be some duplication of spectral classes when clustering independently, these can be easily identified and grouped. More importantly, any classes that represent mixtures of several cover types or pixels that are on the edge between

Table 3.4 -- Comparison between the non-supervised and modified cluster methods for defining training statistics.

	Method Used	
	Non-Supervised	Modified Cluster
Number of Pixels	7844	7844
Number of Training Areas	7	7
Number of Spectral Classes	30	76
Computer Time (Minutes)	68.1	9.7

cover types can be identified and deleted without significantly reducing the number of spectral classes.

The number of cluster classes into which each area is divided varies as a function of the data variability. A comparison of several parameters which may be used to help choose the proper number of clusters indicated that the parameters were closely related. These parameters included average transformed divergence, highest minimum transformed divergence, total variability of all cluster classes, and a transformed scatter ratio (Sinding-Larson, 1974). The transformed scatter ratio, which estimates how well the data are divided, was used throughout this investigation to select the "optimum" number of cluster classes for a training area. Each training area is clustered into 12 through 16 classes and the transformed scatter ratio is calculated for each number of classes. The optimal class number is selected by minimizing the transformed scatter ratio. If the minimum number is 12 or 16, the transformed scatter ratio is then calculated for the next cluster number (e.g., 11 or 17, respectively). This process continues until a minimum scatter ratio is found.

After the "optimum" number of cluster classes is found for a training area, each cluster class must be identified as to the actual cover types it represents, by overlaying the cluster map with the support data. For this SKYLAB study, a base cover type map was prepared through interpretation of the underflight color infrared photography. The

aerial photography could be used directly by projecting the photography onto the cluster map using an overhead projector, zoom transfer scope or vertical sketchmaster. By using the aerial photography directly, more precise and detailed information could be obtained for each cluster class than by simply using cover type maps.

Because several statistics decks are produced by clustering the data from each training area separately, the separability algorithm is used to combine the cluster classes into informational-spectral classes of the final statistics deck. The saturating, transformed divergence value (obtained from the separability algorithm) is a measure of the distance between classes in multidimensional space. This measure, which ranges in value from 0 to 2000, is referred to as the "divergence value". Higher divergence values indicate class pairs which are more separable. Past experience of LARS researchers suggests that class pairs with divergence of 1700 or greater will generally yield a bimodal distribution when grouped (which violates the basic assumption of the maximum-likelihood, Gaussian classifier).

Since a large number of cluster classes are usually obtained by clustering each area independently, simultaneous comparison of all class pairs with divergence values less than 1700 is difficult. For this reason, the combining of similar cluster classes is performed in a series of steps. The first step is to calculate the divergence value for each

pair of cluster classes. Because cover types are included more than once in the many training areas, there should be several similar, spectral classes for each cover type. We found that combining all pairs with a divergence value of 1000 or less reduced the number of cluster classes by nearly one-half. The low divergence value of 1000 indicated that the spectral classes for that pair were very similar. To distinguish these combined classes from the original cluster classes, the combined classes are referred to as "spectral classes".

The second step in combining the classes is to calculate the divergence value for each pair of "spectral classes". In this step, all spectral class pairs with a divergence value of 1500 or less are combined. The value of 1500 was selected because there are usually still too many pairs with a divergence value less than 1700 to allow easy grouping of the spectral classes (and not many below 1200). When combining the spectral classes, the vegetative (or other) cover type is checked for each cluster class included in the spectral class grouping. Any spectral class with more than one cover type present (mixed cover types) is deleted unless the mixed class is a desired informational class. The combined spectral classes are then identified and named, and consequently are called "spectral informational" classes.

The process of calculating divergence values and combining classes is repeated several times until the desired separability is achieved between the spectral-informational

classes. If more detail is desired for one or more cover types, it may be desirable not to combine some spectral-informational classes and therefore accept misclassification between these classes. This is where the objectives of the analysis become important in deciding the disposition of these classes.

As a final check before classifying the entire study area, as a test of the training statistics, the training areas should be classified. The classification results can then be compared with the support data to make sure no errors were made in labelling classes or that any desirable classes were deleted. If no errors were made, the entire study area is classified with the maximum likelihood classifier.

3.3.3 Evaluation Techniques

Once an adequate training set has been defined, it is not difficult to classify a large geographic area using computer analysis techniques. However, unless one can verify the accuracy of such computer classification results, little has been accomplished by simply classifying data over various areas of interest. The real question is whether or not the resultant classification maps and tables are reasonably accurate and have a reasonable level of reliability. In this study, a combination of three different techniques proved most satisfactory to achieve the best possible indication of the classification performance. The three techniques utilized to evaluate the classification results included:

1. Qualitative comparison of the computer classification maps and the maps obtained from interpretation of aerial photos, as well as direct comparison to the aerial photos;
2. Quantitative evaluation of classification performance, utilizing a system of statistically defined test areas; and
3. Quantitative comparison of acreage estimates obtained from the computer classification and from airphoto interpretation on a quadrangle by quadrangle basis.

In the qualitative evaluation, the maps resulting from the interpretation of the aerial photos obtained by NASA were

utilized as baseline data. The computer classification map and the photo interpretation map were compared, and a general assessment of the level of agreement between the computer classification map and the photo interpretation map was ma . This approach provides a general indication of the computer classification performance, but it is difficult to make in-depth or detailed comparisons of classification results, such as determining whether a classification using a certain combination of wavelength bands is better or worse than a classification using a different combination of wavelength bands. Likewise, it is often difficult to determine whether a classification utilizing data from one time of the year is better or worse than a classification utilizing data from another time of the year. For these reasons, a quantitative evaluation technique utilizing test areas provides a more effective method for evaluating computer classification results.

To obtain a quantitative, unbiased evaluation of the SKYLAB classification results, a statistically defined, systematic grid of test areas (each 4 x 4 resolution elements in size), were located on a 9 resolution element interval over the entire Granite Peaks Test Site. Because of the difficulties involved in overlaying LANDSAT, SKYLAB, and topographic data to a ± 1 resolution element accuracy, a one resolution element buffer strip was added around each potential test field. Next, the grid of potential test areas was superimposed on the cover type map that had been

developed from photointerpretation. Any potential test area, including the buffer strip, which fell on a cover type boundary line was eliminated from further consideration as a test area. This process reduced the number of potential test areas to approximately 540 which included approximately 5% of the entire Granite Peaks Test Site. Since each of the 540 test areas consisted of 16 resolution elements (18.4 acres) over 10,000 acres or 4,000 hectares were defined to quantitatively evaluate the classification results. The results of this process is shown in Figure 3.17. The actual cover type for each of the test areas was later double-checked, using the aerial photography obtained during the SKYLAB underflights.

The third method of evaluating the computer classification results involved acreage estimates. In this technique, the X-Y coordinates of a relatively large area (e.g., a 7½' U.S.G.S. quadrangle area) are specified to the computer. The computer tabulated the number of resolution elements within this designated area that had been classified into each of the categories or cover types of interest. In this investigation both the SKYLAB and LANDSAT data sets had been geometrically corrected and overlayed in such a way that when each resolution element is printed out on a standard computer line printer, the result is a 1:24,000 scale line printer "map". At this scale, each resolution element represents an area of 0.46 hectares (1.15 acres) on the ground. By multiplying this area by the number of resolu-

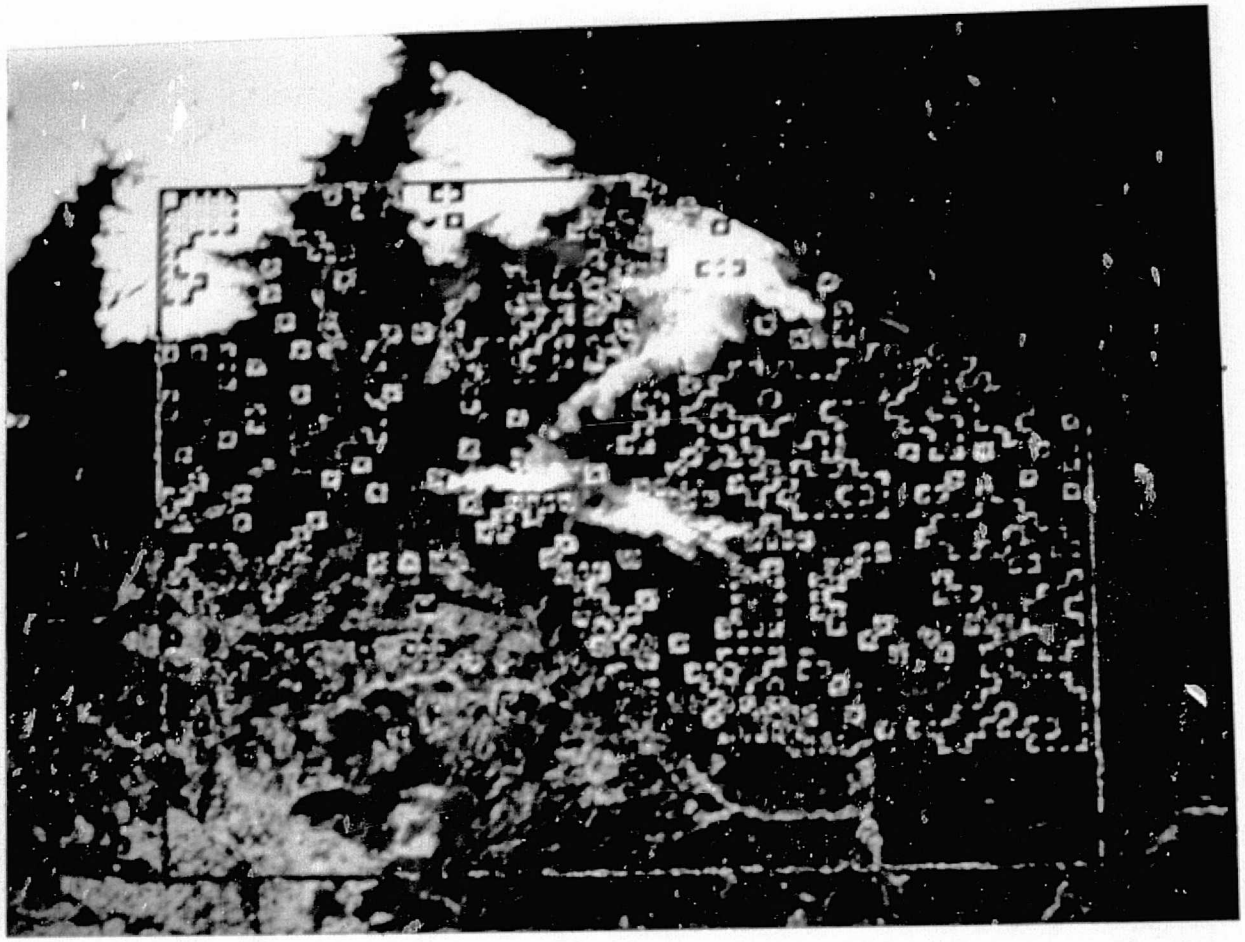

Figure 3.17 Color infrared composite of the Granite Peaks Test Site showing statistically defined grid of test areas used throughout this study

tion elements classified into each cover type category, an acreage estimate for each cover type can be obtained on a quadrangle by quadrangle basis (or for any other size area of interest).

Standard dot grid and planimeter methods were used to obtain acreage estimates from the cover type maps obtained by interpretation of the aerial photos. This was done on a quadrangle by quadrangle basis. This phase of the work was done by our colleagues at the University of Colorado. Thus, the acreage estimates being compared were obtained by two entirely different teams of researchers. The acreage estimate for each cover type was then compared on a quadrangle by quadrangle basis for the SKYLAB MSS analysis and the aerial photo interpretation results. Finally, the correlation coefficient was determined for the overall results.

In summary, unless noted otherwise, throughout all of the final analysis sequences reported upon in the Ecological Inventory portion of this SKYLAB report, the "modified Clustering" technique was utilized for defining training statistics. The maximum likelihood algorithm based on Gaussian distribution and equal apriori probability of occurance was utilized for the computer classification of the multispectral scanner data. The three evaluation techniques described above were then utilized to evaluate the classification results. In many cases, not all of the tables of classification results obtained are shown or discussed, because it was thought that a complete tabulation

and discussion of every analysis completed during the course of the study would only add unnecessary bulk to this final report. Thus only the more pertinent or significant results are reported and discussed.

3.4 COMPUTER-AIDED ANALYSIS OF THE SL-2 S-192 DATA

3.4.1 Introduction

The application of computer-aided analysis techniques (CAAT)to the SKYLAB S-192 multispectral scanner data obtained on June 5, 1973, during the SL-2 mission produced a number of significant results. A geometrically corrected (1:24,000 scale) digital data tape containing all 13 wavelength bands of SKYLAB data, plus three channels of topographic data (elevation, slope, and aspect) was utilized throughout this phase of the study. The "modified cluster" techniques and results evaluation techniques previously described were utilized for the analysis.

The objective of the first phase of this analysis was to determine the accuracy that could be achieved for the computer-aided mapping of major cover types and forest cover types, utilizing the SL-2 S-192 data. The major cover types or "land use" categories and the forest cover types that were found in the Granite Peaks study area are shown on Table 3.5.

Table 3.5 -- Major cover types or "land use" categories and forest cover types found in the Granite Peaks Test Site.

MAJOR COVER TYPES (Land Use Categories 1/)	FOREST COVER TYPES
Water	Water
Exposed Rock and Soil	Exposed Rock and Soil
Grassland	Grassland
Deciduous Forest	Oak
	Aspen
Coniferous Forest	Ponderosa Pine
	Douglas & White Fir
	Engelmann Spruce & Alpine Fir
Tundra	Tundra
Snow	Snow

1/ These major cover types could also be referred to as land use categories, Level II, as defined in U.S.G.S. Circular 671. Exceptions to the definitions given in Circular 671 are in the snow and grassland categories, since this snow cover was seasonal rather than permanent, and because grassland included both pasture in agricultural lands and rangeland grasses.

The first step in the analysis involved definition of the spectral classes that would characterize the area. Initial work with the modified clustering technique resulted in 135 statistically defined cluster classes within the test site. This was far too many to work with effectively, and it was not clear that all 135 spectral classes were really

significant from an information content standpoint. In other words, did each of these classes really contain meaningful information? Possibly some were so similar that they could not be grouped together into spectrally similar classes, each having meaningful information content.

The feature selection algorithm within LARSYS was utilized, and spectral clases having separabilities of less than 1500 were grouped. Interpretation of these results indicated that the spectral classes to be grouped usually were not significantly different in terms of information content (e.g., an aspen stand having 70% crown closure was grouped with an aspen stand having 75% crown closure). Detailed analysis of the spectral classes involved, utilizing the feature selection algorithm in combination with the modified-cluster technique ultimately resulted in the definition of 31 statistically separable spectral classes, each of which had meaningful information content. The characteristics of these "spectral-information" classes were determined through careful examination of the aerial underflight photography obtained by NASA's WB-57F and NC-130 on June 6, in combination with the computer prinouts of the cluster classes of the SKYLAB data obtained on June 5. In general, most of the "spectral-information" classes corresponded to different crown density groupings of forest cover types. After classification of the data using the 31 "spectral-information" classes, those classes which corresponded to

different density groups within a single forest cover type could be combined to allow a forest cover type map or tabular summary to be obtained. The forest cover types could also be combined to produce a major cover type or "land use" map or tabular summary. Table 3.6 shows the relationship between the "spectral-informational" classes, the forest cover type, and the major cover type categories. The crown closure percentages are qualitative estimates based upon interpretation of the aerial photos. These results indicate that the forest stand density is a dominant factor in causing differences in spectral response within individual forest cover types. Differences in percentage of snow cover on the ground were affected by differences in density of the coniferous forest cover (primarily the spruce/fir). In other word, in areas where there was some snow present on the ground, if these was $\leq$ 40% density of spruce/fir only 60% of the ground covered by snow could be seen. This combination of snow and different densities of forest cover resulted in differences in spectral response measured by the S-192 scanner, as will be discussed in more detail in the Hydrological Features portion of this report.

The 31 spectral-information classes resulting from this work are thought to effectively represent the spectral characteristics of this test site area. It should be emphasized that effective man-machine interaction is neces-

Table 3.6 Relationship of spectral-information classes to Forest Cover Types and Major Cover Type Categories

Major Cover Types [1]	Forest Cover Type	Spectral-Information Classes
Water	Water	Water (Shallow) Water (Deep)
Exposed Rock/Soil	Exposed Rock/Soil	Exposed Rock (Spectral Class 1) Exposed Soil (Spectral Class 1) Exposed Soil (Spectral Class 2)
Grassland	Grassland	Range Land (Spectral Class 1) Range Land (Spectral Class 2) Pasture (Spectral Class 1) Posture (Spectral Class 2)
Deciduous Forest	Oak	Oak (Spectral Class 1) Oak (Spectral Class 2)
	Aspen	Aspen(Spectral Class 1) Aspen(Spectral Class 2) Aspen (No Foliage)
Coniferous Forest	Ponderosa Pine	Ponderosa Pine (<10% crown closure) Ponderosa Pine (10-20% crown closure) Ponderosa Pine (20-30% crown closure) Ponderosa Pine (30-50% crown closure) Ponderosa Pine (50-60% crown closure) Ponderosa Pine (60-80% crown closure)
	Douglas Fir and White Fire	D/WFir and Aspen D/WFir(<80% crown closure) D/WFir (80-90% crown closure) D/WFir (90-100% crown closure)
	Engleman Spruce and Alpine Fir	Spruce/Fir(70-80% crown closure) Spruce/Fir(80-90% crown closure) Spruce/Fir(90-99% crown closure)
Snow	Snow	Snow(20-40% ground cover) Snow(50-80% ground cover) Snow(80-90% ground cover) Snow(90-100% ground cover)

[1] Corresponding to Level 2 "Land Use" categories, as defined by USGS Circular 671, that were present in the study area.

sary to define such spectral-information classes. This phase of the study was probably the most critical part of the entire analysis procedure. Considerable time and effort were required on the part of a skilled analyst who was familiar with the ecology and characteristics of the study site. Also, we would like to point out that effective definition of the spectral-informational classes present in the study site could not have been accomplished without the use of the underflight aerial photography. We could define a group of spectral classes without such photography (or current accurate cover type maps), but we would not have been able to relate such spectral classes to the informational categories of interest or significance.

After the final training statistics had been defined, the feature selection processor was utilized to determine the optimum or "best" combination of four wavelength bands of the S-192 MSS data that could be utilized for the classification. In this case, the 0.46-0.51, 0.78-0.88, 1.09-1.19, and 1.55-1.75 μm wavelength bands (channels 2,7,9, and 11) were designated, since this combination yielded the highest "average separability" among the spectral classes involved. Using these four wavelength bands, the entire test site was then classified using the maximum likelihood algorithm.

3.4.2 SL-2 MSS Data Results

3.4.2.1 Major Cover Types

The computer classification and display of major cover types resulted in the map shown in Figure 3.18. This color coded computer classification map was produced on the LARS Digital Display Unit. The entire Granite Peaks Test Site, which encompasses an area of 92,829 hectares, is shown. This map was analyzed in detail and compared to cover type maps developed by interpretation of the aerial photos and to the aerial photos themselves. In general we found that the two cover type maps compared very well for areas below the snow line. For areas above snowline, the cover type map prepared by photointerpretation indicated extensive areas of spruce-fir forest and tundra, whereas these areas are snow-covered on the map obtained using SKYLAB data. The difference occurs because the photo interpreter map was prepared using aerial photography obtained during late summer. Thus, both maps were actually "correct" in these upper elevation areas, even though they were not in agreement.

A comparison between these two cover type maps is shown in Figure 3.19 for a portion of the entire test site. Only a portion of the entire test area is shown because of the complexity of cover types involved, which makes qualitative comparisons for large areas very difficult. As Figure 3.19 shows, the computer classification map compares reasonably well with the map obtained by standard photo interpretation techniques.

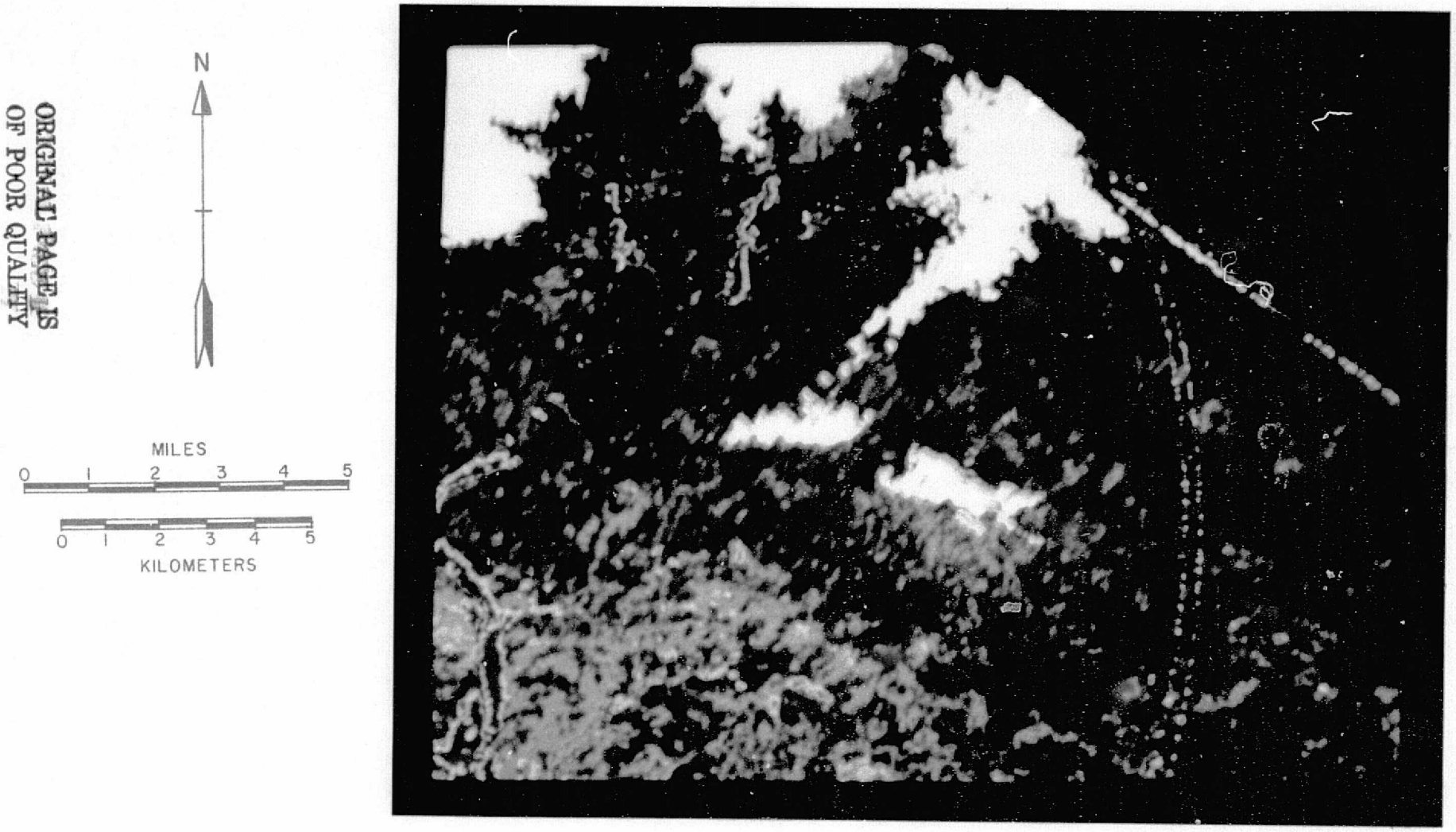

Figure 3.18 Map of major cover types obtained by computer classification of SKYLAB S-192 data. The various cover types are designated by the following colors: white=snow; blue=water; dark green=coniferous forest; light green-deciduous forest; red=grassland; brown=exposed rock and soil; and yellow=boundary areas. The two vertical lines of yellow dots on the right side are bad data lines.

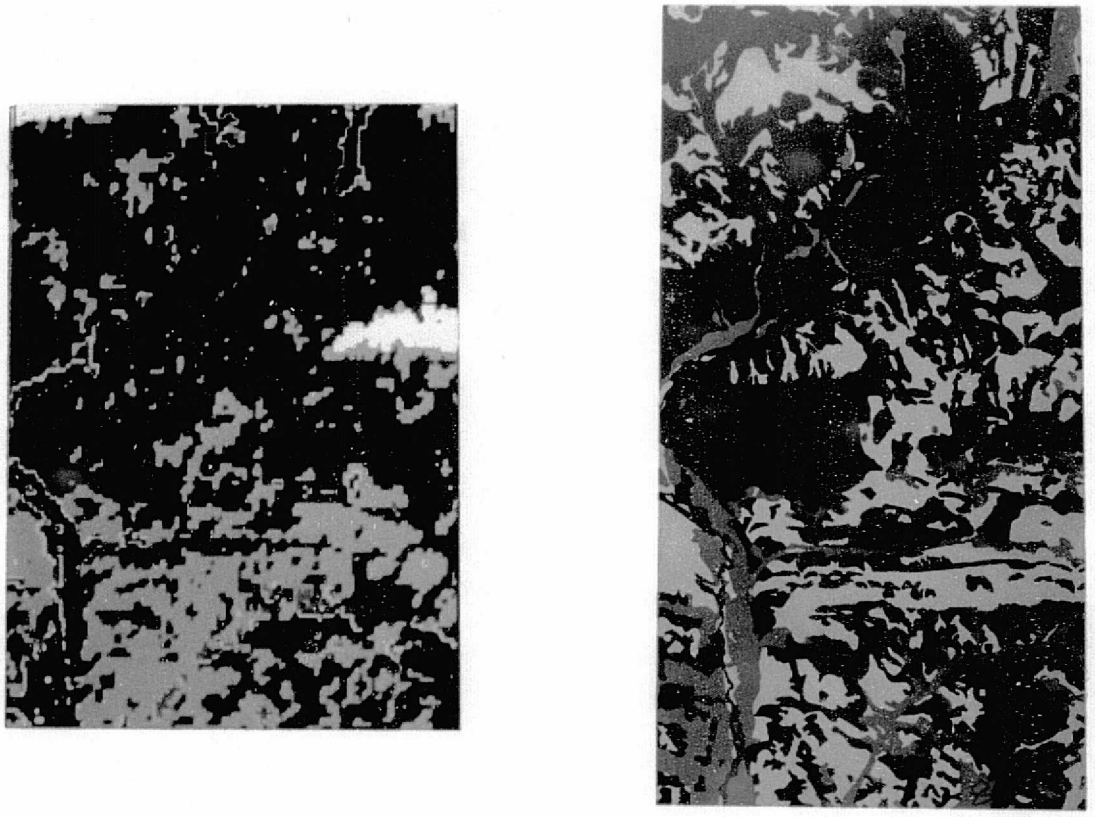

Figure 3.19 Comparison between major cover types obtained by computer classification of SKYLAB S-192 data (left) and manual interpretation of aerial photos (right). The various cover types are designated by: white=snow; blue=water; dark green=coniferous forest; light green=deciduous forest; red=grassland; and brown=exposed rock and soil.

Since the qualitative evaluation indicated the classification was reasonably accurate, an estimate of the areal extent of each cover type was then tabulated. Since each resolution element of the S-192 data represents an area of 0.46 hectares or 1.15 acres, an acreage estimate of the various cover types in the entire test site could be easily obtained (The tabulations required only 45 seconds of computer time for the entire 191,142 acre area). The resulting tabulation is shown in Table 3.7.

Table 3.7 -- Area Estimates for Major Cover Types in the Granite Peaks Test Site, based upon Computer Classifications of SKYLAB S-192 data.

Major Cover Type	No. Scanner Resolution Elements	No. Hectares	No. Acres
Water	2,064	959	2,369
Snow	16,852	7,828	19,343
Grassland	3,397	1,578	3,899
Coniferous Forest	109,975	51,086	126,233
Deciduous Forest	31,370	14,572	36,007
Exposed Rock & Soil	2,865	1,331	3,289
Totals:	166,523	77,354	191,142

To obtain a quantitative evaluation of this classification of major cover types, the grid of 4 x 4 resolution element test areas (described previously) were utilized. A

summary of the classification performance of these test areas is shown in Table 3.8. The number of resolution elements included within the test area in each cover type is shown in the column on the left. The cover type into which the resolution elements were actually classified is shown in the columns on the right. By comparing the number of resolution elements which were actually classified into each cover type with the total number of resolution elements designated as belonging to that cover type, a classification "accuracy" percentage can be obtained which indicates the classification performance on an individual cover type basis and for the overall classification. In this case, the overall classification performance was 85%.

This table (e.g., Table 3.8) allows one to evaluate both the inclusive and exclusive errors in the classification and determine the source of confusion in cases where the classification performance is poor. In this case, one sees that there was a considerable amount of grassland that was misclassified as deciduous forest. We do not believe that this is an inherent difficulty in accurate classification of these two cover types. We feel that this was a confusion due to the condition of the deciduous forest cover at the time of the data collection. Much of the deciduous forest cover, particularly the aspen, was not completely leafed out at the time of the SL-2 overpass. This resulted in the spectral characteristic of deciduous forest appearing like that of the grassland areas. Data collected later

Table 3.8 Classification Performance for Major Cover Types Using Four Wavelength Bands of SKYLAB S-192 Data Obtained on June 5, 1973

Cover Type Group	Number of Samples	Percent Correct	Number of Samples Classified Into:					
			Water	Snow	Grassland	Deciduous	Coniferous	Rock/Soil
Water	96	94.8	91	0	0	0	5	0
Snow	112	100.0	0	112	0	0	0	0
Grassland	128	52.3	0	0	67	28	33	0
Deciduous	368	61.7	0	0	0	227	132	9
Coniferous	1696	90.9	0	2	1	132	1542	19
Total	2400		91	114	68	387	1712	28

Overall Performance (2039/2400) = 85.0%

Wavelength bands utilized: 0.46-0.51, 0.78-0.88, 1.09-1.10, and 1.55-1.75 μm ("Best" 4)

in the growing season would have prevented some of this confusion and enabled a more accurate classification to be obtained. Also note the relatively large amount of interaction between deciduous forest and coniferous forest. We believe that this was caused in part by topographic effects and also because some areas on the ground were actually mixtures of coniferous and deciduous trees. However, because the deciduous trees accounted for a relatively small percentage of the forest canopy in these areas, they were combined with the coniferous forest category.

These results also indicate that if deciduous and coniferous forest samples were grouped into a single "forest cover" category, it would have a very high classification performance (2064/2099=98.3% correct). Thus, it would appear that forest cover as a group can be identified and mapped with a high degree of accuracy, even in this area of rugged mountainous terrain.

The exposed rock and soil category is not shown in the list of cover types on the left side of Table 3.8 because none of the statistical grid of 4 x 4 resolution element test areas fell upon a large enough area of exposed rock or soil to be included. Probably no more than a few areas of more than an acre or two exist in the test site at elevations below timber line, and since the area above timber line was covered with snow at the time of the SL-2 data collection, no exposed rock or soil areas could be included in the test samples. There were some individual resolution elements classified into this category, as indicated by the table.

In several cases, the inclusive and exclusive errors tend to balance out. For example, some of the resolution elements that should have been classified as deciduous were not (i.e., they were excluded), but some of the resolution elements that should have been classified as some other cover type were included in the deciduous category. Thus, among the entire 2400 resolution elements, 368 should have been classified as deciduous forest and a total of 386 resolution elements actually were classified as deciduous. Except for grassland, the total number of samples actually classified into the various cover types is relatively close to the number that should have been classified into that cover type. This is the basic reason why the acreage estimates obtained were relatively accurate, even when the classification did not have as high a level of accuracy.

Table 3.9 provides a more effective method of evaluating the reliability of the classification results. The classification performance (i.e., percent correct classification) for each cover type is based upon a different number of test samples. Therefore,one should not have as much confidence in a 90% accuracy, for example, if that figure was based upon 100 test samples, as a 90% accuracy figure based upon the classification of 1,000 test samples. The 95% confidence boundaries calculated for each cover type and shown in Table 3.9 provide a more meaningful indication of the classification performance than just the percent correct classification figures.

Table 3.9 95% confidence limits for SL-2 classification performance of major cover types, as shown in Table 3.8

Cover Type	No. of Samples	Percent Correct	95% Confidence Limits	
			Lower	Upper
Water	96	94.8	88.5	98.3
Snow	112	100.0	96.4	100.0
Grassland	128	52.3	42.0	62.5
Deciduous	368	61.7	56.5	66.5
Coniferous	1696	90.9	89.0	92.0

3.4.2.2 Forest Cover Types

The next phase of the analysis involved classification of the SL-2 data to obtain a forest cover type map, including each of the forest cover types indicated previously in Table 3.5. The same spectral-informational training classes that had been defined for obtaining the major cover type map were utilized. (These were listed before in Table 3.6.) The procedures followed in the classification and evaluation were the same as those described previously.

Figure 3.20 is an example of a forest cover map for a one 7½' quadrangle area, obtained through interpretation of aerial photos. Forest cover maps such as this were utilized to qualitatively evaluate the map output from the classification of the S-192 data for each of the quadrangles in the Granite Peaks Test Site. As can be seen from Figure 3.20, such forest cover maps are extremely detailed, due to the complexity of the forest cover in the test site area. There are relatively few large homogeneous stands of trees in this region, largely due to the topographic complexity of the area. The detail and complexity of this map also provides some insight into the difficulty that was encountered in obtaining accurate maps and reference data to utilize in evaluating the computer classification results.

The computer classification of forest cover type classes for the same quadrangle is shown in Figure 3.21. This is a reduction of the original 1:24,000 scale computer line printer output. Comparisons between this type of output

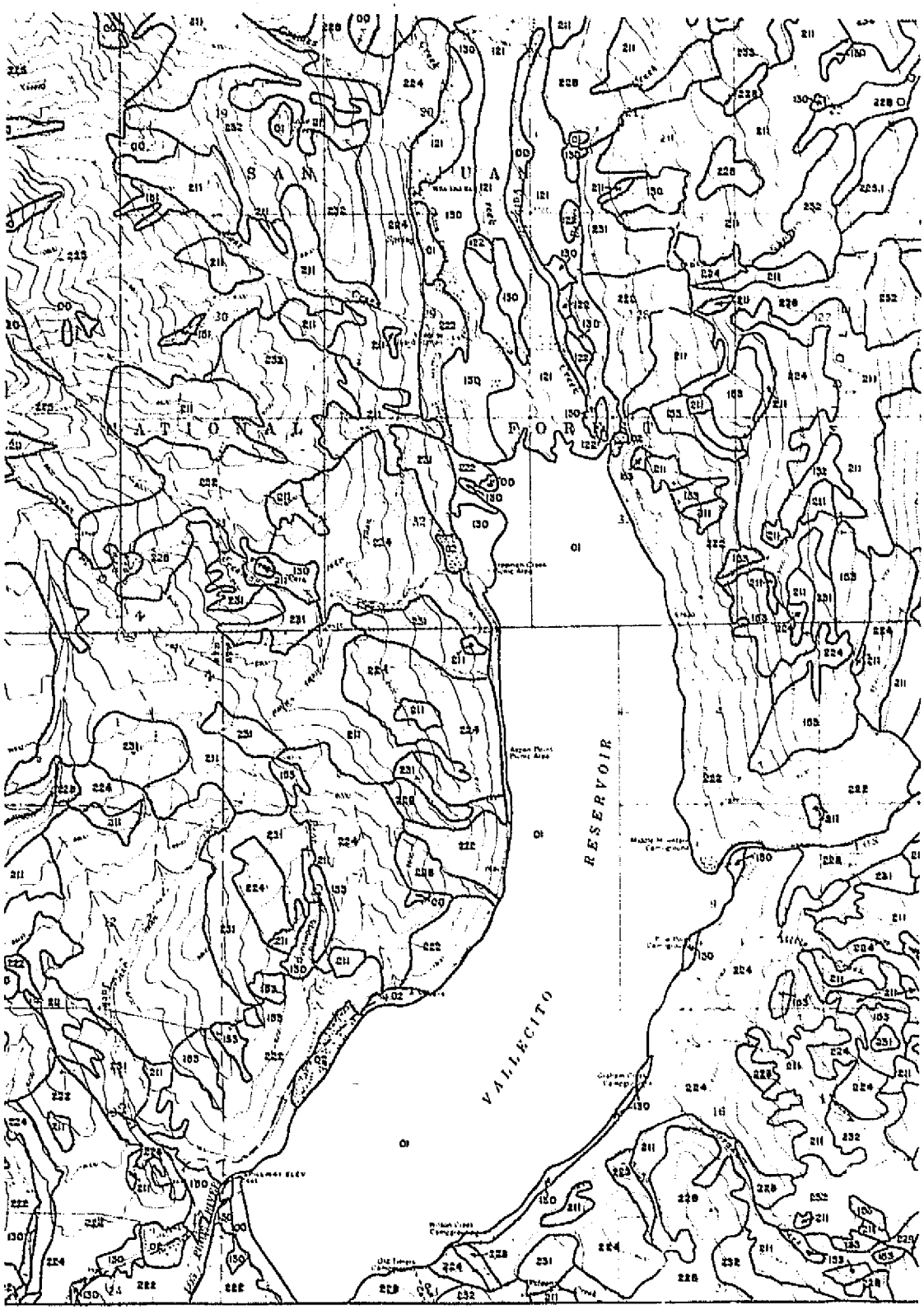

Figure 3.20 Forest Cover map for a portion of the Vallecito quadrangle, obtained by interpretation of aerial photos. The numbers indicate the various cover types (e.g. 01=water, 130=mountain/subalpine meadow, 153=oak, 211=aspen, 222=ponderosa pine, 224=ponderosa pine/Douglas fir, 228-Douglas fir/white fir, etc.)

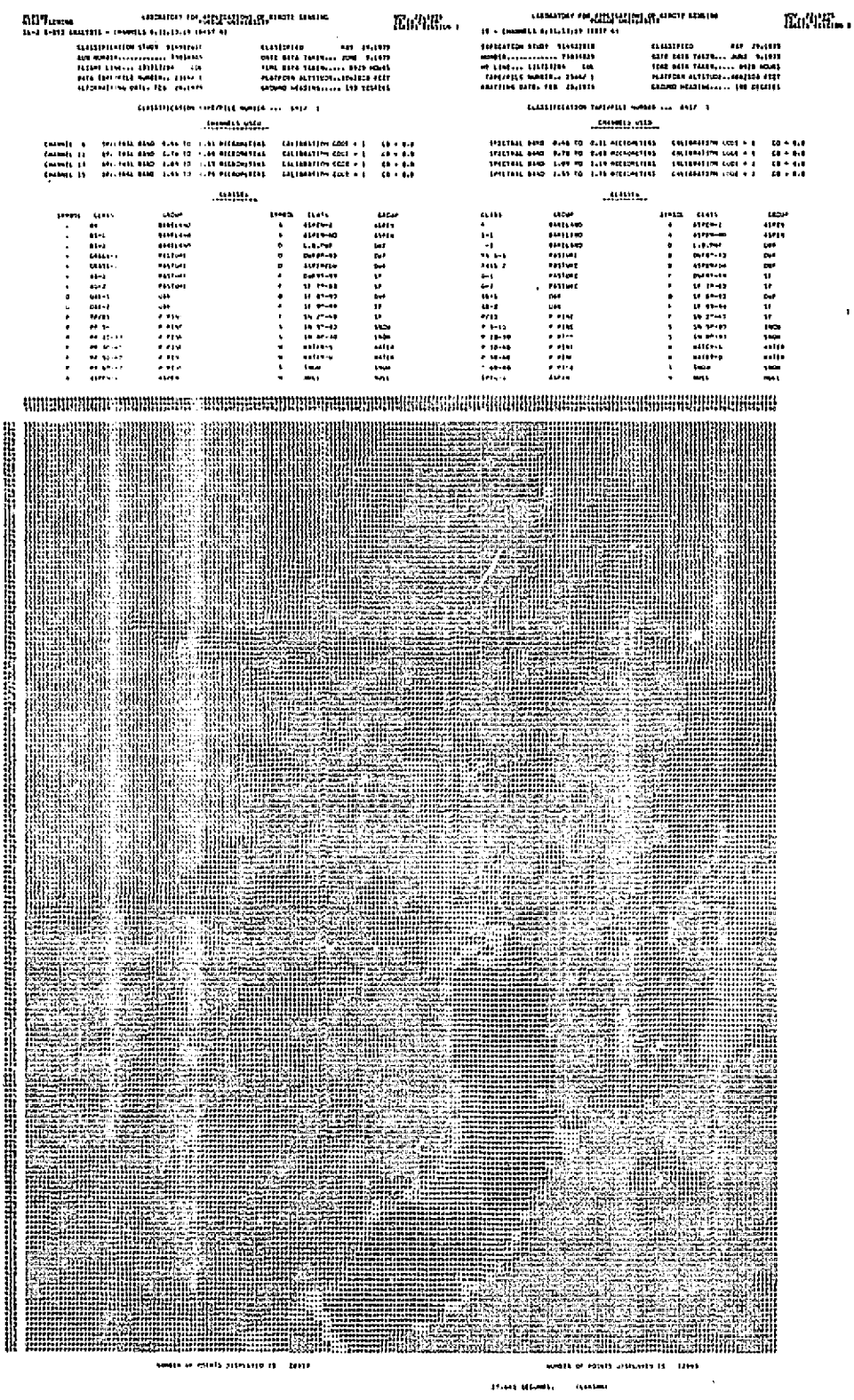

Figure 3.21 Line printer "map" showing the forest cover types in the Vallecito quadrangle obtained by computer classification of SKYLAB S-192 data collected on June 5, 1973. Original scale is 1:24,000. Scale shown is approximately 1:96,000.

and the forest cover map such as shown in Figure 3.20 was utilized to qualitatively assess the classification performance obtained for all quadrangles involved in the analysis. These figures provide an indication of the amount of detail involved in these classification maps and the difficulty of effectively assessing classification performance utilizing the qualitative evaluation approach.

The quantitative tabulation of classification results for the statistical grid of test areas in the entire Granite Peaks Test Site is shown in Table 3.10. The grid of test areas utilized was shown previously in Figure 3.17. As one might expect, the overall classification performance is not as good for this level of mapping as it was for the major cover types, i.e., 71% for forest cover types, and 85% for major cover types. In several forest cover types, we found evidence of classification error due to the effects of topographic interaction with the forest cover types.

We believe that these classification results are relatively good for forest cover type mapping, particularly when the vegetative and topographic complexity of the test site and the relatively noisy quality of the S-192 data is considered. These results are generally better than those that had been previously obtained with LANDSAT data. Therefore, for this area, a 71% classification performance should be considered significant. It is thought that with better quality MSS data and analysis techniques that allow

Table 3.10 Classification performance for forest cover types using four wavelength bands SKYLAB S-192, June 5, 1973 "Best" 4 channels 2,7,9,11

Cover Type	No. of Samples	Percent Correct	Number of Samples Classified Into:								
			Water	Snow	Grass	Oak	Aspen	P.Pine	D/W Fir	Sp/Fir	Rock/Soil
Water	96	94.8	91	0	0	0	0	0	0	5	0
Snow	112	100.0	0	112	0	0	0	0	0	0	0
Grassland	128	52.3	0	0	67	25	3	23	10	0	0
Oak	160	63.7	0	0	0	102	11	37	1	0	9
Aspen	208	54.8	0	0	0	0	114	45	33	16	0
Ponderosa Pine	432	72.9	0	0	0	31	34	315	44	0	8
Douglas and White Fir	1008	76.8	0	2	1	0	57	85	774	86	3
Spruce/Fir	256	50.0	0	0	0	0	10	9	101	128	8
TOTAL	2400		91	114	68	158	229	514	963	235	28

Overall Performance (1703/2400) = 71.0%

Wavelength bands utilized: 0.46-0.51, 0.78-0.88, 1.09-1.19, and 1.55-1.75 μm ("best" 4)

effective utilization of topographic data in conjunction with spectral data, the accuracy of computer-aided mapping of forest cover types could be improved significantly.

The confidence boundaries defined for the results of the forest cover type classification are shown in Table 3.11. Again, one sees that the range varies considerably, depending on the number of samples invovled, as well as the classification accuracy.

To evaluate the classification performance of the forest cover type using the third method described previously (comparison of area estimates), the entire test site was tabulated to determine the areal extent of each cover type. To allow for statistically assessing the accuracy of such areal estimates, this was carried out on a quadrangle by quadrangle basis. The areal estimate of each cover type for each quadrangle, based upon computer classification of the SKYLAB data, could then be compared to similar estimates based upon standard dot grid and planimeter techniques using the cover type maps obtained from interpretation of the aerial photos. The results of this comparison are shown in Table 3.12. Note that the snow and spruce-fir forest cover type have been combined on this table. This was because of the large amount of snow cover present in the test site at the time of this June 5 SKYLAB data collection pass. The tundra areas were all covered by snow, as was a large portion of the spruce-fir forest type, which is predominantly found at elevations above 3100 meters. The cover type maps had been prepared

Table 3.11 95% Confidence Limits for Classification Performances Shown in Table 3.10

	Number of Points	Percent Correct	95% Confidence Limits	
			Lower	Upper
Water	96	94.8	88.5	98.3
Snow	112	100.0	96.4	100.0
Grassland	128	52.3	42.0	62.5
Oak	160	63.7	55.0	71.5
Aspen	208	54.8	42.4	61.5
Ponderosa Pine	432	72.9	68.1	76.1
Douglas and White Fir	1008	76.8	73.5	79.1
Spruce/Fir	256	50.0	43.5	56.5

Table 3.12 Comparison of Area Extimates (Hectares) Obtained From Cover Type Maps (CTM) and Computer-Aided Analysis Techniques (CAAT)

Quadrangle		Exposed	Water	Grassland	Oak	Aspen	Ponderosa	Douglas and White Fir	Spruce/Fir and Snow
Vallecito Reservoir	CTM	449	1160	1021	340	2862	774	5368	3496
	CAAT	155	928	232	108	1609	2553	5740	4146
Granite Peak	CTM	495	0	124	15	990	0	4131	9716
	CAAT	217	31	46	31	1129	1006	5198	7813
Ludwig Mtn.	CTM	170	139	2290	3945	1114	5616	2181	15
	CAAT	665	0	1114	4409	1067	6159	1887	170
Baldy Mtn.	CTM	0	16	542	2058	2243	3264	5136	2212
	CAAT	186	0	93	2150	2259	6312	2924	1547
Devil Mtn.	CTM	15	0	263	402	1887	2831	8772	1300
	CAAT	108	0	93	317	1439	4084	8354	1021
TOTALS	CTM	1129	1315	4240	6760	9096	12485	25588	16739
	CAAT	1331	957	1578	7069	7503	20114	24103	14697

from aerial photos obtained later in the summer, and therefore showed almost no snow cover but did have large areas designated as tundra. Thus, the computer classification results showed large areas of snow cover and relatively small areas designated as spruce/fir forest type, whereas the cover type maps showed large areas of tundra and relatively large areas of spruce/fir forest type, but almost no snow cover. Therefore, the areas from the photo interpretation maps designated as tundra, permanent snow fields, and spruce/fir were combined and compared to the acreage figures for the combination of snow cover and spruce/fir obtained from the classification of SKYLAB data. As can be seen from Table 3.12 in many cases the acreage estimates from the two sources are rather close, but in many other cases, there are significant differences. However, for a large geographic area, an overestimate of one cover type in one quadrangle is often balanced out by an underestimate of the same cover type in another quadrangle. This is indicated by the total acreage estimates shown at the bottom of the table.

A more meaningful indication of the relationship between the area estimates obtained through the use of computer-aided analysis techniques utilizing the SKYLAB data and the area estimates obtained from cover type maps and aerial photography is shown in Figure 3.22. This figure compares the area obtained by computer-aided analysis for each cover type within each quadrangle to the area obtained by photo-interpretation techniques for the same cover type and the same

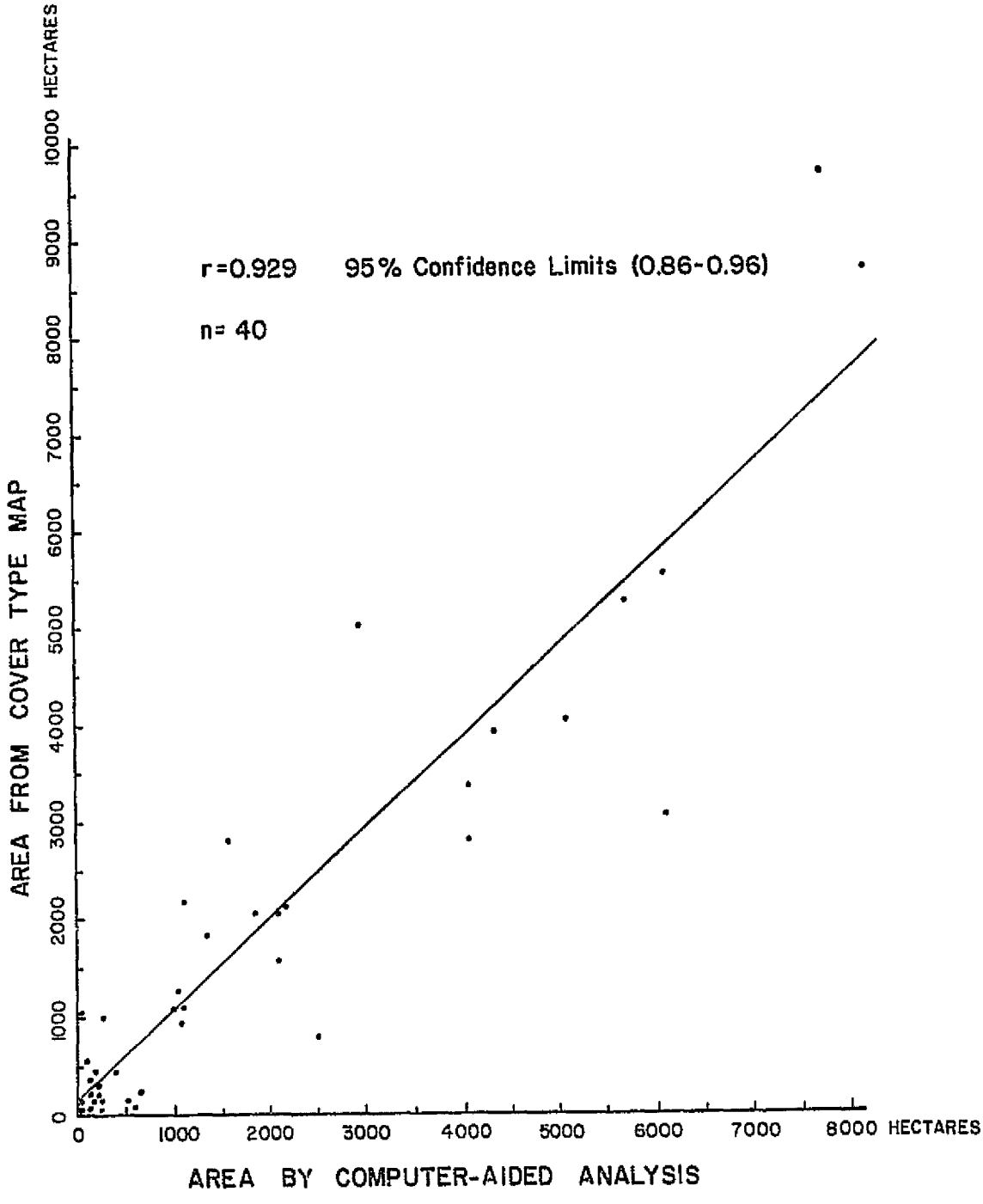

Figure 3.22 Comparison of area estimates obtained from cover type maps and computer-aided analysis of SKYLAB S-192 data

quadrangle. A linear regression was calculated and is also shown. The correlation coefficient between the two data sets was determined to be 0.929, indicating a strong relationship between the acreage estimates obtained by the computer-aided analysis techniques and those obtained by photo-interpretation techniques. The 95% confidence limits for this correlation coefficient are 0.86 and 0.96 (which indicate the range within which the correlation coefficient should be found in 95% of the cases).

The high degree of correlation between these two estimates is considered quite significant. The estimates are similar to the correlation that had been achieved previously during the LANDSAT-1 investigation. Thus, this is not an isolated, single example showing such a high correlation between satellite data analysis results and aerial photo-interpretation data.

These results indicate that acreage estimates of forest cover types, based upon computer-aided analysis of multispectral scanner data obtained from satellite altitudes are quite accurate, provided that areas of reasonable size are involved (i.e., several thousand acres). These results are believed to be of major significance, insofar as forest cover type mapping utilizing remote sensing techniques are concerned.

3.4.3 Classification of the SL-3 MSS Data

As pointed out previously, the S-192 data obtained on August 8, 1973, during the SKYLAB SL-3 mission, was geometrically corrected and overlayed onto the same X - Y grid data base that had been defined for the SL-2 data. This allowed the same training area locations that had been defined during the analysis of the SL-2 data to be utilized for developing training statistics for the SL-3 data. Also, the overlayed data allowed the same test areas that had been used in evaluating the SL-2 data to be utilized for evaluation of the SL-3 data. Therefore, within the area of overlap between SL-2 and SL-3, a very accurate comparison between the classification results between the two data sets could be achieved. There was a small section of the Granite Peaks Test Site that was not present on both of the data sets, so that some of the test areas used in the SL-2 analysis could not be utilized for the SL-3 data, but this was not believed to be a significant problem.

It was decided that since four wavelength bands had been utilized for the SL-2 data classification, four wave length bands should also be utilized for classifying the SL-3 data set. However, the particular combination of wavelength bands could vary between the two classifications, so that the optimal or "best" four bands would be utilized in each classification. For the SL-3 data, the feature selection processor indicated that the 0.52-0.56, 0.98-1.03, 1.09-

1.19, and 1.55-1.75 μm wavelength bands (channels 3,8,9, and 11) would provide the optimal combination of four wavelength bands for the classification. It is significant that the 1.09-1.19 and 1.55-1.75 wavelength bands had also been among the "best" four selected for the analysis of the SL-2 data. For the other two wavelength bands, in the SL-2 analysis, channel 2 was selected rather than channel 3, and channel 7 was selected rather than channel 8. In both cases, the "best" four wavelength bands defined included one band in the visible region, two bands in the near infrared, and the 1.55-1.75 band in the middle infrared. This apparent emphasis on the value of the near infrared region is considered significant in relation to the tentative selection of wavelength bands for the Thematic Mapper on LANDSAT-D.

The classification results are shown in Table 3.13 for the basic cover type (land use) classification, and in Table 3.14 for the forest cover type classification.

As both of these tables show, the classification results from the SL-3 data have a much lower accuracy than those obtained from the SL-2 data. The classification performance for the oak and Douglas/White Fir classes were both more than 30% lower in the SL-3 classification as compared to the SL-2 results These results were contrary to the expected results for two reasons. First, the results of the photo interpretation effort indicated that the various forest cover types could be defined and mapped much more accurately with the color IR photos obtained on August 8 during the SL-3 mission than with the color IR photos ob-

Table 3.13 Classification Performance For Major Cover Types Using Four Wavelength Bands of SKYLAB S-192 Data Obtained on August 8, 1973

Cover Type	No. of Samples	Percent Correct	Number of Samples Classified Into:				
			Water	Pasture	Deciduous	Coniferous	Rock/Soil
Water	96	97.9	94	0	0	2	0
Pasture	48	43.8	0	21	20	6	1
Deciduous	336	63.1	0	32	212	84	8
Coniferous	1504	69.0	0	14	445	1038	7
TOTAL	1984		94	67	667	1130	16

Overall Performance (1365/1984) = 68.8%

Wavelength Bands Utilized: 0.52-0.56, 0.98-1.08, 1.09-1.19, and 1.55-1.75 μm ("Best" 4)

C-3

ORIGINAL PAGE IS
OF POOR QUALITY

Cover Type	No. of Samples	Percent Correct	Number of Samples Classified Into:							
			Water	Grassland	Oak	Aspen	P.Pine	D/W Fir	Spruce/Fir	Rock/Soil
Water	96	97.9	94	0	0	0	0	0	2	0
Grassland	48	43.8	0	21	10	10	3	3	0	1
Oak	96	30.2	0	10	29	32	10	11	0	4
Aspen	240	58.7	0	22	10	141	8	39	16	4
Ponderosa Pine	240	72.5	0	2	0	41	174	23	0	0
Douglas/ White Fir	1008	42.5	0	9	2	371	102	428	92	4
Spruce/Fir	256	28.9	0	3	0	31	29	116	74	3
TOTAL	1984		94	67	51	626	326	620	184	16

Overall Performance (961/1984) = 48.4

Wavelength Bands Utilized: 0.52-0.56, 0.98-1.08, 1.09-1.19, and 1.55-1.75 μm ("Best" 4)

Table 3.14 Classification Performance for Forest Cover Types using Four Wavelength Bands of SKYLAB S-192 Data obtained on August 8, 1973.

tained on June 5 during the SL-2 mission, in spite of the fact that the SL-3 photographs were somewhat underexposed. Since the photointerpretation results indicated the August data would be much better for mapping forest cover types, we had anticipated that the August SL-3 data would also allow a more accurate computer classification to be obtained when utilizing the S-192 MSS data. This obviously did not prove to be the case.

The second reason for anticipating an improvement in classification performance with the SL-3 data was the fact that the SL-2 data had not been put through the digital filtering process which had been developed by J. S. C. to improve the noise characteristics in the data, whereas, the SL-3 data set provided to us for this investigation had been digitally filtered. Thus, we had anticipated an improvement in the quality of the SL-3 data. The apparent decrease in classification performance for the SL-3 data was therefore disappointing and somewhat puzzeling at first. Additional analysis attempts using a different combination of training statistics did not result in improvement in the classification performance.

The reason for the relatively poor classification results when utilizing the SL-3 S-192 data can be seen in Figure 3.23. This figure shows two individual wavelength bands of S-192 data. Notice the sequence of dark linear features beside each of the clouds in the S-192 band 2 data, but not in band 6. These dark areas were not found on the

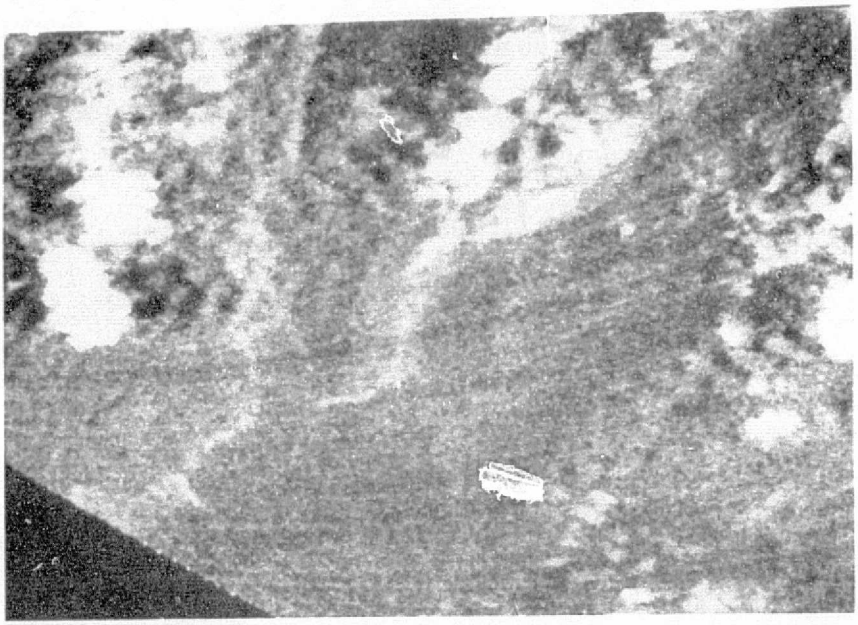

Band 2

Band 6

Figure 3.23 SL-3 data showing the "ringing" effects which caused decreased classification accuracy

S-190 photographic data, but could be observed in several wavelength bands of the S-192 data. Conversations with NASA scientists indicated that the digital filtering process (which had been applied to this set of S-192 data) sometimes causes a "ringing" effect in the data around high contrast objects, such as clouds. Thus, noise has been added to the data in a very irregular manner. It is neither random or systematic noise, and it is particularly bad when there are many clouds, patches of snow, lakes, or other high contrast objects present. In this case, there were quite a few clouds present in the SL-3 data over the Granite Peaks Test Site. Since this problem of data quality was not discovered until relatively late during the contract period, there was insufficient time remaining to request an unfiltered data set to see if it would allow more accurate classification results to be obtained. Apparently, the ringing effect had also been encountered in some of the data sets that had been processed for other investigators, so this was not a phenomena first seen in this particular data set.

Because of the apparent degredation in data quality and resultant poor classification results, and because there were a number of clouds present in the SL-3 data sets, it was decided to utilize only the SL-2 data for the remainder of the investigation, particularly the wavelength band study. Thus, even though the photo interpretation results indicated that the August time period is better than June for vegetation map-

ping, the August (SL-3) S-192 data available was not as good quality as the June (SL-2) data. The relatively poor quality of the SL-3 data made further analysis of this S-192 data set impractical.

3.4.4 Comparison of SKYLAB and LANDSAT Classification Results

The fact that we had been able to successfully overlay the SKYLAB multispectral scanner data with the LANDSAT multispectral scanner data and that both data sets had been collected by satellite on the same day allowed a unique opportunity to compare the classification results obtained from each data set. Qualitative evaluation of the LANDSAT and SKYLAB data indicated that the LANDSAT data had a very good signal-to-noise ratio, better than that of the SKYLAB data. However, the wavelength bands of the SKYLAB data were narrower, thereby providing a better spectral resolution. In addition, the middle infrared and thermal infrared portions of the spectrum were present on the SKYLAB data, but not on the LANDSAT data. We believed that this difference in spectral range available might have a significant impact on the results obtained.

To eliminate as many variables as possible in the comparison, only four wavelength bands of SKYLAB data would be

utilized for the classification, since only four wavelength bands of LANDSAT data were available Therefore, for the first classification with the SKYLAB data, the "best" four wavelength bands defined by the feature selection processor were utilized. This classification involved both the major cover types and the forest cover type levels of detail. The classifications involving the optimum combination of four wavelength bands of SKYLAB data have already been discussed. These classifications resulted in an 85% overall classification performance for the major cover types and a 71% classification performance for the forest cover types (Section 3.4.2).

The next classification sequence involved the four wavelength bands of SKYLAB data that were as similar to the wavelength bands available on the LANDSAT scanner system as possible. In this case, the 0.52-0.56, 0.62-0.67, 0.68-0.76, and 0.98-1.03 μm wavelength bands (channels 3,5,6, and 8) of the SKYLAB data were utilized. The training areas were the same as used previously with the optimum combination of four wavelength bands. The same test areas were used to evaluated all classification sequences. These classifications resulted in an overall performance of 82.5% for the major cover types and 60.2% for the forest cover types.

The final classification sequence involved the LANDSAT data. The four wavelength bands available on LANDSAT included the 0.5-0.6, 0.6-0.7, 0.7-0.8, and 0.8-1.1 μm bands. These four wavelength bands were utilized with the same

training areas that had been used for the SKYLAB analysis to classify the LANDSAT data. The same test areas as used previously with SKYLAB data were utilized to evaluate the classification results. The classification results for the LANDSAT data indicated an overall performance of 85.7% for the major cover type classification and 68.4% for the forest cover type classification. The results of the three classifications of major cover types (or land use classes) are shown in Table 3.15, along with the results obtained for the forest cover types classifications. As this table shows, there is little difference between the three classification results at the major cover type level, but there is a significant difference at the forest cover type level. The fact that the best four wavelength bands from the SKYLAB data set did not allow a significant improvement in the classification performance for the major cover type classification was rather surprising. The spectral resolution of the SKYLAB wavelength bands is better than the LANDSAT wavelength bands, and the additional spectral region involving the middle infrared portion of the spectrum was utilized in this classification. Therefore, the SKYLAB data should have given a higher classification performance. We believe that the reason that the SKYLAB "Best" four results are essentially the same as the LANDSAT results lies in the fact that the data quality (signal/noise ratio) on the SKYLAB data was poorer than that on the LANDSAT data. Therefore, the improved spectral resolution and the spectral range available in the SKYLAB data was offset by the poorer quality

Table 3.15 Comparison of Classification performance using SKYLAB and LANDSAT MSS data

Data Utilized	Wavelength Bands Utilized	Overall Classification Performance	
		Major Cover Types	Forest Cover Types [1]
"Best" 4 Wavelength Bands of SKYLAB Data	0.46-0.51, 0.78-0.88, 1.09-1.19, 1.55-1.75 μm	85.0%	71.0%
SKYLAB Data Using Wavelength Bands that Correspond to LANDSAT	0.52-0.56, 0.62-0.67 0.68-0.76, 0.98-1.08 μm	82.5%	60.2%
LANDSAT Data	0.5-0.6, 0.6-0.7, 0.7-0.8, 0.8-1.1 μm	85.7%	68.4%

1 The same test areas were utilized to evaluate all six classifications

of the data available.

When comparing the results obtained for the forest cover type classification sequence, one sees that the optimal or "best" four wavelength bands of SKYLAB data gave an overall classification somewhat higher than that obtained from the LANDSAT data. The results using the SKYLAB wavelength bands corresponding to those on LANDSAT were significantly lower than either of the other classification results. This indicates that for more detailed analysis, such as that involved with classifying individual forest cover types, the improved spectral resolution and spectral range on the SKYLAB scanner system had a significant impact on the results. The fact that the four wavelength bands of SKYLAB data that corresponded to those available on LANDSAT produced results that were lower would indicate that the poorer data quality in the SKYLAB data did have a significant impact on the classification results.

These results indicate that if the SKYLAB data quality had been comparable to that of the LANDSAT data, the improved spectral resolution and spectral range available on SKYLAB would have allowed a significant improvement in classification performance when individual forest cover types were involved, and at least a modest improvement in classification performance for major cover types. In interpreting these results, however, it is important to remember that the classification performance figures that were obtained are

heavily influenced by the types of materials involved in the classification. Also, these results involve a set of SKYLAB data that had been line-straightened, but had not been put through the digital filtering program developed at J.S.C. to improve the data quality of the SKYLAB data.

We feel that these results offer significant evidence for a need of better spectral resolution and spectral range than is available in the LANDSAT data. These results tend to indicate that the improved spectral resolution and the spectral range tentatively specified for the Thematic Mapper to be installed on LANDSAT-D have tremendous promise for increasing our capability to accurately map vegetative cover types with satellite multispectral scanner data.

3.5 Wavelength Band Evaluation

3.5.1 Introduction

One of the major phases of this SKYLAB investigation involved a series of analyses to determine the relative value of the various wavelength bands and spectral regions for accurately classifying the cover types and forest species present in the test site area. This work involved three major analysis sequences. The first sequence involved classification of the data for major cover types and also forest cover types, utilizing the "best" 1 through 13 wavelength bands for the classifications. The second phase of this work involved evaluation of the importance of individual wavelength bands for accurately classifying various forest and other cover types. The third analysis sequence involved determination of the importance of the different spectral regions for accurately classifying the various major cover types and forest cover types.

3.5.2 Classification Performance Versus Number of Wavelength Bands Utilized

In the first analysis sequence, classification results for both major cover types and forest cover types were obtained when 1 through 13 wavelength bands were utilized in the classification. The feature selection processor of LARSYS was utilized to select the "best" single wavelength band to use for classification, then the "best" combination of two wavelength bands, the "best" combination of three wavelength bands, etc. These various combinations of "n" wavelength bands were then utilized to classify the data.

The data were classified and the results tabulated using the set of test fields previously defined. Overall performance figures were obtained for each number of wavelength bands utilized. Figure 3.24 shows the results of this analysis sequence. For purposes of comparison, this figure shows the test field results of the classification using LANDSAT data (four bands involving the 0.5-0.6, 0.6-0.7, 0.7-0.8, and 0.8-1.1μm wavelengths). The classification results using the four wavelength bands of SKYLAB data that most closely approximated the LANDSAT data (0.52-0.56, 0.62-0.67, 0.68-0.76, and 0.98-1.08μm wavelength bands) are also included in this figure. As indicated in Figure 3.24, the classification of Major Cover Types (or Land Use Categories) resulted in classification performance ranging from approximately 76 to 86%, whereas the more complex classification of individual Forest Cover Types resulted in classification performances ranging from 48 to 71%. In both cases, the classification is relatively low when only a single channel was utilized, as might be expected.

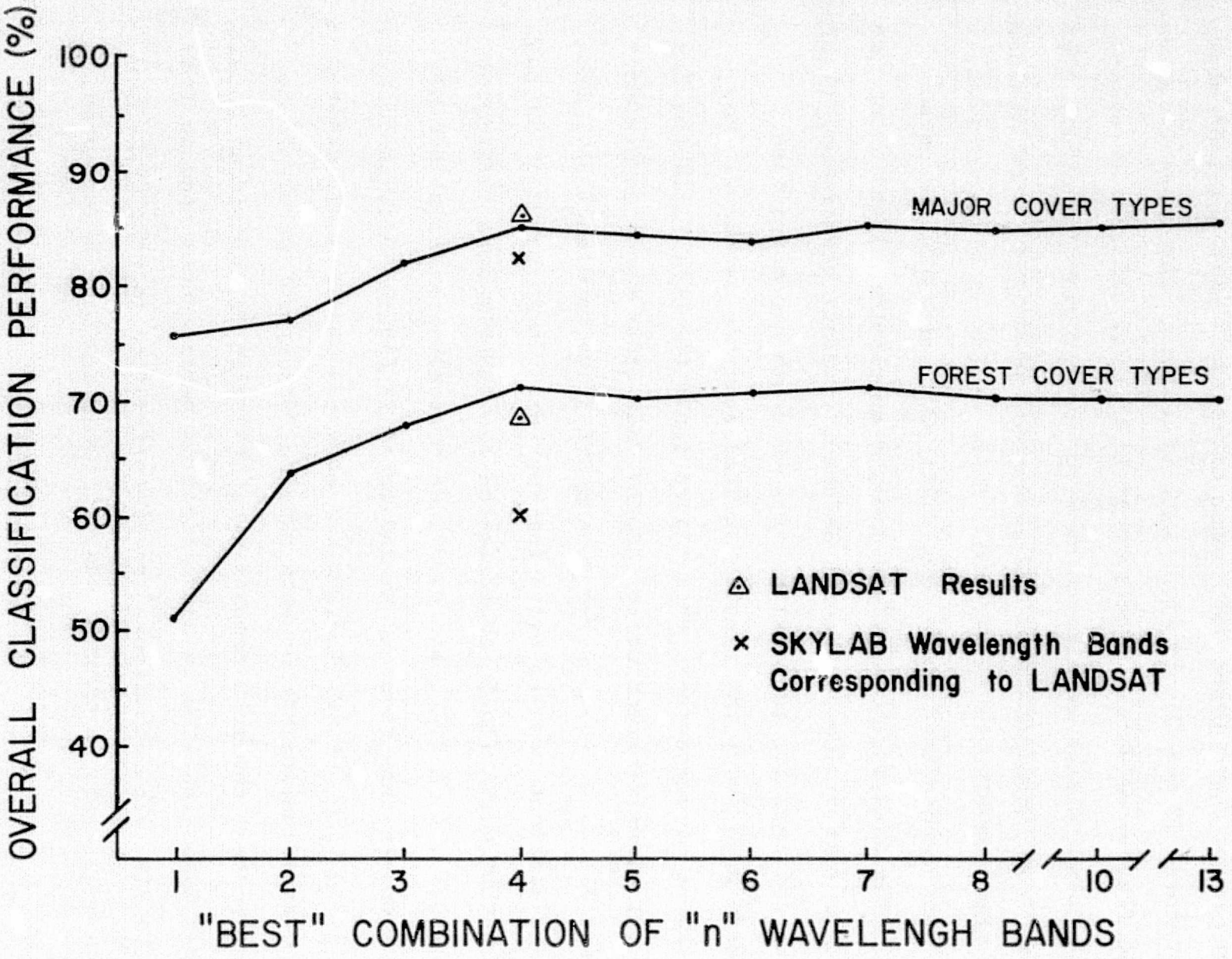

Figure 3.24 Overall classification performance versus number of wavelength bands utilized

When two, and then three wavelength bands were utilized, the classification performance increased significantly, and the highest classification performance was achieved when four or more wavelength bands were utilized. A slight decrease in classification performance occurred when five or six wavelength bands were utilized, but the differences in classification performance when more than four wavelength bands were used are not considered to be significant.

The results of this analysis sequence substantiate earlier work, both theoretical and emperical, which indicated that significant improvements in classification accuracy are not obtained when more than four wavelength bands are utilized in the classification (Coggeshall & Hoffer, 1973). However, the amount of computer time increases significantly as more wavelength bands are used to classify the data, as shown in Figure 3.25. This particular figure resulted from a classification sequence involving twelve wavelength bands of aircraft MSS data, and clearly shows that relatively small increases in classification performance were obtained when more than six or even four wavelength bands were utilized, but the classification time (and therefore the cost) increased rapidly as more and more channels (wavelength bands) were utilized. Thus, there is a clear need to define the point of diminishing returns, where the small improvement in classification accuracy achieved by using additional numbers of wavelength bands is not worth the cost of the additional computer time involved. The overall results of the SKYLAB analysis sequence indicated that four wavelength bands would be optimal. However to achieve maximum classification accuracy for individual cover types,

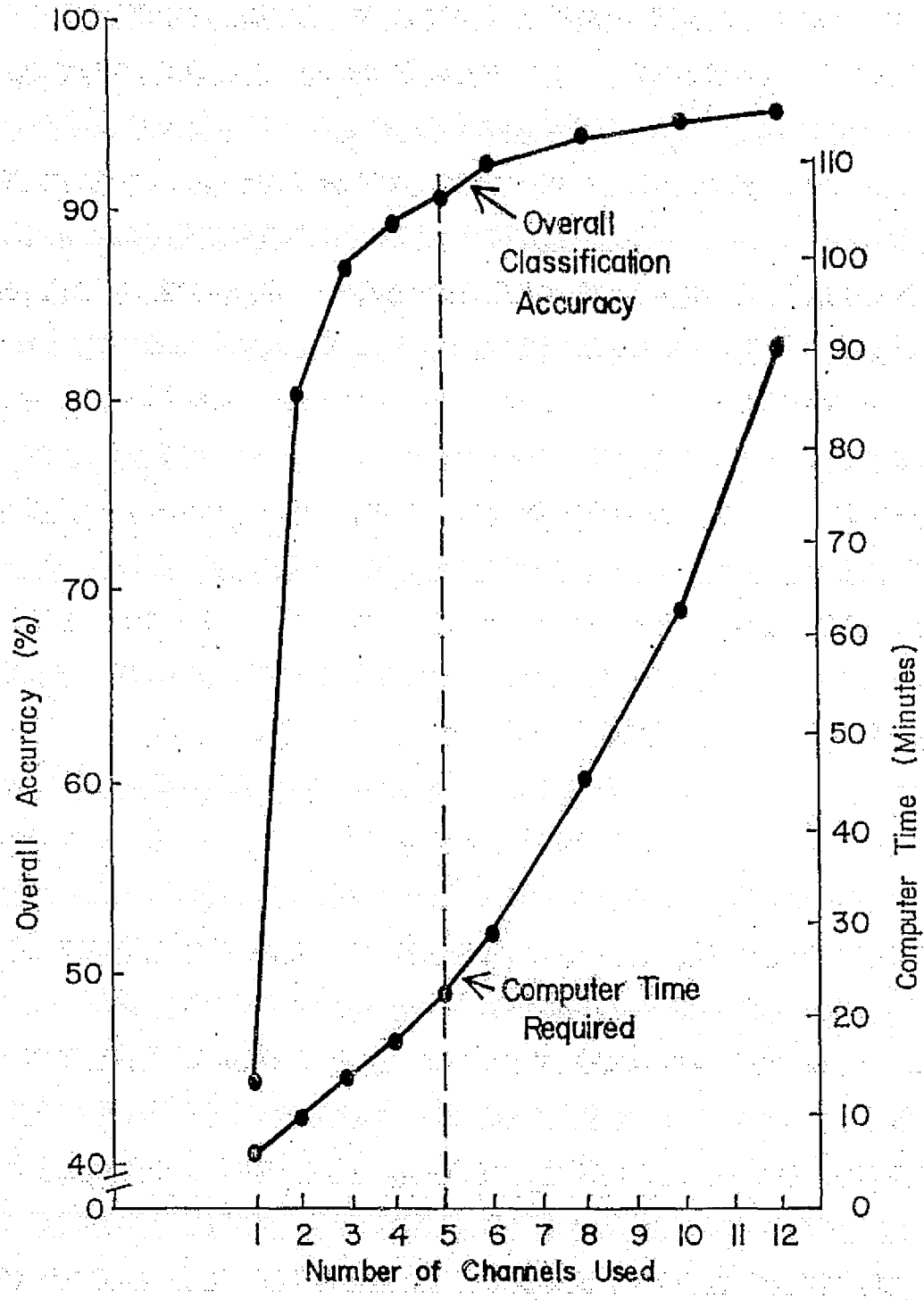

Figure 3.25 Overall classification accuracy and computer time required versus number of channels used. (From Coggeshall and Hoffer, 1973).

different combinations of four wavelength bands might be required for the various cover types.

The last part of this first phase of the wavelength band study involved examination of the individual wavelength bands that were designated by the feature selection processor. Tables 3.16 and 3.17 show which wavelength bands were defined by the feature selection processor as the optimal combinations of wavelength bands to be used in the classification sequence. These tables also show the overall classification performance obtained when the various numbers of wavelength bands (or "channels") were utilized. Table 3.16 contains the results for the major cover types, and Table 3.17 provides the results for the forest cover types. The results for the individual forest cover type classification gave the same sequence of wavelength bands since both classification sequences were based on the statistics for the same 31 spectral-informational training classes.

As can be seen from Table 3.16, the 1.09 to 1.19 wavelength band was selected as the single best wavelength band. Also note that the wavelength bands selected for the best four combination included only those channels which had a very good signal to noise ratio (as expressed by a low data quality index), indicating that the data quality in these channels were relatively good as compared to some of the other channels. However, when the best combination of five wavelength bands was defined, the 0.56 to 0.61 wavelength band was selected. This channel has a very poor data quality index and yet it was selected ahead of some of the other channels that had a better data quality. This would seem to indicate that

Table 3.16 Wavelength Band Selection Sequence For Major Cover Types, Using SKYLAB S-192 Data Obtained on June 5, 1973

Spectral Regions		Visible					Near Infrared					Middle Infrared		Thermal	Overall Classification Performance
Channel Number		1	2	3	4	5	6	7	8	9	10	11	12	13	
Wavelength Band		0.41 to 0.46	0.46 to 0.51	0.52 to 0.56	0.56 to 0.61	0.62 to 0.67	0.68 to 0.76	0.78 to 0.88	0.98 to 1.08	1.09 to 1.19	1.20 to 1.30	1.55 to 1.75	2.10 to 2.35	10.20 to 12.50	
Data Quality Index		7.13	1.99	1.79	14.85	12.12	4.08	2.24	5.59	1.76	6.21	1.59	2.93	11.86	
Number of "Best" Channels	1									X					75.7
	2		X							X					76.8
	3		X					X		X					81.9
	4		X					X		X		X			85.0
	5		X		X			X		X		X			84.1
	6		X		X			X		X		X		X	83.7
	7		X		X			X		X		X	X	X	85.3
	8	X	X		X			X		X		X	X	X	84.1
	10	X	X		X			X		X	X	X	X	X	85.2
	13	X	X	X	X	X	X	X	X	X	X	X	X	X	86.0

Table 3.17 Wavelength Band Selection Sequence For Forest Cover Types, Using SKYLAB S-192 Data Obtained on June 5, 1973

Spectral Regions		Visible					Near Infrared					Middle Infrared		Thermal	Overall Classification Performance
Channel Number		1	2	3	4	5	6	7	8	9	10	11	12	13	
Wavelength Band		0.41 to 0.46	0.46 to 0.51	0.52 to 0.56	0.56 to 0.61	0.62 to 0.67	0.68 to 0.76	0.78 to 0.88	0.98 to 1.08	1.09 to 1.19	1.20 to 1.30	1.55 to 1.75	2.10 to 2.35	10.20 to 12.50	
Data Quality Index		7.13	1.99	1.79	14.85	12.12	4.08	2.24	5.59	1.76	6.21	1.59	2.93	11.86	
Number of "Best" Channels	1									X					48.1
	2		X							X					63.8
	3		X					X		X					67.7
	4		X					X		X		X			71.0
	5		X		X			X		X		X			70.0
	6		X		X			X		X		X		X	70.4
	7		X		X			X		X		X	X	X	71.0
	8	X	X		X			X		X		X	X	X	70.4
	10	X	X		X			X	X	X	X	X	X	X	70.8
	13	X	X	X	X	X	X	X	X	X	X	X	X	X	70.4

the information content available in this channel is significant, and that the spectral information content in the various wavelength bands can be a more important factor than the data quality. It is also possible that the relatively poor data quality in this channel may, in part, be responsible for the decrease in overall performance of the classification result when five rather than four bands were utilized. If the data quality had been better for this wavelength band, the overall accuracy might have gone up instead of showing the slight decrease indicated. The same comments could be made in respect to the selection of the thermal channel when the optimum combination of six channels were defined by the feature selection processor. It is apparent from the high data quality index and by looking at the imagery shown previously (Figure 2.17) that the thermal channel is of relatively poor data quality, yet this channel was among the first six selected for the classification procedure, apparently because of its information content. Again, it seems reasonable that if the data quality in the thermal channel had been better, the classification performance would have been better.

Since these results seem to indicate that a reasonably good classification performance can be achieved with a combination of four wavelength bands, it was decided to carry out the remainder of the wavelength band evaluation classifications using various combinations of four wavelength bands.

3.5.3 Channel Selection Sequence

The next phase of this wavelength band evaluation study involved the examination of the ability of each of the individual channels to spectrally discriminate between the various cover types present in the study area. This phase of the analysis took two forms. The first was to compare the average separability value for each cover type against all other cover types on a wavelength band by wavelength band basis. These results are shown in Table 3.18. Each column in Table 3.18 has one wavelength band that is marked with an asterisk and one marked with a small circle. The asterisk indicates the wavelength band that is best for separating that particular cover type from the average of all other cover types. The circle indicates the wavelength band which is the poorest for separating that cover type from the other cover types. Because of the extremely poor data quality of channel 1, it was not evaluated in this table. In reviewing this data set, it becomes apparent that the channel 9 data (1.09-1.19μm) allows optimal separation between many of the cover types, and that the channel 5 wavelength band (0.62-0.67μm) has the poorest separation among many of the different cover types. In some cases, the same wavelength band is best for identifying certain cover types and relatively poor for others. For example, the Douglas/White Fir cover type can best be defined using Channels 6 (0.68-0.76μm), but at the same time Channel 6 is poorest for separating the Exposed Rock/Soil from all other cover types. This provides some indication of the complexity of the problems involved in defining the optimal combination of wavelength bands for classification of a variety of cover types in a topographically complex

Table 3.18 Average spectral seperability in each wavelength band of individual cover types versus all other cover types, based upon training statistics from SL-2 data

Channel Number	Spectral Region	Wavelength Band	Water	Snow	Grassland	Oak	Aspen	P. Pine	D/W Fir	Spr/Fir	Rock/Soil
1		0.41-0.46	363	1813	337	282	287	339	291	368	299
2		0.46-0.51	807	1969	721	592	516	770	677	875	926
3	Visible	0.52-0.56	661	7000*	594	584	479	656	830	646	900
4		0.56-0.61	527	1421	526°	549	550	604	815	579	1666*
5		0.62-0.67	402°	1826	537	529°	403°	518°	677	484°	907
6		0.68-0.76	1428	1978	1272	959	726	801	1669*	654	741°
7		0.78-0.88	1817	1761	1562*	1296	847	1017	1287	874	833
8	Near IR	0.98-1.08	1889	1690	1479	1221	981	1055	1210	1279	981
9		1.09-1.19	1971*	1585	1510	1516*	1261*	1413*	1497	1709*	1102
10		1.20-1.30	1745	909°	1191	1018	1005	946	1035	1552	849
11	Middle IR	1.55-1.75	1313	1337	1049	1329	946	1042	1193	1338	1399
12		2.10-2.35	961	1001	758	1196	817	889	825	1133	1458
13	Thermal IR	10.2-12.5	755	1212	593	718	516	573	518°	965	795
Elevation			1975	1616	1175	1078	1239	1098	1054	1389	1607

area. One can see from this table that snow and exposed soil can best be differentiated from the other cover types using channels in the visible wavelength region. The near infrared portion of the spectrum is optimum for separating various vegetative cover types from the other materials in the test site area and for separating water from other cover types.

This first approach, involving the average separability for each cover type as compared to the average for all other cover types, provides some insight into the value of the various wavelength bands, but does not effectively indicate the ability to utilize various wavelength bands to discriminate between individual cover types present in the test site area. In other words, the results shown in Table 3.18 show for example, that the 1.09-1.19μm wavelength band is best for separating spruce/fir from the average of all other cover types, but it doesn't indicate which wavelength band is best for separating spruce/fir from Douglas and white fir or from ponderosa pine, etc. Therefore, the next phase of this analysis involved an attempt to quantitatively define the ability to spectrally discriminate individual cover types on a wavelength band by wavelength band basis.

As a first step in this analysis, the separability program was again utilized, but this time individual forest cover types were compared. In this way, the effects of non-forest cover types would be minimized, and the wavelength bands of most significance for separating individual forest cover types could be defined. The results of this analysis sequence are shown in Table 3.19.

Table 3.19 Seperability of individual forest cover types as a function of spectral differences in individual wavelength bands

Wavelength Region	Visible					Near Infrared					Middle Infrared		Thermal	Elevation
Channel Number	1	2	3	4	5	6	7	8	9	10	11	12	13	
Wavelength Band	0.41 to 0.46	0.46 to 0.51	0.52 to 0.56	0.56 to 0.61	0.62 to 0.67	0.68 to 0.76	0.78 to 0.88	0.98 to 1.08	1.09 to 1.19	1.20 to 1.30	1.55 to 1.75	2.10 to 1.35	10.20 to 12.50	
Forest Cover Types Compared	Separability Indicator													
Oak VS Aspen							-	-	-	-			-	
Oak VS P Pine									-		-			
Oak VS DWF				-		-	+	+	‡	-	‡	+		
Oak VS Spr/Fir		-					-	+	‡	‡	‡	‡	+	+
Aspen VS P Pine														-
Aspen VS D/WFir										-	-			
Aspen VS Spr/Fir									-	+	‡	+	-	
P Pine VS D/WFir							-	-	-		-			
P Pine VS Spr/Fir		-						-	‡	+	‡	+	-	+
D/WFir VS Spr/Fir		-									-			-

1. Seperability Indicator is based upon the following values:

   Blank = Not Separable

   - = Partially Separable (1000 < Divergence < 1500)

   + = Separable (1500 < Divergence < 1800)

   ‡ = Very Separable (Div 1800)

In this analysis, divergence values were utilized as a measure of separability. Divergence values of less than 1000 indicate that the two forest cover types cannot be spectrally separated. Values of 1000-1500 indicate some separability is possible, but not very reliable. Reasonably good separability occurs if divergence values are between 1500-1800, and quite reliable spectral differentiation is obtained if the divergence values are over 1800.

The results shown in Table 3.19 are significant in that they clearly indicate the value of the middle infrared and near infrared wavelength regions for spectrally separating individual forest cover types. It is also significant that the longer wavelength bands within the near infrared portion of the spectrum are generally better than the shorter wavelength bands within this region. This should be considered in selecting the specific locations of the wavelength bands to be utilized on the Thematic Mapper scanner system for LANDSAT-D.

The next phase of this analysis involved actual classification of the data. Table 3.20 shows the results of a series of classifications of the SKYLAB data and also the LANDSAT data when individual wavelength bands were used to classify the various cover types. The first column indicates the overall classification for the major cover types and the second column indicates the overall classification results for the individual forest cover types when using only the designated wavelength band for the classification. In evaluating these classification results, it

Table 3.20 Classification results for each cover type using individual wavelength bands of both LANDSAT and SKYLAB data

Channel	Wavelength Band	Classification Performance											
		Overall (Major Cover Type)	Overall (Forest Cover)	Water	Snow	Grassland	Deciduous	Conifer	Oak	Aspen	Ponderosa Pine	Douglas Fir/ White Fir	Spruce/Fir
1	0.41-0.46	24.1	10.2	5.2	100.0	42.2	0.0	24.5	0.0	0.0	15.5	0.4	2.0
2	0.46-0.51	42.2	17.9	7.3	100.0	53.9	11.5	46.7	0.0	18.8	43.5	1.2	0.8
3	0.52-0.56	50.5	30.0	2.1	97.3	37.5	17.5	58.9	8.7	20.0	44.7	31.3	0.0
4	0.56-0.61	57.2	29.4	2.1	0.0	0.0	15.5	78.2	10.0	16.2	49.8	40.6	12.9
5	0.62-0.67	61.4	35.4	3.1	100.0	0.0	32.2	73.6	27.5	23.7	58.8	38.8	0.0
6	0.68-0.76	74.7	34.8	63.5	97.3	35.2	36.5	85.8	23.1	22.1	60.6	20.2	29.3
7	0.78-0.88	77.9	43.4	93.8	89.3	34.4	52.5	85.6	35.0	35.0	54.9	37.2	27.0
8	0.98-1.08	56.9	31.4	100.0	63.4	52.3	57.7	54.2	15.0	60.0	47.9	5.1	40.2
9	1.09-1.19	75.7	48.1	100.0	50.9	43.0	32.7	88.6	25.0	23.3	56.3	50.9	43.0
10	1.20-1.30	68.5	47.1	87.5	0.9	34.4	27.5	84.1	22.5	19.2	52.3	58.7	45.7
11	1.55-1.75	46.5	31.3	31.3	22.3	51.6	16.7	55.7	26.9	2.9	32.4	40.5	16.4
12	2.10-2.35	50.1	27.1	0.0	29.5	16.4	19.5	64.0	23.7	11.7	78.7	8.4	44.9
13	10.2-12.5	47.1	27.4	0.0	74.1	37.5	7.0	58.2	0.0	9.2	27.3	30.6	34.4
14	*0.5-0.6	72.3	47.5	21.9	100.0	0.0	15.5	92.2	28.1	0.0	37.0	75.3	23.0
15	*0.6-0.7	70.6	45.4	94.8	100.0	17.2	3.0	87.3	0.0	1.2	43.3	62.4	23.8
16	*0.7-0.8	63.6	35.4	100.0	100.0	24.2	52.5	64.7	60.6	12.1	27.5	31.3	24.2
17	*0.8-1.1	67.6	33.1	100.0	91.1	48.4	57.5	68.0	75.0	5.8	19.2	25.1	28.9

*LANDSAT Wavelength Bands

is important to note that by using only one wavelength band for classifying the data, the power of the multispectral approach is not being utilized. In other words, multispectral analysis is based upon the concept that materials will reflect differently in different wavelength bands, and by combining data from several wavelength bands, one might be able to spectrally separate and identify the various cover types of interest. When using only a single wavelength band to classify the data, one is doing little more than level slicing or density slicing of that wavelength band. However, use of the individual wavelength bands for classifying the data does provide an indication of the value of each wavelength band for discriminating and identifying various cover types of interest.

In an attempt to make Table 3.20 a little easier to understand and interpret, Figures 3.26, 3.27 3.28 and 3.29 show the same data in a graphical format. Four separate figures were used in order to keep from having too many lines on any single graph. Figure 3.26 shows the overall classification results for Major Cover Types (Level 2), and Forest Cover Types when using the individual wavelength bands. (These data values were shown in columns 1 and 2 of Table 3.20.) Also shown in Figure 3.26 are the classification performances for snow and water using individual wavelength bands. The reason for the discontinuity in classification performance for snow cover when using channel 4 (0.56-0.61μm) was because of detector saturation on the S-192 scanner. This causes a singular co-variance matrix in the data, with a consequent inability to classify the data.

Figure 3.26 clearly shows the value of the visible wavelengths for separating snow from the other cover types present

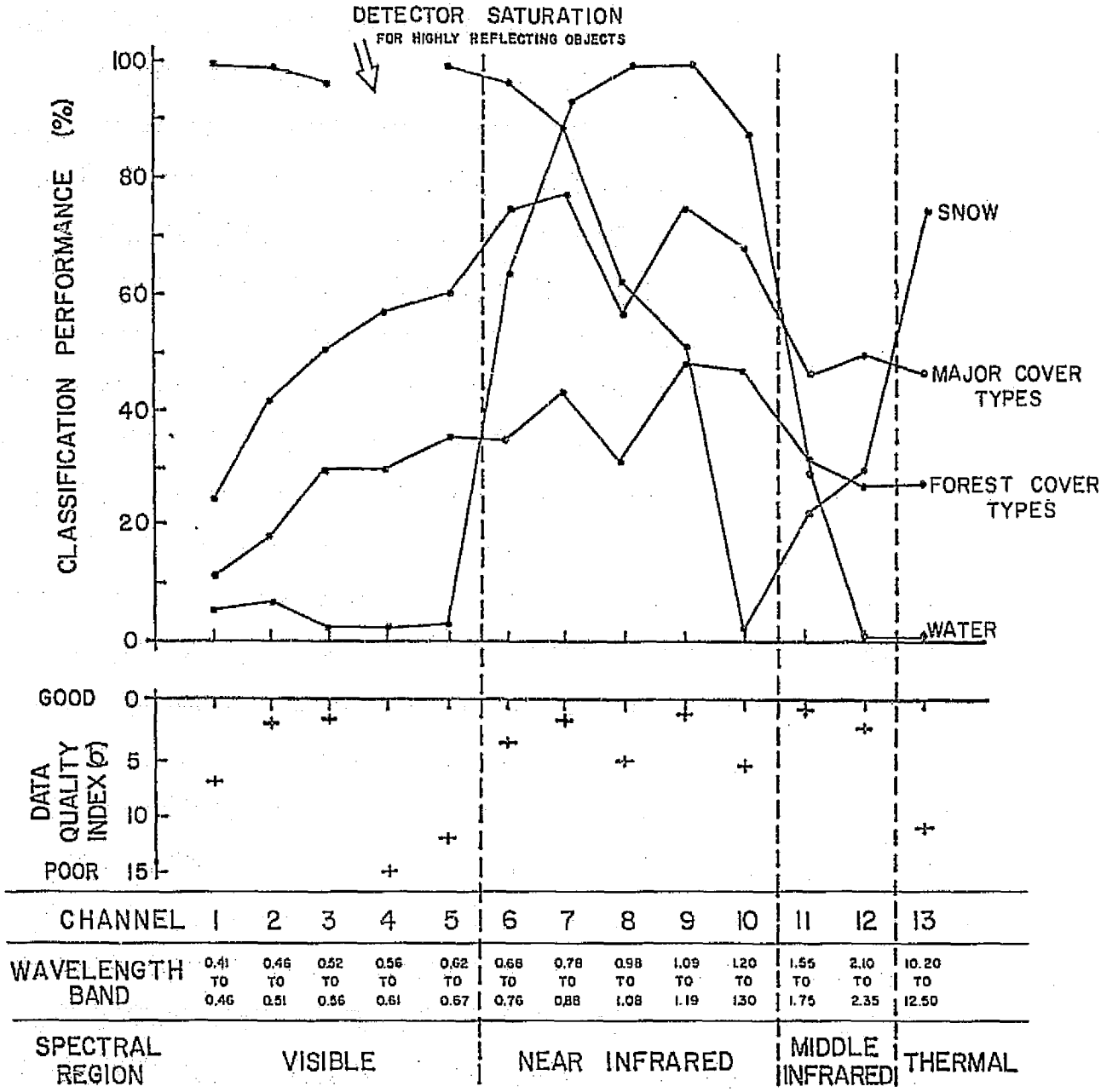

Figure 3.26 Classification results for major cover types, forest cover types, water, and snow using individual wavelength bands.

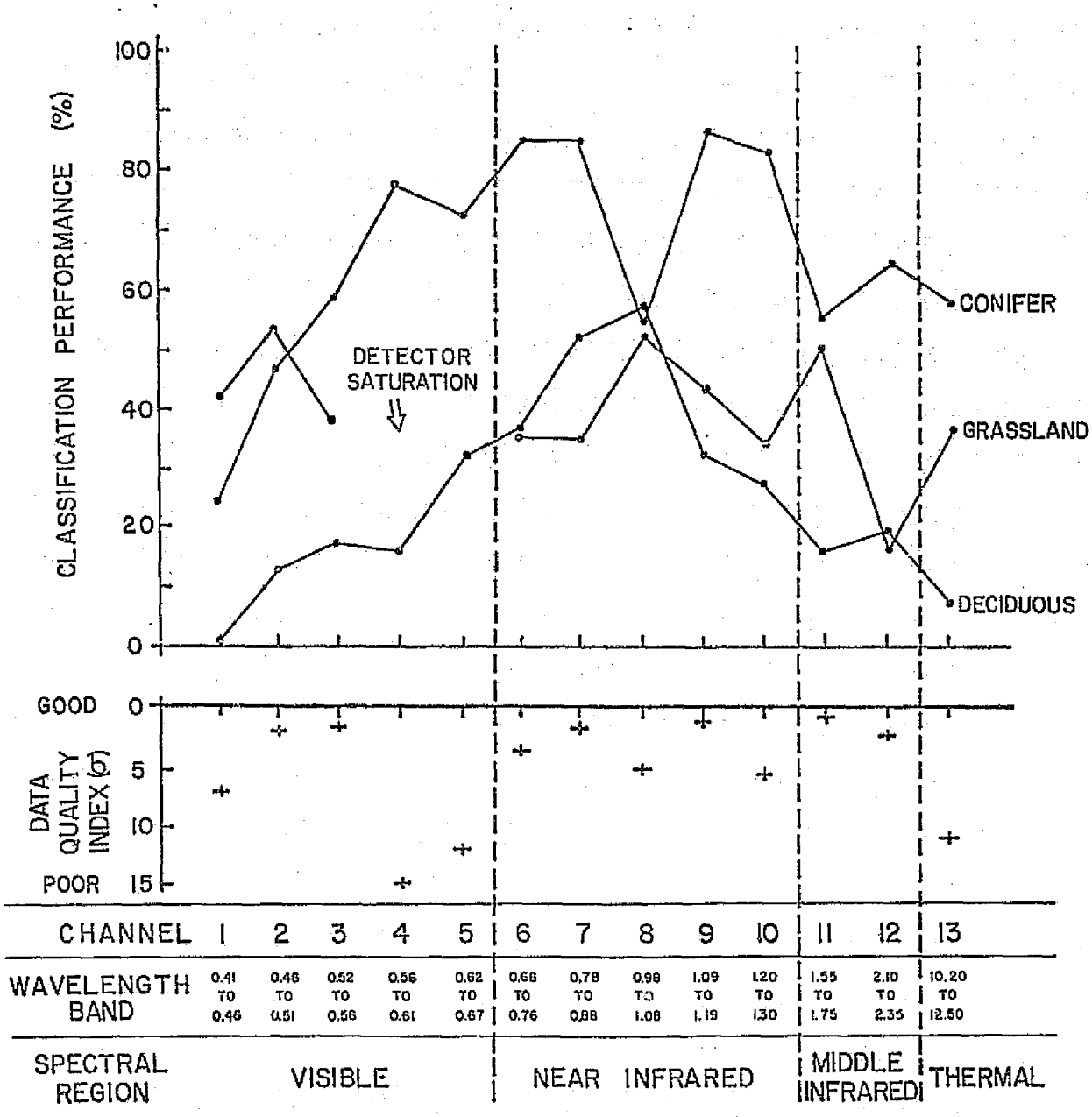

Figure 3.27 Classification results for deciduous forest cover, coniferous forest cover, and grassland, using individual wavelength bands

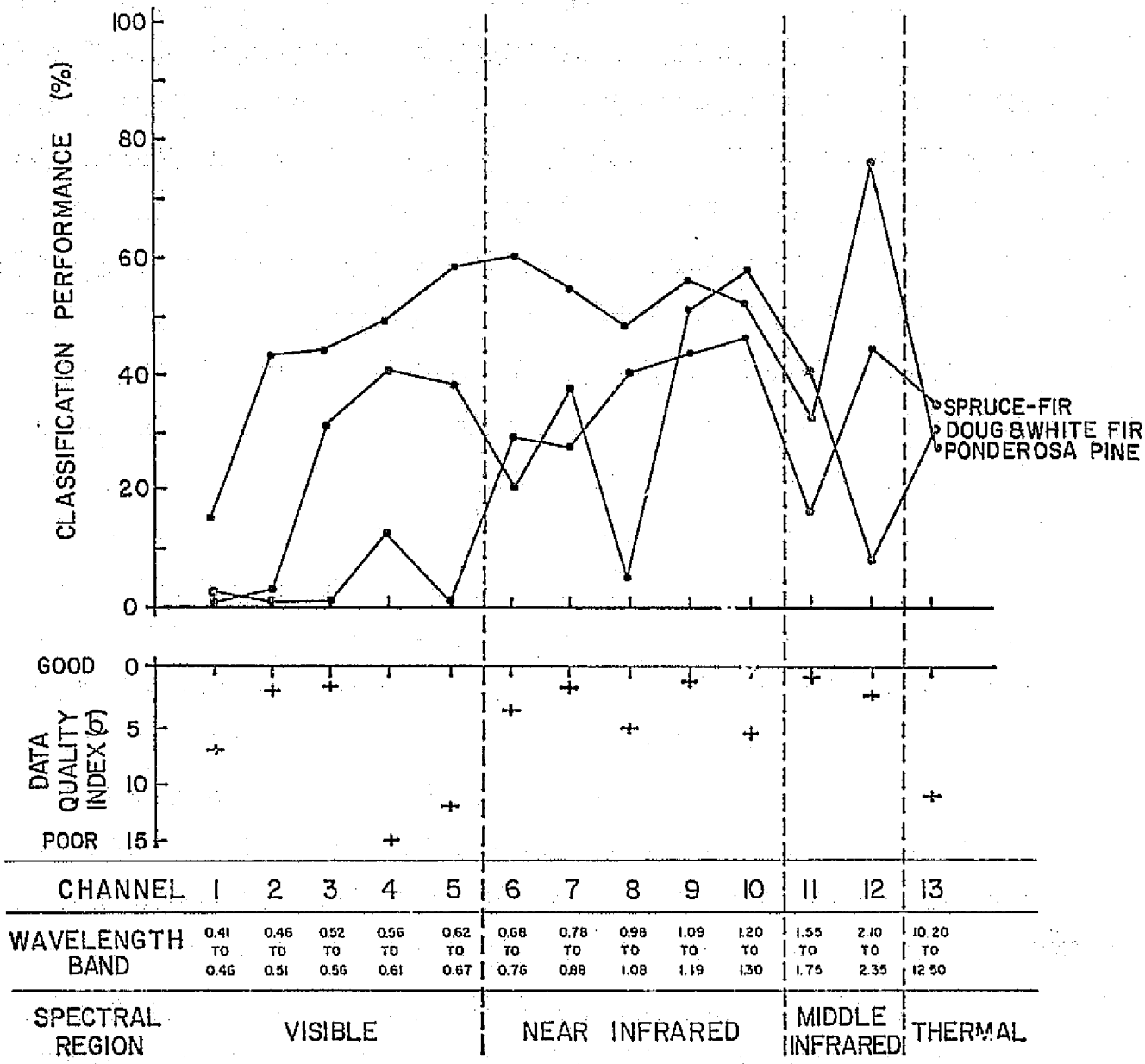

Figure 3.28 Classification results for ponderosa pine, Douglas fir/White fir, and Englemann spruce/subalpine fir, using individual wavelength bands

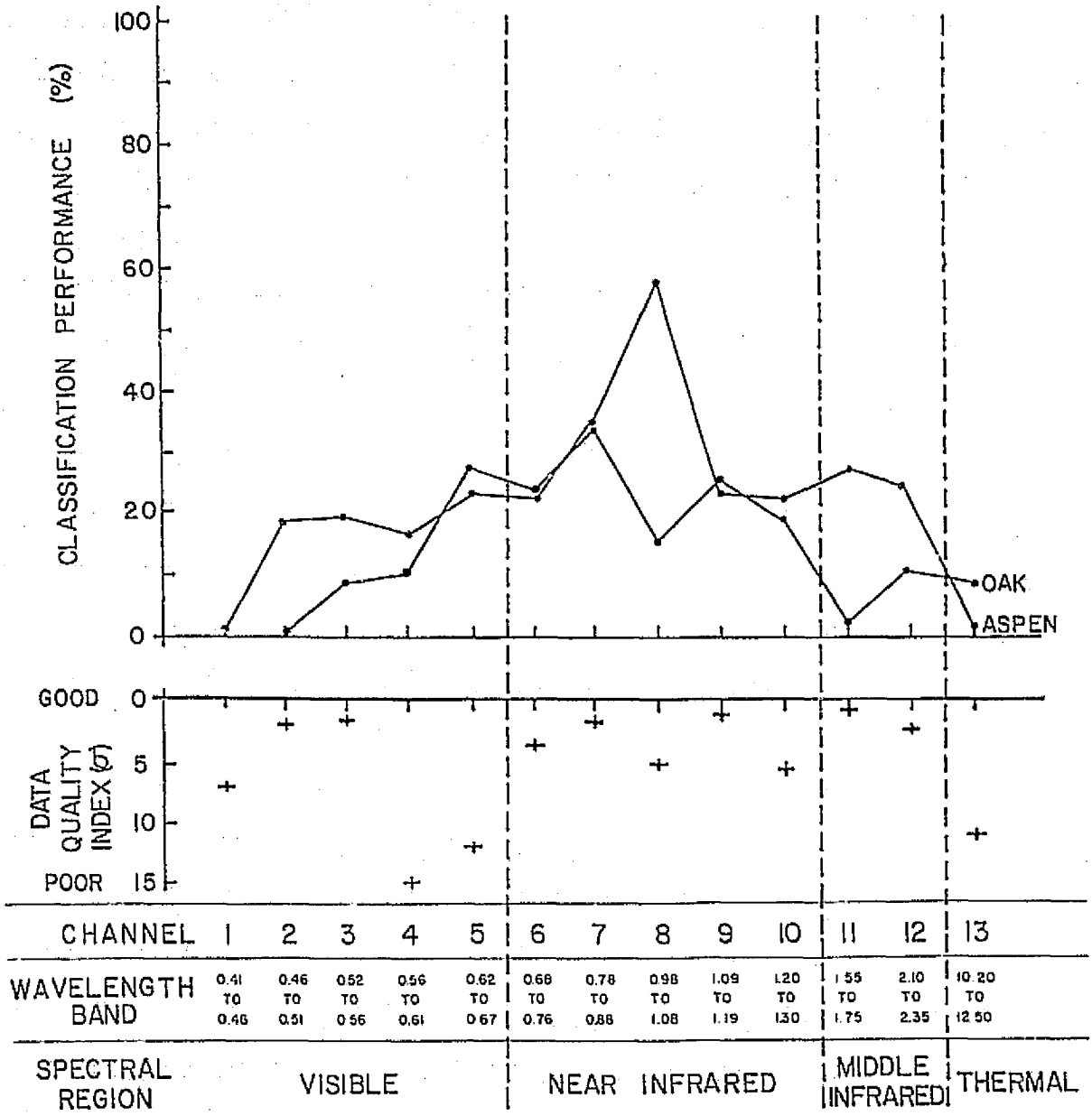

Figure 3.29 Classification results for aspen and oak forest cover types, using individual wavelength bands

in the test site. The visible wavelengths are extremely poor for separating water from the other cover types, whereas the near infrared portion of the spectrum is extremely good for separating water from other cover types.

Figure 3.27 shows the classification performance values when using individual wavelength bands for identifying coniferous forest cover, deciduous forest cover, and grassland. This figure also has a discontinuity for grassland in Channels 4 and 5 because of detector saturation, apparently due to the high reflectance of the grassland and the gain-setting on the scanner system. In evaluating this figure, one must take into account the data quality index that is shown. For example, it would appear that all three of these cover types can be classified much better using Channel 2 than Channel 1. However, the data quality index indicates that the data quality for Channel 2 was much better than for Channel 1, and this might explain the reason for the improved classification performance. Just because one channel produces a better classification performance than another channel, one cannot assume that the result obtained is only due to the differences in spectral information content in the various channels. The data quality index must be taken into account. Thus, when comparing Channels 2 and 3, one sees that Channel 3 does a better job of classifying conifers than Channel 2, but a poorer job of classifying grasslands. This difference can be assumed to be due to the spectral differences of the materials involved since both Channels 2 and 3 have approximately the same data quality index. Another example is seen in the 0.98-1.08μm (Channel 8) wavelength band

which has a poorer data quality index than either Channel 7 or Channel 9. However, the classification accuracy for both the deciduous forest cover and grassland is much higher in Channel 8 than either Channel 7 or Channel 9. This would indicate that the spectral information in the 0.98-1.08μm wavelength band is extremely important for accurate classification of deciduous and grassland cover types. The decreased classification accuracy for Channel 8 for the coniferous forest cover is largely due to the fact that Douglas and White fir forest cover cannot be accurately identified in this wavelength band, although the decrease in data quality in this channel may also be affecting these results. Figure 3.27 also shows a significant increase in classification for the conifer cover when going from Channel 3 to Channel 4, in spite of the fact that the data quality in Channel 4 is extremely poor as compared to Channel 3. This could be interpreted to mean that the spectral information content in Channel 4 (and also in Channel 5) is extremely important for accurate classification of coniferous forest cover.

Figures 3.28 and 3.29 provide a closer look at the classification performance of individual channels for each of the various forest cover types involved in this analysis. Figure 3.28 shows the classification performance for the three coniferous forest cover types, and Figure 3.29 shows the classification performance for the two deciduous forest cover types.

Figure 3.28 shows the difficulty in defining a single set of wavelength bands for use under all circumstances and where many different cover types are involved. Channel 5, for example,

seems to be the best of the visible channel for separating ponderosa pine from other cover types, but is extremely poor for separating the spruce-fir cover types. In fact, Channel 4, in spite of its very poor data quality index, is the only visible channel that is at all useful for separating spruce-fir from other cover types. Comparisons of Channels 8 and 10 show that both have about the same data quality index. However, Channel 8 is relatively poor for identifying Douglas and white fir forest cover, whereas Channel 10 is the best of any of the SKYLAB channels for this particular forest cover type. An interesting pattern is also shown in the middle infrared wavelength bands, in which Channel 12 is much poorer than Channel 11 for the Douglas and white fir, but much better than Channel 11 for both the ponderosa pine and the spruce fir.

Figure 3.29 indicates that the near infrared portion of the spectrum is extremely useful for identifying the deciduous forest cover types. Channel 8 appears to be of particular importance in identifying aspen. This figure also shows why it is important to evaluate the actual classification performance results and to examine ability of individual wavelength bands to separate and identify the individual cover types, rather than to simply rely on the feature selection processor to indicate the ability of a single channel to separate a particular cover type in comparison with the average of all other cover types. For example, Figure 3.29 shows that Channel 8 is best for actually classifying aspen, but Table 3.18 (based upon use of the feature selection processor) indicated that Channel 9 gave the best separation between aspen and the average of all other cover types. Also, Table 3.18 did not indicate that either of the wavelength bands in the middle

infrared portion of the spectrum would be best for identifying any individual cover types, but Figure 3.28 shows that in actual classification, the 2.10-2.35μm channel is best for identifying ponderosa pine. Thus, when working with the classification of individual cover types, the results can be different than when comparing a particular cover type against the average of all other cover types in the scene. These classification results tend to be in reasonable agreement with the separability data shown in Table 3.19, where the separability values for individual cover types were compared.

In an attempt to summarize the results shown in Table 3.20 and in Figures 3.26 through 3.29, Table 3.21 shows the best wavelength band (or bands in some cases) in each portion of the spectrum for actually identifying individual cover types. The table does not indicate which combination of wavelength bands would be optimum for each of the various cover types concerned, but it does indicate which individual wavelength band seems to be the best in each of the different portions of the spectrum for identifying the various cover types.

This table brings out the fact that the 0.62-0.67μm channel is particularly important for the deciduous forest but the 0.56-0.61 seems to be the more important of the visible channels for identifying coniferous forest cover. In the near infrared portion of the spectrum, the 0.98-1.08 seems to be more important for deciduous forest whereas the 1.09-1.19 seems to be more important for coniferous forest. For individual forest cover types still other channels are more important, such as the 1.20-1.30μm for the Douglas and white fir forest cover, and the spruce-fir forest cover types. Both of the channels in the middle IR seem to be

Table 3.21 Best wavelength band in each spectral region for identifying individual cover types.

Spectral Region:	Visible					Near IR					Middle IR		Thermal IR
Wavelength Band:	0.41 to 0.46	0.46 to 0.51	0.52 to 0.56	0.56 to 0.61	0.62 to 0.67	0.68 to 0.76	0.78 to 0.88	0.98 to 1.08	1.09 to 1.19	1.20 to 1.30	1.55 to 1.75	2.10 to 2.35	10.2 to 12.5
Channel Number:	1	2	3	4	5	6	7	8	9	10	11	12	13
Cover Type													
Deciduous Forest					X			X				X	X
Aspen					X			X			X		X
Oak					X		X					X	X
Coniferous Forest				X		(X)[1]	(X)		X			X	X
Ponderosa Pine					X	X						X	X
Douglas and White Fir				X						X	X		X
Spruce-Fir				X						X		X	X
Grassland		X[2)]						X			X		X
Water		X							X				
Snow	X[2)]	(X)	(X)	(X)	(X)	X						X	X
Overall, Major Cover Types					X		X					X	X
Overall, Forest Cover Types					X				X		X		X

1) X in parantheses indicates equally good wavelength bands
2) Channels 4 & 5 could not be evaluated for grasslands due to detector saturation and Channel 4 could not be evaluated for snow.

important for various cover types. Since only one channel in the thermal infrared channel was available, this channel was marked for all cover types. This table clearly shows the complexity of selecting a single wavelength band that is optimum for all cover types of interest or concern. Rather, various wavelength bands are of optimum value for various cover types. This leads to a question concerning the importance of one wavelength band as compared to another when utilizing a multispectral classification approach, rather than evaluating bands on an individual basis. For example, in a multispectral analysis involving four or five wavelength bands, if the 0.78-0.88μm wavelength band were utilized rather than the 0.98-1.18μm band, would there be a significant difference in the classification results obtained? This led to the third phase of the wavelength band evaluation study.

3.5.4 Wavelength Region Evaluation

The third analysis sequence in the wavelength band evaluation study involved use of the multispectral approach to evaluate the importance of the different spectral regions for accurately classifying both the major cover types and forest cover types. In this classification sequence, five wavelength bands were utilized for all classifications insofar as possible. First the feature selection processor was utilized to select the optimum combination of five wavelength bands when all 13 channels were available for consideration. Next, only the visible channels were considered. Then only the near infrared channels were considered, then the middle infrared, and then the thermal infrared. After that, the visible portion of the spectrum was excluded from consideration and the feature selection processor was asked to select the best five wavelength band combination using only channels in the near infrared, middle infrared, and thermal infrared portions of the spectrum. Next, the near infrared was excluded from consideration, and the future selection processor defined the optimum combination of five wavelength bands from the visible, middle IR and thermal IR, etc. In each case, after the five wavelength bands were defined by the feature selection processor, those channels were used to classify the data. At least one wavelength band was always included from each of the spectral regions considered by the feature selection processor. For example, when all spectral regions were considered by the

feature selection processor, we required the five wavelength bands used in the classification to include at least one band from the visible, one from the near infrared, one from the middle infrared, and the thermal infrared. Consequently, we sometimes utilized a combination of five wavelength bands that were not the "best" five bands, but that did include each of the various spectral regions.

The results of these classifications are shown in Table 3.22. To more graphically illustrate the results, Figures 3.30-3.41 are shown. When only the middle infrared portion of the spectrum was available for consideration, only two channels were used in the classification rather than five, and this may have caused some of the decrease accuracy when only the middle IR was involved in the classification. The same thing could be said for the thermal infrared, since in this case only a single wavelength band was involved in the classification.

The results shown in Figures 3.30 through 3.41 demonstrate a number of interesting interactions. For example, Figure 3.30 (Overall Major Cover Type, or Level 2 results) indicates that when the visible channels are excluded from consideration, the classification accuracy is almost as high as when all four of the major spectral regions were involved in the classification. Also, the exclusion of the thermal channel did not cause any decrease in classification performance. Interestingly, when only the near infrared portion of the spectrum considered, classification performance was almost as high as when all four regions were used.

Table 3.22 Multispectral classification results using wavelength bands from various combinations of spectral regions.

	All Regions Included	Visible Only	Near IR Only	Middle IR Only	Thermal IR Only	No Visible	No Near IR	No Middle IR	No Thermal IR
Overall (Major Cover Type)	85.3	57.6	81.4	57.3	47.1	83.9	66.0	80.6	84.8
Overall (Forest Cover Type)	69.9	36.0	64.1	40.5	27.4	67.4	49.2	67.6	70.2
Coniferous	89.9	66.9	87.9	68.9	58.2	89.6	73.3	87.9	90.4
P Pine	70.8	44.2	63.4	63.2	27.3	70.4	51.2	61.6	67.1
DWF	77.9	36.0	68.8	43.8	30.6	71.3	53.5	79.1	76.7
SF	49.6	23.8	44.1	21.9	34.4	41.8	43.4	47.7	50.0
Deciduous	58.7	19.5	54.2	31.0	7.0	62.7	39.7	51.0	64.2
Aspen	51.4	25.8	52.5	28.3	9.2	57.5	30.4	44.2	61.7
Oak	60.0	5.0	51.2	28.7	0.0	63.7	31.3	55.6	61.2
Grassland	51.6	37.5	50.8	30.5	37.5	51.6	28.1	48.4	53.1
Water	94.8	31.3	97.9	38.5	0.0	94.8	57.3	94.8	94.8
Snow	100.0	100.0	100.0	22.3	74.1	100.0	100.0	100.0	100.0

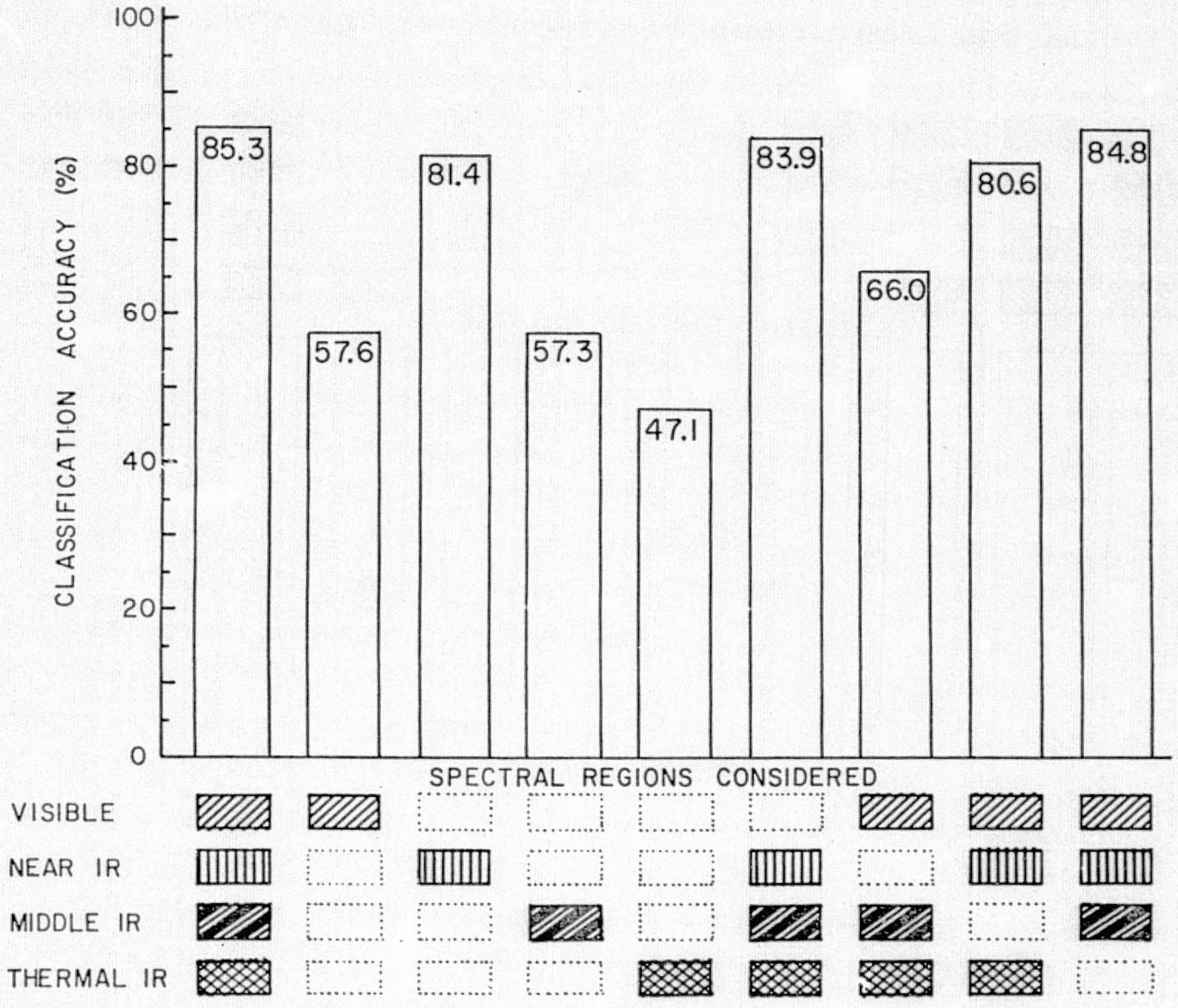

Figure 3.30 Wavelength region evaluation for major cover types

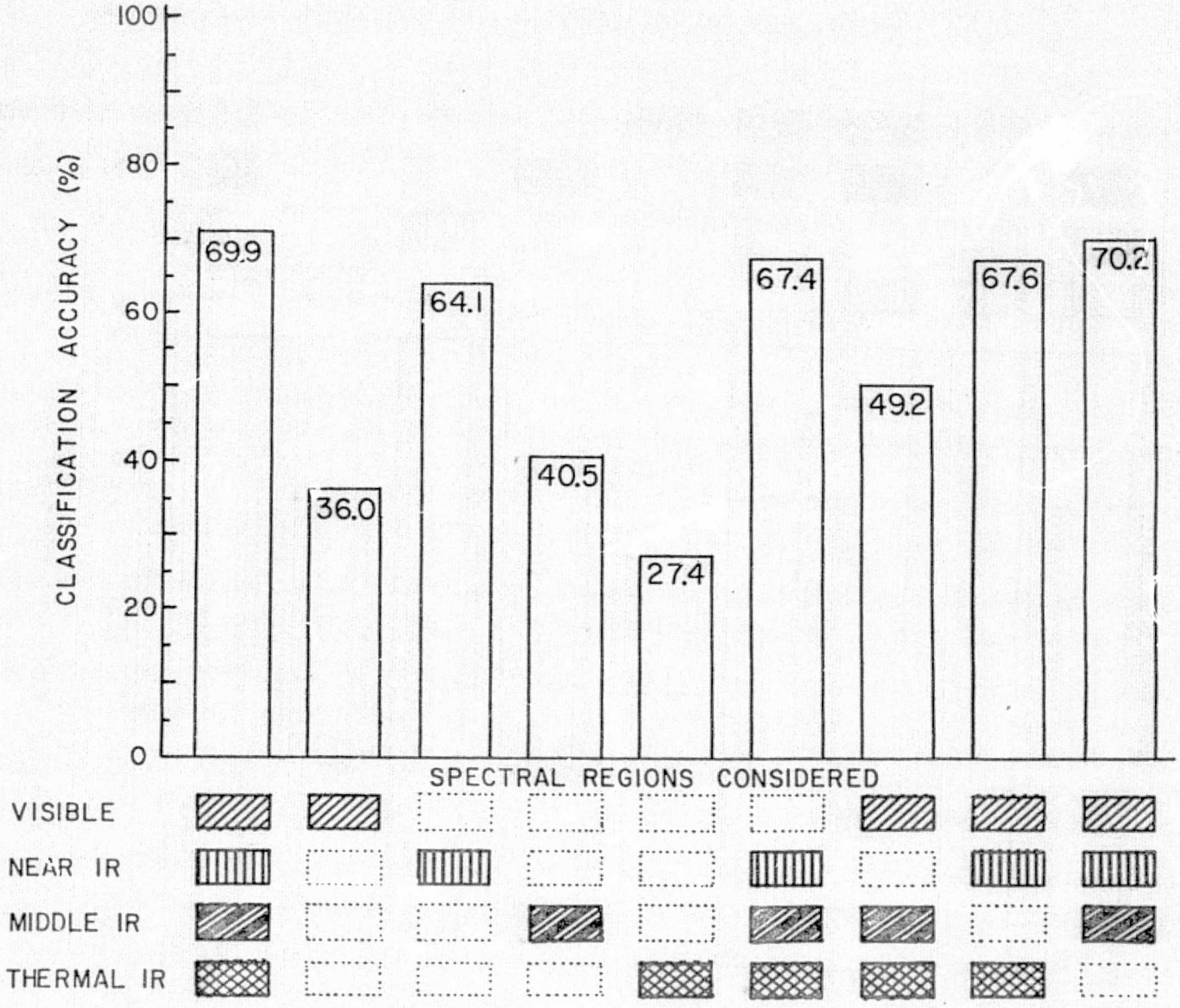

Figure 3.31 Wavelength region evaluation for forest cover types

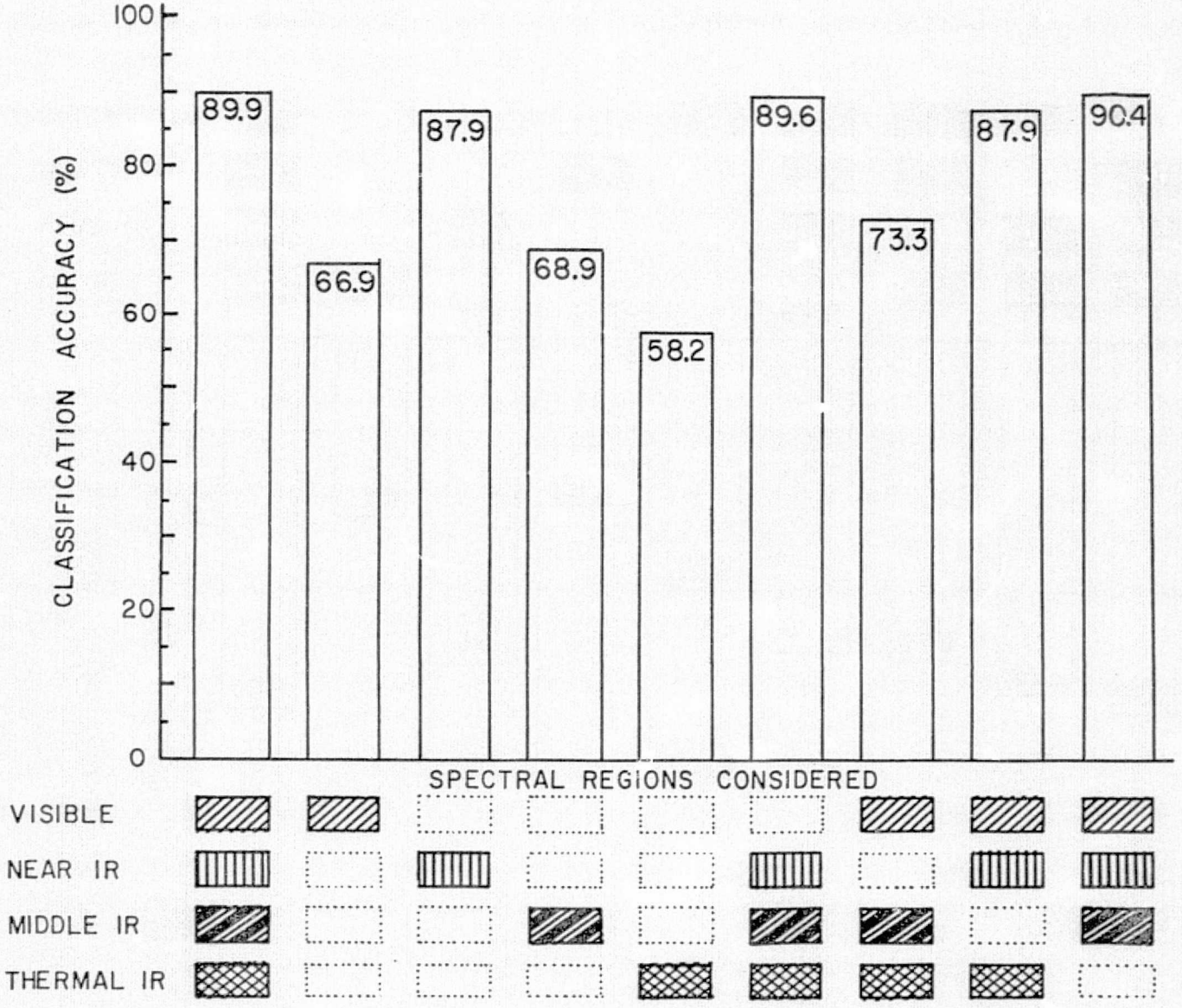

Figure 3.32 Wavelength region evaluation for coniferous forest cover types

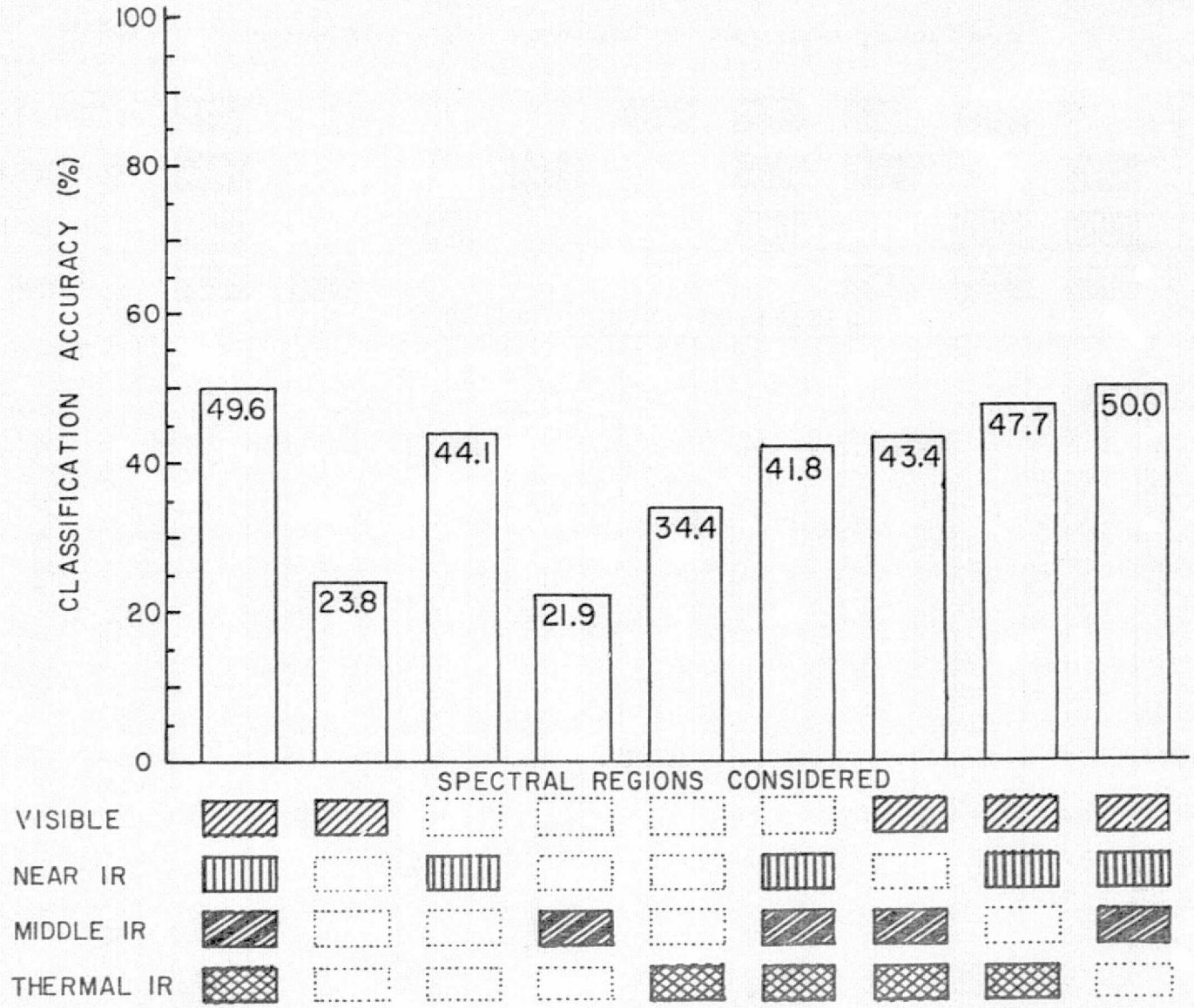

Figure 3.33 Wavelength region evaluation for Englemann spruce/subalpine fir cover types

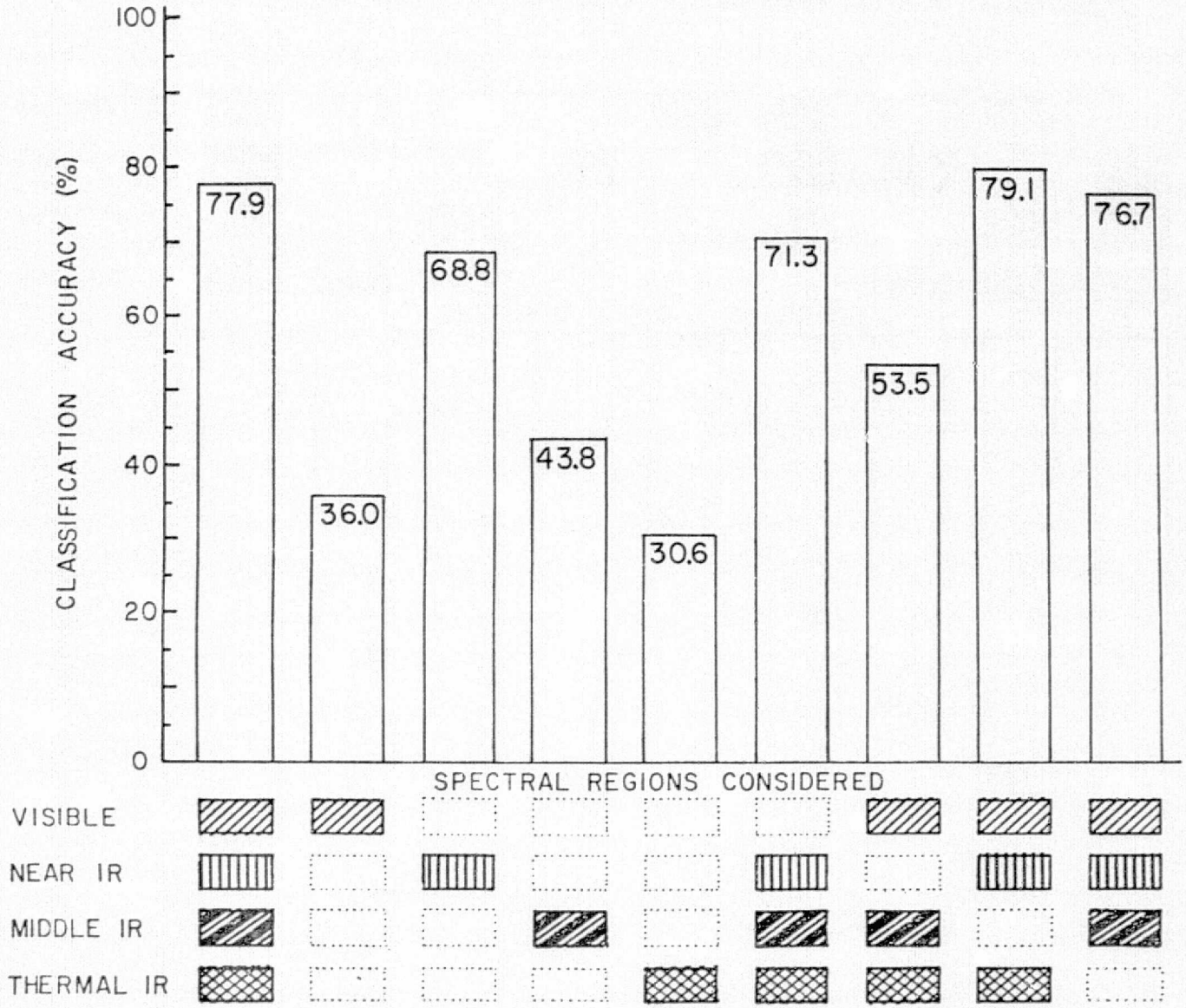

Figure 3.34 Wavelength region evaluation for Douglas fir and white fir cover types

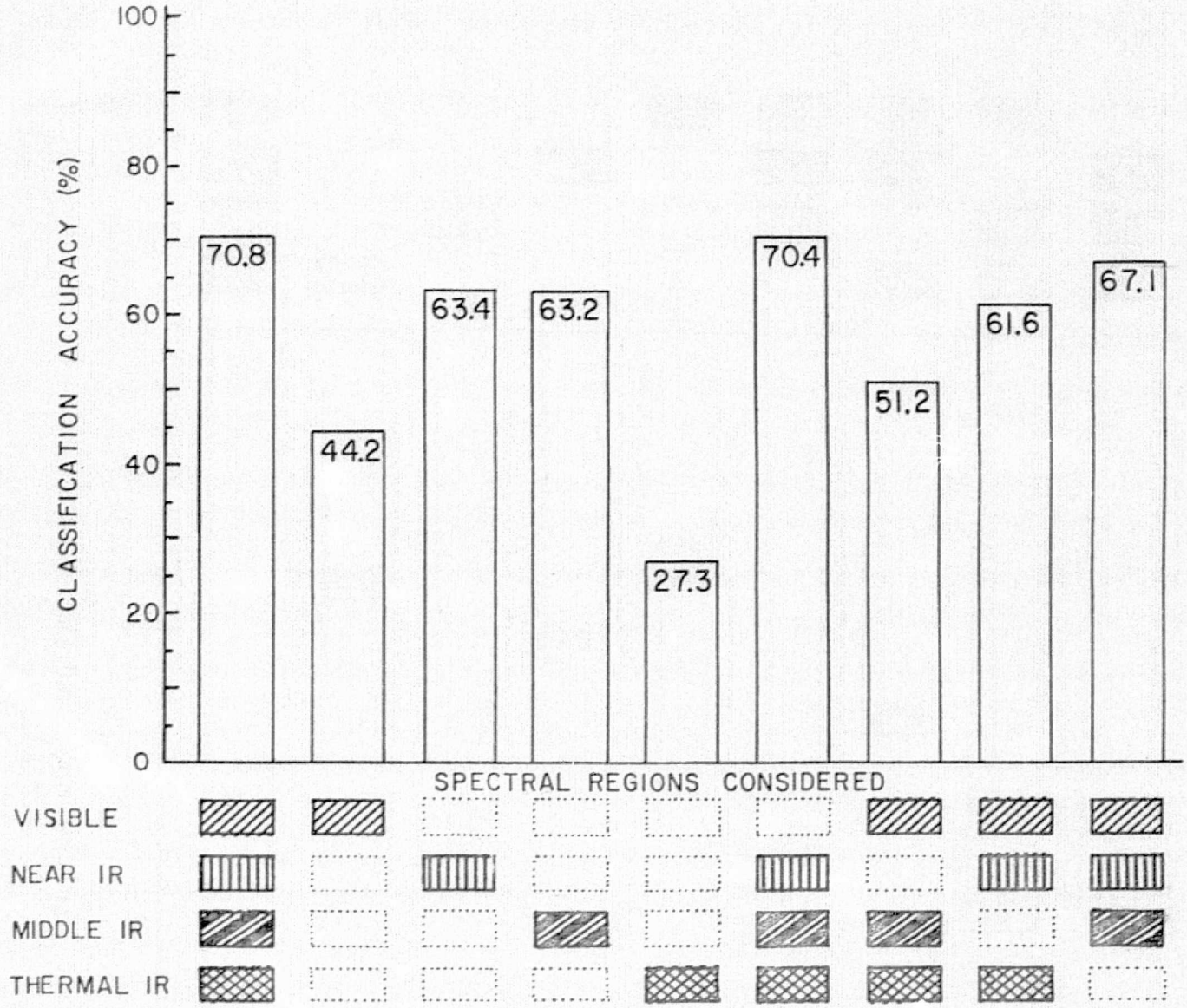

Figure 3.35 Wavelength region evaluation for ponderosa pine cover type

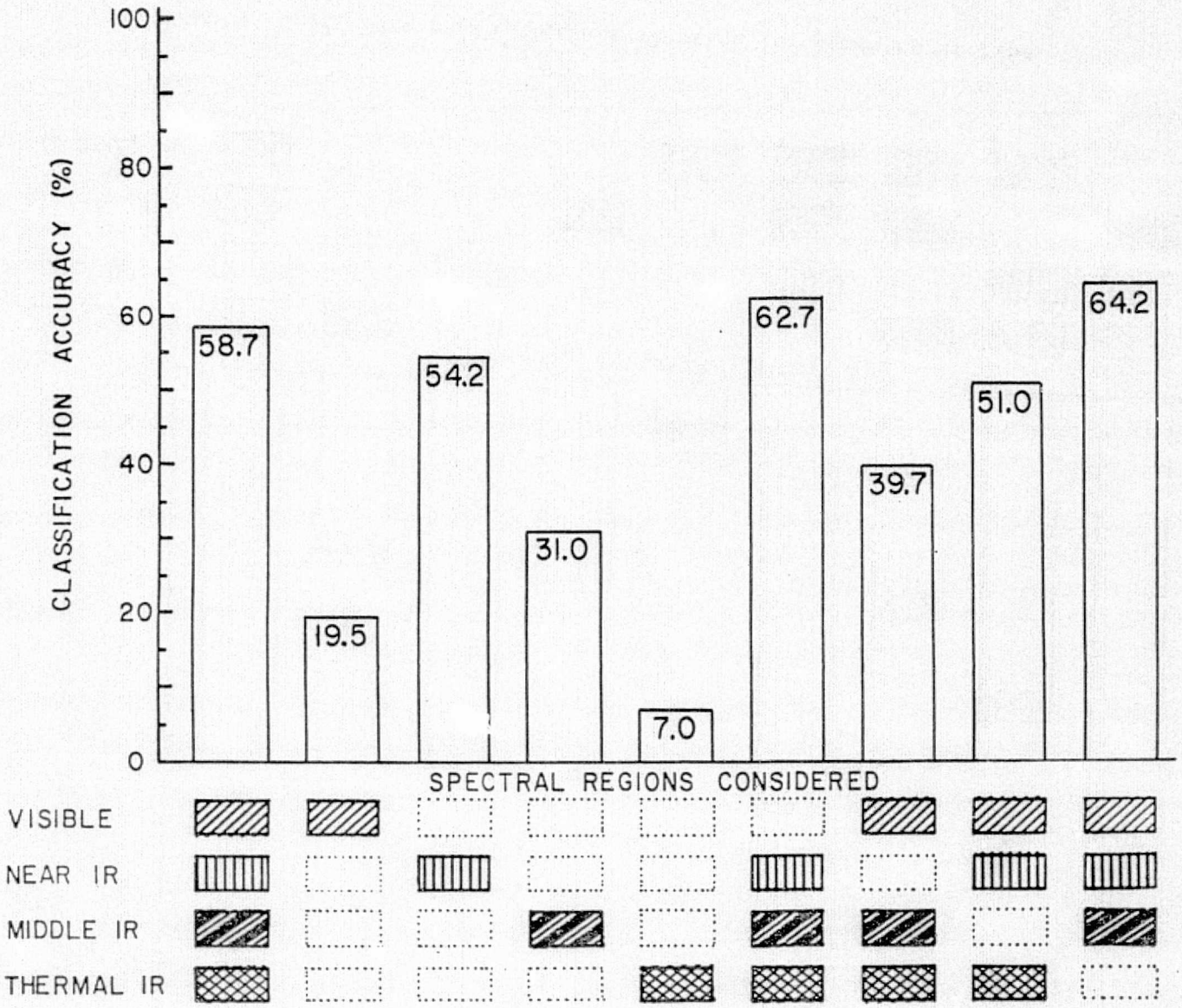

Figure 3.36 Wavelength region evaluation for deciduous cover types

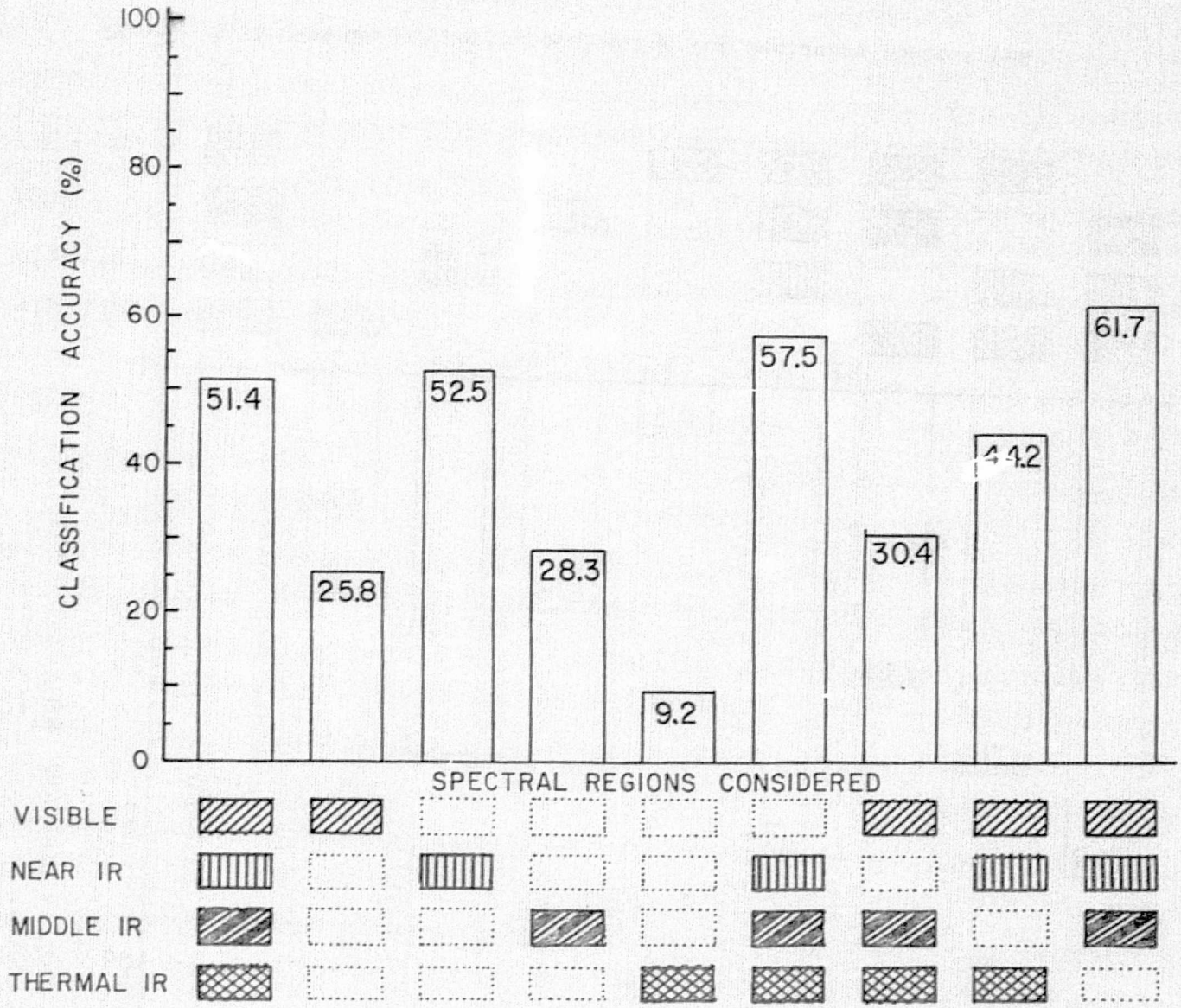

Figure 3.37 Wavelength region evaluation for aspen cover type

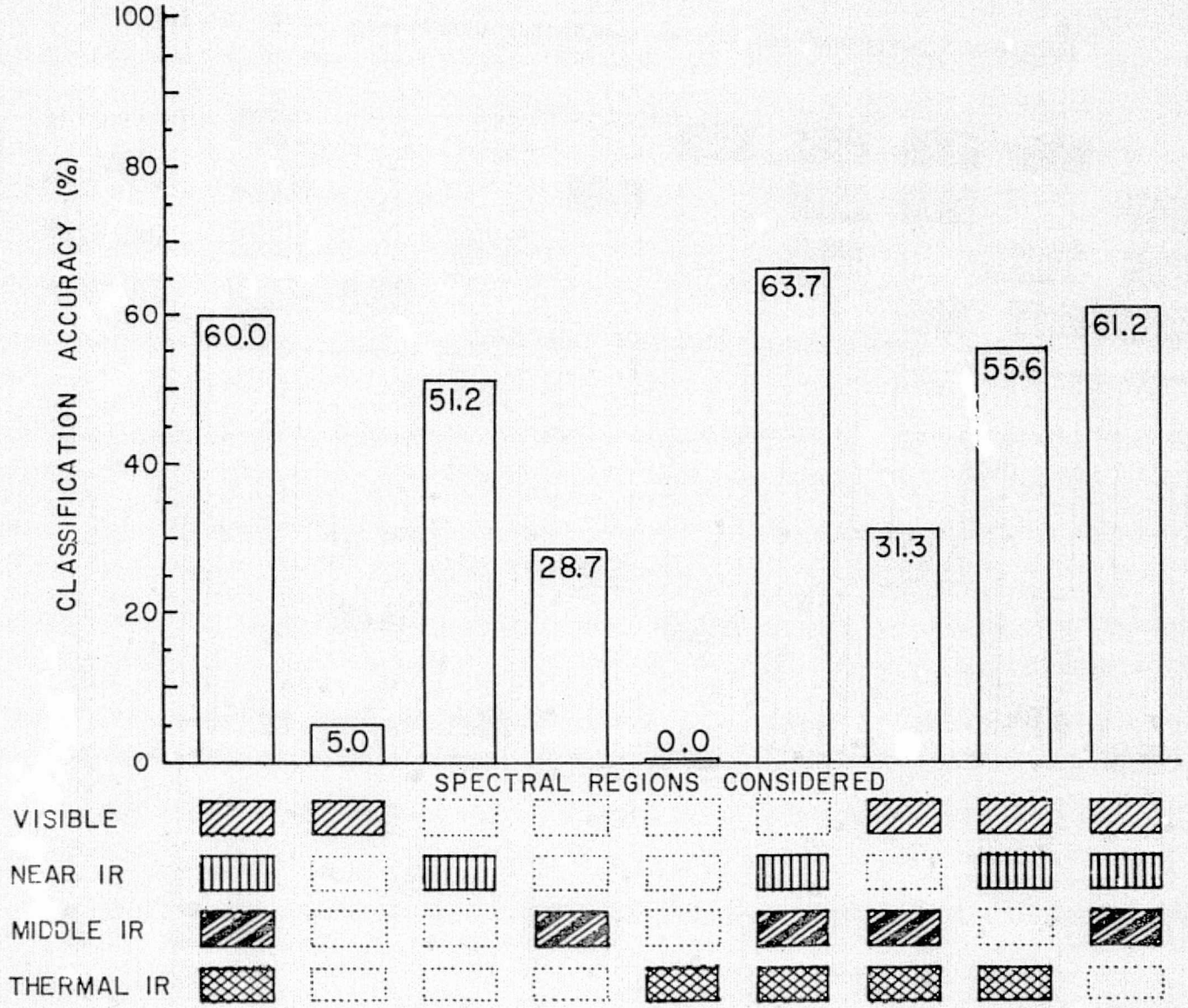

Figure 3.38 Wavelength region evaluation for oak cover type

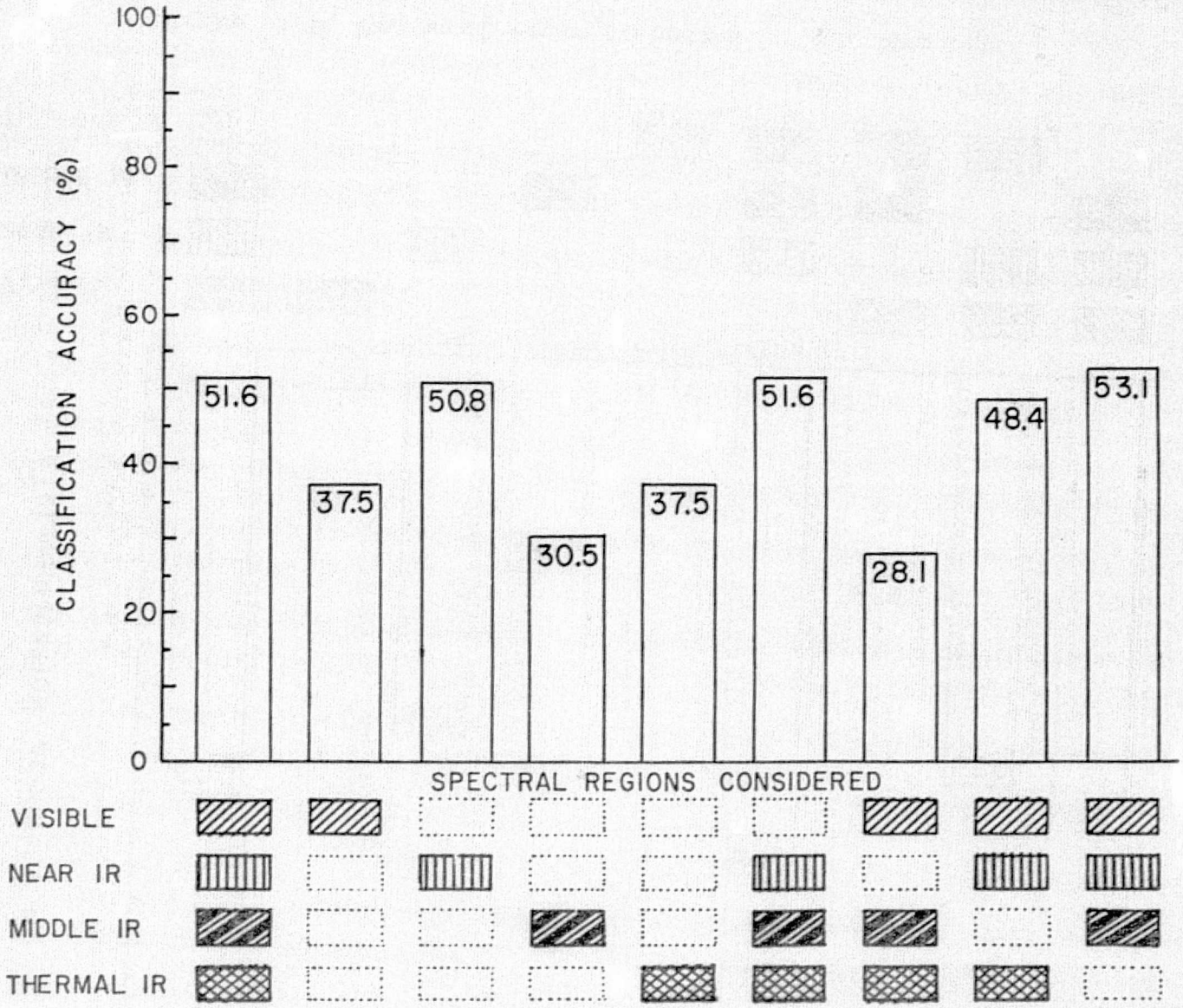

Figure 3.39 Wavelength region evaluation for grassland cover type

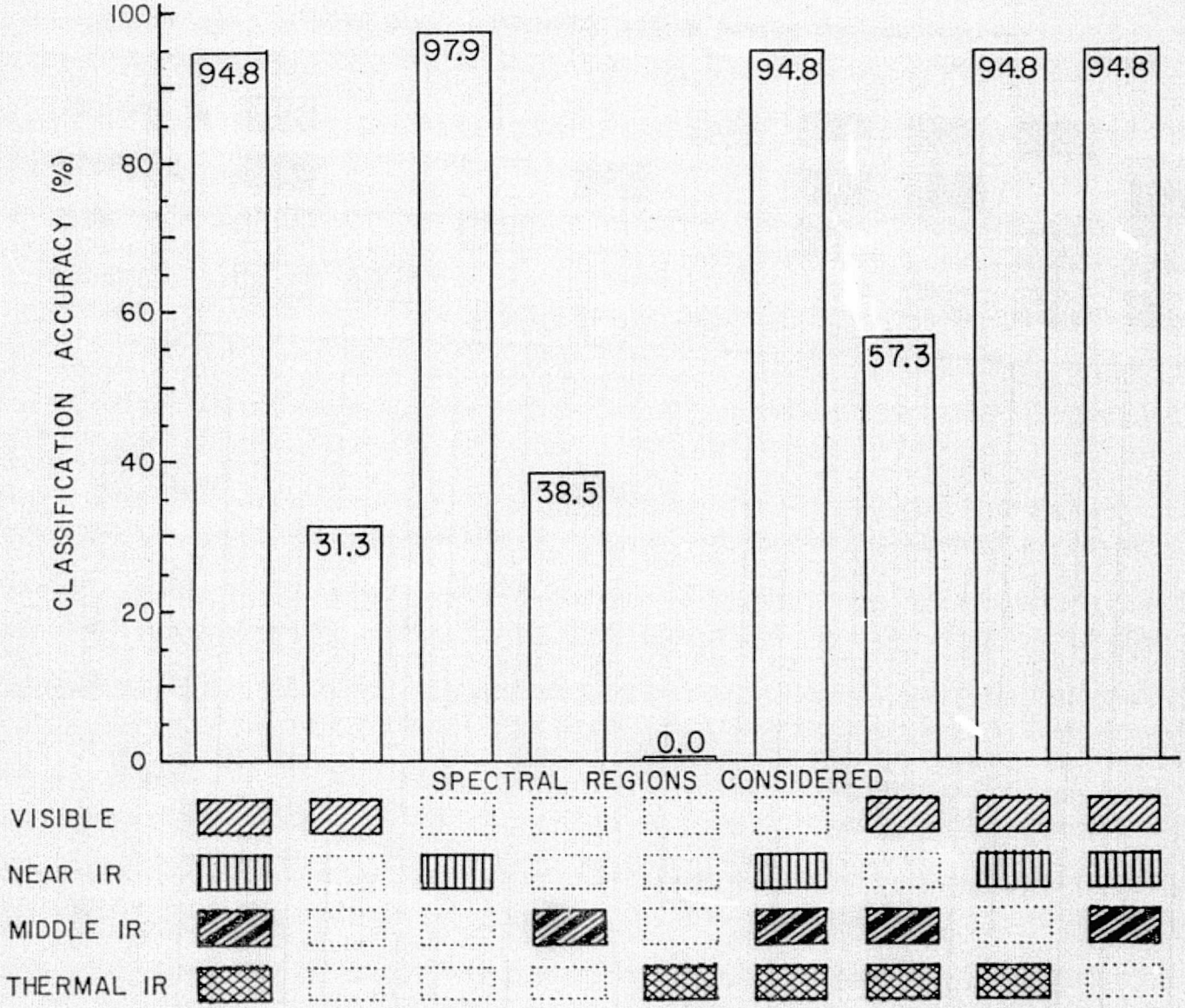

Figure 3.40 Wavelength region evaluation for water

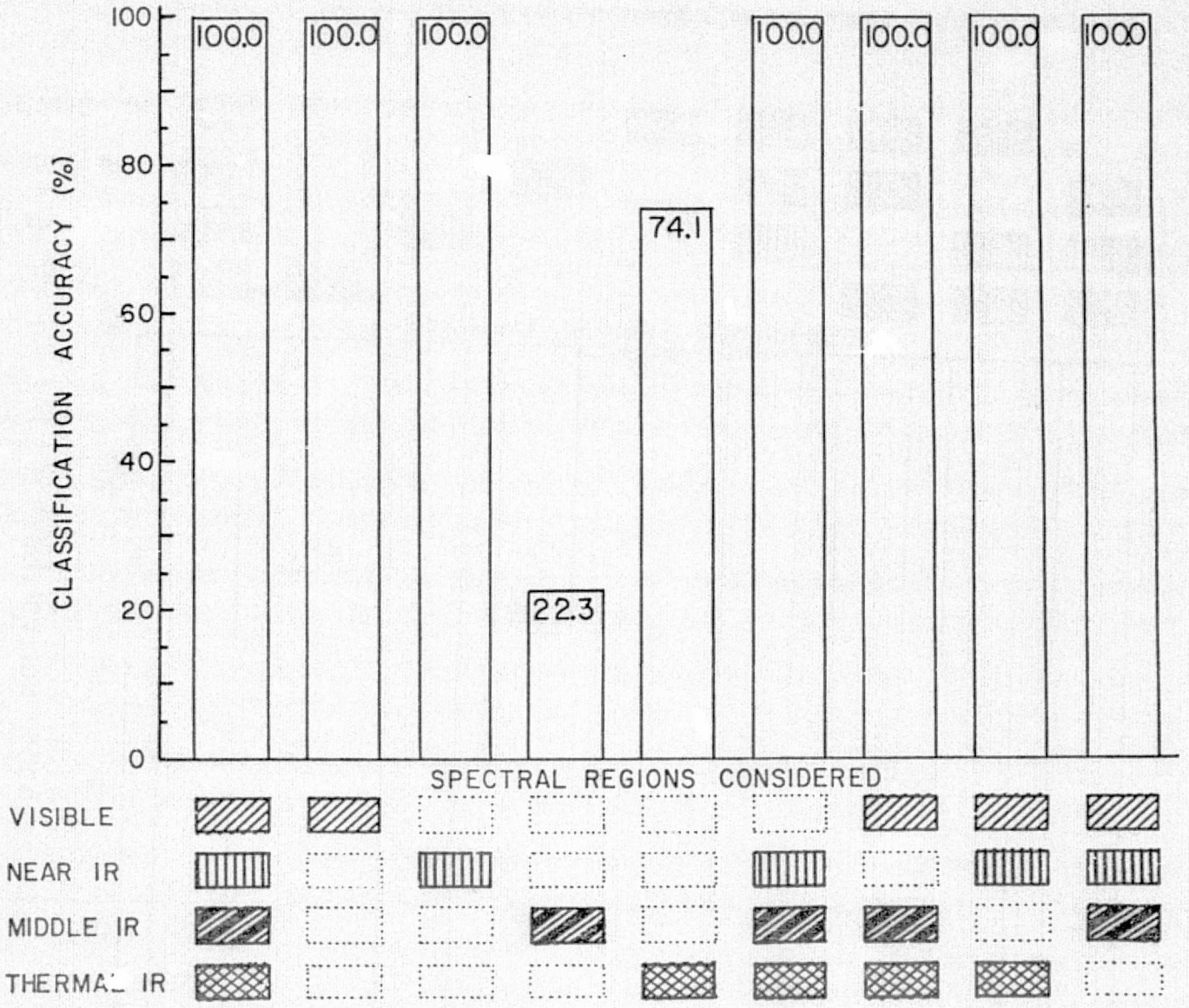

Figure 3.41 Wavelength region evaluation for snow

Figure 3.31 shows the same pattern when classification of forest cover types was involved. A very similar pattern is also shown for the overall coniferous cover type classification (Figure 3.32). However, when evaluating the individual forest cover types within the onifer group, one sees some somewhat different trends occurring. For example, the spruce-fir classification sequence (Figure 3.33) indicates that when only the thermal IR is considered, a much higher classification occurs than when only the middle infrared portion of the spectrum is involved. However, when the thermal infrared is excluded from consideration, the classification is a little higher than when the middle infrared is excluded from consideration and the thermal infrared is included, as shown in the last two bars. This indicates the interaction effects that can occur when channels in other spectral regions are involved in a classification. Figure 3.34 shows the importance of the near infrared for accurate classification of Douglas and white fir. Both the near and middle infrared wavelength regions are much more important than the visible portion of the spectrum for identifying ponderosa pine, as shown in Figure 3.35. Figures 3.36, 3.37, and 3.38 show similar patterns for the aspen, oak, and combined deciduous cover. In this case, the importance of the near infrared is again indicated. These results also indicate that when the thermal infrared is not included, the classification is significantly higher than when the thermal infrared channel is present. A similar pattern is evident in Figure 3.39 for grasslands. However, this was not the case for the Douglas and white fir forest cover type, since Figure 3.34 indicated that when the thermal infrared channel was not included, the classification was somewhat lower than when all four spectral

regions were present or when the middle infrared was deleted.

Figure 3.40 clearly shows the importance of the near infrared portion of the spectrum for effective classification of water. Where the near infrared was not included in the consideration, the classification dropped significantly but when even the near infrared was included, the classification accuracy is approximately 95%.

Figure 3.41 shows the importance of either the visible or the near infrared wavelength bands for classification of snow. When either of these spectral regions was included, the classification accuracy was 100%, but if only the middle or thermal infrared channels are considered, classification is much lower. A point of interest here is the considerable improvement when the thermal infrared is involved in the classification as compared to the middle infrared. In chapter four, the value of the middle infrared for spectrally separating snow and clouds is clearly shown, but here the middle infrared is not particularly useful for classifying snow because of the relatively low spectral response of snow in these wavelength bands. Such a low spectral response causes snow to be confused with other cover types.

A key result that these graphs emphasize is the importance of the near infrared for accurately classifying vegetative cover types. In most cases, the near infrared allows a significantly higher classification accuracy than the visible wavelengths, and in several instances, (such as with the spruce-fir, ponderosa pine, or oak forest cover types) the middle infrared channels also allow a much better classification than the visible channels.

The results of the final step in evaluating the importance of the various wavelength bands are shown in Table 3.23. In this case, 18 channels of the overlaid data tapes were used in the feature selection processor. These channels included the 13 wavelength bands of SKYLAB data, the four wavelength bands of LANDSAT data, and the channel including the elevation data. The feature selection processor ranked each channel according to the average saturating transformed divergence values for all of the test field statistics in the data set. This provided an opportunity to work with a larger data set than was included in only the training fields. Also, by using the test field data, another opportunity was provided to evaluate the various wavelength bands using a different set of statistics than had been involved in the evaluations considered earlier in this section.

These results again point out the importance of the near infrared portion of the spectrum. In looking at "Spectral Region" column of Table 3.23, one sees that other than for the elevation channel (ranked third), all of the SKYLAB and the LANDSAT near infrared wavelength bands were selected before any wavelength bands in the middle infrared, visible or thermal infrared regions. Also, in some cases, poorer quality data in the near infrared region was selected as having more information content than better quality data in the middle infrared or visible wavelengths. These results clearly demonstrate the value and importance of the near infrared wavelength region for computer-aided mapping of major (land use) cover types and forest cover types.

Rank	Source	Wavelength Band	Spectral Region	Qualitative Data Quality Rating	Quantitative Data Quality Rating	Average Saturating Transformed Divergence
1	SKYLAB	0.98-1.08	near IR	Very good	Fair	1311
2	LANDSAT	0.80-1.10	near IR	Excellent	Excellent	1305
3	DMA	Elevation				1302
4	SKYLAB	1.09-1.19	near IR	Very good	Very good	1299
5	LANDSAT	0.70-0.80	near IR	Excellent	Excellent	1296
6	SKYLAB	0.78-0.88	near IR	Very good	Good	1227
7	SKYLAB	1.20-1.30	near IR	Good	Fair	1057
8	SKYLAB	0.68-0.76	near IR	Fair	Fair	1036
9	SKYLAB	1.55-1.75	middle IR	Very Good	Very good	860
10	LANDSAT	0.50-0.60	visible	Excellent	Excellent	820
11	LANDSAT	0.60-0.70	visible	Excellent	Excellent	766
12	SKYLAB	0.52-0.56	visible	Very good	Very good	619
13	SKYLAB	0.46-0.51	visible	Poor	Good	598
14	SKYLAB	2.10-2.35	middle IR	Good	Good	579
15	SKYLAB	10.20-12.50	thermal	Poor	Poor	569
16	SKYLAB	0.56-0.61	visible	Poor	Poor	555
17	SKYLAB	0.62-0.67	visible	Fair	Poor	471
18	SKYLAB	0.41-0.46	visible	Very poor	Fair	416

Table 3.23 Information content ranking based on divergence values of all data sets (SKYLAB, LANDSAT, Elevation)

Another indication of the importance of data quality is that both of the visible wavelength bands of LANDSAT data had excellent data quality and were ranked ahead of any of the visible wavelength bands of SKYLAB data, which had poorer quality but better spectral resolution. Also, note that the last four wavelength bands listed in Table 3.23 had only fair or poor data quality. One last point of significance shown in this table is that the 1.55-1.75 middle infrared wavelength band is ranked ahead of any of the visible wavelengths, again indicating the value of this middle infrared portion of the spectrum.

3.6 ADVANCEMENTS IN THE STATE-OF-THE-ART IN COMPUTER-AIDED ANALYSIS TECHNIQUES

3.6.1 Spatial Data Analysis

The normal classification procedure and the results described thus far involve a "per-point" classification technique in which the computer classifies each individual resolution element into one of the spectral classes defined by the training statistics. The spectral classes are then grouped into the information class of interest and a cover type map is obtained, as was discussed previously.

Meetings and discussions with personnel from the U.S. Forest Service, National Park Service, and other user groups indicated that for some purposes, the detail that was present on the per-point classification map was very useful, but for other purposes, it appeared that the per-point classification maps contained more detail than could be effectively utilized. For example, the per-point classification results sometimes have shown a single resolution element of "pasture" surrounded by a large area of coniferous forest. Such a result might be caused by a clearing in a forest stand, which would be of great interest to the wildlife manager because of the potential for wildlife habitat. However, for many of the other forest resource managers, a more generalized forest cover type map without such detailed information is much more useful. For most purposes, these user agency personnel indicated that they preferred small scale maps which have fairly generalized boundaries among the various

cover types (such as might be obtained if mapped with 10-acre minimums), rather than the extreme detail that is shown when every resolution element is classified independently.

A recently developed analysis procedure, referred to as the "ECHO" (Extraction and Classification of Homogeneous Objects) classifier has been developed. This technique involves the use of an algorithm which first defines the boundary around an area of similar spectral characteristics and then the area within the boundary is classified into a single spectral class. This procedure is somewhat similar to the "Per Field"classifier which has been used previously at LARS, except that with the "Per Field" classifier, the analyst must specify the area to be classified (boundaries). The ECHO classifier has the capability of specifying the boundary as part of the computer analysis procedure. Thus, it appeared that the ECHO classifier might enable us to obtain the more generalized cover type maps preferred by the U.S. Forest Service and the other user agency personnel to whom we had talked.

A study was therefore carried out to evaluate the results that would be obtained when utilizing the per-point classifier and the ECHO classifier, and secondly, to determine the classification performance that would be obtained when using the per-point classifier, the ECHO classifier, and the per-field classifier. The same set of 4 x 4 test areas that had been used in the previous classification sequences of SL-2, S-192 data were utilized. The classification re-

sults are shown in Figure 3.42 and Table 3.24.

As shown in Figure 3.42, the per-point classifier gives a rather salt and pepper effect to the classification results, whereas the ECHO classifier produced a cover type map that appears to be much more like those obtained through normal photo interpretation techniques. That is, larger areas of a single cover type are grouped together, and one does not get all of the fine detailed information obtained when using the per-point approach. It would therefore appear that the ECHO classification technique might be much more useful to the resource manager for many application needs. U.S. Forest Service personnel with whom we have discussed these results and who have seen the output maps have indicated enthusiasm for the ECHO classification output. They indicated that this type of computer classification map would indeed be very useful for many application needs and provide a product more amenable to existing map systems.

The results shown in Table 3.24 indicate that the ECHO classifier improves the classification performance significantly, as compared to the per-point classifier. This was particularly true for the pasture, aspen, and ponderosa pine cover types, which each showed increased performances of 10% or more. The per-sample classifier had significantly increased performance over the per-point classifier and, in most cover types, over the ECHO classifier as well. However, from a practical standpoint, since the boundary of the area of interest (i.e., the "sample") must be specified by hand in

"Per-point" Classification

"ECHO" Classification

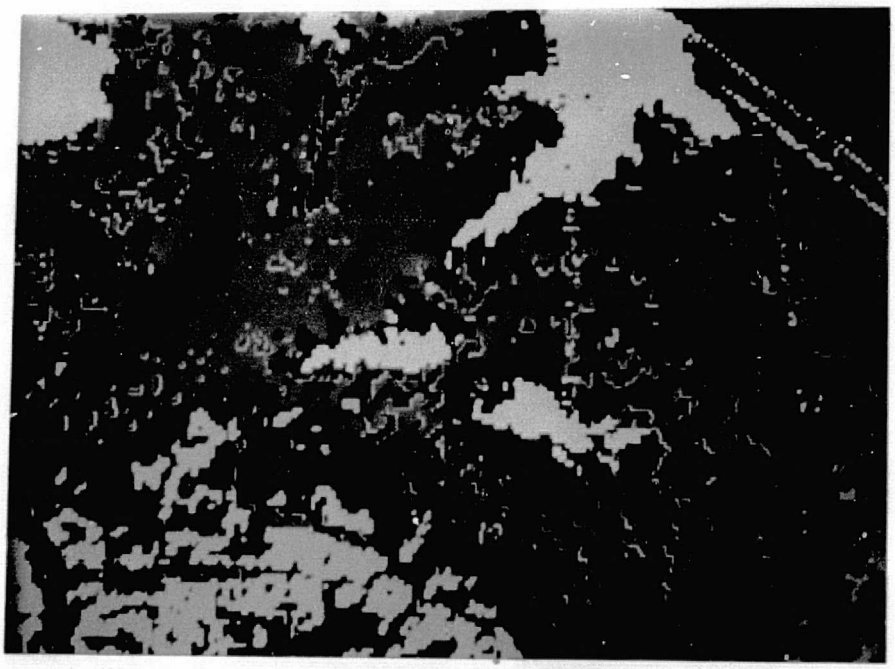

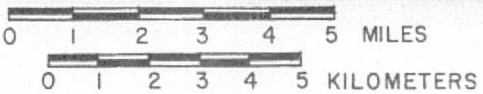

Figure 3.42 Comparison of "Per Point" and "ECHO" classification results for forest cover types

Table 3.24 Comparison of Classification Results Using Three Different Analysis Techniques (SL-2 SKYLAB S-192, "BEST" 4 Channels -- 6, 11, 13, 15)

	Per-Point Classifier	ECHO Classifier	Per-Sample Classifier
Water	94.8	95.8	100.0
Snow	100.0	100.0	100.0
Pasture	52.3	67.2	87.5
Deciduous	61.7	70.7	78.3
Oak	63.7	67.5	80.0
Aspen	54.8	65.4	69.2
Coniferous	90.9	91.0	96.2
Ponderosa Pine	72.9	82.9	77.8
Douglas/White Fir	76.8	79.1	82.5
Spruce/Fir	50.0	52.7	50.0
Overall: Major Cover Types	85.0	87.2	93.3
Overall: Forest Cover Types	71.0	76.0	78.7

order to use the per-sample classifier, but the ECHO classifier automatically defines the boundary of each forest stand or cover type area, the results for the ECHO classifier are much more important. As Figure 3.42 and Table 3.24 indicate, the ECHO classifier produces a more accurate classification results and the cover type map produced is in a more usable and desirable format for the user agencies. Further evaluation of these products will be carried out as part of our LANDSAT-2 project.

3.6.2 Refinement of Classification Analysis Procedures

During the analysis of the SKYLAB S-192 data, a number of questions and problems arose which indicated a need to further refine and test some of the basic analysis procedures being utilized. This portion of this report discusses three activities in which we became involved during the Ecological Inventory portion of this SKYLAB investigation.

The first activity involved a method to effectively reduce a large number of spectral classes down to a reasonable number of spectral-information classes. The initial analysis of the June 5, 1973, S-192 data involved nine training areas, each 40 x 40 resolution elements. The modified clustering technique was utilized to develop the training statistics. As was briefly described previously, the complexity of the test site lead to a total of 135 individual spectrally separate cluster classes within the nine training areas utilizing seven wavelength bands. To reduce the number of spectral classes involved, the separability algorithm was used to pool the similar spectral cluster classes, based upon a transformed divergence of 1500. If the transformed divergence was less than 1500, it was assumed that the two cluster classes were spectrally similar and could be pooled together. The statistics for the 135 cluster classes were thus pooled into 97 spectral classes, each of which had a spectral separability value greater than 1500. It was obvious that 97 spectral classes was still an unreasonable number to work with for the final classification sequence, so a spectral separability

value of 1700 was set as the threshold. However, this meant that in some cases spectral classes containing different cover types would be pooled into a single set of training st tis-tics. In such cases the analyst must make a decision whether the entire spectral class should be deleted or whether one of the cover types should be eliminated from that spectral class. In many cases, it was found that one of the cover types was of relatively minor importance whereas the other was of major importance in the test site area, and so the cover type of least importance could be eliminated from the spectral class. If both cover types were of equal importance, and if the number of resolution elements involved was relatively small, the entire spectral cluster class was eliminated from the training statistics deck. Through the judicuous use of a spectral separability limit of 1700, the 97 spectral classes were reduced to 31 spectral classes which allowed a reasonably accurate but not overly complex classification. Through comparison of these spectral classes with the underflight aerial photos, we could associate important characteristics of the earth surface features with each spectral cluster class (e.g. percent crown closure in forested areas, turbidity of water, etc.). For this reason, we refer to the final set of training data a spectral informational classes.

After a set of spectral-information (spectral) classes have been developed, there are two methods of reducing the spectral classes to informational categories to be utilized in producing the final maps and tables desired. One method

is to pool the statistics for all spectral classes within each information class before classifying the data. The second method is to group the spectral classes for each information class after classifying the data.

There are advantages to each method. By pooling the statistics before classifying, the number of classes are reduced, thereby reducing the amount of computer time required to classify the data. However, by pooling statistics, the separability between the classes used to classify is reduced. This is because the combination of classes that are spectrally separable (if training was properly done), will create bimodal distributions and therefore increase the variance. Although grouping classes after classifying will require additional computer time to do the classification, the classification accuracy should be higher when classes are grouped rather than pooled.

To determine the effects, in terms of computer classification time and classification accuracy, of pooling and grouping, the 31 spectral informational classes (described previously) that had been developed with the SL-2 data were utilized in conjunction with the "Best 4" wavelength bands previously selected as having the highest average transformed divergence for the 31 training classes.

The Granite Peaks test site was classified using these 31 spectral-informational training classes, first by pooling appropriate training classes before classification, and secondly, by grouping the classes after classification. In each case,

the final results were maps and tables for both the major cover types and forest cover types. Quantitative evaluation of the classifications was accomplished using the statistical grid of test fields described previously.

The results (Table 3.25) indicate that pooling statistics greatly reduces the amount of CPU time required to do the classification (from 2869 sec. to 701 seconds) and the drop in classification accuracy was not as large as was expected (85.0% to 82.6% for the major cover types, and 71.0 % to 68.9% for the forest cover types). This indicates that the pooling approach could be utilized under the proper conditions, but further work is recommended to define the circumstances under which this approach could be safely utilized.

Table 3.25 Comparison of Pooling and Grouping Techniques for Cover Type Mapping (SL-2 Data, "BEST" 4 Channels -- 2, 7, 9, 11)

Analysis Technique	Overall Classification Performance		Computer Time Required (Minutes)	
	Major Cover Types (Land Use Categories	Forest Cover Types	Major Cover Types	Forest Cover Types
Classification with 31 Spectral Classes, Then Grouping Results	85.0%	71.0%	47.8	47.8
Pooling Statistics, Then Classifying	80.5%	68.7%	11.7	16.0

3.6.3 Topographic Data Utilization

In areas of mountainous terrain, there is a distinct impact on the vegetation due to the topography of the area. This effect could be clearly seen in Figures 1.2 and 3.2. Figure 3.2 in particular, clearly demonstrates the impact of elevation on forest cover types. It is believed that in some cases, spectral differences could not be defined between two different forest cover types, but that a separation could be made between the cover types on the basis of elevation. For example, Engelmann spruce and subalpine fir, comprising the spruce-fir cover type, are primarily found at elevations above 2900 meters, whereas Douglas and white fir, which are spectrally rather similar, are predominantly found at elevations below 2900 meters. Therefore, elevation data should allow a more accurate separation between these forest cover types than can be achieved using spectral data alone, particularly when one considers the variation in spectral response due to stand density, slope and aspect and related shadow effects.

Since the SKYLAB data set had been overlaid with the topographic data (elevation, slope and aspect), a potential existed to examine the improvement in classification accuracy that could be achieved through utilization of the elevation data as a very preliminary test of the utilization of elevation data in conjunction with spectral data, the maximum likelihood classifier was utilized to classify the SL-2 data into the various forest cover types. A three-step sequence was pursued in this classification, involving:

1. Classification of forest cover types using the "best" three wavelength bands.
2. The classification using the same three wavelength bands plus the elevation data.
3. The classification of the data using the "best" four wavelength bands.

By following such a sequence, we could evaluate the improvement and performance when the elevation channel was added to the best three bands of spectral data. However, since we would then be comparing results of a three "channel" vs. four channel classification, it is felt that we should also classify the data using the "best" four wavelength bands of data, so that we could compare a four channel classification involving the elevation data with a four channel classification not including the elevation data.

The results of this analysis sequence were particularly striking in relation to the improvement in classification for the spruce-fir forest cover types, and for the aspen forest cover type. In the case of spruce-fir, the best three wavelength bands gave a classification performance of 49.2% and the best four wavelength bands resulted in a 54.7% classification performance. However, the best three wavelength bands plus elevation gave a classification performance of 65.2%, for an improvement of 16% over just using the best three wavelength bands of spectral data alone and an improvement of 10.5% over using the four channels of spectral data without the elevation data. In the case of aspen, the best three

channels of spectral data gave a classification performance of 45.7%, but the addition of the elevation data allowed a classification of 56.3% to be obtained. In this case, there had been no improvement in classification performance when four channels of spectral data alone had been utilized as compared to only three channels of spectral data. Since the oak forest cover type had shown an improvement of approximately 8% when the elevation data was added to the best three spectral channels, the deciduous forest cover in total showed an improvement from 52.4% for the best three spectral wavelength bands to 53.0% for the best four wavelength bands and a 64.5% classification performance for the best three spectral bands plus the elevation channel.

It is clear from these results that the use of the elevation data offers considerable potential for improving the classification performance that can be achieved for individual forest cover types. In some cases, the classification performances were not improved and it is clear that a better analysis technique must be utilized to effectively incorporate the topographic data in the analysis procedure.

In another approach to demonstrate the utility the multiple source data tape incorporating elevation, slope, and aspect data, a series of tables were generated for the test site showing the hectares, acres, and percent of total area within the test site within each elevation zone, aspect zone, or slope group. These summaries are shown in Tables 3.26, 3.27, and 3.28. Such information could also be shown in a map-type format, as seen in Figures 3.43, 3.44, 3.45, and 3.46.

Table 3.26 Area in Granite Peaks Test Site as a function of elevation

ELEVATION	HECTARES	ACRES	% AREA
Under 2000 meters	0	0	0.0
2000-2100	371	918	0.4
2100-2200	4,270	10,551	4.6
2200-2300	5,663	13,992	6.1
2300-2400	10,675	26,379	11.5
2400-2500	10,768	26,608	11.6
2500-2600	9,097	22,479	9.8
2600-2700	10,675	26,379	11.5
2700-2800	9,933	24,544	10.7
2800-2900	9,840	24,314	10.6
2900-3000	7,148	17,662	7.7
3000-3100	4,920	12,157	5.3
3100-3200	3,527	8,716	3.8
3200-3300	1,949	4,817	2.1
3300-3400	1,393	3,441	1.5
3400-3500	1,393	3,441	1.5
3500-3600	928	2,294	1.0
3600-3700	279	688	0.3
over 3700	0	0	0.0
TOTAL	92,829	229,380	100%

Table 3.27 Area in Granite Peaks Test Site as a function of aspect

ASPECT	HECTARES	ACRES	% AREA
N	13,553	33,489	14.6
NNE	5,848	14,451	6.3
ENE	8,726	21,562	9.4
E	7,612	18,809	8.2
ESE	6,405	15,827	6.9
SSE	3,249	8,028	3.5
S	650	1,606	0.7
SSW	3,156	7,799	3.4
WSW	5,291	13,075	5.7
W	7,241	17,892	7.8
WNW	9,840	24,314	10.6
NNW	6,405	19,827	6.9
FLAT	14,853	36,701	16.0
TOTAL	92,829	229,380	100.0%

Table 3.28 Area in Granite Peaks Test Site as a function of slope

SLOPE	HECTARES	ACRES	% AREA
$<3^{o}$	14,853	36,701	16.0
$3-5^{o}$	15,781	38,995	17.0
$5-10^{o}$	26,085	64,456	28.1
$10-15^{o}$	19,216	47,782	20.7
$15-22.5^{o}$	11,139	27,575	12.0
$22.5-50^{o}$	5,663	13,992	6.1
$50-90^{o}$	93	229	0.1
TOTAL	92,829	229,380	100.0%

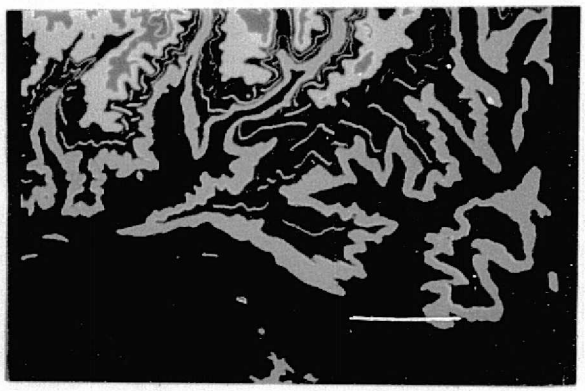

Figure 3.43 Color Coded Image of Elevation in 200 m intervals
Dark blue=200^0-2200 meters, brown=2200-2400 meters, etc.

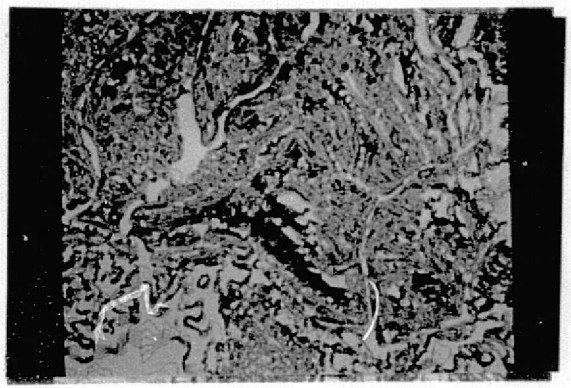

Figure 3.44 Color Coded Image of Slope
white=flat, red=1^o-10^o, yellow=10^o-15^o, green=15^o-50^o, blue=50^o-90^o

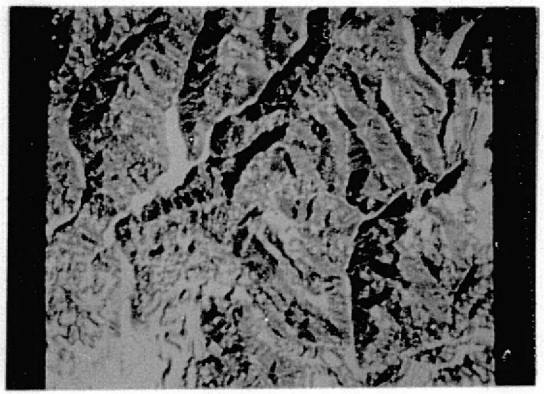

Figure 3.45 Color Coded Image of Aspect
White=flat, red=north, yellow=east, green=south, blue=west

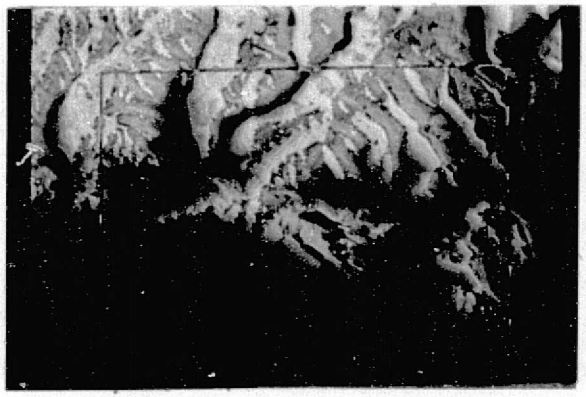

Figure 3.46 False color composite of topographic data. red filter = elevation, blue filter = slope green filter = aspect

In Chapter 2, some black and white illustrations of the topographic data were shown. During the analysis of the forest cover types, utilizing the topographic data, a technique was developed to color code the data and obtain color displays of the elevation, aspect, slope, and a color combination of all three topographic characteristics. Figures 3.43, 3.44, 3.45, and 3.46 show these color coded displays of the topographic data that were utilized.

3.7 SUMMARY AND CONCLUSIONS

Many of the results obtained during this portion of the investigation are significant advances in the state-of-the-art of remote sensing technology. These results obtained should be considered to be quite data-dependent due to the characteristics of the test site, the quality of the data, and the analysis and evaluation techniques which were utilized. These facts must be taken into account if any attempts are made to generalize these conclusions to other data sets or geographic locations. However, because this test site was in an area of rugged mountain terrain having a complex vegetation pattern, and because the quality of the MSS data was not optimum, these results could be considered as representative of a "worst case" situation. Geographic locations without such a complex vegetative pattern or terrain effects and higher quality data sets should allow better results to be obtained in the future.

The modified cluster approach to classification of multispectral scanner data proved to be the optimal analysis procedure. For areas of natural vegetative conditions, such a modified cluster technique is far superior to a supervised analysis procedure or to the standard clustering (or non-supervised) procedure. In some cases, the analyst was working with as many as 135 separate spectral classes of data. Without the effectiveness of the modified cluster technique, the analysis of this data would have been extremely difficult.

The modified cluster technique significantly reduced the amount of computer time involved, increased the accuracy of the classification, and enabled better man-machine interactions to be achieved.

Reasonable accuracy and reliability can be achieved for mapping major cover types (land use categories) Level II) and forest cover types (species association), even in regions of rugged topographic relief using computer-aided analysis techniques and multispectral scanner data from satellite altitudes. Using the "Best" four wavelength bands of SKYLAB data, a classification performance of 85% was obtained for the major cover types, and the forest cover type classification resulted in a 71% overall correct classification.

Based on comparisons between photointerpretation results and computer analysis of SL-2 SKYLAB and LANDSAT data, our results ($r=0.929$) indicate that highly accurate acreage estimates can be obtained using computer-aided analysis techniques and satellite data sources.

Seasonal effects were significant when comparing the results of the June and August data analysis. Photointerpretation indicated that the August spectral characteristics of the data obtained during SL-3 (August 8, 1973) were significantly better than the spectral characteristics present in the SL-2 (June 5, 1973) data. A map accuracy index of 87% was obtained when using the August 8 color infrared photos, and 40% when using the June 5 color infrared photos. If better quality data had been available from the

SL-3 mission, the accuracy of the results of the computer-aided analysis of the MSS data would probably have been significantly improved.

The digital filtering procedure applied to the SL-3 S-192 data improved the data quality in some respects, but also caused new "noise" problems in the data. In particular areas around clouds had a "ringing" effect. This distortion in the SL-3 data caused poor computer-aided classification results (68.8% overall classification performance). Consequently, the detailed wavelength band evaluation study was conducted with the June SL-2 data set since the overall data quality seemed to be better, even though the photointerpretation results indicated that the spectral information content from the August (SL-3) data set was apparently better than the spectral information content present in the June data set.

The spectral information content present in individual wavelength bands of S-192 data is more important than the noise characteristics of the data. In the wavelength band evaluation phase of this study, wavelength bands that were relatively noisy were frequently selected as being more important for the multispectral classification than other channels that have better data quality characteristics.

Each of the four major spectral regions (visible, near infrared, middle infrared, and thermal infrared) is vital for effective computer classification of multispectral scanner data. The importance of the different spectral regions varies as a function of the cover type to be mapped. The near infrared portion of the spectrum was found to be particularly im-

portant for mapping various forest cover types. The 1.09-1.19 micrometer wavelength bands was found to be the most important wavelength band.

The best combination of six wavelength bands included two in the visible, two in the near infrared, one in the middle infrared, and the thermal infrared band. This result is significant in terms of the proposed configuration for the Thematic Mapper scanner on LANDSAT-D. The results of this investigation support the selection of wavelength bands tentatively scheduled for the Thematic Mapper, with the exception of the second channel in the near infrared region. Our results indicate that adjacent bands in the near infrared portion of the spectrum would not be as effective as two wavelength bands that are spectrally separated in this region. It is recommended that the wavelength bands tentatively scheduled for the Thematic Mapper in the 0.80-0.91 micrometer region be changed to a longer wavelength in the 1.10-1.30 micrometer region. In comparison to LANDSAT, the spectral resolution of the SKYLAB wavelength bands did not allow an improvement in results to be achieved for mapping major cover types or land use classes, but did allow a more accurate classification of forest cover types to be achieved. This result was because of the improved spectral resolution of the SKYLAB scanner as compared to the broader wavelength bands present on the LANDSAT scanner system, even though the data quality on SKYLAB S-192 data was not as good as the

LANDSAT data quality. Comparing the classification performance for forest cover types over exactly the same test area, the LANDSAT scanner data resulted in a classification performance of 68.4% whereas the higher spectral resolution of the SKYLAB data resulted in a classification performance of 71.0% (utilizing the best four wavelength bands of SKYLAB data).

The newly developed "ECHO" classifier produced results that were more accurate, from a quantitative standpoint, than the standard classification of each data point. Of more importance was the fact that the maps resulting from the ECHO classification had an appearance similar to a standard land use or forest cover type map. Therefore, the map output using the ECHO classifier was preferred by user agency personnel.

The capability to overlay topographic data onto multispectral scanner data offers significant potential for more effective forest cover type mapping in mountainous areas. Our results showed a 10% increase in classification performance for some forest cover types when elevation data was combined with SKYLAB spectral data. However, this analysis also indicated that different analysis procedures will need to be developed to effectively utilize the capability to combine topographic and multispectral satellite data sets.

The underflight color infrared aerial photos obtained by NASA were vital in conducting this research. Without the aircraft photography, detailed evaluation of the classi-

fication results achieved by computer-aided analysis of the SKYLAB scanner data could not have been achieved.

Discussions with user agency personnel concerning the results obtained with the SKYLAB satellite data produced somewhat varied responses depending on the individuals involved (primarily U. S. Forest Service and National Park Service personnel), their level within the organization, the information requirements which these individuals faced, and the willingness of the individual to consider alternative ways of obtaining various types of information. In general, the more local users expressed relatively little interest in the data derived from satellite altitudes because it was too generalized and broad in scope, but were quite interested in the information that could be obtained from the 1:60,000 scale aerial photos over their areas of interest. On a regional basis, the need for information over a large geographic area and in a more generalized map and tabular format was evident, and there was considerable interest expressed in the possibilities for obtaining such information using digital computer processing techniques and satellite data. Some evaluations of the products supplied to these users are still being conducted. Another general trend observed in talking to user agency personnel involved the status of existing information. If existing information was detailed and fairly accurate, relatively little interest was expressed in the potential for obtaining maps and tabular information with remote sensing techniques.

However, if the users had relatively little up-to-date, accurate information available to them, strong interest was expressed in the possibility of obtaining the needed information with remote sensing, using either the satellite data or the small-scale aerial photography. The third general area of user reaction which was encountered involved concern over the somewhat different format and reliability of the type of data that could be obtained through computer processing of satellite scanner data. Because the computer classification maps involved a statistical probability of correct classification of any one resolution element, they believed that they would need to evaluate these types of products and determine how to effectively utilize them. They tended to like the idea that the computer-aided analysis techniques produce quantitative results,which, if they are not correct, are at least biased in a consistent, definable manner.

A permanent display was built and installed in the Headquarters Museum of Mesa Verde National Park. This display features SKYLAB S-190 B photos of Mesa Verde and a computer-produced vegetation map of the park. The display was opened in late October, 1975. It is anticipated that this display may be viewed by over 600,000 visitors during the next year alone.

In summary, we believe that several of these results are significant advances in the development of remote sensing technology. The current capabilities for mapping land use and forest cover types in areas of mountainous terrain were

shown, the wavelength bands of most value in future satellite systems were studied, the potential for combining spectral data and topographic data was indicated, and valuable potentially significant interactions with user agency personnel were made possible through this SKYLAB research.

CHAPTER IV -- HYDROLOGIC FEATURES SURVEY

by

L. A. Bartolucci

4.1 INTRODUCTION

The hydrologic features survey portion of this SKYLAB final report incorporates three major areas of activity including:

- snow/cloud differentiation
- snow cover mapping
- thermal data calibration

Previous experience with LANDSAT-1 data had indicated that snow and clouds could not be spectrally differentiated in the visible and near infrared portions of the spectrum. However, spectral analysis of snow by a number of researchers indicated that snow cover should have a relatively low reflectance in the middle infrared portion of the spectrum, whereas theoretical considerations of the scattering phenomenon would indicate that non-selective scattering would cause clouds to have a high reflectance throughout these same wavelengths. SKYLAB data offered the first opportunity to test the hypothesis that snow and clouds could be effectively differentiated based on their spectral response in the middle infrared portion of the spectrum.

Interpretation of aerial photos obtained by NASA aircraft underflights during the SKYLAB SL-2 mission indicated that the areas which appeared to be solid snowcover on the satellite data were actually a combination of snow and trees in many areas, particularly in the areas at lower elevations.

Preliminary analysis of the SKYLAB data indicated that there were several differences in spectral response within various areas of the snow pack. This led to the possibility of utilizing the SKYLAB S-192 data to define and map different levels of spectral response within the snow pack area, and to relate these to the different characteristics of the ground scene. Inability to effectively differentiate and map various characteristics of a snow pack area would be of considerable value for more accurately predicting water run-off from mountain snow pack areas.

Because the SKYLAB data had been digitally overlaid onto a 1:24,000 scale data base, and topographic data had also been overlaid with the SKYLAB data, the potential also existed to define snow pack areas within individual watersheds. The potential also existed for tabulating acreages of the various spectral groups within the snow pack area as a function of elevation. Thus, a capability to spectrally map variations within the snow pack and to relate this to elevation and other topographic parameters offers considerable promise. This study pursued the development of a demonstration of such a capability. Also included in the snow cover mapping phase of the study was an evaluation of different analysis techniques that could be utilized for such applications.

The final phase of the hydrologic features survey portion of this SKYLAB study involves the calibration of the thermal channel in the SKYLAB data, in order to determine the ability to effectively utilize such data to study the thermal characteristics of mountain lakes, snow packs, and other earth sur-

face features. Although the data quality of the thermal channel of the SL-2 data was relatively poor, the calibration results indicated a surprisingly high correlation with the surface temperature measurements.

4.2 SNOW/CLOUD DIFFERENTIATION

4.2.1 Introduction

During the early 1960's the problem of differentiating snow-covered areas from cloud formations was first identified by those researchers interpreting early meteorological satellite imagery. At the time, however, their primary concern was the study of cloud types and patterns. More than a decade ago, while referring to the study of clouds as observed by the TIROS satellites, Conover (1964) stated that "clouds are easily confused by the interpreters with snow cover."

Today, with the improved spatial and spectral resolution of orbiting sensor systems such as the SKYLAB and LANDSAT multispectral scanners, a greater emphasis has been placed in the utilization of the multispectral data for hydrological applications, one of which is snowcover mapping.

Promising results were obtained in utilizing LANDSAT data to map the areal extent of snow fields. However, one of the drawbacks is still the difficulty in differentiating snowcover from clouds, especially when using computer-aided analysis of spectral information only, as reported by Hoffer and Staff (1974). This difficulty was encountered on several data sets

during the analysis of the LANDSAT-1 MSS data collected over the Colorado Rocky Mountains. Many other investigators have reported similar difficulties. Meier (1973), in his report on the evaluation of LANDSAT imagery for mapping and detecting changes of snowcover on land and on glaciers, stated that "it is difficult for an experienced observer to distinguish some types of clouds and fog from snow even with all possible radiometric information." Barnes and Bowley (1973) have also pointed out that "cloud interference, which limits the number of usable satellite observations for snowcover mapping, remains a problem."

With the advent of the SKYLAB mission, multispectral scanner data over an extended spectral region (0.41-12.5μm) became available, thereby offering a potential for effective snow/cloud differentiation.

This investigation was primarily concerned with the quantitative analysis of the SKYLAB-2 (SL-2) S-192 MSS digital data collected over the La Sal Mountains, Utah, where both clouds (cumulus) and snow were present in the scene. The specific objectives were:

1) to measure the spectral separability between snow and clouds in the 13 different wavelength bands of the SL-2 S-192 MSS data,
2) to define the wavelength bands that could be best utilized tc reliably differentiate snow from clouds,
3) to classify the snow and clouds using a maximum likelihood classifier and determine the percent correct classification.

4.2.2 Test Site Description

The SKYLAB-2 S-192 MSS data utilized in the study of snow/cloud spectral separability was collected over the La Sal Mountains in southeastern Utah during the fifth EREP pass of the space laboratory (see Chapter II for data description and assessment of its quality).

At the time of the spacecraft overpass (June 5, 1973), the northern part of the La Sal Mountains was covered by a series of cumulus clouds. Figure 4.1 shows a color photograph (SL-2, S-190B) of the area under study. This figure also shows the actual area covered by the S-192 multispectral scanner data.

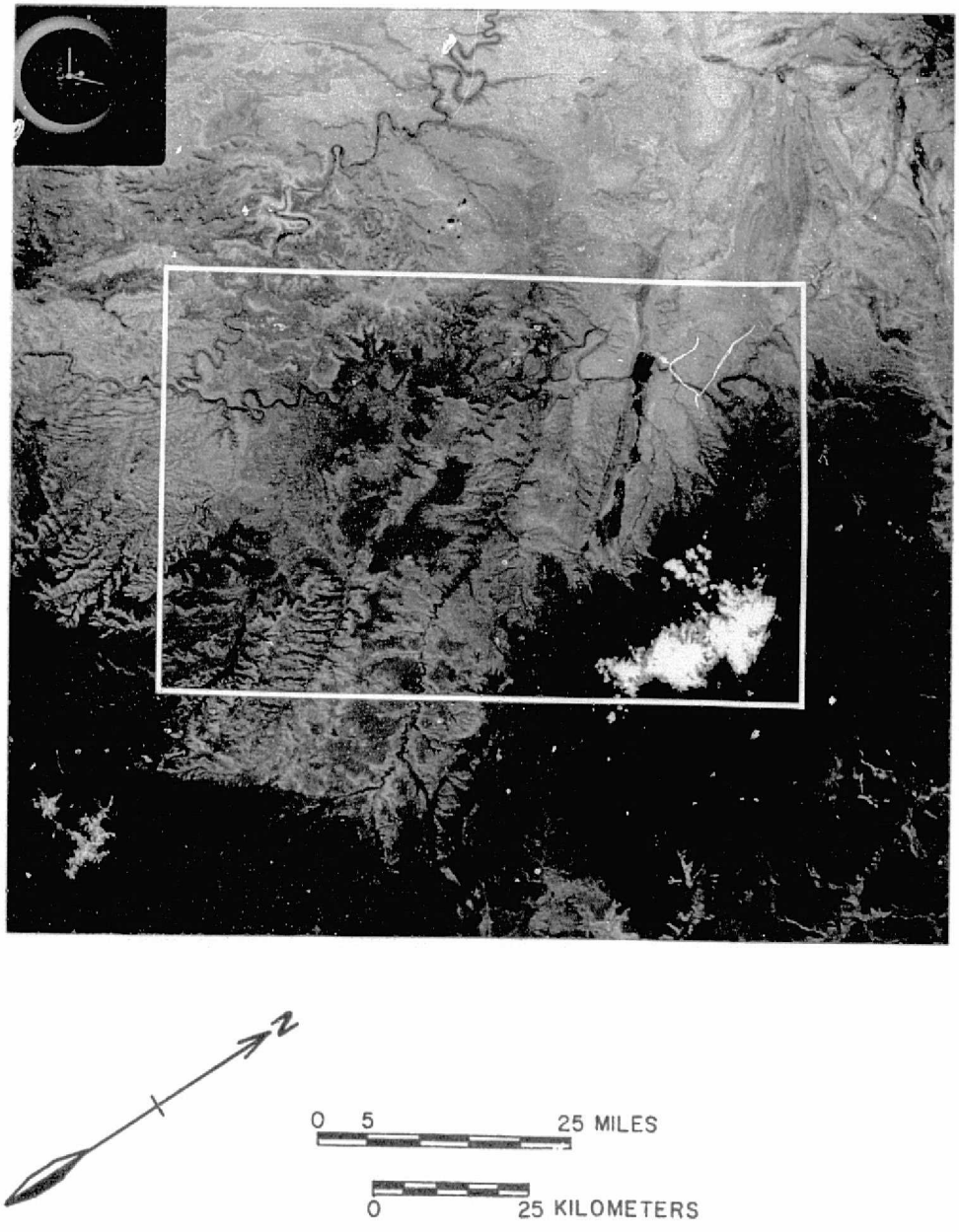

Figure 4.1 SKYLAB-2 S-190B photograph of the La Sal Mountains test site. The rectangle indicates the area covered by the S-192 data used in the snow/cloud differentiation study.

4.2.3 Analysis Sequence

The SL-2 S-192 MSS digital data collected over the La Sal Mountains were first straightened from its original conical scan format, and then reformatted to obtain a LARSYS compatible data tape.

Thirteen S-192 images obtained from the LARS digital display unit and corresponding to the 13 spectral bands of the S-192 systems are illustrated in Figure 4.2. They are representative of the four different portions of the spectum (visible, near infrared, middle-infrared, and thermal infrared). A simple inspection of these images shows that both the snow and clouds have similar spectral responses in the visible (0.41-0.67μm), the near infrared (0.68-1.30μm) and the thermal infrared (10.2-12.5μm) portions of the spectrum. Only in the middle infrared bands (1.55-1.75μm and 2.10-2.35μm) does the spectral response of clouds diverge considerably from that of snow. Clouds still continue to show a high response in the middle infrared, while the snow shows an appreciable drop in reflectance. It should be noted that energy in this portion of the spectrum cannot be detected by photographic emulsions or by means of the LANDSAT multispectral scanner system.[1/]

[1/] Photographic emulsions are not sensitive to wavelengths longer than 0.9μm. The LANDSAT MSS detector system is sensitive up to 1.1μm.

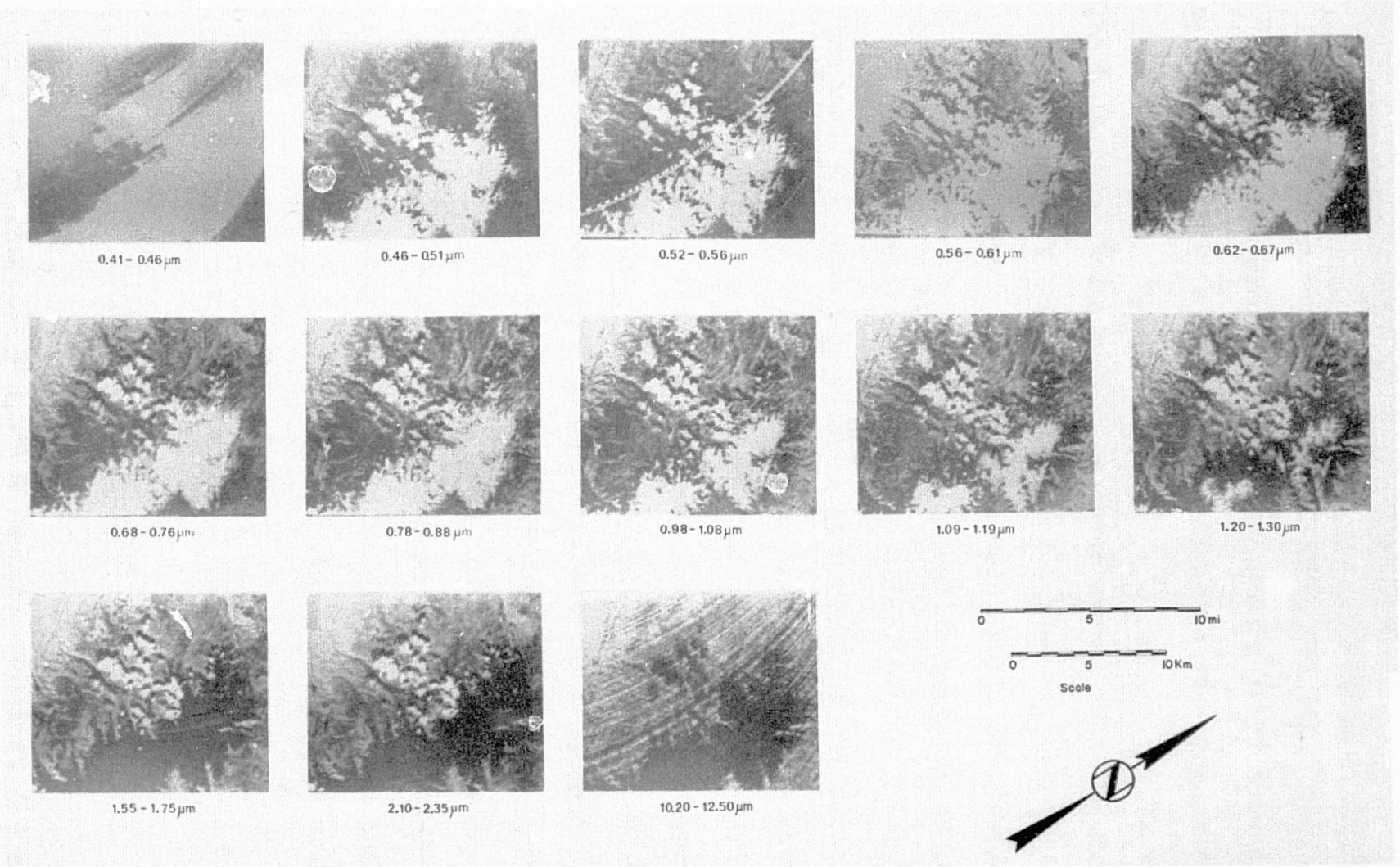

Figure 4.2 SKYLAB-2 S-192 imagery from 13 wavelength bands.

4.2.3.1 Statistics Calculation

The imagery in Figure 4.2 illustrate (qualitatively) the spectral behavior of clouds and snow in the different portions of the spectrum. However, to quantitatively determine the spectral separability between snow and clouds for computer-assisted multispectral classification purposes, training samples of both snow and clouds were selected and their statistics (mean and standard deviation) were computed. The resulting statistics are shown in Table 4.1.

Table 4.1. Statistics for Snowcover and Clouds from the SL-2 MSS Data, 5 June 1973, La Sal Mountains, Utah.

	Snowcover		Clouds	
Spectral Band(μm)	Mean	S.D.	Mean	S.D.
0.41-0.46	128	0	127	2
0.46-0.51	125	8	124	10
0.52-0.56	115	19	114	19
0.56-0.61	128	0	126	1
0.62-0.67	127	3	127	4
0.68-0.76	123	11	123	11
0.78-0.88	115	19	115	18
0.98-1.08	91	22	111	21
1.09-1.19	82	17	114	16
1.20-1.30	53	11	105	21
1.55-1.75	17	8	81	17
2.10-2.35	20	8	80	16
10.2-12.5	34	9	31	7

A comparison of the spectral response of clouds and snow is shown in Figure 4.3, where the means (plus or minus one standard deviation) for two visible, two near infrared, two middle infrared, and one thermal band are illustrated in the form of a coincident spectral bar graph. Figure 4.3 illustrates the overlap in spectral response for snow and clouds in the visible, near infrared, and thermal infrared bands. Figure 4.3 shows that the spectral response distributions for snow and clouds are substantially separated from each other in the two middle infrared bands.

The spectral characteristics of snow and clouds in the reflective portion of the spectrum have been extensively investigated under both laboratory conditions and field environments. The results of these investigations have indicated that the spectral responses of clouds and snow are very high and quite similar in the visible portion of the spectrum, but in the near infrared and especially in the middle infrared region their spectral responses differ considerably (Chapursky, 1966). Figure 4.4 shows a typical spectral reflectance cover for snow in the red, near and middle infrared regions as reported by O'Brien and Munis (1975).

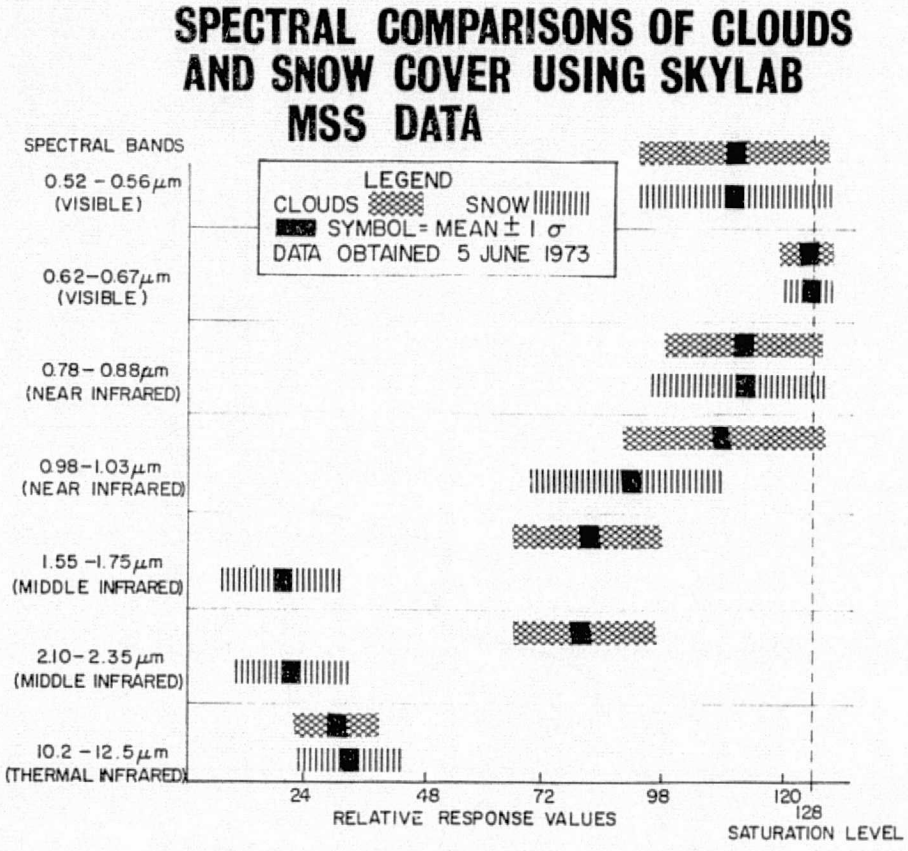

Figure 4.3 Comparison of the spectral response of clouds and snow from SKYLAB-2 MSS data.

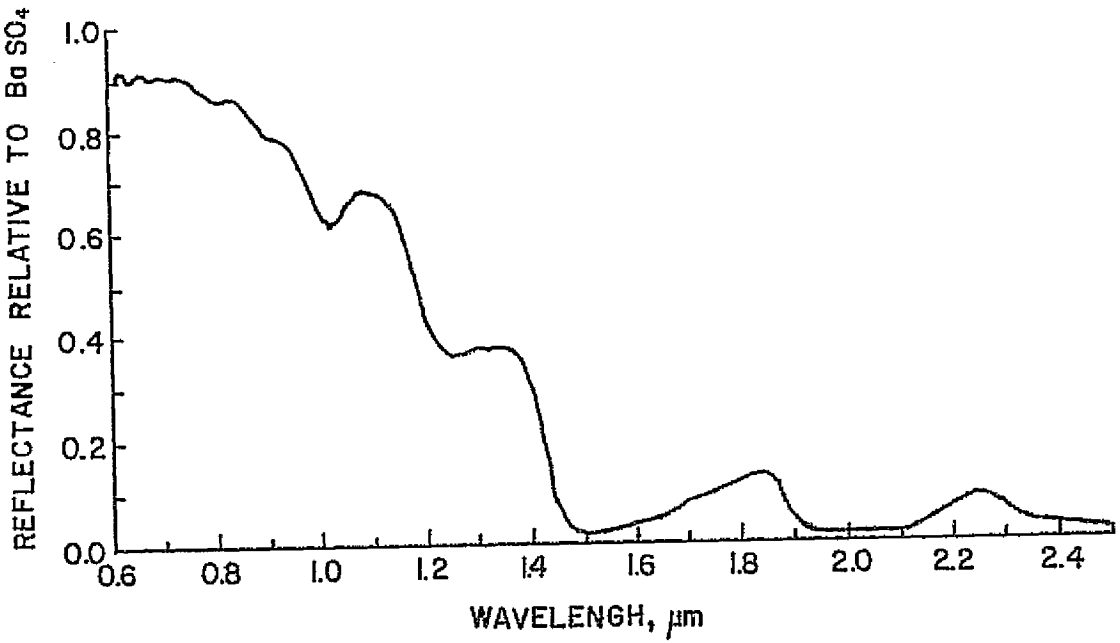

Figure 4.4 Typical spectral reflectance curve for snow. (After O'Brien and Mumis, 1975).

4.2.3.2 Detector Saturation

The output from the detectors have been quantitized into 128 discrete levels[1], where zero corresponds to absence of radiation and 128 corresponds to the maximum radiation intensity that would yield a linear response of the detectors. Thus, a radiation intensity equal to or greater than 128 would saturate the detectors. The response of snow and clouds in the visible and part of the reflective portion of the spectrum is usually quite high, and the output from some of the SL-2 S-192 detectors in the visible and part of the reflective infrared shows saturation, as illustrated in Table 4.1 by the mean values of 128 and zero standard deviation.

The detector saturation has caused severe problems in both LANDSAT and SKYLAB MSS data analysis. If a bright spectral class has caused the saturation of the detector(s) in one or more spectral bands, the resulting statistics will contain a singular covariance matrix which impedes further computer-assisted analysis of the data. There are two important LARSYS processors that are susceptible to singular covariance matrices: (1) the spectral separability or divergence measure (*SEPARABILITY) and (2) the classification algorithm (*CLASSIFYPOINTS).

---

[1] Originally, the SKYLAB S-192 MSS data were quantitized into 256 levels. However, for purposes of comparison with the LANDSAT data, the SKYLAB S-192 data were quantitized into 128 levels.

4.2.3.3 Spectral Separability Measure

In order to determine quantitatively the optimum subset of spectral bands for the classification of multispectral data, a feature selection algorithm is available in the LARS system (Swain et al., 1971; and Swain and Staff, 1972) which in fact measures the spectral divergence between all possible pair combinations of spectral classes. Figure 4.5 shows a bar graph illustrating the resulting spectral separability between snow and clouds. Note that in those bands where there was detector saturation (indicated by asterisks in Figure 4.5), the spectral separability was not computed, i.e. bands 1 and 4. Because the divergence is a monotonic function and increases without bound as separability increases, whereas the probability of correct classification saturates at 100%, the *SEPARABILITY processor contains an option that artificially saturates the separability measure at a value of 2000 and is referred to as the transformed divergence measure.

Based on experience at LARS on the use of the transformed divergence algorithm and following the results obtained by Swain and King (1973) on the relationship between the separability measure and the percent correct classification, values of transformed divergence greater than 1750 between a pair of spectral classes are considered to indicate complete spectral separability, as illustrated by the shaded area in Figure 4.5.

It is also interesting to note (in Figure 4.5) the trend in separability as a function of wavelength. The separability starts increasing in band 8 (0.98-1.03μm) or near infrared re-

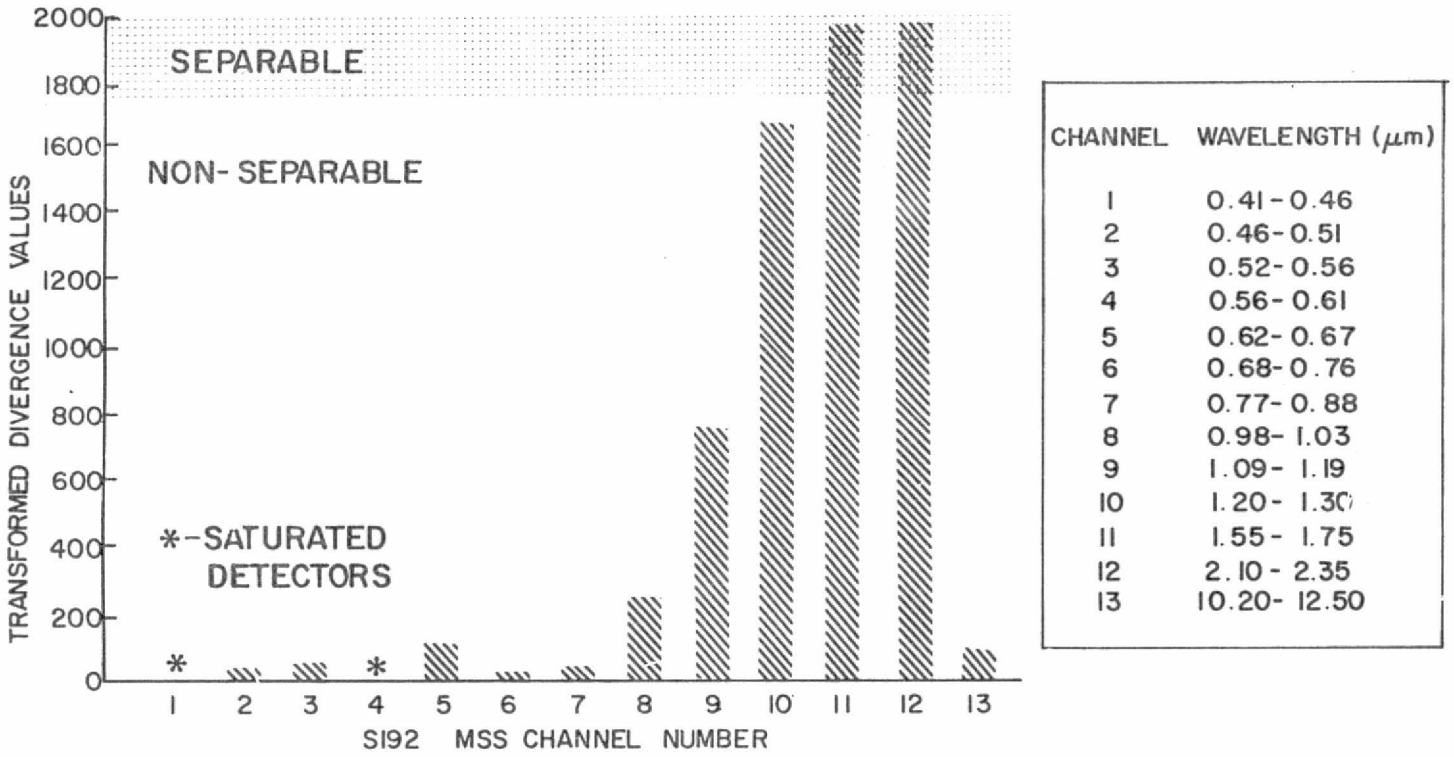

Figure 4.5 Spectral separability of snow and clouds in the 13 SKYLAB-2 S-192 wavelength bands.

gion and continues increasing through the middle infrared portion of the spectrum. However, there is a sharp drop in separability in the thermal infrared, which was expected because the radiant temperatures of the clouds and the snow as measured by the thermal band of the S-192 system were very similar.

The most relevant aspect of Figure 4.5 is that it clearly shows that snow and clouds can be spectrally separated only in bands 11 and 12 (middle infrared bands).

4.2.3.4 Multispectral Classification of Snow and Clouds

The final step in the study of the spectral differentiation of snow and clouds involved the classification of the multispectral data set using (1) a layered classification approach and (2) the standard LARSYS maximum likelihood classifier (*CLASSIFYPOINTS).

The decision tree (or layered classification) approach to multispectral classification was utilized to classify the La Sal Mountains data set into three spectral classes: (1) snow, (2) clouds, and (3) other (i.e., everything other than clouds and snow). The layered classifier processor has been described in detail by Wu et al. (1974), and was developed to improve the classification accuracy and to optimize the computational efficiency (reduce computer time) of multispectral classifications.

The decision tree may be constructed either automatically or in an interactive mode, i.e., by the researcher. In the case of the snow/cloud classification, because of the small number of classes involved (three spectral classes), the decision tree was constructed by the researcher with the aid of the coincident spectral plot for the "snow", "clouds" and "other" spectral classes, and the respective decision tree boundaries. Note in Figure 4.6 that the decision boundary separating the spectral class "other" (C) from both the snow and cloud classes (A and B) could have been drawn in either channel 2 (0.46-0.51μm band) or in channel 3 (0.52-0.56μm band) because both channels show a good spectral separation between the "snow" and "cloud" classes, and the spectral class "other". However, the boun-

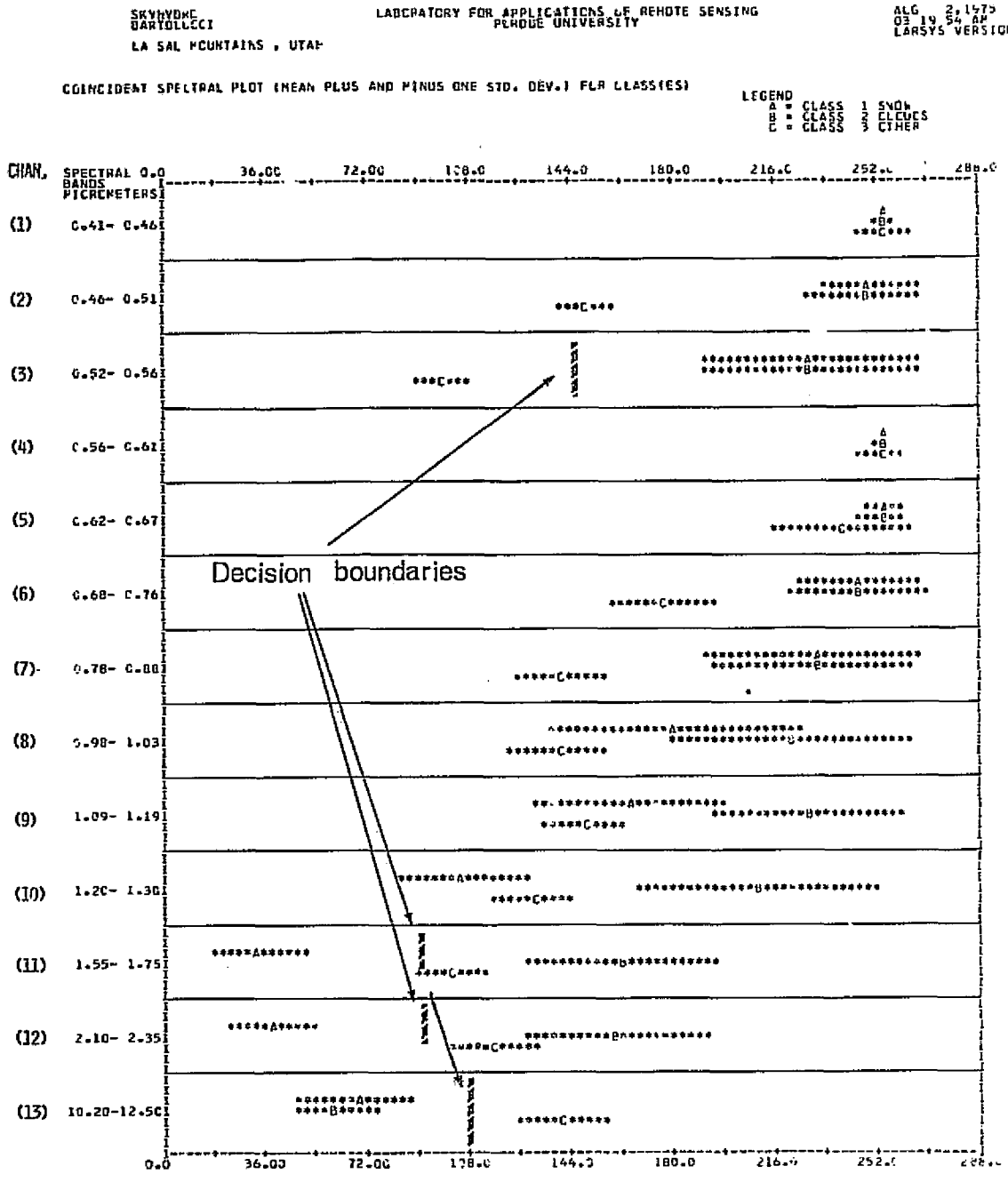

Figure 4.6 Coincident spectral plot for "snow", "clouds", and "other" spectral classes.

dary was drawn in channel 3 because the assessment of the data quality indicated that the signal to noise ratio (S/N) was higher in channel 3 than in channel 2. In conjunction with channel 3, channel 13 (10.2-12.5μm band) was also utilized for the separation of the class "other" from the snow and cloud classes. The reason for using the thermal band (channel 13) in addition to the visible band (channel 3) was to avoid possible spectral confusion between the highly reflective snow and clouds, and the sands that also have a high reflectance in the visible portion of the spectrum. In June, the snow and the clouds should be at a much lower temperature than the sands in the river valley. Thus, the thermal band should allow the reliable separation of any "other" bright cover types from the snow and clouds.

Once the layered classifier separates the spectral class "other" from the snow and cloud classes (in the first step or layer), then the classifier is provided with another subset of channels (spectral bands) for the separation of the snow from the cloud spectral class. The coincident spectral plot in Figure 4.6 clearly indicates that the decision boundaries necessary to separate the snow class from the cloud class (which are the only two spectral classes remaining after the first layer) should be drawn in channels 11 (1.55-1.75μm) and 12 (2.10-2.35μm). A schematic illustration of the decision tree structure is shown in Figure 4.7, where the ovals are referred to as "nodes" of the tree, and the lines are known as its branches.

The resulting layered classification is shown in Figure 4.8,

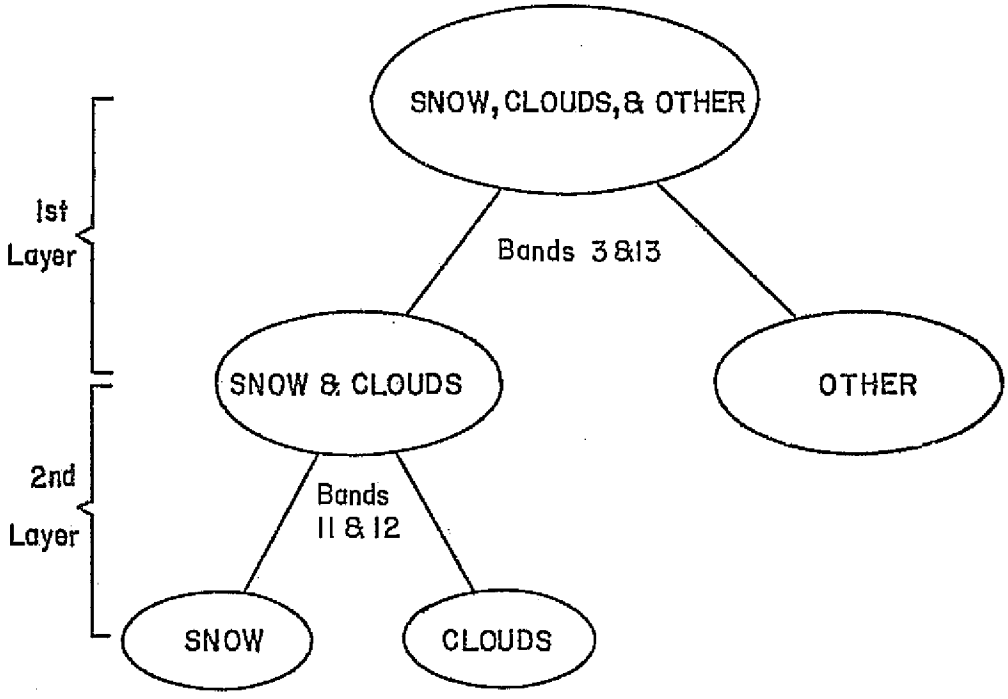

Figure 4.7 Decision tree structure for the layered classification of snow and clouds.

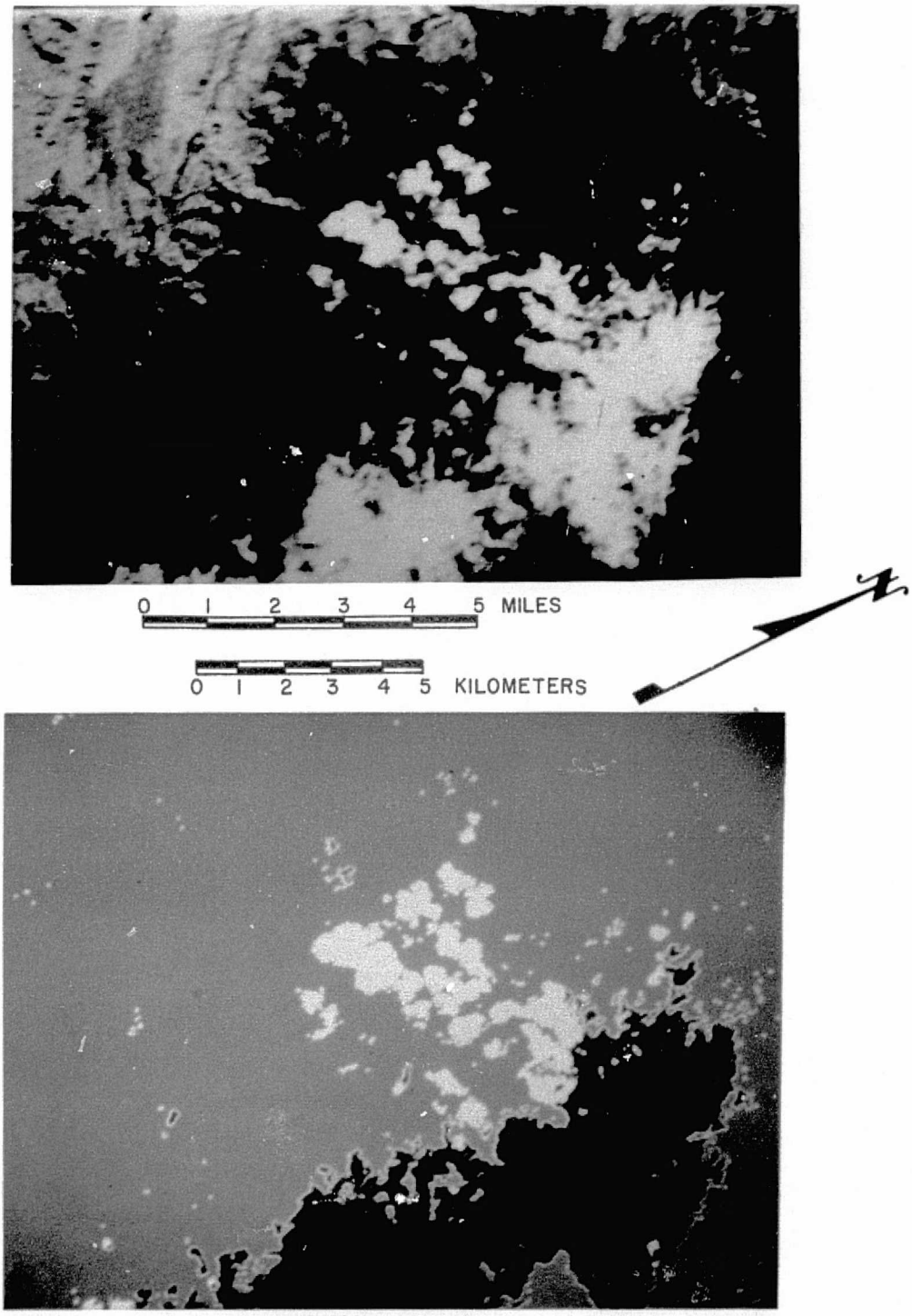

Figure 4.8 Color IR composite of the La Sal Mountains test site, and color-coded multispectral classification map of the same area.

together with a color infrared composite of the same areas.[1] The blue areas in the classification represent the snow, the white represents the clouds, and the green represents the spectral class "other", i.e., all the non-snow and non-cloud cover types present in the scene.

The layered classification of the La Sal Mountains test site (10,956 pixels) took 198 seconds of CPU (Central Processing Unit) time, and the accuracy of the classification (test field performance) was 99.7% overall correct classification as shown in Table 4.2.

Table 4.2. Classification Performance of the Layered Classifier.

Class	Number of Samples	Percent Correct	Number of Samples Classified Into		
			Snow	Clouds	Other
Snow	806	100.0	806	0	0
Clouds	238	99.2	0	236	2
Other	440	99.9	0	5	435
Overall Correct Classification		99.7%			

The same set of statistics utilized in the layered classifier was used as input to the standard LARSYS classifier (*CLASSIFY-POINTS) to compare the performance accuracy and the computational efficiency of both classification processors. The same bands used in the layered classification were utilized in the LARSYS classification (i.e., bands 3, 11, 12 and 13). The CPU time

[1] In order to obtain the color IR composite image, three of the SL-2 S-192 spectral bands were utilized: band 3 (0.52-0.56μm), band 5 (0.62-0.67μm) and band 8 (0.98-1.03μm).

involved in the LARSYS classification of the La Sal Mountains test site (same area processed by the layered classifier) was 235 seconds as compared to 198 seconds for the layered classifier. The layered classifier was, therefore, 16% faster (more efficient) than the LARSYS classifier. The performance accuracy of the standard LARSYS classifier was 97.5% overall correct classification as shown in Table 4.3.

Table 4.3. Classification Performance of the Standard LARSYS Classifier.

Class	Number of Samples	Percent Correct	Number of Samples Classified into		
			Snow	Clouds	Other
Snow	806	100.0	806	0	0
Clouds	238	99.6	0	237	1
Other	440	93.0	0	29	411
Overall Correct Classification		97.5%			

A comparison of the results shown in Tables 4.2 and 4.3 indicates that the Layered Classifier yielded a 2.2% higher classificacion accuracy than the standard LARSYS classifier.

4.2.4 Summary of Results and Recommendations

The results obtained in the present investigation concerning the spectral separability of snow and clouds may be summarized in the following statements:

1) The detector saturation caused by the high spectral response of clouds and snow, impedes the utilization of those bands where the saturation has occured even though those same bands might be desirable for the separation of other cover types.
2) The spectral responses of clouds and snow in the visible and part of the reflective infrared (0.41-1.3μm) region of the spectrum are so close to one another that it is impossible to obtain a reliable spectral separation of the snow and clouds in the 0.41-1.3μm region using existing computer-aided analysis techniques.
3) The thermal band (10.2-12.5μm) was found to be of no use in the separation (discrimination) of snow-covered surfaces and clouds, because both the clouds and the snow-cover were at approximately the same radiant temperature.
4) Clouds can be reliably and accurately separated from snow when using spectral information in the middle infrared region (1.55-2.35μm interval) of the spectrum.
5) The multispectral classification results shown in Tables 4.2 and 4.3 indicate that the Layered Classifier approach yielded a 2.2% higher classification accuracy than the standard LARSYS classifier. The comparison of the two classification approaches also showed that the Layered

Classifier was (in this particular case) 16% more efficient with respect to computational time than the LARSYS classifier.

In order to meet the requirements of the snow hydrologists, future operational earth observation systems should include at least one band in the middle infrared portion of the spectrum, preferably in the 1.55-1.75μm interval, in order to enable a reliable spectral discrimination of clouds and snow. Furthermore, it is recommended that the amplifier gains in future satellite detecting systems should be set so as to avoid saturation problems caused by the high spectral response of snow and clouds.

4.3 SNOWCOVER MAPPING

4.3.1 Introduction

The water supply for much of the southwestern United States comes from snowmelt in the watersheds of the Colorado Rocky Mountains. Information on the amount of snow accumulated during the winter months is necessary for making accurate predictions of spring runoff. Leaf and Haeffner (1971) have pointed out that an important index of runoff during the snowmelt season is the areal extent of the snowcover.

For more than thirty years snow hydrologists have made innumerable attempts to correlate the areal extent of snowcover and subsequent runoff. Parshall (1941) and Potts (1944) have estimated the areal extent of snow fields for runoff forecasting using ground photography. From the late forties to date, many studies have included use of aerial photography to measure the areal extent of snowcover (Parsons and Castle, 1959; Finnegan, 1962; Leaf, 1969). However, it was not until the early 1960's that one could attain a synoptic view of large geographical areas through earth orbiting satellites. Today, a wide variety of environmental satellites are collecting an astronomic amount of data that potentially could be utilized to map the areal extent of snowcover in a repetitive mode. Wiesnet (1974) has stated that "our capacity for collecting data on snow and ice far exceeds our ability to analyze the data." Therefore, in order to keep up the pace with the existing and highly advanced data collection technology, computer-aided analysis techniques (CAAT) need to be further developed and evaluated.

4.3.2 Test Site Description and Data Utilized

For the snowcover mapping study the San Juan Mountains test site was selected because this area is fairly typical of the Rocky Mountains Region in terms of water resources. A general description of the test site location and characteristics has been reported in section 1.3.

The topography of the test site area is rugged, ranging in elevation from less than 2000 meters to over 4200 meters. Timberline in the region is at approximately 3600 meters, and extensive areas of tundra are found above this elevation. In the data set analyzed in this study, this tundra area was completely covered by snow. Below timberline, there are several different forest cover types that are distributed as a function of the topography (elevation, slope and aspect). There are many variations in stand density between and within the different forest cover types. Such stand density variations become important in interpreting the spectral characteristics of the SKYLAB S-192 MSS data for snowcover mapping purposes, as will be discussed later.

This study involved an unusual and particularly valuable set of data that were obtained over the test site during the SKYLAB (SL-2) mission as outlined in Table 2.1.

4.3.3 Spectral Definition and Classification of Snowcover

An inspection of Figure 4.9 shows that the snowcover has a high reflectance throughout the visible wavelength data (channels 1 through 5, from 0.41 to 0.67μm). On data in the near infrared wavelengths (channels 6 through 10, from 0.68 to 1.39μm), the areal extent of the snowpack seems to decrease in size with increase in wavelength. In the middle infrared region (channel 11, 1.55 to 1.75μm, and channel 12, 2.10 to 2.35μm), the snowcover is very low in reflectance and appears nearly black. Finally, in the thermal infrared data (channel 13, 10.2 to 12.5μm), the snow is relatively cold in relation to the other earth surface features, so it appears dark in tone on the imagery.

The apparent decrease in areal extent of the snowpack throughout the reflective infrared portion of the spectrum seems to be caused by two factors. First, water in liquid form has very little reflectance above 0.8μm, and since the snowpack was in the process of melting by June 5, particularly at the lower elevations, the snow crystals have a coating of liquid water which causes a lower reflectance. The second factor is that the forest stand is denser at lower elevations, resulting in a higher proportion of forest canopy than snowcover at the lower elevations. Examination of the aerial photos (taken the day after the SKYLAB data were obtained) showed that only the tundra areas at the highest elevations had a pure snow cover, without any trees present to cause a decreased reflectance.

The computer-assisted analysis of the SL-2 S-192 MSS data for mapping snowcover involved several processing steps. The first consisted of the automatic definition (classification)

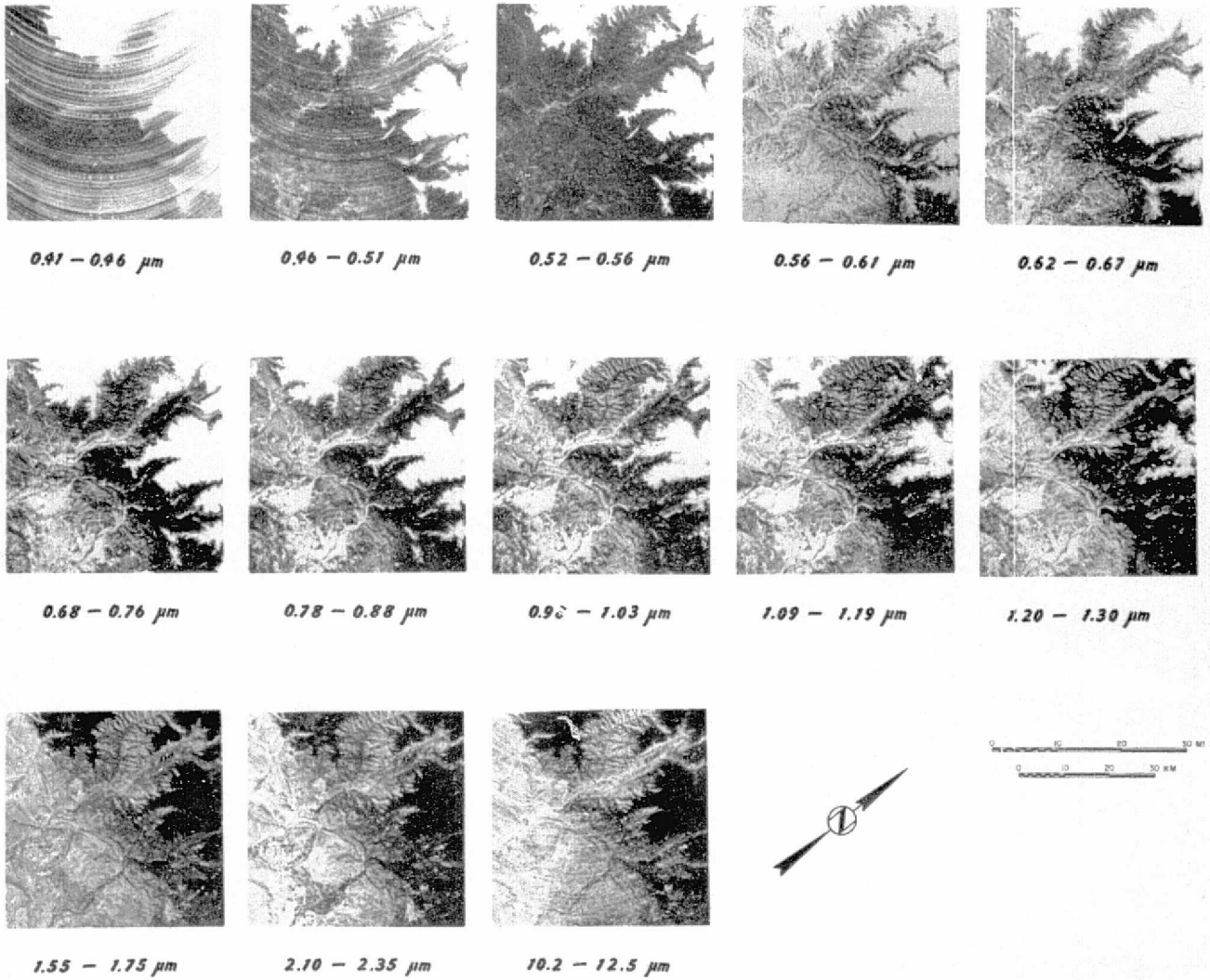

Figure 4.9 SKYLAB-2 S-192 scanner imagery. San Juan Mountains, Colorado, June 5, 1973.

of the maximum number of spectrally separable classes or categories of snowcover present in the scene. This step is referred to as the "multispectral clustering" or "non-supervised classification" approach. In this manner, five distinct spectral classes of snowcover were defined. Subsequently, their statistics (means and covariance matrices) were used as training input for the final maximum likelihood classification of the entire data set. Table 4.4 shows the mean spectral response of the five snowcover classes and of forest spectral class.

Table 4.4. Mean Spectral Response of Five Snowcover Classes and a Forest Spectral Class.

	Spectral Classes					
Band (μm)	Snow 1	Snow 2	Snow 3	Snow 4	Snow 5	Forest
(0.41-0.46)	255*	255*	255*	255*	255*	205
(0.46-0.51)	255*	255*	255*	197	162	110
(0.51-0.56)	254*	252*	219	120	93	56
(0.56-0.61)	255*	255*	255*	253	251	131
(0.62-0.67)	255*	255*	255*	255*	237	72
(0.68-0.76)	255*	255*	255*	240	166	89
(0.78-0.88)	255*	255*	255*	193	148	113
(0.98-1.08)	255*	255*	194	138	108	102
(1.09-1.19)	251	196	137	104	89	92
(1.20-1.30)	185	148	98	76	68	83
(1.55-1.75)	64	61	56	54	59	72
(2.10-2.35)	19	17	14	11	13	21
(10.2-12.5)	99	100	101	105	110	124

* - Denotes detector saturation

After the automatic definition (through the LARSYS clustering processor) of the maximum number of separable spectral groups of snowcover present in the San Juan Mountains test site (five snowcover spectral groups), in order to be able to spectrally classify the entire data set it was necessary to train the computer to recognize other major ground cover types also present in the scene, i.e., water, forest, agricultural vegetation, and a specular reflection class to take into account the intense glittering effect encountered in certain parts of the surface water bodies. Therefore, a total of nine spectral groups were involved in the final multispectral classification of the data.

Figure 4.10 shows a coincident spectral plot of the nine classes considered in the multispectral classification. Because some of the snow spectral groups had a saturated spectral response (255 digital counts) in some of the channels, it was not possible to utilize the standard LARSYS classifier (*CLASSIFYPOINTS). Therefore, a new approach to multispectral classification was used, i.e., the decision tree classifier or layered classifier. In essence, the layered classifier utilizes a maximum likelihood algorithm in a sequential or layer-by-layer mode. The major advantage of this classification approach is that it allows the multispectral discrimination of certain spectral classes using an optimum subset of spectral bands. A further separation of these spectral classes may be accomplished in a subsequent classification step (layer) using another set of the most appropriate spectral bands for that particular purpose.

SKYHYORD
BARTOLUCCI

LABORATORY FOR APPLICATIONS OF REMOTE SENSING
PURDUE UNIVERSITY

MAY 27,1975
06 25 04 PM
LARSYS VERSION 3

COINCIDENT SPECTRAL PLOT (MEAN PLUS AND MINUS ONE STD. DEV.) FOR CLASS(ES)
SNOW-COVER MAPPING, SKYLAB-2 S192 MSS DATA
GRANITE PEAKS TEST SITE, JUNE 5, 1973

LEGEND
A = CLASS 1 CROPS
B = CLASS 2 TREES
C = CLASS 3 WATER
D = CLASS 4 SPECREFL
E = CLASS 5 NS- 1/ 5
F = CLASS 6 NS- 2/ 5
G = CLASS 7 NS- 3/ 5
H = CLASS 8 NS- 4/ 5
I = CLASS 9 NS- 5/ 5

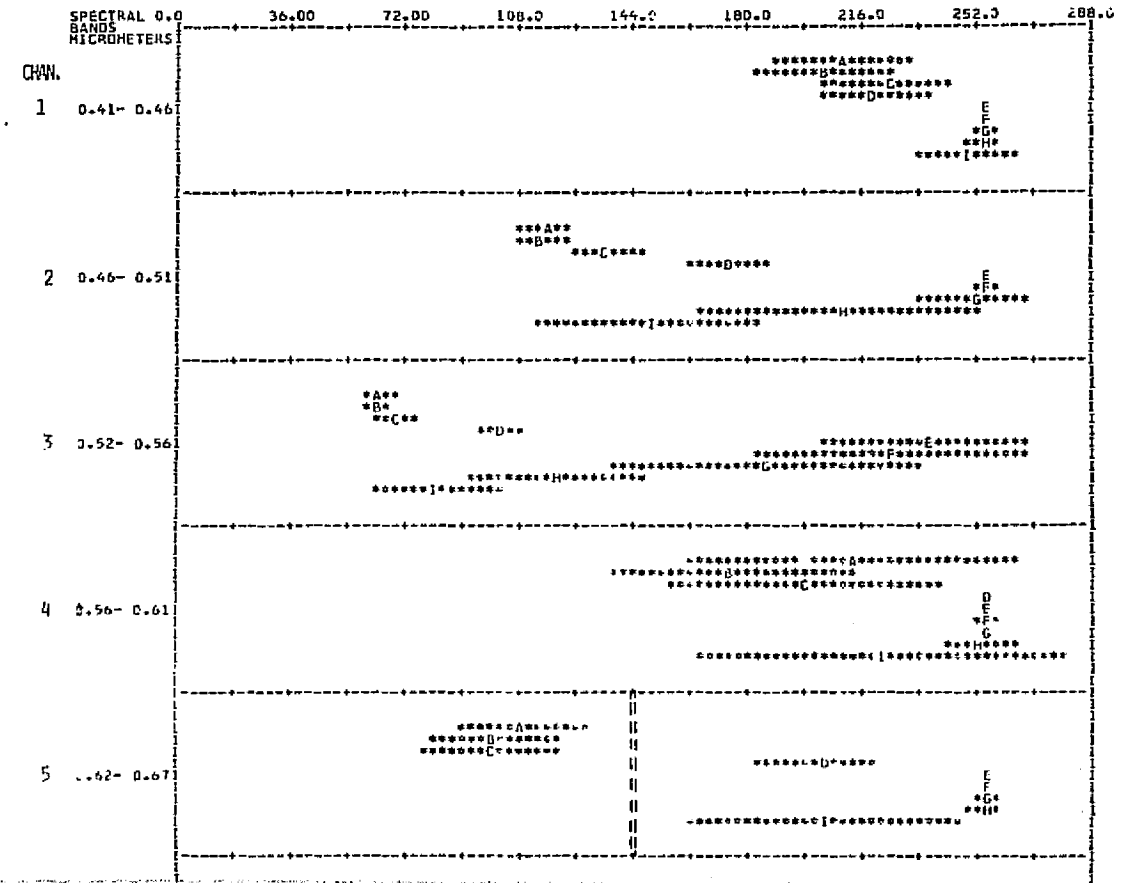

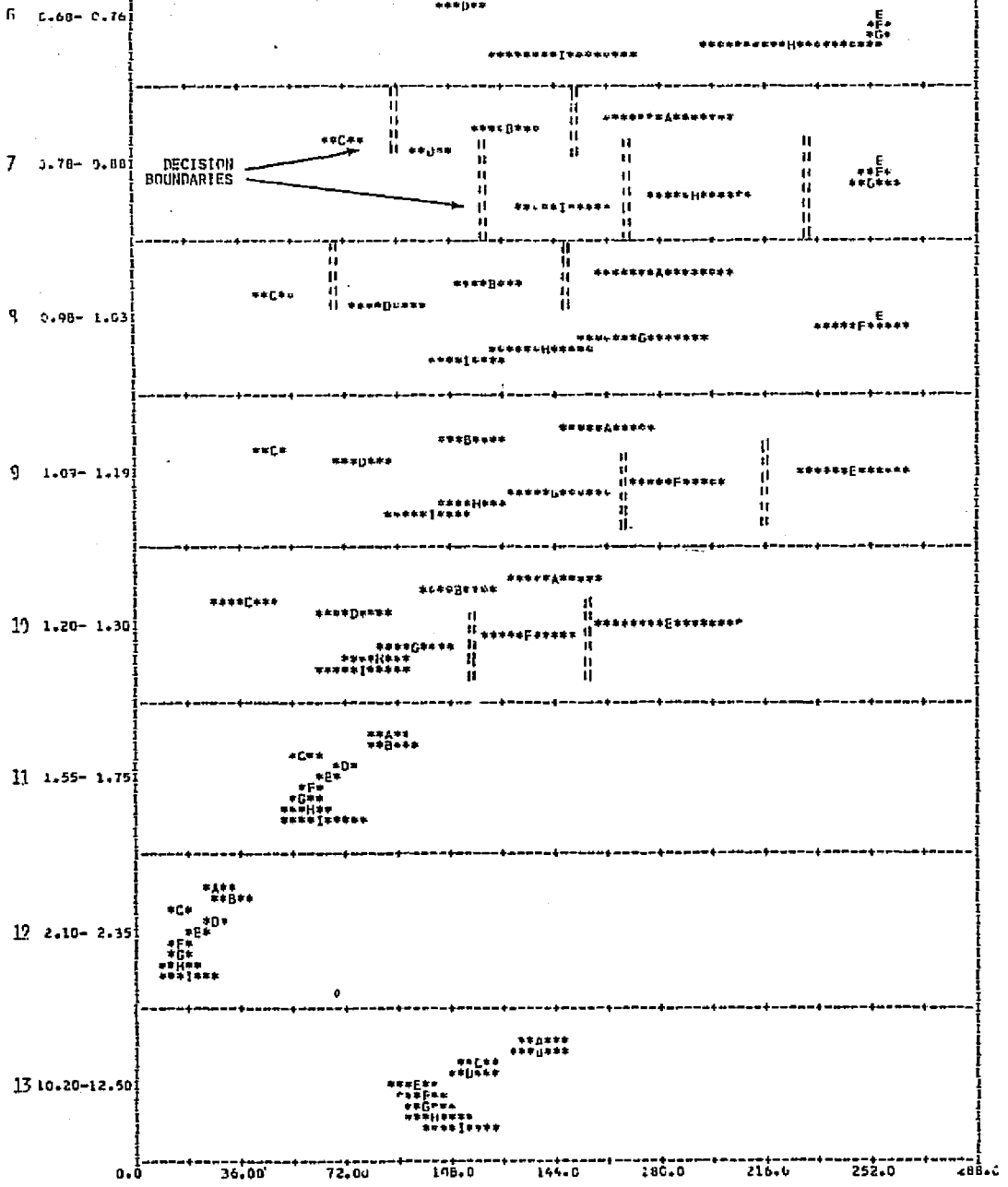

Figure 4.10 Coincident spectral plot of nine ground cover spectral classes.

FOLDOUT FRAME 2

In Figure 4.10 one can see that in order to separate the crops, trees, and water spectral classes from the specular reflection and the five classes of snow, only band 5 (0.62-0.67μm) is needed. If a further separation among the crops, trees and water classes is desired, then band 7 (0.78-0.88μm) and 8 (0.98-1.08μm) may be used for this purpose. Finally, in order to discriminate the specular reflection class from the five snowcover classes, and furthermore, to separate the five snowcover classes among themselves, two sequential classification steps are needed. That is, in one step, bands 7 (0.78 0.88μm) and 13 (10.2-12.5μm) are used to separate the specular reflection class from snow-4, snow-5, and a group of snow-1, snow-2 and snow-3. Then, bands 9 (1.09-1.19μm), 10 (1.20-1.30μm) and 13 (10.2-12.5μm) are utilized to separate the snow-1, snow-2 and snow-3 among themselves. The above classification sequence may be easily visualized by means of a diagram which is referred to as the "decision tree" and it is illustrated in Figure 4.11.

The result of the multispectral classification of the SL-2 S-192 scanner data is a snowcover map (Figure 4.12) in which the spectral classes of interest have been color coded. The colors in Figure 4.12 indicate a specific spectral class as illustrated in Table 4.5.

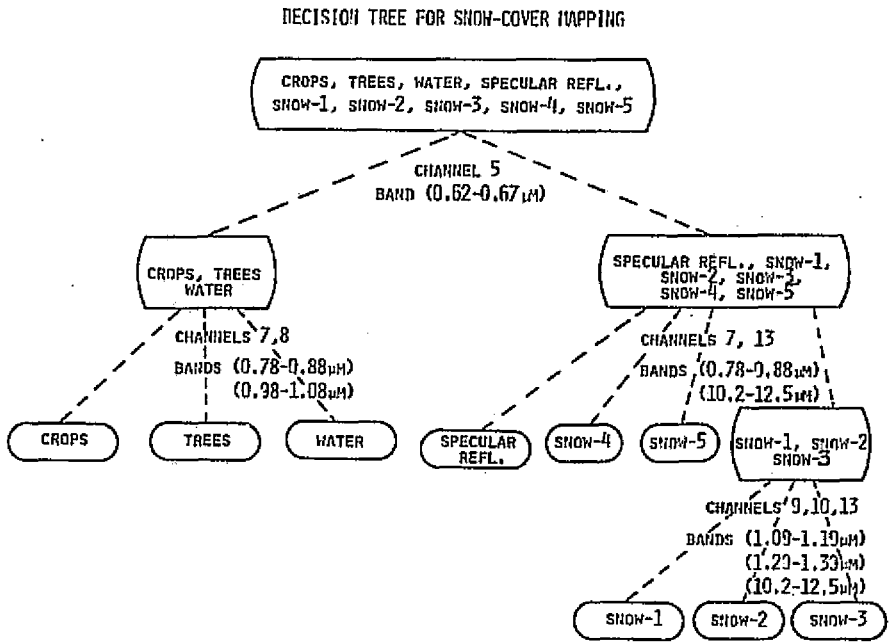

Figure 4.11 Multispectral decision tree for the classification of snow cover .

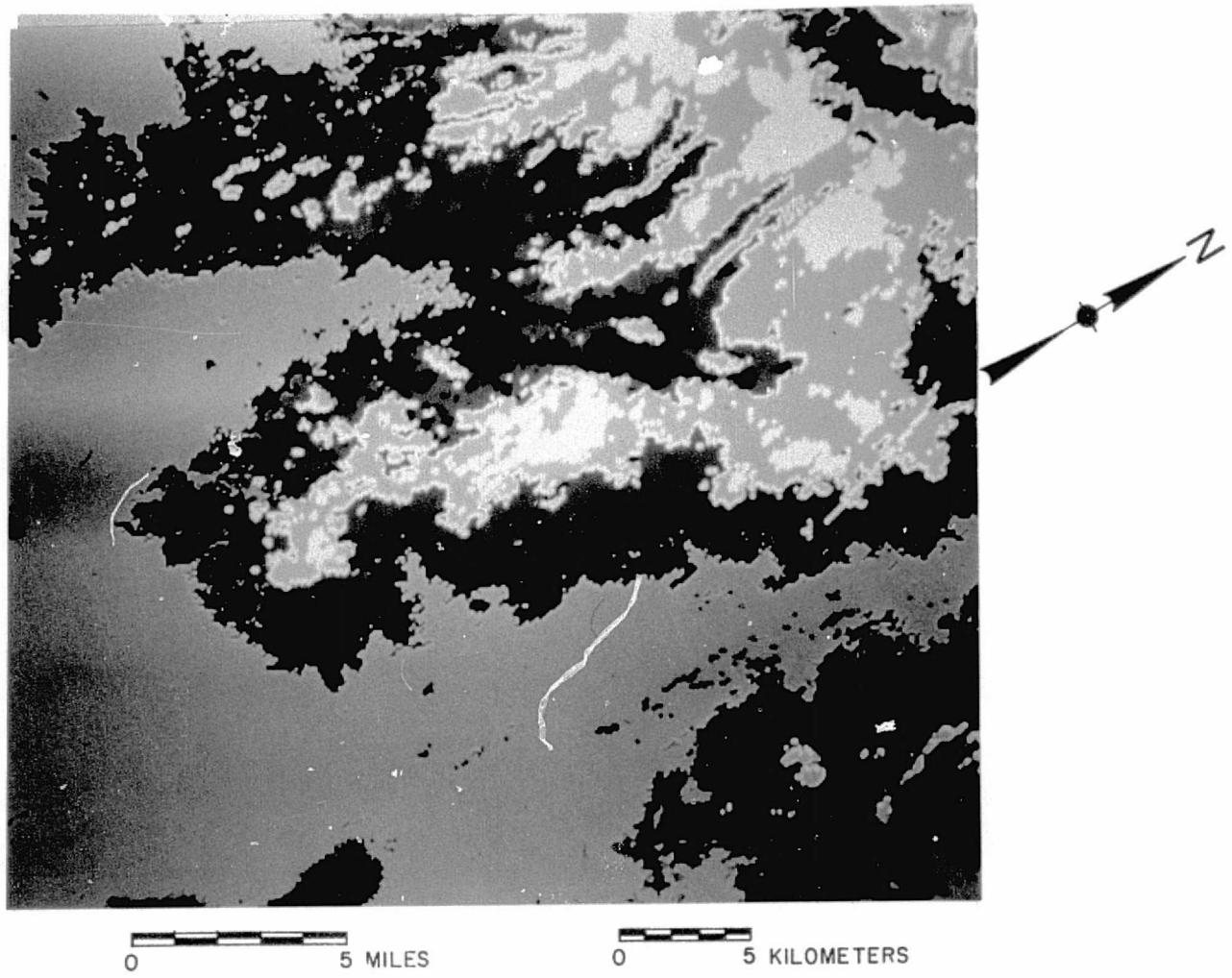

Figure 4.12 Color-coded snowcover map. (Results from the multispectral layered classification).

Table 4.5. Spectral classes shown in Figure 4 and their corresponding colors.

Spectral Class	Color-code
snow-1	white
snow-2	yellow
snow-3	light blue
snow-4	dark green
snow-5	red
water specular reflection	dark blue
crops forest	light green

Comparison of the resulting snowcover classification map (Figure 4.12) with the aircraft (NC-130 and WB-57) photography taken one day after the SKYLAB-2 overpass indicated that the five different spectral classes of snowcover were primarily related to the different proportions of snow and forest cover present in the individual resolution elements (pixels) of the SKYLAB-2 S-192 MSS data.

Figure 4.13a shows an area of the S-192 classification map illustrating the five different spectral classes of snowcover.

Figure 4.13b shows a photographic print of the same area (shown in Figure 4.13a) taken by NASA's WB-57 aircraft from an altitude of 18,288 meters (60,000 feet). Comparison of Figures 4.13a and 4.13b clearly indicate that the different spectral classes of snowcover (Figure 4.13a) correspond to the different proportions of snow and forest (Figure 4.13b) present in the scene.

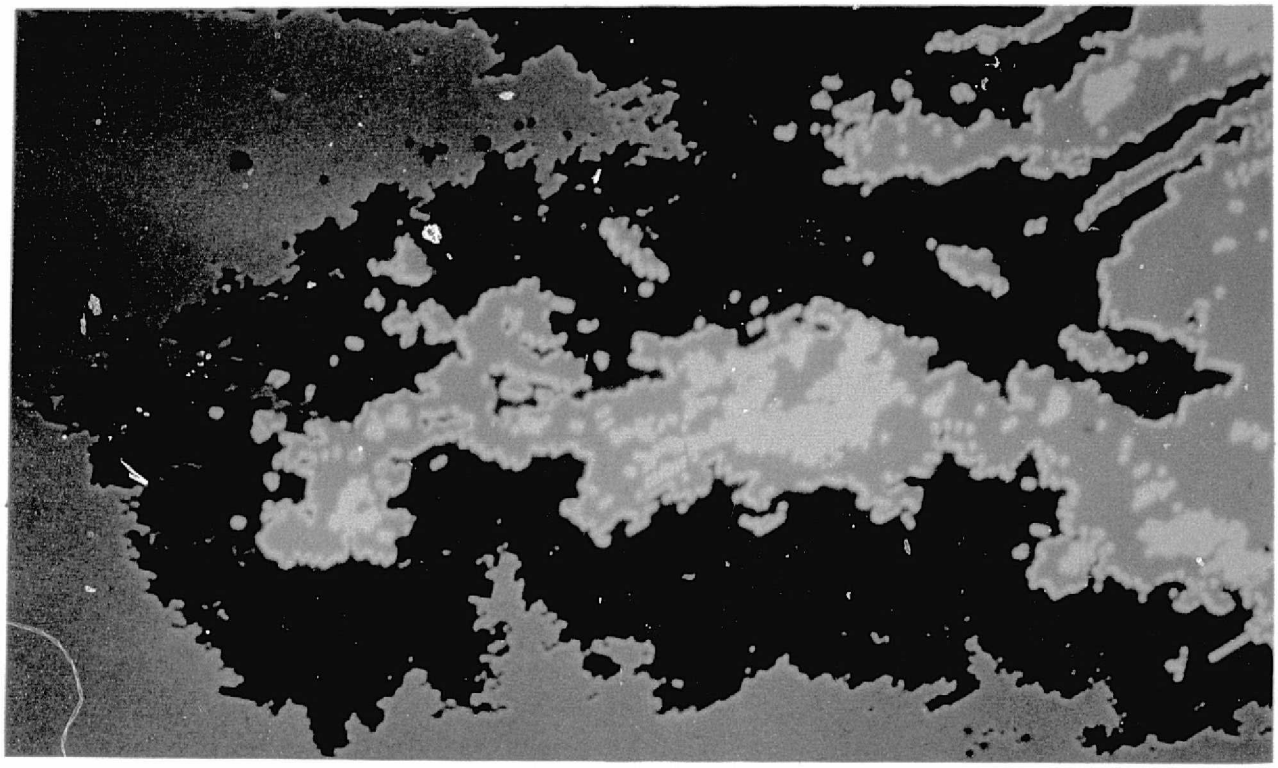

Figure 4.13.a Multispectral classification of snowcover using SL-2 S-192 MSS data.

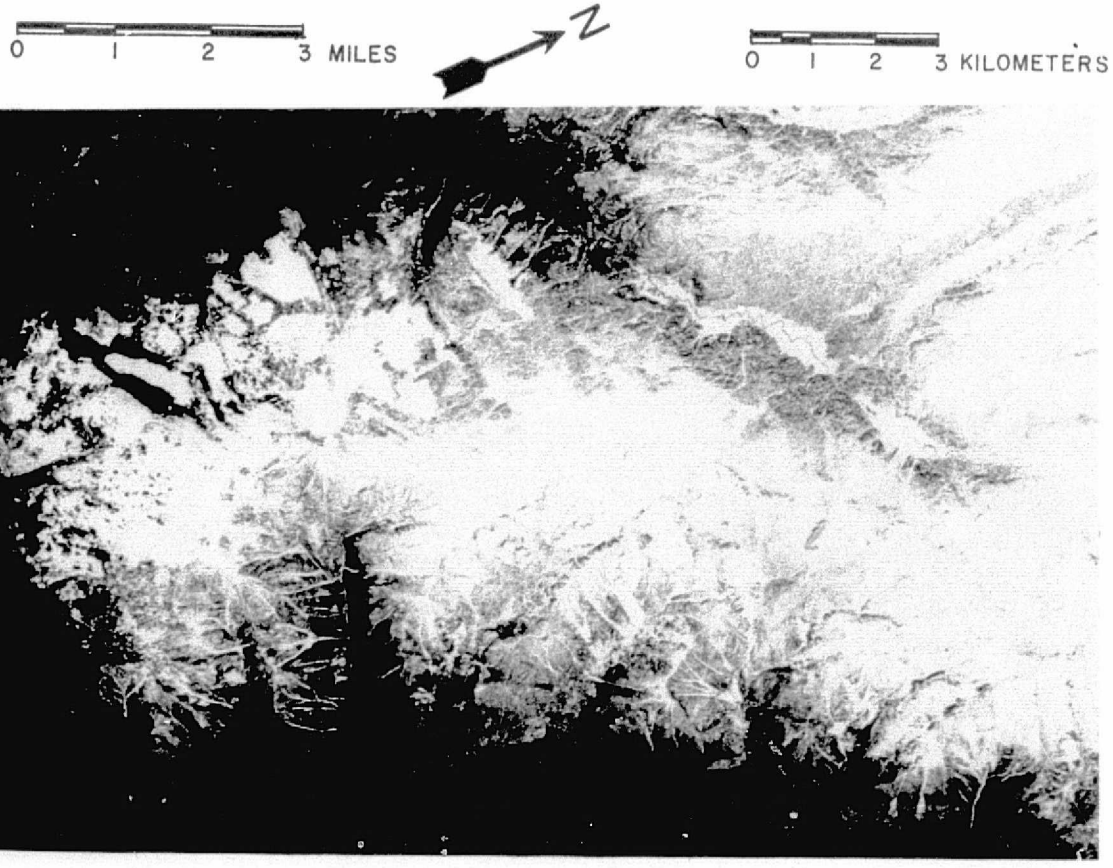

Figure 4.13.b Color IR photo taken by NASA's WB-57 aircraft of the same area shown in Figure 4.12.a .

Since the snowcover map shown in Figures 4.12 and 4.13a is actually composed of a number of individual resolution elements (pixels) that represent a specific area on the ground (≈ 0.47 hectares), it is quite easy to determine quantitatively the areal extent of the snowpack. The areal extent of the snow-covered area is calculated by multiplying the number of pixels classified as snowcover times the conversion factor of 0.47 hectares per resolution element.

Many water runoff prediction models utilize either the total area (in hectares or acres) covered by snow or the percent of snow in a particular watershed (Peck, 1972). In order to demonstrate the capability of using computer-aided analysis techniques to determine (in a quantitative manner) the areal extent of snowcover in a particular basin, a watershed in the San Juan Mountains test site was outlined on the SKYLAB MSS data, and a computer tape containing data of only the area inside the watershed was produced. Figure 4.14 shows the five snowcover spectral classes inside the Lemon Reservoir watershed. The areal extent of the five snowcover spectral groups inside the watershed is shown in Table 4.6.

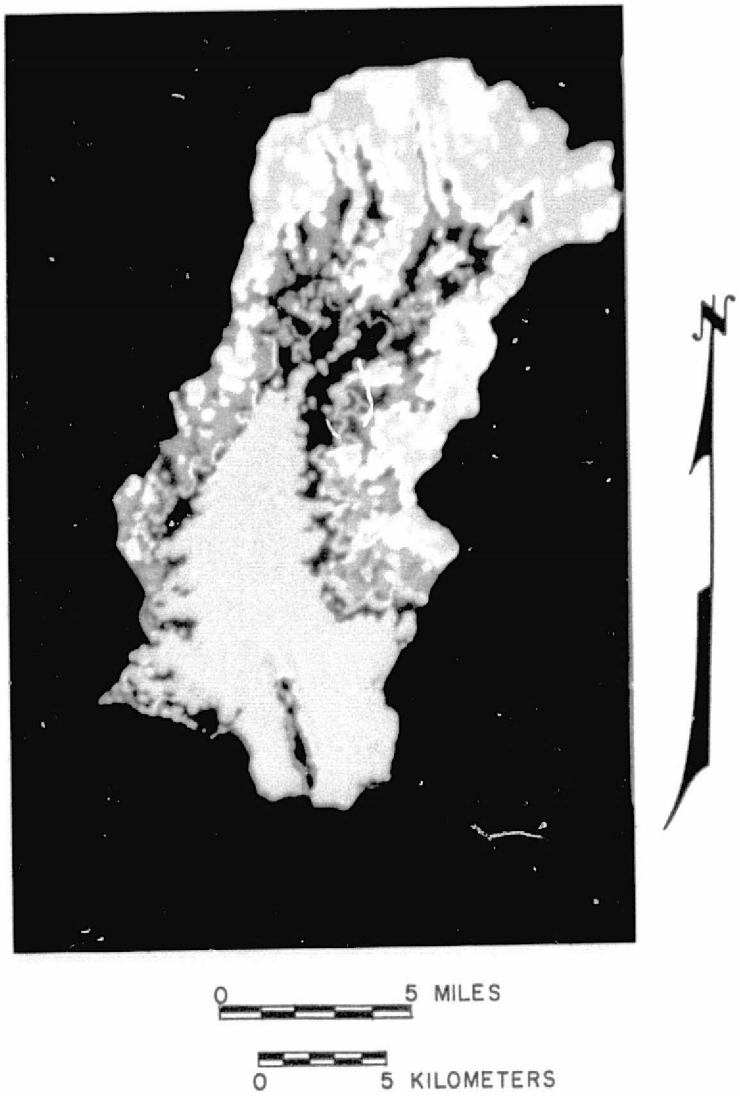

Figure 4.14 Snowcover map of the Lemon Reservoir .

Table 4.6. Area Extent of Snowcover in the Lemon Reservoir Watershed - June 5, 1973.

	Area (hectares)	% Cover
Watershed-Entire Area	17,866	100.0
Snow-1	1,021	5.7
Snow-2	3,717	20.7
Snow-3	3,395	19.0
Snow-4	2,221	12.3
Snow-5	1,322	7.3
Total Snow Cover	11,676	65.0

The spatial distribution of the five spectral classes of snowcover shown in Figures 4.12, 4.13a, and 4.14 is highly correlated to the topography of the area. The "snow-1" spectral class is found at higher elevations. The other four snowcover classes tend to follow the elevation contours of the area. Also, the thermal response (in the 10.2-12.5μm band) corresponding to each of the five spectral classes of snowcover (Table 4.4) are inversely related to the elevation of the area. The lower temperatures (snow-1) correspond to higher elevation. However, in order to establish a more quantitative correspondence between the five spectral classes of snowcover and the topography of the area, digital topographic data were overlaid onto the multispectral scanner data.

4.3.4 Topographic Effects on Snowcover Distribution

Digital tapes containing elevation data had been developed by the Defense Mapping Agency, using 1:250,000 scale U.S.G.S. topographic maps. These DMA elevation data tapes were obtained for the entire San Juan Mountains area and rescaled to match the 1:24,000 scale SKYLAB and LANDSAT data tapes. From this data, an interpolation procedure was developed and utilized in conjunction with the elevation information to obtain data on slope and aspect for each resolution element.

The final result of this data processing procedure (overlay), therefore, was a single digital data tape containing 13 channels of SKYLAB MSS data, four channels of LANDSAT MSS data, and three channels of topographic data (one channel each for elevation, slope, and aspect), all at a 1:24,000 geometrically correct scale. This data tape was subsequently utilized in 11 of the analysis sequences for the SKYLAB multispectral scanner data.

Figure 4.15 shows a topographic digital map of the San Juan test site, in which the different elevations are shown as different gray tones. The white tone (in Figure 4.15) represents elevations above 3600 meters, the darkest tone represents areas below 2000 meters, and the intermediate gray tones indicate elevation increments of 200 meters each.

To obtain an indication of the value of the topographic overlay data, the elevation data were combined with the results of the snowcover classification. The area of each of the five classes of snowcover was quickly determined as a function of elevation (using 100 meter elevation increments).

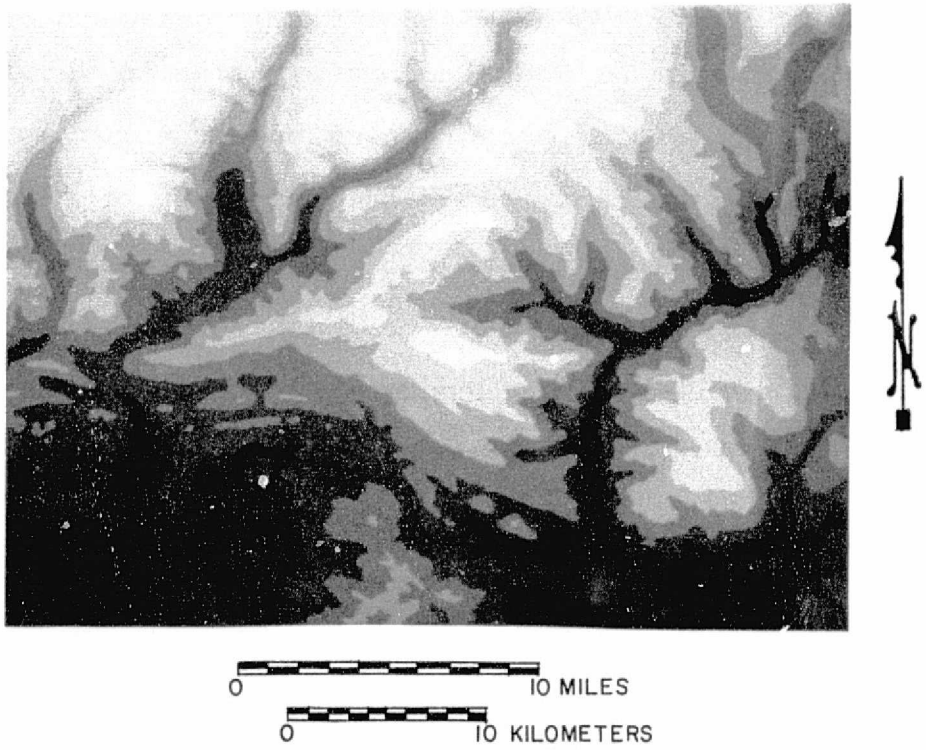

Figure 4.15 Topographic digital map.

These results are shown in Table 4.7.

Table 4.7. Snowpack area (in hectares) within 100 meter elevation increments

Elevation (meters)	Spectral Class of Snowcover 1	2	3	4	5	Total Area (hectares)
Above 3700	1179	2464	308	108	7	4086
3600-3700	400	1914	694	135	37	3180
3500-3600	129	1868	1858	517	61	4433
3400-3500	45	904	1858	1266	280	4353
3300-3400	13	378	1305	1417	812	3925
3200-3300	7	94	922	1258	1298	3579
3100-3200	6	22	529	793	1540	2890
3000-3100		6	213	433	1041	1893
2900-3000		1	38	188	535	752
2800-2900			4	54	289	347
2700-2800			1	13	147	181
2600-2700				1	95	96
Below 2600					79	79
TOTALS	1779	7651	7730	6183	6221	29564

The results of applying computer-aided analysis techniques to a combined set of multispectral and topographic digital data (Table 4.2) reveal the tremendous potential that these techniques offer to the snow hydrologist.

The utility of being able to rapidly and accurately determine the areal extent of snowcover at different elevations becomes clear when this type of information is used in con-

junction with previous results obtained by Caine (1975) on the relationship between the peak snow accumulation (water equivalent) and elevation in the San Juan Mountains. Caine's work demonstrated that the normals of peak accumulation in the San Juan Mountains increase with elevation in a predictable fashion. His results suggest a snow accumulation gradient of 65.5 cm of water equivalent per 1000 meter elevation increment with a non-accumulation level at 2400 meters. Thus, the combination of accurate estimates of the areal extent of snowcover at different elevations and the predictable information on the water equivalent at the various elevations should permit a more accurate estimation of the amount of runoff to be expected during the snow melt season.

4.4 S-192 THERMAL INFRARED DATA STUDY

4.4.1 Introduction

Within the past few years, thermal scanner systems on board aircraft platforms have been successfully utilized to detect the onset of volcanic eruptions (Parker and Wolfe, 1966), sea ice and crevasses in Arctic regions (McLerran, 1964), geothermal activity (McLerran and Morgan, 1966; Smedes, 1968), subsurface fires in coal mining districts (Slavecki, 1964), circulation patterns in the oceans (McLeish, 1964), and thermal effluents from power generating plants (Bartolucci et al., 1973).

For more than a decade, thermal infrared radiation meters have also been used in orbiting space platforms, primarily as vehicle attitude control systems (horizons sensors). Since the early 1960's, the TIROS Operational Satellites (TOS) and the NIMBUS meteorological satellites have been equipped with infrared radiometers for temperature monitoring of atmospheric conditions. However, it was not until the advent of the SKYLAB mission that a thermal infrared scanner system was available for measuring radiant temperatures of earth surface features with a very high spatial resolution (≈ 80 m square ground coverage).

4.4.2 Sensor Description

The SKYLAB S-192 multispectral scanner contains 13 detectors, one of which is responsive to emitted radiation in a portion of the 8-14μm thermal infrared atmospheric window. The actual spectral width of the S-192 thermal band ranges from 10.2μm to 12.5μm, and the shape of the detector's spectral response is shown in Figure 4.16.

The S-192 detectors were housed in a package known as the cooler/dewar/preamplifier (C/D/P) assembly. During the first two data gathering missions (SL-2 and SL-3) a primary detector array was used and it was designated as the Y-3 C/D/P assembly. The SL-4 flight crew carried and installed a spare C/D/P assembly which produced an improved thermal infrared data quality and it was referred to as the X-5 C/D/P assembly. The thermal infrared data used in this investigation were collected by the SL-2 crew with the Y-3 detector system.

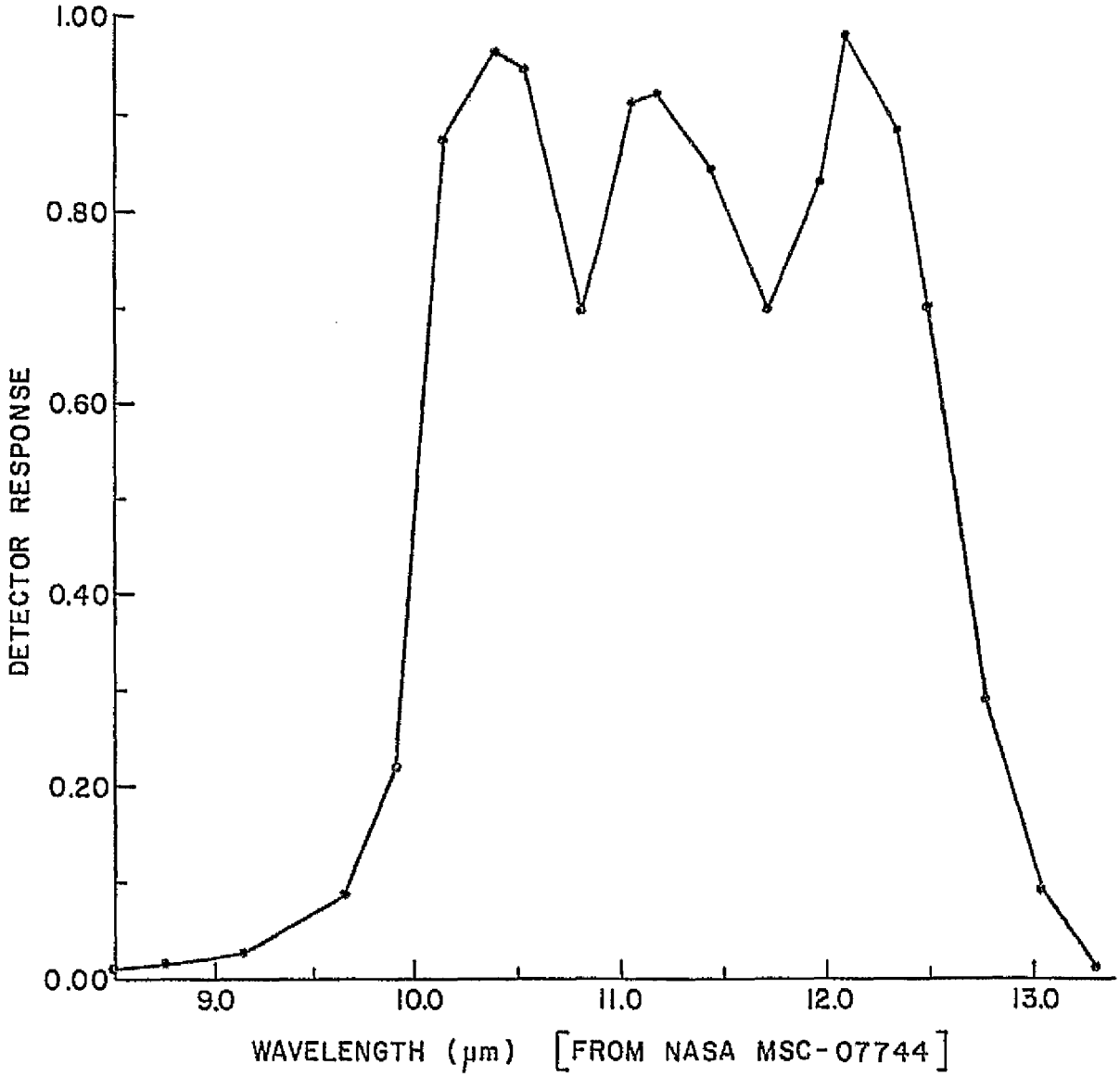

Figure 4.16 Spectral response plot of the SKYLAB-2 S-192 thermal infrared detector.

4.4.3 Surface Reference Data

During the time of the SL-2 pass (June 5, 1973) field teams from INSTAAR and LARS collected surface temperature data. Collection of the temperature data was made from an aircraft by using a BARNES PRT10 thermal infrared thermometer. Due to the nature of the instrument (no internal temperature reference) the results obtained using this instrument were not considered to be reliable. A second data gathering trip was undertaken June 9 and 10 to compensate for the unreliability of the PRT10 thermal IR thermometer. A thermister thermometer was used to measure the water temperatures. Twenty sample points in the reservoir and several other cover types were recorded. Location and temperatures of the sample points are illustrated in Figure 4.17.

Due to the lack of reliability of the reference data (ground truth temperatures) obtained over the Vallecito Reservoir, these data were not used in this investigation. A field team from Martin-Marietta Co., however, collected a set of valuable reference data at the Vallecito Reservoir site simultaneously with the SKYLAB overpass. These data have been published in NASA MSC-05531 report, August 1973. Figure 4.18 shows a number of reference water temperatures (numbers in parentheses) at Vallecito Reservoir obtained by the Martin-Marietta crew. These water temperatures were utilized in this investigation to check the accuracy of the calibrated SKYLAB-2 S-192 thermal data.

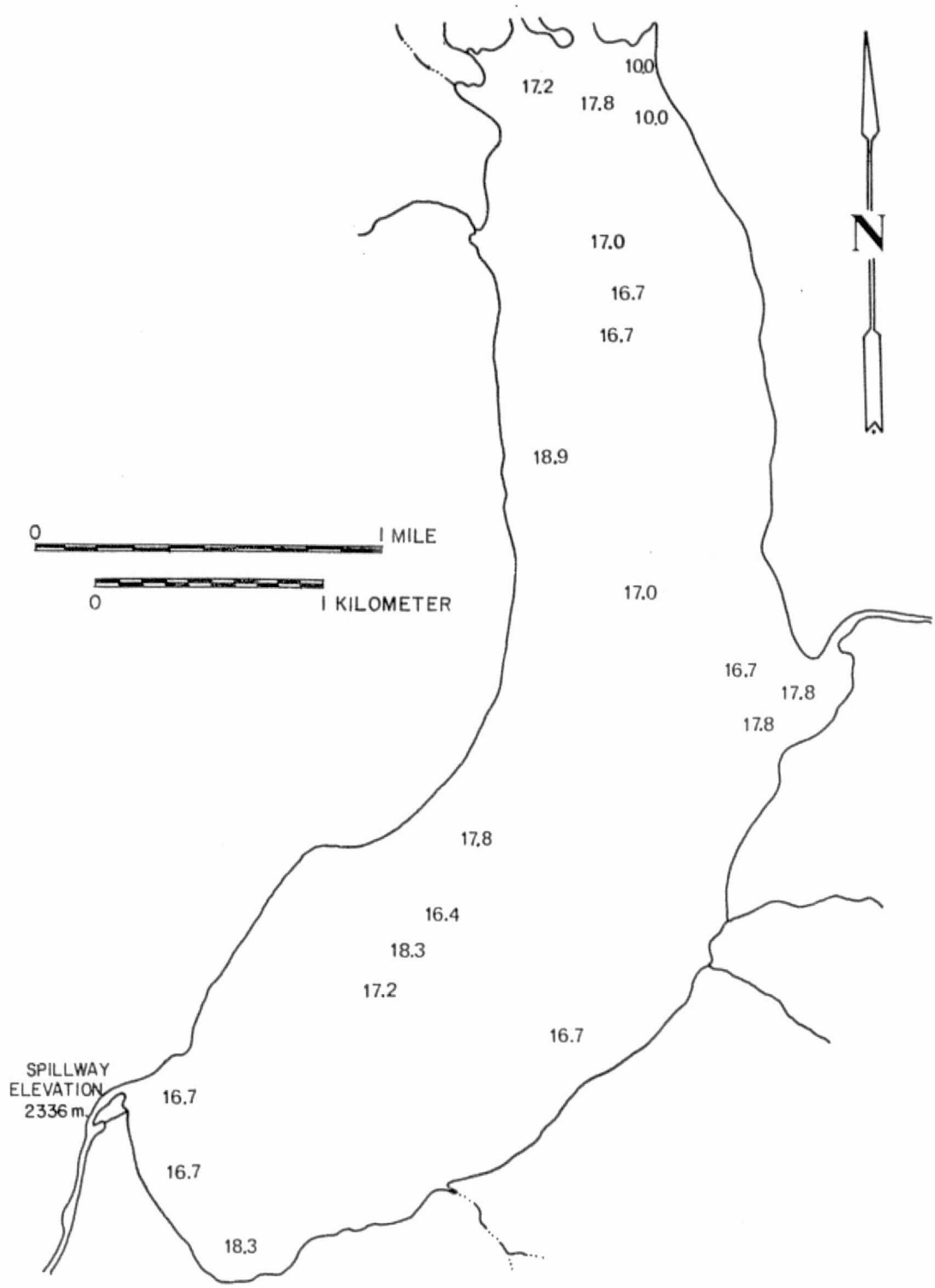

Figure 4.17 Vallecito Reservoir temperature measurements (^{0}C.) collected by INSTAAR on June 5, 1973 from 12:14 p.m. to 2:31 p.m. MST. The temperatures were measured at 10cm of depth.

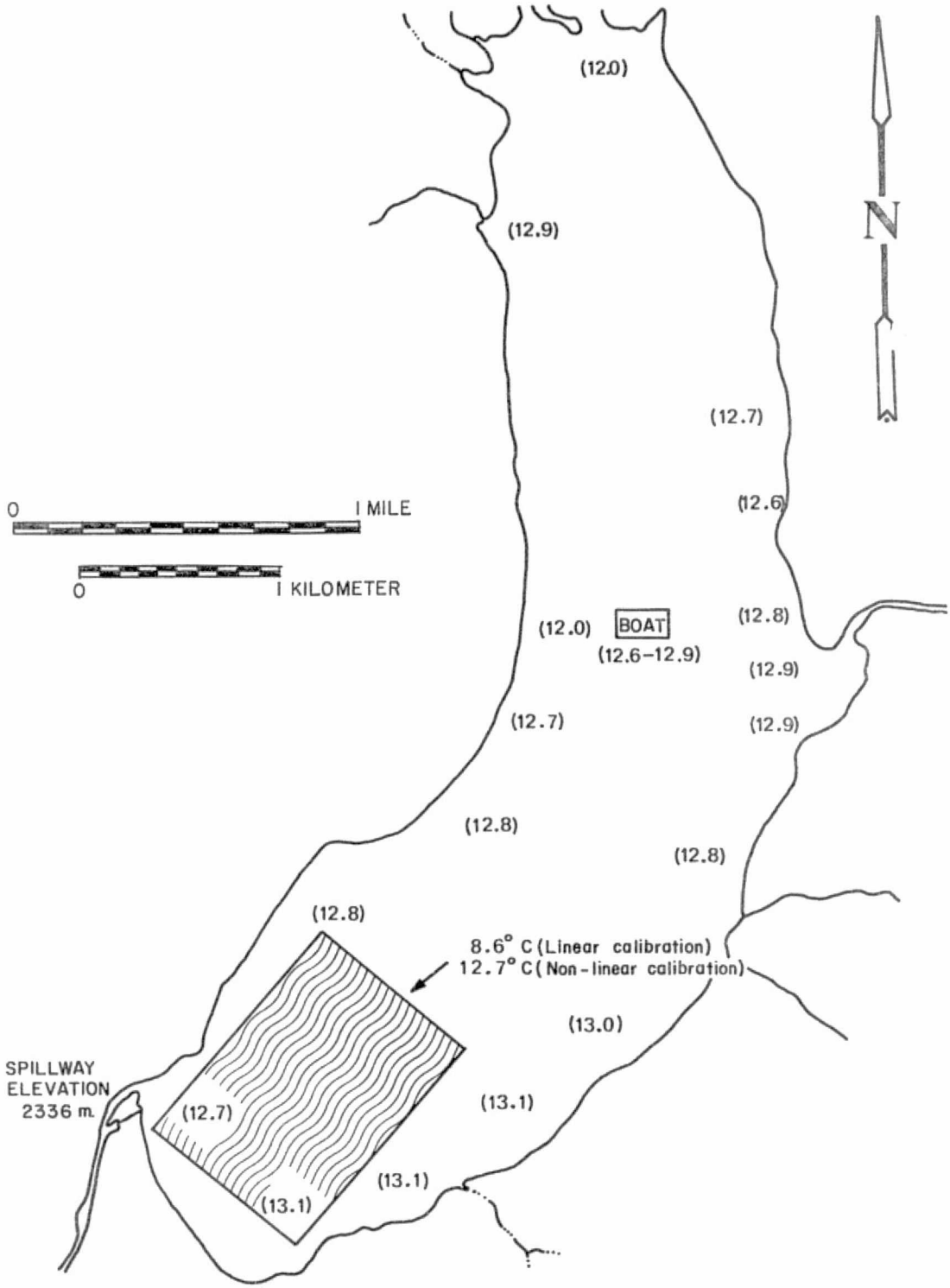

Figure 4.18 Vallecito Reservoir. The numbers in parenthesis show the reference temperatures in $^{o}C.$, and the shaded rectangle shows the area on the reservoir used to calculate the mean radiant temperature from the calibrated S-192 thermal IR data.

4.4.4 S-192 Thermal Infrared Data Calibration

In order to convert the relative response from the S-192 thermal band (band 13) into absolute temperature values, an "internal calibration" procedure was carried out.

The S-192 MSS system contains a set of two internal calibration sources which consist of two blackbodies maintained at constant and known temperatures during the data gathering period. The rotating scanner mirror views these two blackbodies once every revolution, thus, for every scanline of data the thermal detector senses and records a set of two radiances corresponding to the energy emitted by the blackbodies as a function of their temperature.

Therefore, with the knowledge of the temperatures of the blackbodies and their corresponding radiances and applying Planck's radiation theory it is possible to relate to every relative thermal radiance from a scene on the earth surface a corresponding temperature value. This procedure is referred to as the internal calibration of the data, and can be done automatically for every spatial resolution element (pixel) through a calibration function available in the LARS software processing system. The LARSYS calibration procedure has been described in detail by Bartolucci et al., (1973). Basically, the LARSYS calibration algorithm is a linear function which relates the thermal data "D" to a specific temperature value "T" as shown in Equation 4.1:

$$T = aD + b \qquad (4.1)$$

where a and b are coefficients derived from the known temperatures and radiances corresponding to the two reference blackbodies. If D_C, T_C, D_H, and T_H are the known radiances and temperatures for the cold and hot blackbodies respectively, then the coefficients a and b can be obtained from Equations 4.2 and 4.3:

$$a = \frac{T_C - T_H}{D_C - D_H} \tag{4.2}$$

$$b = \frac{T_H D_C - T_C D_H}{D_C - D_H} \tag{4.3}$$

The assumption that the amount of thermal energy emitted by a blackbody is linearly related to its temperature is only valid for a restricted number of situations, i.e., in those cases in which the Rayleigh - Jean approximation holds true. Because the S-192 thermal infrared data utilized in this investigation had to be calibrated between a wide range of temperatures (cold blackbody = -12.8°C, hot blackbody = 48.2°C) the linearity assumption is not valid. Therefore, an integration of Planck's Equation was performed for a 10.2-12.5μm wavelength interval (SKYLAB S-192 band 13) and for a range of temperatures between -12.8°C and 48.2°C, at ΔT increments of 0.1°C. The results of the integration were then plotted as a function of temperature as illustrated by the curve (asterisks) in Figure 4.19. Note in Figure 4.19 that if a linear function (straight heavy line) was used for the calibration of the thermal S-192 data, an error of approximately 4.5°C would be obtained.

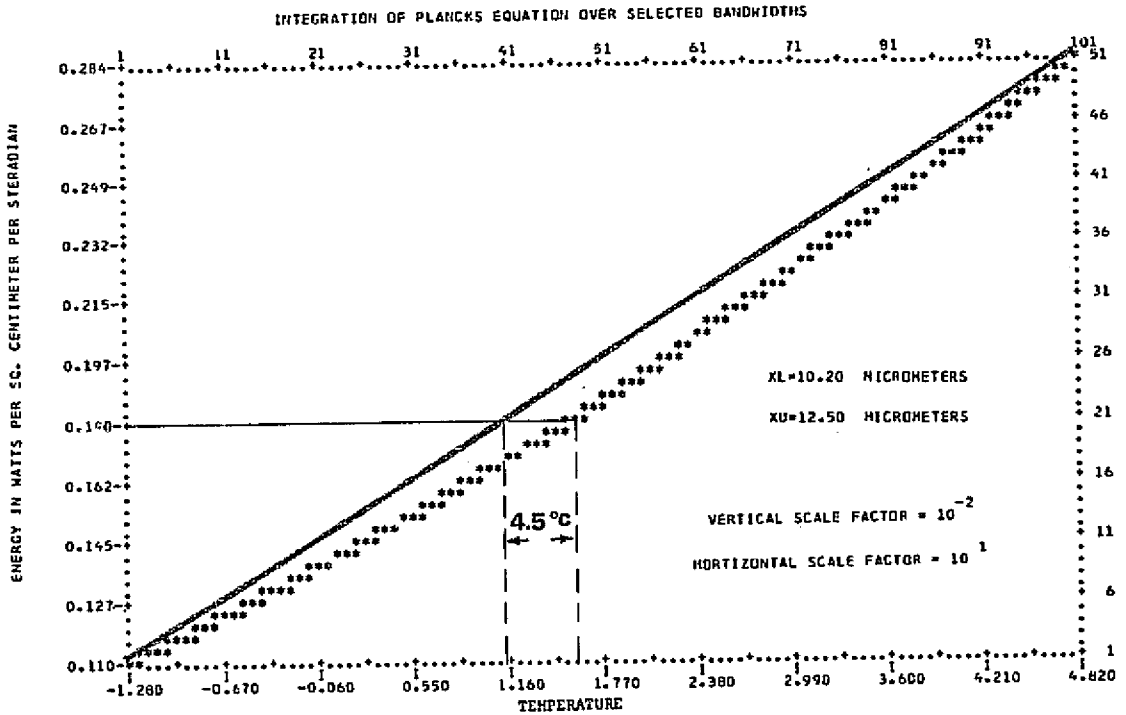

Figure 4.19 Non-linear relationship (asterisks) between the amount of energy emitted by a blackbody and its temperature in the 10.2-12.5 μm wavelength band.

The results of the data quality assessment indicated that strong noise components were present in the thermal S-192 data. This noise produced a banding effect in the calibrated thermal SL-2 imagery as illustrated in Figure 4.20. Therefore, a weighted average of the thermal data was accomplished by substituting line "n" by a line resulting from averaging line "n-1" (weighted 0.1) and line "n" (weighted 0.9). Figure 4.21 shows the smoothed thermal imagery.

Figure 4.18 shows an area of Vallecito Reservoir (shaded rectangle) for which the thermal S-192 response was calibrated through a linear and a non-linear calibration function. The numbers in parentheses (Figure 4.18) indicate the reference (ground truth) temperatures obtained by the Martin-Marietta Co. team. It should be understood, however, that the calibrated SL-2 S-192 data (radiant temperatures) shown in Figure 4.18 indicate the mean temperature of all the resolution elements (pixels) contained in the shaded rectangular area. Because of the noise in the data the standard deviation for the water temperature of Vallecito Reservoir is on the order of 4°C.

It is interesting to note that the mean radiant temperature of the water in Vallecito Reservoir, as determined through the non-linear calibration of the SKYLAB-2 S-192 thermal data, agrees with the reference temperature data obtained at approximately the same time of the spacecraft overpass. On the other hand, the mean radiant temperature as determined through the

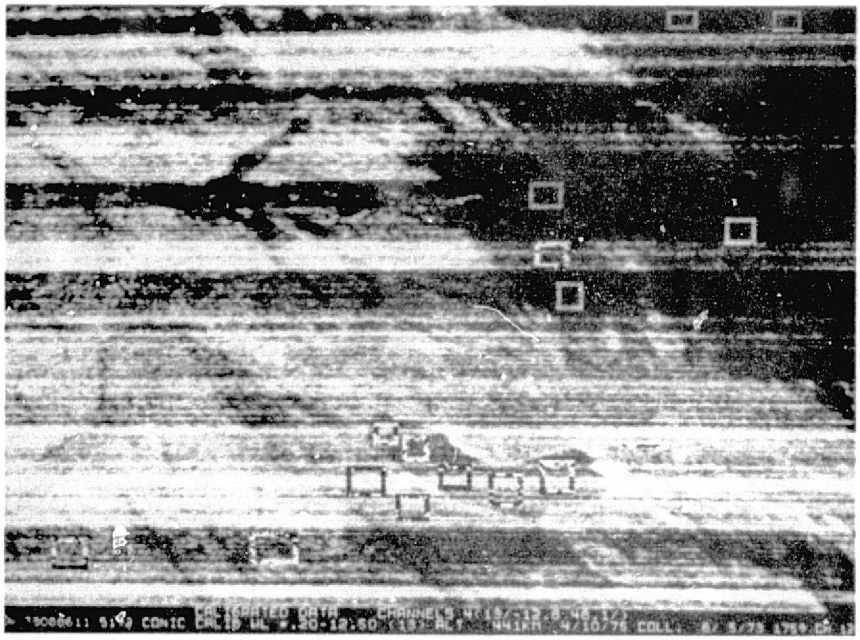

Figure 4.20 Calibrated (unsmoothed) SL-2 S-192 thermal infrared data .

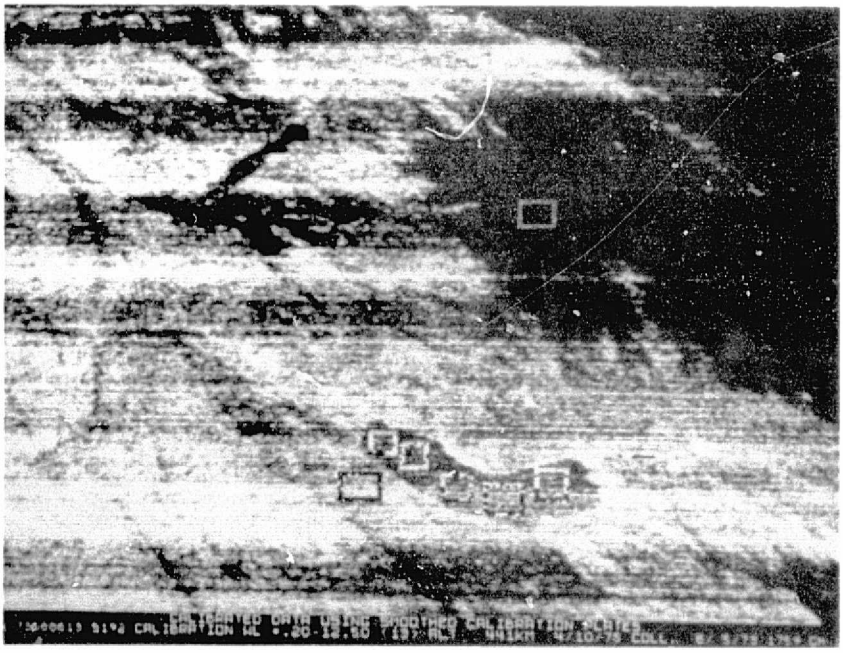

Figure 4.21 Calibrated (smoothed) SL-2 S-192 thermal infrared data .

linear calibration function is about 4°C lower than the reference temperatures.

These results suggest that the emissivity less than unity of the water and the partial atmospheric transparency in the 10.2-12.5μm spectral region do not have a significant effect on radiant temperatures obtained from orbiting space platforms, provided a proper calibration function is utilized.

4.4.5 Summary of Results

The above results indicate that through proper calibration of thermal infrared data gathered by orbiting sensor systems, it is possible to obtain accurate information on the thermal regime of water-bodies. However, one of the limitations found in the SL-2 S-192 thermal data was its low signal to noise ratio (S/N) which produced large variations in the temperatures being measured.

The internal calibration sources have proven to be a desirable feature to be included in future thermal sensor systems because they allow the determination of absolute temperatures without the need for reference data (ground truth).

It should be also pointed out that from a snow hydrology point of view, knowledge of the thermal state of snow-covered areas is of significant importance in the prediction of the amount and time of snow melt and subsequent runoff.

4.5 CONCLUSIONS

The snow/cloud differentiation study clearly indicated that spectral differentiation between snow and clouds could only be achieved reliably in the middle infrared portions of the spectrum, specifically in the 1.55-1.75 and 2.10-2.35 micrometer wavelength bands. This ability to spectrally separate snow and clouds in these wavelengths is because of the relatively low reflectance of snow in this portion of the spectrum whereas clouds have a very high spectral response due to non-selective scattering phenomena. Snow has a decreasing reflectance with increasing wavelengths throughout the near infrared portions of the spectrum (0.7-1.3 micrometer), thereby allowing a certain degree of separation to be achieved in these wavelengths, particularly in the 1.2-1.3 micrometer band, but a reliable separation is only achieved in the middle infrared wavelengths.

The computer classification of the test site containing 5,040 hectares (12,600 acres) into snow, clouds, and other cover types required less than 3-1/3 minutes of computer time with a resultant cost of only $0.0013 (13/100¢) per acre. Since this classification was done on a medium speed, general purpose scientific computer, it is anticipated that a special purpose high speed digital computer could carry out such classifications of snow cover on a much more cost effective basis.

The layered classification system for analyzing the SKYLAB data gave slightly better classification results and was

slightly faster in terms of computer time (16%) in carrying out the snow/cloud/other classification, as compared to the maximum likelihood classifier available in the LARSYS software system.

Detector saturation due to the high spectral response of clouds and snow causes several of the SKYLAB channels to be unusable in this analysis of snow cover. The thermal band (10.2-12.5 micrometer) was of no use in this study for separating snow cover surfaces and clouds, because both the clouds and snow cover were at approximately the same radiant temperature in this data set.

In the snow cover mapping phase of the investigation, five spectral classes of snow were defined and mapped utilizing the layered classification procedure. The five spectral classes of snow cover were related to differences in the mixture of snow and forest canopy present in the resolution elements of the SKYLAB scanner data. Denser stands of forest cover resulted in a mixture of approximately 20% snow and 80% forest cover (spectral class 5), whereas spectral class 2, in areas having low forest cover density, had approximately 80% snow and only 20% forest cover. In alpine areas at higher elevations or areas where the forest had been clear cut, there was 100% snow cover, causing these areas to be mapped as spectral class 1. This relationship between the forest stand density and the amount of actual snow cover present could be clearly seen on the underflight photography.

A second reason for the differences in spectral response among the five classes of snow that were defined using the S-192 data (particularly in the near infrared wavelengths) is believed to be due to snow melt. A rocket-sonde air temperature profile was obtained over Vallecito Reservoir within 15 minutes of the SKYLAB SL-2 overpass[1], and this data indicated that the air temperature ranged from 7 to 15°C for the elevations at which the snowpack around Vallecito Reservoir was located, with the higher temperatures corresponding to the lower elevations. Therefore, it is probable that the snowpack was melting, and it seems logical that the higher temperatures at the lower elevations would cause more melting to occur in these lower elevation ranges. This would cause a higher liquid water content in the snow-pack at the lower elevations, thereby causing a lower reflec-tance in the near infrared wavelengths (O'Brien and Munis, 1975). However, even though it seems logical that the five spectral classes of snow which were mapped represent differ-ent amounts of snow melt (as well as different proportion of snow and forest cover) we were not able to obtain adequate "ground truth" data in this test site area to definitely prove that such a spectral class/snow melt relationship existed at the time these SL-2 data were obtained. We could prove that the spectral classes that were mapped were related to a

---

[1] Data gathered by Martin-Mariette Co. and published in NASA MSC-05531 report, August 1973.

forest canopy/snow cover mixture. Therefore, in summary, we believe that in all probability, the spectral classes of snow that were defined and mapped using the S-192 data and computer-aided analysis techniques are a function of both the forest stand density and the snow melt.

A single watershed area was digitally defined on the data tapes and the area of each of the spectral classes of snow cover and other cover types was tabulated for the entire watershed area.

A further demonstration of the utility of multiple data sets in a digital format was shown when the different spectral classes of snow cover were tabulated as a function of elevation for the entire test site area, using 100 meter elevation increments. This result was obtained through use of the topographic overlay with the SKYLAB data, and indicates a significant potential for effectively utilizing remotely sensed data to more accurately predict water runoff from mountain snow pack areas.

Underflight aerial photography was found essential in effective analysis of the SKYLAB scanner data for the snow cover mapping portion of this SKYLAB investigation. Use of a two point non-linear calibration procedure with the thermal channel of the SKYLAB data resulted in a calibrated temperature value of 12.7^{o}C for a portion of Vallecito Reservoir, while surface temperature measurements for the same portion of the reservoir at the time of the SKYLAB overpass ranged from 12.7 to 13.1 degrees Centigrade. Therefore, in spite of

the relatively noisy quality of the thermal channel, accurate reading temperature measurements could be obtained from spacecraft altitudes in this mountainous test area where there is relatively little atmospheric attenuation.

A particularly significant result involved the digital overlay of 13 channels of SKYLAB data, four channels of LANDSAT data and topographic data including elevation, slope, and aspect. These data were first geometrically corrected to a 1:24,000 scale base and then overlaid using digital analysis techniques. Due to the orbital characteristics of the two satellites involved, the SKYLAB data had to be rotated approximately 45 degrees west with respect to north, whereas the LANDSAT data had to be rotated approximately 12 degrees east with respect to north; but in spite of the complexity of the geometric corrections involved, statistical analysis of the overlaid data indicated root mean square errors ranging from .54 to .97 in an east-west direction and .81 to 1.2 in a north-south direction for the combined topographic LANDSAT and SKYLAB SL-2 and SKYLAB SL-3 data sets. A September LANDSAT data was also overlaid onto this data base with significantly lower RMS errors (0.48 east-west and 0.39 north-south). The overlay of these large blocks of data, involving totally different data sources having considerably different geometric characteristics (mainly SKYLAB, LANDSAT, and topographic data including elevation, slope,

and aspect) is a first in the machine processing field at LARS, and it is believed that this is the first time that such a complex large multiple overlay has ever been achieved in the remote sensing community worldwide. The capability for such multiple data sets has tremendous potential for enabling more accurate and productive analysis of remotely sensed spectral data for a variety of discipline application needs. Preliminary demonstrations of the applications of the overlaid topographic data with the spectral data obtained by SKYLAB were demonstrated in the snow cover mapping and forest cover type mapping phases of this SKYLAB experiment.

CHAPTER V -- GEOLOGICAL STUDY

by

Don W. Levandowski and Robert Borger

5.1 INTRODUCTION

Digital processing of satellite MSS data from LANDSAT has provided new information useful to a variety of natural resources investigations including mineral exploration. Previous experience has revealed that digital processing is a feasible and efficient method for extracting the maximum amount of valuable geological information contained in satellite MSS data. This study provided an opportunity to evaluate computer-aided analysis of SKYLAB data from the San Juan Mountains, Colorado test site, which is an area of significant metallic mineralization.

5.2 OBJECTIVES

The overall objective of the Geological Study was to develop effective computer-aided analysis techniques for regional mineral exploration using remotely sensed data from space platforms by determining the extent to which SKYLAB and related data could be utilized in identifying and delineating geological features favorable to the localization of mineral deposits.

Specific objectives of the geological study were (1) identification and mapping of lithologic units, (2) recognition and interpretation of degrees and types of rock alteration within these units, (3) interpretation of structural features based on interruptions in spectral patterns, and (4) evaluation of thermal scanner data for use in locating areas of recent or current, shallow igneous activity which could potentially be related to mineralization.

No success was achieved in the identification and mapping of lithologic units. This lack of success can be attributed to: 1) a general lack of spectral discriminability among the various lithologies present, and 2) insufficient exposures of outcrop detectable from satellite altitude. The volcanic extrusive rocks which make up by far the greatest portion of all rocks present in the test site show monotonously similar spectral characteristics as reported by Hunt *et al.*, 1973. Additionally, our own Exotech spectral radiometric studies indicated that only extreme spectral variations involving extensive, distinctive alterations

could be detected.

The definition of the Silverton area as a study site provided additional problems when the SKYLAB data was received. The study area was completely snow covered in the SKYLAB SL-2 data, precluding completely its use in the structural analysis (Objective 3). The SKYLAB SL-3 data was about 75% cloud covered in the Silverton area, making it extremely difficult to utilize effectively. Therefore, because both data sets obtained over this study area were essentially unusable, the structral analysis portions of the structural analysis objective could not be completed.

5.3 GEOLOGICAL SETTING

The test site is situated at the southwest end of the famed Colorado mineral belt. Most of the metal mining districts of Colorado occur in this belt, a generally narrow but somewhat irregular strip that extends southwestward across the state of Colorado from the Front Range near Boulder to the San Juan Mountains. The mineral belt is, in general, an elevated zone containing many of the highest peaks in Colorado, and closely parallels the Continental Divide. The belt coincides with an ancient zone of weakness defined by north-east-trending, Pre-cambrian shear zones (Tweto and Sims, 1963). Magma invaded the regional zone of shearing and imparted to it the present features that characterize the mineral belt's intrusive and extrusive bodies and ore deposits.

The test site, which contains a number of major silver, gold, lead, copper and zinc mining districts including Creede, Lake City, Ouray, Silverton, and Telluride, is located near the western border of the San Juan volcanic plateau. The region is a topographic high with several peaks over 4667 meters (14,000 feet). It is also a structural high and consists of a relatively thin series of Paleozoic and Mesozoic sedimentary rocks on a highly elevated basement of Pre-cambrian crystalline rocks consisting of schist, gneiss, quartzite and slate. The region is overlain by a thick series of Tertiary volcanics consisting of flows, tuffs, and breccias of rhyolitic, andesitic, and

latitic composition. In some areas of the region, the sedimentary rocks are missing and the volcanics lie unconformably on the crystalline basement. The volcanic rocks have been intruded by a number of stocks and irregular bodies of quartz monzonite, by many dikes of andesite and latite, and by a few dikes of granite porphyry and rhyolite.

The structure of the area is dominated by several collapse centers. These centers are characterized by fault and joint systems typically associated with calderas developed during repeated cycles of doming and collapse (Leudke and Burbank, 1968; Smith and Bailey, 1968). These structural features largely controlled the distribution and localization of the ore deposits. In fact, every major mining district in the San Juan Mountains can be directly related to a caldera (Bird, 1972). Among the more important are the Silverton and Lake City cauldrons, each about 15 kilometers in diameter, that lie within the northeast-trending older and larger San Juan volcanic depression which is about 25 by 50 kilometers in size. These major structures are the result of successive and repetitive stages of eruption, intermittent subsidence of some blocks, partial engulfment of volcanic piles, and resurgent magma that caused broad uplift and radial and concentric fracturing (Leudke and Burbank, 1968).

Intrusive masses, mainly gabbro rhyolite, stocks, dikes, and plutons, were emplaced contenporaneously with the fracturing in the ring-fault zones and elsewhere in and near the calderas.

Post-volcanic faulting, fissuring, and intrusive activity in part was accompanied and in part was followed by pervasive rock alteration and the formation of the major late Tertiary ore deposits.

The ore deposits localized mainly in the radial and concentric fractures and in the associated graben faults, include fissure veins, chimneys, replacements, and disseminations in volcanic and sedimentary rocks.

5.4 MULTISPECTRAL MAPPING OF AREAS OF HYDROTHERMAL ALTERATION

5.4.1 Introductory Statement

Three types of hydrothermal alteration are common in the San Juan Mountains: propylitization, solfataric alteration and "vein-type" alteration (Burbank and Leudke, 1961).

Most of the rocks within and closely surrounding the cauldrons were initially subjected to pervasive propylitic alteration caused by effusions of water and carbon dioxide. This type of alteration occurred during and after late igneous activity. In all cases the propylitization has been pre-ore, i.e., it occurred prior to the deposition or emplacement of ore minerals. Propylitization may have assisted in creating an environment favorable to the deposition of ores by making the rock hard and brittle. Hard, brittle rock units are more highly fractured than less brittle rocks. Ore deposition favors the fractured rocks.

Solfataric alteration is the result of exposure to hydrothermal solutions rich in sulfur and highly ionized sulfurous compounds. This alteration was immediately pre-ore and in some cases continued during the ore deposition stage. During the alteration, the rocks involved were extensively bleached creating a highly porous and permeable setting for ore deposition.

In addition, ferromagnesian minerals present in the

rock were broken down and the iron reduced to pyrite. The pyrite produced during this alteration rapidly oxidized to hematite, limonite and goethite when exposed at or near the surface. These minerals produce a very distinctive red, orange or occasionally yellow staining or coloration known as a gossan.

The "vein-type" alteration is highly variable and directly associated with mineralized fractures or fissures. The most common types involve sericitization or kaolinization and commonly extensive pyritization. The "vein-type" alteration is co-genetic with the mineralization and the variability is due to the variability of the mineralizing solutions. This type of alteration is usually of very small scale affecting only a few centimeters of rock on either side of the vein. The alteration is most often indistinct and magnification is required to observe the presence of the alteration minerals. However, when abundant pyrite is present in the altered zone, a distinct gossan may be developed.

For the purpose of this project we chose to concentrate on the delineation of areas of solfataric alteration. The areas of solfataric alteration are directly associated with areas of ore mineralization and historically have been used by prospectors in the search for ore deposits. The Red Mountain section, an area of approximately 16 square kilometers (six square miles) in the northwest portion

of the Silverton caldera has produced extensive amounts of silver, gold, lead, zinc, and copper from vein, chimney or pipe and replacement bodies in the solfataricly altered rock.

The size of the solfataricly altered areas also enables them to be detected from satellite altitudes. They are large enough to be detectable with a resolution such as SKYLAB's, but are not so extensive as to lose their importance as a guide to the localization of ore deposits.

The gossan of the area of solfataric alteration is highly distinctive. The iron oxides making up the gossan show a characteristic decrease in reflection below approximately .55-.60 μm and may show a distinct absorption band centered near .85 μm (Hunt et al., 1973). Such spectral characteristics allow the use of LARSYS CAAT spectral analysis techniques to be applied to delineate the gossan. These spectral characteristics also allow the use of ratio techniques to aid in mapping the alteration areas. Specific areas of study are shown in Figure 5.1.

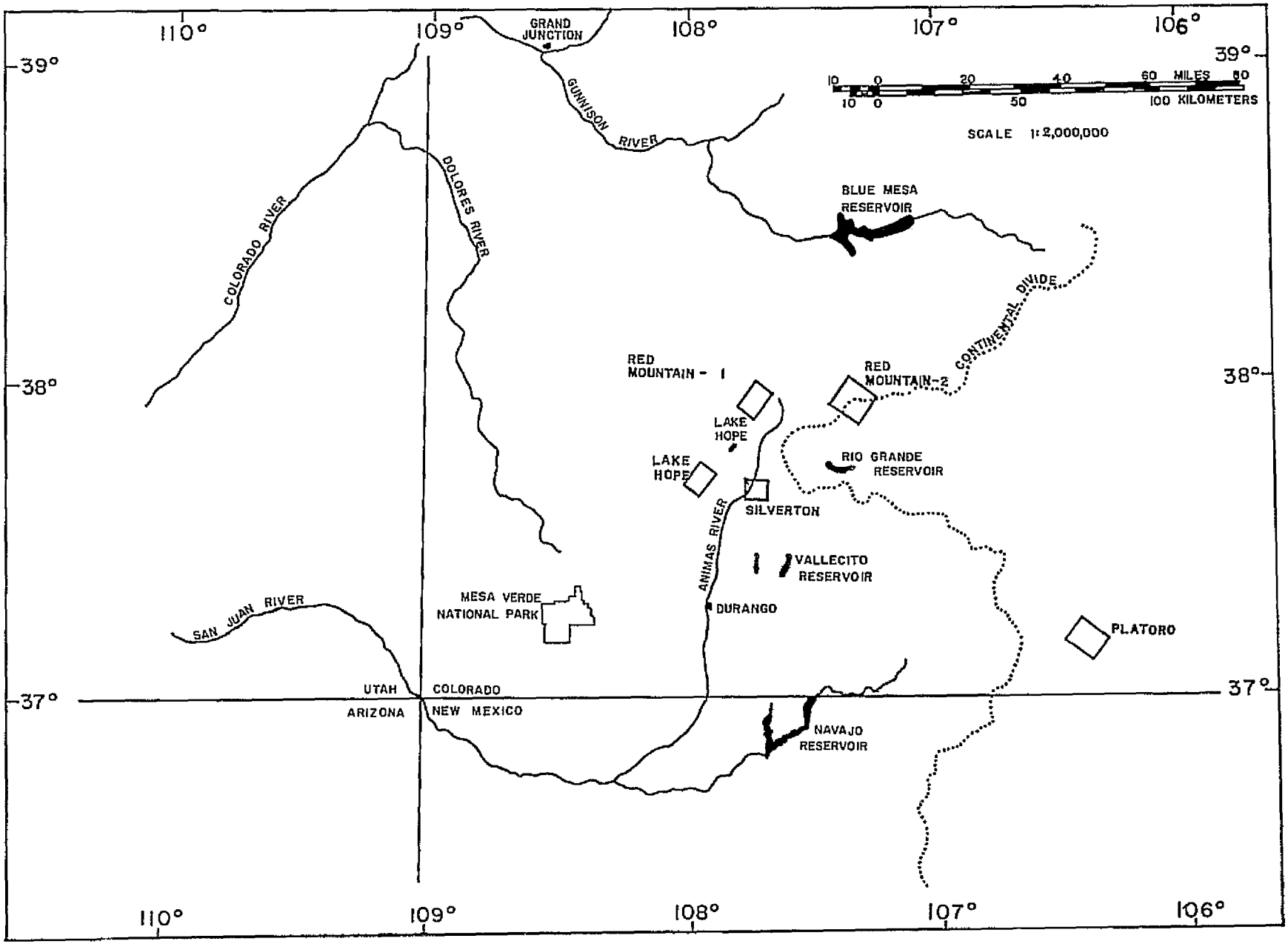

Figure 5.1 Index map showing areas of geological investigation.

5.4.2 LARSYS Classification of Hydrothermally Altered Areas

A series of vein or vein-like alteration patterms can be observed (Figure 5.2) on a ridge northwest of San Miguel Peak and west of Lake Hope (Ophir Quadrangle). The altered areas show a typical red-orange color due to the presence of hematite and limonite. The scree in the area also contains varying amounts of altered or iron-stained material. The NC-130 MSS data over this area were classified to determine the feasibility of using this type of data for determining the alteration.

In order to spectrally differentiate the altered rock from the unaltered rock and other cover types in the scene, a series of training samples representative of each cover type was selected. The general cover types were forest, meadow, mixed forest and meadow, water, mixed snow and rock and bare rock.

A training procedure, called the modified clustering technique described by Fleming, Berkebile and Hoffer (1975), was used to cluster the NC-130 data from the initial set of training fields into a larger number of subclasses. The 0.40-0.44, 0.53-0.58, 0.65-0.69, and 0.82-0.88 μm wavelength bands were chosen to do the training and classification. This set of channels should detect the decrease in reflectance below 0.60 μm, and the presence of the 0.85 μm absorption band. The result of the final classification is shown in Figure 5.2.

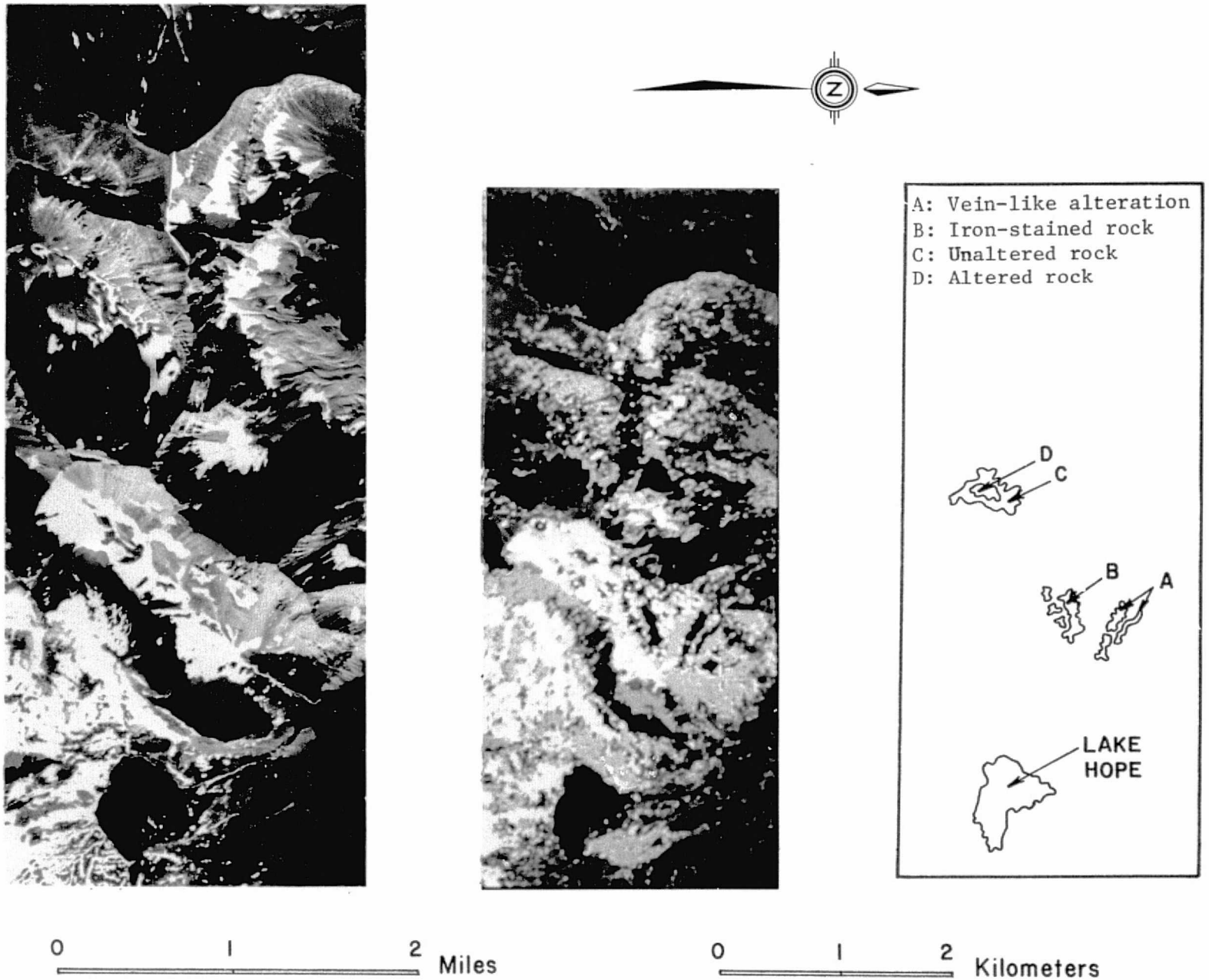

Figure 5.2 Color photography and computer classification of NC-130 MSS data, Lake Hope, Colorado.

The 54 resultant classes shown in the final classification are composed of 22 vegetation classes, four snow classes, two deep shadow classes, one water class, and two altered rock classes. The altered rock classes represent one sunlit and one shadowed class. The two vein-like areas of alteration (area A in Figure 5.2) and the hillwash composed of altered and iron-stained rock (area B in Figure 5.2) are immediately apparent. These represent the areas of primary interest and are well delineated.

Another feature detected by the classification was a small oval patch of shadowed alteration which had previously been undetected during the airphoto examination. Area C is the lightly shadowed unaltered rock floor of a cirque, while Area D is a shadowed altered rock class. The photography collected concurrently with the scanner data was used to verify the presence of the alteration. Although the alteration is subtle, it can be seen in the photography. The alteration is associated with a roughly circular, textural is subtle, it can be seen in the photography. The alteration is associated with a roughly circular, textural and structural pattern in the floor of the cirque. The feature is approximately 120 meters (400 feet) in diameter and is contained within an intrusive. It is interpreted to represent the surface expression of a breccia pipe. There are many such pipes in the area, particularly to the north and northeast. The pipes are associated with intrusives and are circular to elliptical

in cross section and range from 90 to 150 meters (300 to 500 feet) in diameter. Many of these breccia pipes have served as the foci of mineralization.

The SKYLAB-3 S-192 data were also classified in a attempt to determine of these type of data were suitable for alteration mapping. The S-192 data quality varied considerably from channel to channel, as discussed in Chapter II. Cloud cover over the San Miguel Peak, Lake Hope and Silverton areas during the S-192 data collection precluded the possibility of performing a classification over the same area that was chosen for the NC-130 data classification. Consequently, the area classified was shifted to the Platoro-Summitville mining district (Figure 5.3). The training areas were clustered into a total of 30 subclasses which were then recombined into 19 classes for the final classification. A color-coded classification result is shown in Figure 5.4. The areas of alteration can be seen as dark red with scree being pink.

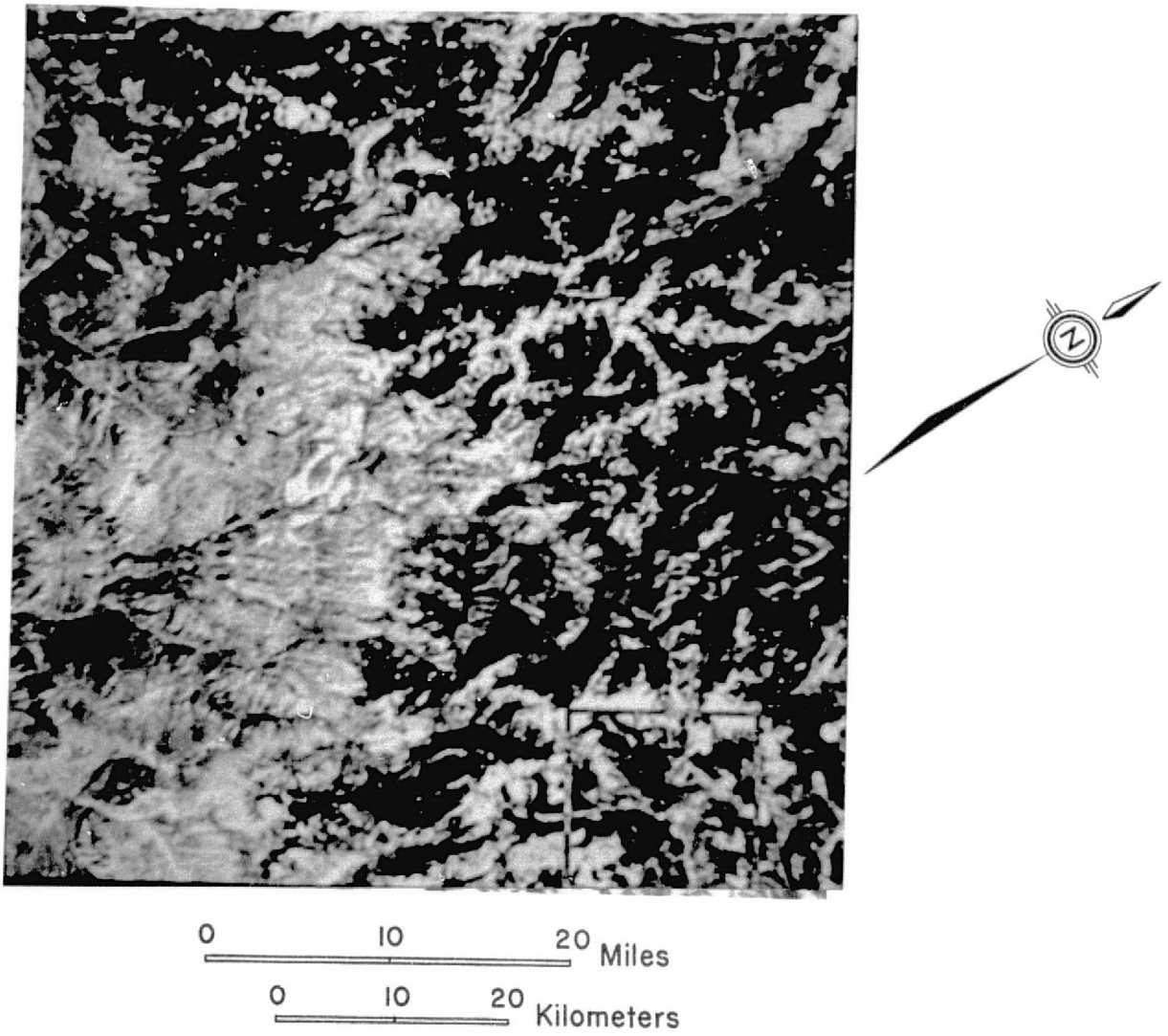

Figure 5.3 Color composite of channels 3, 5, and 8 of SKYLAB III S-192 MSS data of Platoro-Summitville area. The rectangle in the lower right indicates the classified area shown in Figure 5.4.

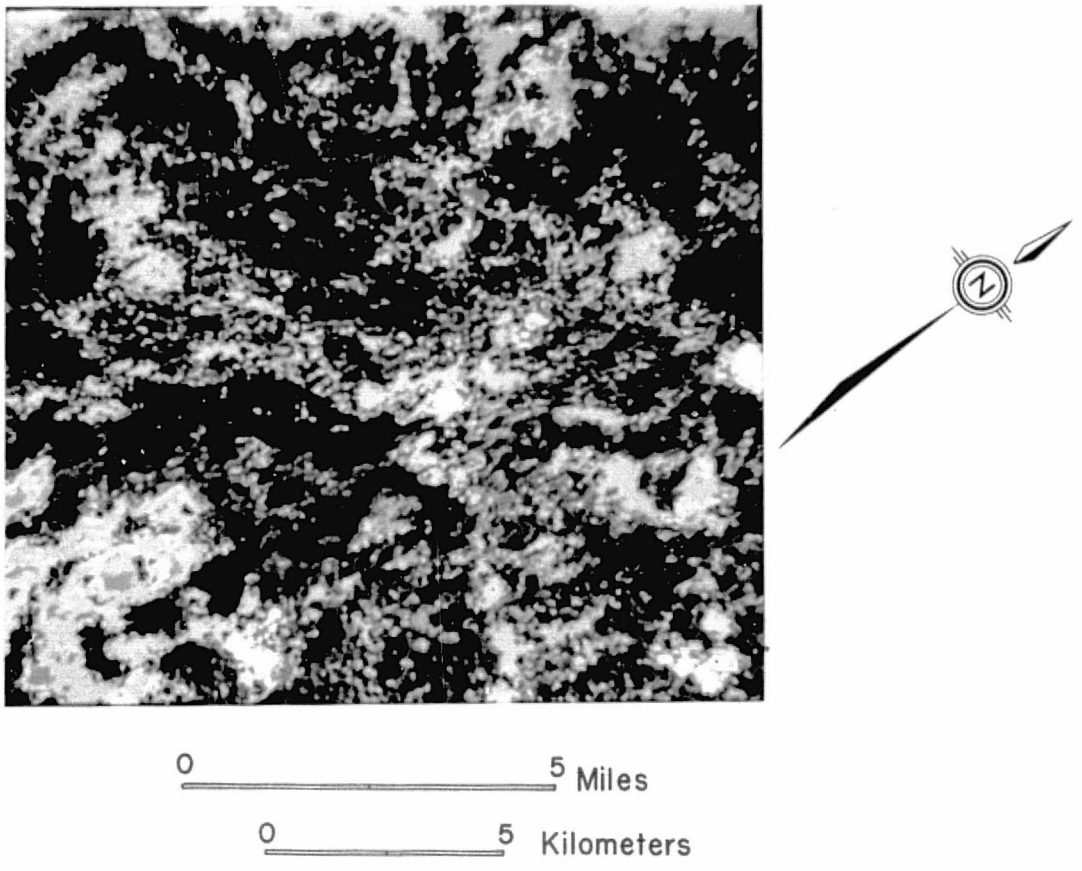

Figure 5.4 Classification of SL-III S-192 data of Platoro-Summitville area. (Altered rock - red; bare rock - brown and yellow; water - blue; shadow - black; vegetation - green.)

5.4.3 Discrimination of Hydrothermally Altered Areas by Ratioing

Another method used to detect and map hydrothermally altered areas is through the use of ratios of various channels of spectral data. The ratios may involve single channel pairs (A/B) or various combinations of channels (A+B/C+D). In order to compare the effectiveness of the ratioing of various types of data for discriminating between altered and unaltered areas of rock, ratioing was applied to a portion of a frame of LANDSAT data, to Mission 247 MSS data of the Lake Hope area, and to SKYLAB SL-3 S-192 data.

For LANDSAT data, the most widely used ratio for the discrimination of areas rich in iron oxides is the ratio of bands 5/7 (Vincent, 1972). Other band combinations, namely 4/5, 5/6, and 6/7 have been successfully used by Rowan et al. (1974) to form a color composite image in which iron oxide enriched, altered rock display distinctive colors. Both of these types of ratioing techniques were performed in this study. In addition, two other types were investigated. One is a variation of the single channel pair method (A/B), and the other involves ratioing between a single channel of a set and the sume of all the channels of the set (A/A+B+C+D).

The band ratios 5/4, 6/5, 7/6, and 4/SUM, 5/SUM, 6/SUM and 7/SUM (where SUM = 4+5+6+7) were applied pixel by pixel to the portion of interest of the LANDSAT-1 frame to create a new data tape. The resultant data tape

was then used to create a set of color composite images of the area. Although a variety of combinations of ratios were examined, most of the combinations failed to enhance the alteration. For example, the band-ratio combinations used by Rowan et al. (1974), i.e., 4/5, 5/6 and 6/7, did not distinguish alteration from snow. The most successful combinations for delineating alterations were the combination 4/SUM, 6/SUM, and 7/SUM. A color composite of these ratios for the Silverton area is shown in Figure 5.5. This color composite was produced with the LARS digital display with 4/SUM as blue, 6/SUM as green, and 7/SUM as red. The areas of alteration are black.

The ratios performed on Mission 247 aircraft MSS data (See Table 2.2) were 4/6, 6/8, 8/10, involving wavelength bands similar to those used by Rowan et al. (1974), 3/8 equivalent to the bands used by Vincent (1972) and 4/SUM, 6/SUM, 8/SUM, and 10/SUM. None of the various combinations tried appeared to delineate or enhance areas of alteration. Apparently there was insufficient spectral contrast betweeen the areas of normal bare rock and altered rock. In an effort to improve the contrast, a new set of histograms was prepared with only the area of bare rock histogrammed. This procedure effectively decreases the number of gray levels used in the surrounding areas of vegetation and increases the number of gray levels used in the bare rock areas. The process

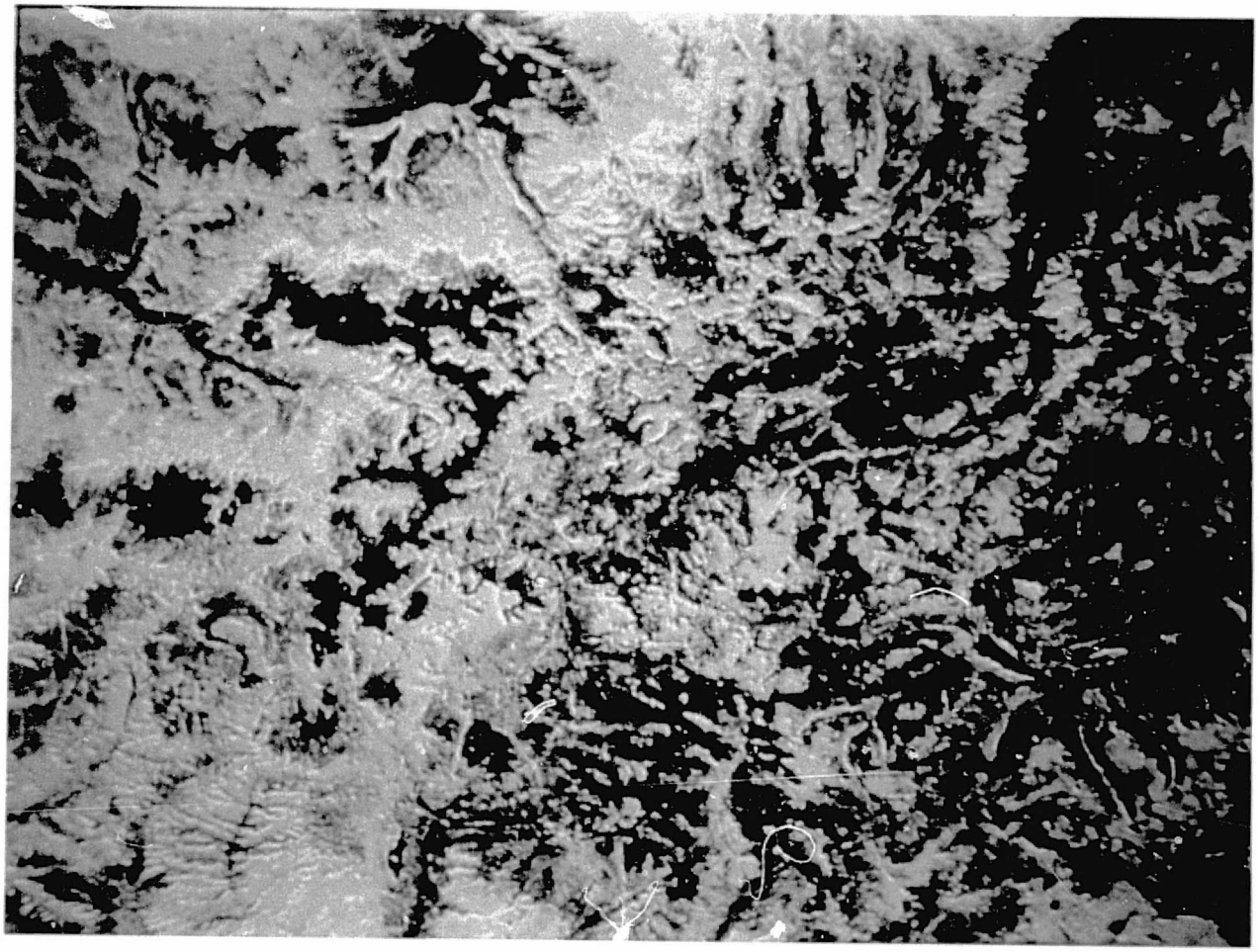

Figure 5.5 Three component color-ratio composites of LANDSAT data, Silverton areas, Colorado. Areas of alteration appear black.

produces a result similar to contrast stretching as reported by Rowan et al., 1974. Color composite images of various sets of ratios comparing regular and contract histograms were prepared of data over the Lake Hope area. No enhancement of alteration was obtained with the set 4/6, 6/8, and 8/10. Individual black and white images of these ratios distinctly showed the alteration areas. These were 3/8 as blue, 4/SUM as green, and 6/SUM as red as shown in Figure 5.6. Both composites show the alteration very distinctly, but with the contrast increasing histograms much more detail can be discerned. In particular, the alteration associated with the breccia pipe discerned in Section 5.4.2 is much more distinct when the contrast is increased.

The SKYLAB SL-3 S-192 data were treated with a set of ratios similar to those used for the LANDSAT and aircraft Mission 247 data, plus an additional set of ratios specific for this data set. The SKYLAB bands chosen for ratioing were 3,4,5,6,7,8,9,10, and 11 (see Table 2.2). Bands 1,2,12, and 13 were not utilized because of data quality problems. The ratios performed were 4/6, 6/7, 7/9, 4/SUM, 6/SUM, 7/SUM, and 9/SUM. In addition, a set specific for these data 3/8, 4/9, 5/10 and 6/11 was also used. Color composites of various combinations of these ratios were prepared for the Red Mountain I and Red Mountain II areas (Figure 5.7 and 5.8). The most noticeable effect of ratioing is the tremendous enhance-

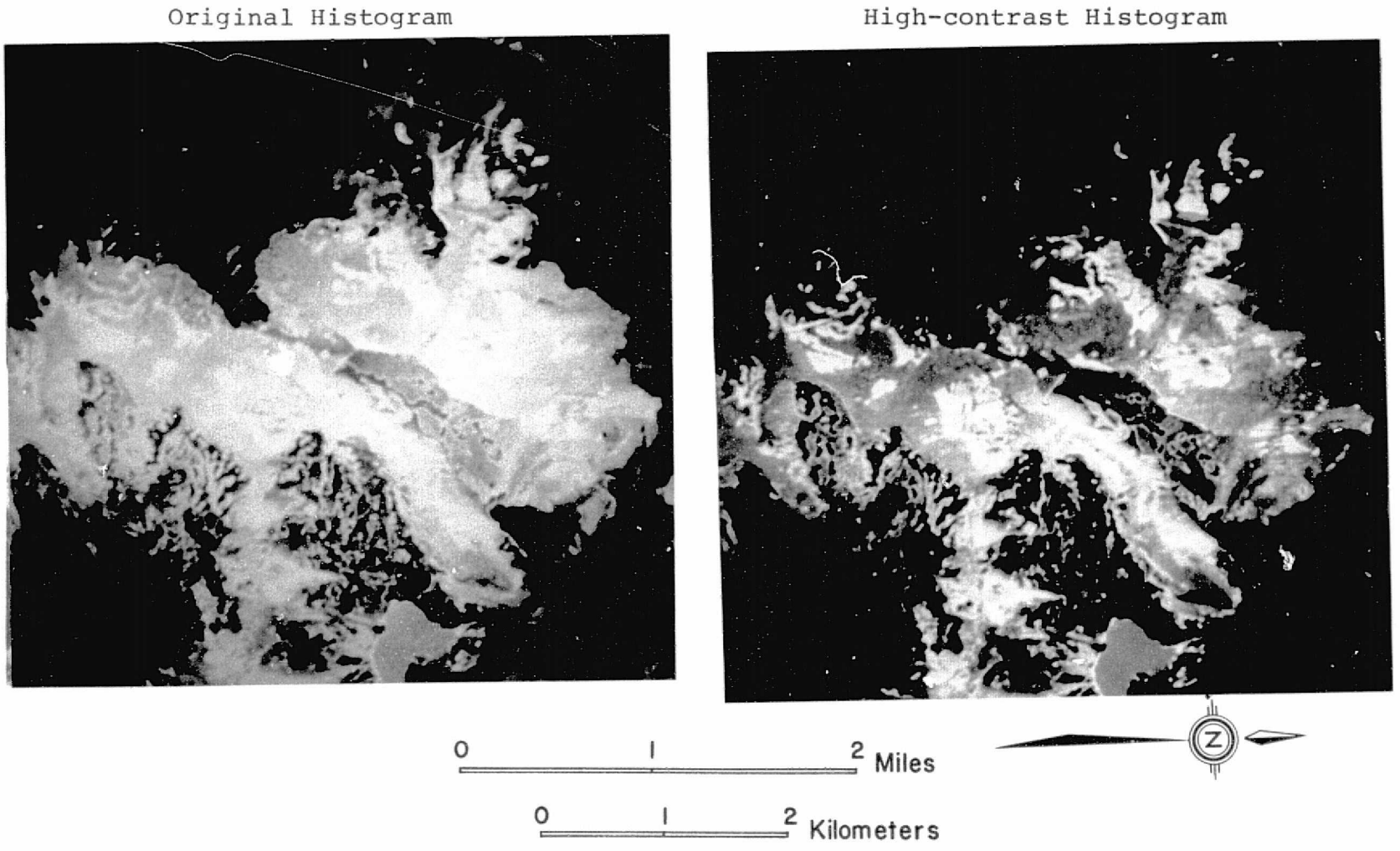

Figure 5.6 Three component color-ratio composites of MSS NC-130 data of the Lake Hope area using 3/8 (blue), 4/SUM (green) and 6/SUM (red).

ment of noise present in the S-192 data. Noise completely obscures the details of any scene. Only the most obvious features are discernible. In spite of the noise effects, three combinations appeared to be effective in enhancing the alteration: (3/8,4/9, 6/11), (3/8, 5/10, 6/11) and (4/SUM, 7/SUM, and 9/SUM). As an example of this enhancement, Figure 5.7 is a three component color ratio composite with 3/8 as blue, 5/10 as green, 6/11 as red. Areas of alteration are shown as red. For comparison, the color composite of the combination (4/SUM, 6/SUM, and 7/SUM) is shown in Figure 5.8 in which there is no enhancement of the alteration.

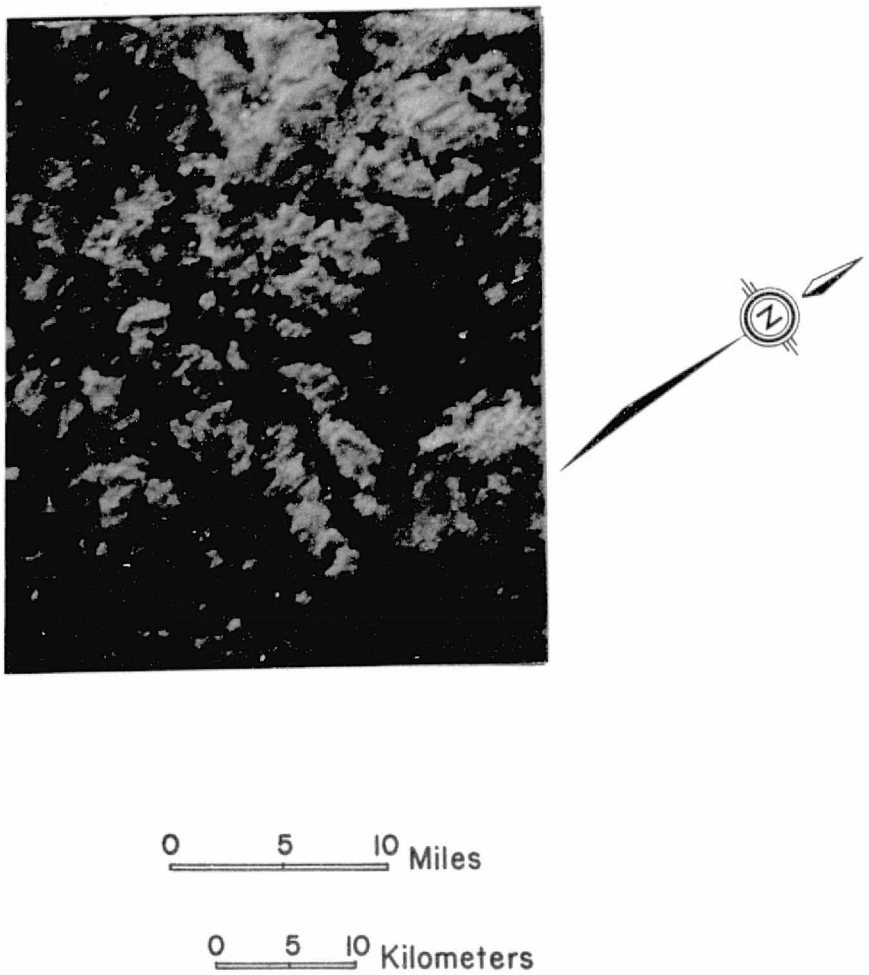

Figure 5.7 Three component color-ratio composites of 3/8 (blue), 5/10 (green), and 6/11 (red). Areas of alteration are red.

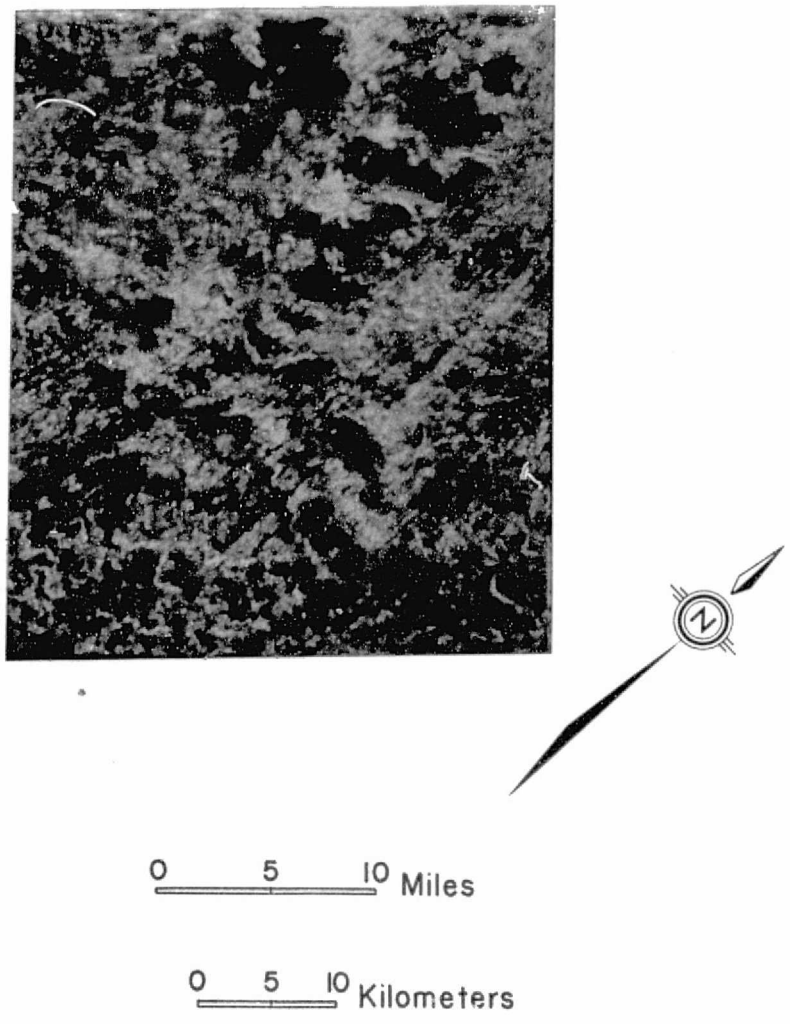

Figure 5.8 Three component color-ratio composites of 4/SUM (blue) 6/SUM (green), and 7/SUM (red).

5.5 CONCLUSIONS AND RECOMMENDATIONS

The results of this study show that computer aided analysis techniques applied to the multispectral scanner data will allow gossan associated with solfataric alteration and vein pyritization in the study area to be separated on the basis of spectral response differences recorded from aircraft or satellite altitudes.

Classification techniques provide the most definitive approach for delineating alteration areas, provided adequate training samples are available. This limits the application of the technique to areas where a reasonable amount of information exists so that adequate training samples can be selected.

Ratioing of properly pre-processed data, i.e., contrast stretched data, and the production of ratio color composite images also is capable of enhancing areas of alteration. This technique may be particularly useful for areas in which little supportive knowledge of geology is available. An additional advantage of ratioing over the classification technique is that computer time is less, resulting in a substantial cost saving. The major problem associated with ratioing is the lack of repeatability. That is, a set of ratios which may be established for one area or one data set, may not work for another area or for another data set. Ratioing was found to enhance the noise characteristics of the data, thus causing a degradation of the data quality.

Additional work is necessary both in the laboratory

and in the field in order to define the effects of spatial resolution, intervening atmosphere, topography, and lithological (mineralogical and textural) features on spectroradiometric measurements. An especially critical need exists for in situ spectroradiometric measurements of various rock types and altered rocks coordinated with detailed sampling for subsequent mineralized and textural analysis in a variety of geologic and environmental conditions. Such studies would provide some of the data necessary for establishing the proper physical basis for ratioing.

Although many questions have been left unanswered by this study, the general results indicate that geologic exploration can benefit substantially by the use of digital computer processing of multispectral scanner data collected at aircraft and/or satellite altitudes.

5.6 GEOMORPHOLOGICAL ANALYSIS

Initially, a number of objectives were defined for this phase of the project, including: (1) landform family mapping, (2) landslide hazard delimitation, (3) thermal characteristics of alpine soil moisture and permafrost, and (4) cultural geomorphic features. However, between the time that the objectives were initially defined and SKYLAB data became available, a considerable amount of experience had been gained in working with LANDSAT-1 data in the same general test site area. Since the spatial resolution of the SKYLAB S-192 data was known to be similar to that of the LANDSAT-1 MSS, the work with the LANDSAT data offered considerable insight into the capabilities and limitations (based on spatial resolution considerations) of the S-192 data. Thus, it was recognized that only the larger landslide areas could be defined using MSS satellite data, and many of the smaller areas of interest would not be evident. Similarly, most mine tailings and dumps (i.e., "cultural geomorphic features") would not be of sufficient size to define and map using the S-192 data. Therefore, the project objectives were revised, and both of those objectives (2 and 4 above) were deleted.

Additionally, after the SL-2 mission was completed, the quality of the S-192 thermal infrared data was not believed to be adequate to allow for effective mapping of the thermal characteristics of alpine soil moisture

and especially permafrost areas. The investigators working on this phase of the project had also experienced difficulties in defining effective techniques to obtain adequate quantities of "ground truth" or reference data. Therefore, the phase of the geomorphic study involving the thermal data was also deleted.

Following these modifications of the original objectives, the major thrust of the geomorphological analysis activity therefore centered on the mapping of landforms. It was decided that S-190A color and color IR photos obtained during SL-2 would be utilized for the majority of this analysis effort, since this S-190 data arrived before the S-192 data were available. Two maps were compiled from stereoscopic analysis of the S-190A color and color IR photos: (1) a generalized geologic map and (2) a major landform feature physiographic map.

In developing the geologic map, it was found that color and texture were the primary photographic characteristics used for recognition of major lithologic units. Most formation units of the region's stratigraphical section were recognizable on both the color and color IR photographs. For example, the Triassic Wingate Sandstone is dark red in color. This unit is overlain by the Triassic Kayenta and Jurassic Entrada sandstones which are white. Such color differences allowed discrimination between these two lithologic units. The Wingate is underlain by interbedded red sandstones and slabs of

the Chinle Formation. The photo-texture of interbedded resistant and non-resistant rocks of the Chinle differs markedly from the even texture of the massive Wingate sandstone cliffs. Thus, texture could be used to delineate the boundary between the Wingate and Chinle formations.

Color and texture, in addition to relative differences in relief (as determined by the stereoscopic analysis of the photos) were the primary photographic characteristics utilized in developing the physiographic map. The major physiographic features of the area could be satisfactorily mapped using either the color or color IR S-190A photos.

Neither of the maps developed during this phase of the project contained any new or unusual features. In both cases, standard photointerpretation techniques were utilized, and the resultant maps were generally similar to existing maps of the area (therefore, they are not reproduced in this report). Considerable experience was gained in this photointerpretation activity and insight was obtained concerning the spatial characteristics of the features of interest. Because of this experience, and because we knew that the spatial resolution of the S-192 data would not be as good as the S-190 data with which we had been working, and also because of the somewhat poor quality of the S-192 data and consequent delay in the availability of this data set, it was decided not to

attempt any computer-aided analysis of the S-192 data for purposes of geomorphologic mapping. The geomorphologic phase of the SKYLAB project was, therefore, terminated upon completion of these rather preliminary mapping activities involving standard photointerpretation techniques.

Although there were no particularly significant results from this geomorphologic phase of the project, these results did indicate that lithologic features of interest and major physiographic features could be defined and mapped using either the color or color IR S-190A photography, and that the synoptic view and small scale of the SKYLAB photography was satisfactory for this type of small scale, generalized mapping.

CHAPTER VI -- SIGNIFICANT RESULTS, CONCLUSIONS, AND RECOMMENDATIONS

by

Roger M. Hoffer

This SKYLAB investigation produced many significant results, some of which should be considered important advances in the state-of-the-art of remote sensing technology. A brief synopsis of the major results and conclusions reached during the course of this research is given in this chapter. The reader is also referred to the "Summary and Conclusions" sections of the individual chapters of this report. The results which are considered particularly important are designated by two or, in a few cases, three dots.

These results should be considered to be rather data-dependent, due to the quality of the data, the characteristics of the test site, and the analysis and evaluation techniques which were utilized. These facts must be taken into account if any attempts are made to generalize these conclusions to other data sets or geographic locations. However, because this test site was in an area of rugged mountain terrain having a complex vegetation pattern, and because the quality of the SKYLAB S-192 data was not optimum, these results could be considered as representative of a "worst case" situation. Geographic locations without such a complex vegetative pattern or terrain effects and higher quality data sets should allow better results to be obtained in the future.

DATA OVERLAY AND ANALYSIS TECHNIQUES

●●● Among the more significant results of this SKYLAB investigation was the successful and highly accurate geometric correction and digital overlay of multiple data sets consisting of SKYLAB, LANDSAT, and topographic (elevation, slope, and aspect) data.

An unusual and extremely valuable multistage set of data were obtained during the SKYLAB SL-2 mission (Table 2.1, p. 24). This data set consisted of SKYLAB and LANDSAT-1 data (both obtained under cloud-free conditions on June 5, 1973), in addition to WB-57 color infrared photography and NC-130 color infrared photography and 24-channel multispectral scanner data (obtained on June 6, 1973). "Ground truth" teams also collected a variety of support data. Thus, an excellent multistage, multispectral data set was available for the subsequent data analysis efforts. During the SL-3 mission (August 4-8, 1973) additional SKYLAB, WB-57, and NC-130 data were obtained over a portion of the same area, thereby offering the opportunity for multi-temporal data analysis.

A geometric correction procedure was applied to the satellite data which geometrically corrected the data and successfully adjusted for the difference in orbital paths of the SKYLAB and LANDSAT satellites (approximately 58^{o}). Elevation data were obtained from the DMA digital topographic tapes and an interpolation procedure was developed to determine slope and aspect (Figures 2.21-2.27, pp. 74-75). These data sets were then geometrically corrected to the same X-Y grid base. Lastly, all data sets were overlayed. Thus, the final result was a single digital data tape containing a total of 20 channels of data which consisted of 13 channels of SKYLAB S-192 data, four channels of LANDSAT MSS data, an elevation channel, an aspect channel, and a slope channel, all geometrically corrected to a 1:24,000 scale data base (Table 2.13, p. 78).

Since the LANDSAT and SKYLAB MSS data were both obtained on the same date (June 5, 1973), the geometric correction and overlay procedure allowed a direct comparison between the classification results obtained from SKYLAB and those obtained from LANDSAT analysis. The 1:24,000 scale also facilitated the data analysis, since it allowed printouts of satellite data to be overlayed directly onto 7½ minute USGS topographic maps and other 1:24,000 scale type maps that had been prepared.

Both SL-2 and SL-3 SKYLAB data were geometrically corrected and overlayed with LANDSAT data. Since the SL-2 and SL-3 data were on the same X-Y grid base, the test areas were exactly the same for both data sets, thereby allowing

study of the temporal characteristics as well as the spectral characteristics of these MSS data sets (Figure 2.20, p.66).

To the best of our knowledge, this represents the first time that such a geometric correction and digital overlay involving SKYLAB S-192, LANDSAT, and topographic data, has been achieved anywhere.

- The "modified clustering technique" proved to be superior to both the "supervised" and "non-supervised" (or clustering) techniques that have been used in the past to define the training statistics for computer aided analysis of multispectral scanner data.

The modified cluster technique significantly reduced the amount of computer time involved, increased the accuracy of the classification, and enabled better man-machine interactions to be achieved (pp. 130-142).

- A newly developed analysis algorithm referred to as the "ECHO" classifier produced a more accurate classification result and also produced a map output product having a more useful format than that obtained by the standard per-point classification technique (Figure 3.42, P. 237).

Pasture, aspen, and ponderosa pine each had increases of 10% or more in classification performance for the ECHO classifier, as compared to the per-point classifier (Table 3.24, p. 238). U.S. Forest Service personnel evaluated the cover type maps obtained from the ECHO classifier and indicated that for many purposes, the ECHO cover type maps were a more desirable and useful format than the per-point classification maps.

- A combination of three different evaluation techniques provided the best overall approach for evaluation of the results of the computer-aided analysis of the SKYLAB data.

The evaluation techniques used included 1) qualitative comparisons between the computer classifications and maps and aerial photos of the area, 2) quantitative evaluation of

the classification performance utilizing a system of statistically defined random sample of test areas (Figure 3.17, p. 146), and 3) quantitative comparison of acreage estimates obtained from the computer classification from air photo interpretation on a quadrangle by quadrangle basis (pp. 143-148).

- Quality of multispectral scanner data can only be effectively evaluated by quantitative techniques, rather than qualitative techniques, if the data are to be analyzed by computer.

The data quality of the S-192 data was evaluated by both qualitative and quantitative techniques, and the results clearly indicated that qualitative evaluation of individual channels of multispectral scanner data does not provide a reliable indication of the spectral information content of the data. The results of the quantitative evaluation indicated that the square root of the autocorrelation for zero displacement (standard deviation) of the calibration signals provided the best technique for evaluating the data quality and obtaining a reliable data quality index (Table 2.11, p. 62).

- The digital filtering procedure applied to the SL-3 S-192 data improved many aspects of the data quality, but also created new "noise" problems in the data, due to a "ringing" effect around clouds present in the test site.

The ringing effect was particularly noticeable (visually) in the visible wavelengths (Figure 3.23, p. 180). It caused the computer-aided classification results obtained for the SL-3 (August 8, 1973) S-192 data to have relatively low accuracy (Tables 3.13 and 3.14, pp. 177-178).

- The availability of overlayed topographic data allowed the test site to be easily and rapidly tabulated and displayed into areas within various elevation zones as well as slope and aspect groupings.

This capability is of particular interest to user agencies, such as the U.S. Forest Service, since it allows a rapid summarization of the topographic characteristics within various areas of interest (Tables 3.26-3.28 and Figures 3.43-3.46, pp. 248-251).

° The point of diminishing returns between classification performance and cost of the classification was achieved when four wavelength bands were utilized to classify the SKYLAB S-192 data.

Overall computer classification performance did not improve when more than four wavelength bands were utilized, but the cost of classification increased substantially as more wavelength bands were added (Figures 3.24 and 3.25, pp. 190 and 192). However, various combinations of four wavelength bands were required to achieve optional classification performance of the different individual cover types. This indicates that a scanner system having more than four wavelength bands should be utilized to obtain the data, and then various optimized combinations of approximately four wavelength bands could be utilized in the classification and analysis of the data.

LAND USE AND FOREST COVER TYPE MAPPING

°°° Accurate Level II land use maps were obtained through the use of computer-aided analysis of SKYLAB S-192 data, even in this area of rugged mountainous terrain and spectrally complex cover types (Figure 3.18, p. 156).

"Major Cover Types" or "Level II Land Use Classes" (based on USGS Circular 671) present in the area and mapped by computer-aided analysis techniques included coniferous forest, deciduous forest, grassland, exposed rock and soil, water, and snow. An overall classification performance of 85% was obtained for these cover types, using the SL-2 data obtained on June 5, 1973, and the "Best" 4 bands of the S-192 data which included the o.46-0.51, 0.78-0.88, 1.09-1.19, and 1.55-1.75 µm wavelength bands. [1] (Table 3.8, p. 160, and Table 3.9, p. 163)

---

1) The classification performance figures cited are based upon the statistically defined random sample of test areas, which included 2,400 resolution elements of SKYLAB S-192 data.

oo Reasonable accuracy in mapping forest cover types was achieved, using SKYLAB S-192 multispectral scanner data and computer-aided analysis techniques (Figure 3.21, p. 166).

The forest cover types mapped, using the same SL-2 data indicated above, included ponderosa pine, douglas and white fir, spruce-fir, oak, and aspen, as well as grassland, exposed rock and soil, water, and snow. An overall classification performance of 71% was obtained, which is considered to be very good in view of the complexity of the vegetative and topographic characteristics of the test site (Table 3.10, p. 168 and Table 3.11, p. 170).

ooo Acreage estimates of forest cover types, based upon computer-aided analysis of the SKYLAB S-192 data, were highly correlated (r=0.929) with acreage estimates obtained through standard photo interpretation techniques using aerial photography.

These results, coupled with similar results obtained previously with LANDSAT-1 data, indicate that acreage estimates of land use categories and forest cover types, based upon computer-aided analysis of multispectral scanner data obtained from satellite altitudes, are reasonably accurate for relatively large geographic areas.

oo Differences in spectral response within individual forest cover types were closely related to differences in stand density (Table 3.6, p. 153).

Differences in elevation aspect and slope also caused significant variations in spectral response within several forest cover types. However, in general density differences tended to dominate spectral variations within an individual forest cover type, while differences in elevation, slope, and aspect significantly influenced the geographic location of the various forest cover types. Therefore, spectral differences between forest cover types were significantly influenced by topographic relationships, whereas spectral variations within individual forest cover types were influenced most by differences in stand density.

●● When different cover types are spectrally similar but occur in different elevation zones, the combination of elevation plus multispectral scanner data allows significant improvements to be obtained in accurately differentiating and mapping such cover types.

A combination of elevation plus SKYLAB S-192 spectral data resulted in a significant improvement (over 10%) in classification performance for both spruce-fir and aspen forest cover types, as compared to the use of spectral data alone (pp. 246-247).

●●● Each of the four major spectral regions-visible (0.4-0.7 μm), near infrared (0.7-1.3 μm), middle infrared (1.3-3 μm), and thermal infrared (3-14 μm)-is vital for effective computer classification using multispectral scanner data of natural resources. The relative importance of the different spectral regions and the individual wavelength bands varies significantly as a function of the cover types to be mapped.

The wavelength band phase of this study indicated that the best combination of four wavelength bands included the 0.46-0.51, 0.78-0.88,1.09-1.19, and 1.55-1.75 μm wavelength bands, while the best combination of six wavelength bands included the previous four along with the 0.56-0.61 and 10.2-12.5 μm wavelength bands (Table 3.17, p. 195).

Evaluations of the best wavelength bands within each of four major spectral regions (visible, near infrared, middle infrared, and the thermal infrared) indicated that almost every one of the S-192 wavelength bands was of value for mapping one or more forest cover types (Table 3.21, p.212). Overall, the 0.62-0.67 band was most valuable of the visible wavelength bands for mapping both major cover types (land use classes) and forest cover types. In the near infrared, the 0.78-0.88 μm band was of most value for major cover types, and the 1.09-1.19 μm band was of most value in the mapping of forest cover types. In the middle infrared portion of the spectrum, the 1.55-1.75 μm band was of most value for the forest cover types, while the 2.10-2.35 μm band was of most value for the major cover types. Since the 10.2-12.5 μm channel was the only one available in the thermal wavelengths,

it was selected in each case as being of most value for this spectral region.

- For mapping land use classes and forest cover types, the best combination of six wavelength bands of S-192 data included two in the visible, two in the near infrared, one in the middle infrared, and the thermal infrared band, as indicated above. This result is singled out as being particularly significant because of the similarity of the best combination of six wavelength bands indicated by this study and the proposed configuration for the Thematic Mapper scanner on LANDSAT-D.

The results of this investigation generally support the selection of wavelength bands tentatively scheduled for the Thematic Mapper, with the exception of the second channel in the near infrared region. Our results indicate that adjacent bands in the near infrared portion of the spectrum would not be as effective as two wavelength bands that are spectrally separated in this region. (See recommendations)

- The near infrared portion of the spectrum was found to be particularly important for spectrally discriminating and mapping vegetative cover (either land use classes of forest cover types) in several phases of this study (Table 3.22, p. 216).

The wavelength band evaluation study indicated that the 1.09-1.19 μm wavelength band was the single most important wavelength band. When all SKYLAB S-192 and LANDSAT MSS wavelength bands were individually evaluated using the feature selection processor, all five of the near infrared S-192 wavelength bands and both of the near infrared LANDSAT wavelength bands were selected as being spectrally more valuable than any of the visible or middle or thermal infrared wavelength bands (Table 3.23, p. 232). In some cases, even poorer quality data in the near infrared region was selected as having more information content than better quality data in the middle infrared or visible wavelengths. These results indicate the value and importance of the near infrared wavelength region for computer-aided mapping of vegetative cover.

- The improved spectral resolution and the increased spectral range available in scanner systems such as the SKYLAB S-192 (as compared to the LANDSAT-1 MSS system) will enable a significant improvement in classification performance to be achieved, particularly for forest cover types.

Quantitative comparisons were made between the computer-aided classification results using S-192 data from SKYLAB and the MSS data from LANDSAT-1 (Table 3.15, p. 185). (Both data sets had been obtained on June 5, geometrically corrected and overlayed, and the comparison was based upon a statistically defined random sample of 2,400 resolution elements.) The "Best" four wavelength bands of SKYLAB S-192 data (0.46-051, 0.78-0.88, 1.09-1.19, and 1.55-1.75 μm bands) resulted in a forest cover type classification of 71% compared to a classification performance of 68.4% for the LANDSAT data, and 60.2% for the four wavelength bands of S-192 data that most closely corresponded to the LANDSAT bands (0.52-0.56, 0.62-0.67, 0.68-0.76, and 0.98-1.08 μm wavelength bands). The 8.2% difference between the classification result using LANDSAT data and the corresponding wavelength bands of S-192 data indicates a serious degredation in classification accuracy, due to the poor quality of the S-192 data as compared to the LANDSAT data. However, the 10.8% improvement in classification obtained by using the "Best" four wavelength bands (as compared to the four wavelength bands most closely corresponding to those of LANDSAT) indicates the significant improvements in classification performance that can be achieved when the optimum combination of wavelength bands are utilized. These results indicate the importance of good quality data and use of the optimum combination of narrow, effectively located, spectral bands for computer-aided cover type mapping.

- The spectral information content present in individual wavelength bands of multispectral scanner data can be more important than the noise characteristics of the data for computer-aided analysis of MSS data.

In the wavelength band evaluation phase of this study, relatively noisy wavelength bands were frequently selected by the "Feature Selection Processor' as being more important for the multispectral classification than other channels that had better data quality characteristics (Tables 3.16 and 3.17, pp. 194-195).

- Use of color infrared photography and the synoptic view obtained from SKYLAB allowed effective small scale (1:250,000) mapping of vegetative cover types (Figure 3.6, p. 100).

Existing vegetation maps, developed previously with use of aerial photos and standard photo interpretation techniques, could be significantly improved through the use of the SKYLAB color infrared photography. Comparisons with existing small scale maps clearly indicated the value of the satellite imagery for obtaining more accurate small scale vegetation maps than have ever before been possible.

- Seasonal effects in vegetative condition were significant when the SL-2 photographic data analysis results were compared to the SL-3 photographic data results.

For vegetative mapping purposes, the satellite photos obtained on August 8, 1973 (during SL-3), were superior to the photos obtained on June 5 (during SL-2) because of the difference of the vegetative conditions existing in the test site at the time of each mission (Figure 3.9, p. 108). In general the deciduous forest species had not leafed our completely at the time of the SL-2 mission, particularly at the higher elevations.

The computer-aided analysis of SL-3 data produced much poorer results than had been obtained from the SL-2 data, apparently because of the relatively poor quality of the SL-3 data (Table 3.10, p. 168, and Table 3.14, p. 178). Had better quality data been available from the SL-3 mission it is probable that more accurate cover type classification could have been achieved using computer-aided analysis techniques. This would be due to better spectral differentiation in August using the cover types present, as was indicated by the photo interpretation comparisons of the SL-2 and SL-3 data.

- A computer-aided analysis of multispectral scanner data of Mesa Verde National Park has resulted in an up-date of the existing 1938 vegetation map of the park.

The map and acreage tables derived from this classification have proven of value and are being utilized in various management decisions by park personnel (pp. 113-123).

- A permanent display centered around SKYLAB photography and the computer-derived vegetation map of Mesa Verde National Park was developed and installed in the Headquarters Museum of Mesa Verde National Park.

We believe that this material should be of considerable benefit to NASA and the remote sensing community in general in explaining the value and application of the U.S. Space Program to "user" agencies such as the National Park Service (Figures 3.12-3.15, pp. 126-129).

- Discussions with personnel from various user agencies (primarily the U.S. Forest Service and National Park Service) concerning the application and use of SKYLAB satellite data and the results obtained from it produced somewhat varied responses, depending on the individuals involved in the discussions, their position within the organization, the information requirements which these individuals faced, and the willingness of the individual to consider alternative ways of obtaining various types of information.

In general, the more local users expressed relatively little interest in the data derived from satellite altitudes because it was too generalized and broad in scope, but were quite interested in the information that could be obtained from the 1:60,000 scale aerial photos over their areas of interest. On a regional basis, the need for information over a large geographic area and in a more generalized map and tabular format was evident, and there was considerable interest expressed in the possibilities for obtaining such information using digital computer processing techniques and satellite data. Some evaluations of the products supplied to these users are still being conducted.

Another general trend observed in talking to user agency personnel involved the status of existing information. If existing information was detailed, up-to-date, and fairly accurate, relatively little interest was expressed in the potential for obtaining maps and tabular information with remote sensing techniques, regardless of the method that had

been utilized in obtaining the existing information. However, if the users had relatively little up-to-date, accurate information available to them, strong interest was expressed in the possibility of obtaining the needed information with remote sensing, using either the satellite data or the small-scale aerial photography.

The third general area of user reaction which was encountered involved concern over the somewhat different format, cost and reliability of the type of information that could be obtained through computer processing of satellite scanner data. There was a general concern about future costs involved in obtaining cover type maps and acreage tabulations using these methods. They tended to like the idea that the computer-aided analysis techniques produce quantitative results, which, if they are not correct, are at least biased in a consistent, definable manner. Because the computer classification maps involve a statistical probability for correct classification of any individual resolution element, there is a need to evaluate these types of products in detail and determine how to utilize them most effectively.

HYDROLOGIC FEATURES MAPPING

- SKYLAB S-192 data has demonstrated for the first time that spectral discrimination between snow and clouds can be achieved reliably through the use of data in the middle infrared portion of the spectrum, specifically in the 1.55-1.75 and 2.10-2.35 μm wavelength bands (Figure 4.8, p. 281).

In the middle infrared wavelengths, snow has a relatively low reflectance (therefore, appearing black on the imagery) whereas clouds have a very high spectral response due to non-selective scattering (therefore, appearing white on the imagery) (Figure 4.2, p. 268). Such spectral differentiation cannot be accomplished with LANDSAT data due to detector saturation problems and the limited spectral range of the LANDSAT MSS system. Also, photographic systems, including the SKYLAB S-190A, cannot obtain a spectral separation between snow and clouds because of their limited spectral range.

Snow has a decreasing reflectance with increasing wavelengths throughout the near infrared portions of the spectrum (0.71-1.3 μm), thereby allowing a limited degree of separation to be achieved in these wavelengths (parti-

cularly in the 1.2-1.3 μm band). However, a reliable separation is achieved only in the 1.55-1.75 and 2.10-2.35 μm middle infrared wavelengths (Figure 4.5, p. 275).

ooo Using the SKYLAB S-192 data and computer-aided analysis techniques, different spectral classes of snow cover could be defined and mapped, due to difference in the mixture of snow and forest cover present inthe resolution elements of SKYLAB scanner data, and probably also due to differences in snow melt (Figure 4.12, p. 295).

Underflight aerial photos showed a distinct relationship between the spectral classes defined in the S-192 data and the porportion of snow and forest canopy present in the area (Figure 4.13, a and b, p. 297). Although it could not be positively proven, it is probable that the different spectral classes also represent differences in liquid water content within the snow pack due to melting snow.

ooo Different spectral classes of snow were tabulated as a function of elevation by using the combination of S-192 spectral data and the overlayed topographic data. This result indicates a significant potential for effectively utilizing remotely sensed data to predict water run-off from mountain snow pack areas more accurately.

Tabulations of the areal extent of each of the spectral classes of snow cover were obtained for the entire test site, and then a single watershed area was digitally defined on the data tapes and the area of each of the spectral classes of snow cover and other cover types was tabulated for only this individual watershed (Table 4.6, p. 300). Timely, economical, and accurate information concerning the area of snow cover in various conditions on individual watersheds or on a regional basis, would be of tremendous help in more effective reservoir management and watershed management programs. This SKYLAB study demonstrated that remote sensing technology has the potential for providing information in the formats required, using rapid analysis techniques, once the data became available. (See Recommendations.)

- The layered classifier provided the best approach for snow/cloud differentiation and for mapping the various spectral classes of snow cover (Figure 4.7, p. 280, and Figure 4.11, p. 294).

In the snow cover classifications using SKYLAB S-192 data, the layered classifier gave slightly better classification results, and was somewhat faster in computer time (16%) than the standard maximum likelihood classification approach (Tables 4.2 and 4.3, pp. 282-283).

- The surface temperature of a mountain reservoir was accurately determined from satellite altitudes using a two-point non-linear calibration technique and SKYLAB S-192 thermal scanner data (Figure 4.18, p. 310).

The calibration technique, utilizing only data obtained from SKYLAB, resulted in a temperature determination of 12.7°C. for a portion of Vallecito Reservoir, while the reference temperature measurements obtained for the same portion of the reservoir at the time of the SKYLAB overpass ranged from 12.7° to 13.1°C. This would indicate that the atmosphere is sufficiently transparent in the 10.2-12.5 μm wavelength band and at these altitudes to allow reasonably accurate measurements of radiant temperatures to be obtained from orbital platforms for water bodies at higher elevations (see Recommendations).

GEOLOGICAL STUDY

- Oxidized areas of hydrothermal alteration could be spectrally delineated and mapped by computer classification of SKYLAB and NC-130 aircraft multispectral scanner data.

The most effective procedure for mapping areas of altered rock involved the modified cluster technique. This technique requires a better knowledge of the area and more computer time than is the case with the ratioing approach, but more accurate, consistent results were also obtained when the modified cluster technique was utilized.

- Ratios involving various combinations of wavelength bands of SKYLAB and NC-130 multispectral scanner data produced variable results.

Many sets of single channel and combined channel ratios were analyzed in this study, and in some cases, the geologic features of interest could be defined and enhanced with these techniques. However, consistent results could not be obtained from one area to another or from one data set to another. Ratio combinations recommended by other investigators did not produce satisfactory results in this study. These results indicate a need for better knowledge of the spectral characteristics of the earth surface features of interest, and to better understand the theory involved in the ratio approach for analysis of multispectral scanner data.

RECOMMENDATIONS

●●● It is recommended that the wavelength band tentatively scheduled for the Thematic Mapper to be used on LANDSAT-D in the 0.80-0.91 μm region be changed to a longer wavelength in the 0.96-1.08 or 1.16-1.30 μm region. Such a change would provide better spectral separation between the two near infrared wavelength bands currently defined for the Thematic Mapper. Such a change should enable better classificaiton accuracies to be obtained for various vegetation cover types. The 0.74-0.80 μm band should remain as scheduled. This recommendation is based on the results of the SKYLAB investigation, which clearly indicated the importance of the near infrared portion of the spectrum for vegetation mapping purposes when using computer-aided analysis techniques, as well as on the basis of previous studies which indicate that sometimes when there is little spectral differentiation present in the shorter near infrared wavelengths, reasonably good spectral discrimination can be achieved in the longer near infrared wavelengths, and vice versa. By causing both near infrared channels to be spectrally adjacent, it is likely that much of the capability to spectrally discriminate between natural objects, and much of the power of existing computer-aided analysis techniques would be significantly reduced.

●● A software and hardware system should be developed at one of the NASA centers to geometrically correct satellite data, such as that obtained from the SKYLAB or LANDSAT

multispectral scanners, on a routine, cost effective basis. Data overlay procedures should also be established so that temporal changes in spectral response could be studied effectively for a variety of situations. Such geometric corrections are nearly essential for detailed analysis of existing satellite MSS data and as more and more people start working with such data, the demand for geometrically correct, overlayed data will grow. Such data processing could be done at a large size central facility more cost-effectively than to have various individual groups do their own, using a variety of techniques.

- Further study of digital filtering techniques is needed, so that guide-lines can be established as to the conditions under which such techniques will effectively improve data quality, and the level of improvement that can be expected under a variety of circumstances.

- Methods of evaluating the quality of multispectral data for purpose of both qualitative (visual) interpretation and more quantitative analysis should be defined. Subsequently, the standardized data quality index should be provided, as part of the data set, for all future investigations involving analysis of multispectral scanner data. Such an approach will allow more effective comparison of results throughout the scientific community.

- The results of the wavelength band study described in this report involved a single test site. It is recommended

that additional sets of SKYLAB data, with the associated reference data, be defined and that wavelength band studies be carried out for a variety of test sites and cover types. Data quality should be adjusted to be approximately the same in all channels as one phase of such additional studies.

●● Additional research is needed to determine the effectiveness of utilizing multispectral scanner data in combination with topographic data, and to define the most effective analysis techniques for utilizing such combinations of data. Effects of slope and aspect on the spectral response of vegetative cover require further study.

●●● A system needs to be developed to be able to provide MSS satellite data to users on a very fast turn-around basis. Many potential users of multispectral satellite data are not interested in it at present because their requirements for certain types of information dictate a rapid analysis of the data after it is collected, and at present, they cannot obtain the data soon enough after it is obtained to meet their needs. Until the data collection-dissemination turn-around time is fast enough to satisfy such users, they will not be attempting to utilize this data source to meet their information needs.

● Further study is required to evaluate the effectiveness and potential of the two-point non-linear calibration technique for mapping the thermal characteristics of earth surface features.

C.5

[66] Additional research is needed to better define the relationship between spectral reflectance of earth surface features and ratioing techniques. Application of ratio combinations recommended by other investigators for geologic applications produced variable results in this study. Because of the difficulties inherent in obtaining in situ spectral reflectance measurements of geologic features of significance, there is a general lack of knowledge concerning the spectral reflectance characteristics of these materials. When working with many wavelength bands of MSS data a large number of ratio combinations are possible. Therefore, there is a distinct need to define the most appropriate ratio combinations to enable reliable and predictable results to be obtained.

REFERENCES

1. Anderson, J. R., E. E. Hardy, and J. T. Roach. 1972. "A Land Use Classification System for Use With Remote Sensor Data", U.S.G.S. Circular 671, U.S. Geological Survey, Washington, D.C., 16 pp.

2. Anonymous, 1974. "Corn Blight Watch Experiment Final Report, Volume III: Experiment Results", NASA, Johnson Space Center, May, 1974. (Report cooperatively written and published by Purdue University, the Johnson Space Center, and the U.S. Department of Agriculture). pp. 68-70.

3. Anuta, P. E., 1970. "Spatial Registration of Multispectral and Multitemporal Digital Imagery Using Fast Fourier Transform Techniques", IEEE Transactions on Geoscience Electronics, Vol. GE-8, No. 4, pp. 353-368.

4. Anuta, P. E., and M. E. Bauer, 1973. "An Analysis of Temporal Data for Crop Species Classificatio n and Urban Change Detection", LARS Information Note 110873, Purdue University.

5. Barnes, J. D., and C. J. Bowley, 1973. "Use of ERTS Data for Mapping Snow Cover in the Western United States", Proceedings of the Symposium on Significant Results Obtained from ERTS-1, NASA, Goddard Space Flight Center, NASA sp-327, pp: 855-862.

6. Bartolucci, L. A., R. M. Hoffer, and T. R. West, 1973. "Computer-aided Processing of Remotely Sensed Data for Temperature Mapping of Surface Water from Aircraft Altitudes", LARS Information Note 042373, LARS/Purdue University, W. Lafayette, Indiana, 143 pp.

7. Bird, W. H., 1972. "Mineral Deposits of the Southern Portion of the Platoro Caldera Complex: Southeast San Juan Mountains, Colorado". The Mountain Geologist, Vol. 9, no. 4, p. 379-387.

8. Burbank, W. S. and Luedke, R. G., 1961. "Origin and Evolution of Ore and Gangue-forming Solutions, Silverton Caldera, San Juan Mountains, Colorado", U.S. Geol. Survey Prof. Paper 424-C, p. C7-C11.

9. Caine, N., 1975. "An Elevational Control of Peak Snowpack Variability", Water Resources Bulletin, Vol. 11, No. 3, pp: 613-621.

10. Chapursky, L. I., "Experimental Investigations of the Spectral Brightness Characteristics of Clouds, the Atmosphere, and the Underlying Surface in the 0.3-2.5 Micron Interval", Transactions Main Geophysical Obs, Issue 196, Leningrad.

11. Coggeshall, M. E., and R. M. Hoffer, 1973. "Basic Forest Cover Mapping Using Digitized Remote Sensor Data and ADP Techniques", LARS Information Note 030573, Purdue University, W. Lafayette, Indiana, 131 pp.

12. Coggeshall, M. E., R. M. Hoffer, and J. S. Berkebile, 1974. "A Comparison Between Digitized Color Infrared

Photography and Multispectral Scanner Data Using ADP Techniques", Proceedings of the 4th Biennial Workshop on Aerial Color Photography in the Plant Sciences, American Society of Photogrammetry, Washington, D.C., pp. 43-56. Also LARS Information Note 033174.

13. Conover, J. H., 1964. "The Identification and Significance of Orographically Induced Clouds Observed by TIROS Satellites", Journal of Applied Meteorology, Vol. 3, pp: 226-234.

14. Finnegan, W. H., 1962. "Snow Surveying with Aerial Photographics", Photogrammetric Engineering, Vol. 28, No. 5, pp: 782-790.

15. Fleming, M. D., J. S. Berkebile, and R. M. Hoffer, 1975. "Computer-aided Analysis of LANDSAT-1 MSS Data: A Comparison of Three Approaches, Including a 'Modified Clustering' Approach", Machine Processing of Remotely Sensed Data Symposium Proceedings, Laboratory for Applications of Remote Sensing, W. Lafayette, Indiana.

16. Hoffer, R. M., M. D. Fleming, and P. V. Krebs, 1974. "Use of Computer-aided Analysis Techniques for Cover Type Mapping in Areas of Mountainous Terrain", LARS Information Note 091774, Laboratory for Applications of Remote Sensing, Purdue University, W. Lafayette, Indiana.

17. Hoffer, R., and Staff, 1975. "Natural Resource Mapping in Mountainous Terrain by Computer Analysis of ERTS-1 Satellite Data", Research Bulletin 919, Laboratory for Applications of Remote Sensing and Agricultural Experi-

ment Station, Purdue University, W. Lafayette, Indiana, 124 pp.

18. Hunt, G. R., Salisbury, J. W., and Lenhoff, C. V., 1973. "Visible and Near-infrared Spectra of Minerals and Rocks-VIII. Intermediate Igneous Rocks". Modern Geology, Vol. 4, No. 4, p. 237-244.

19. Kettig, R., 1975. "Fast Fourier Transform Software Programs", Laboratory for Applications of Remote Sensing, Purdue University, W. Lafayette, Indiana.

20. Kuchler, A. W., 1964. "Potential Natural Vegetation of the Conterminous United States", American Geographical Society Special Publication No. 36, New York. Map (39 x 60 inches) plus manual (150 pp., photographs).

21. Leaf, C. F., 1969. "Aerial Photographs for Operation Streamflow Forecasting in the Colorado Rockies", proceedings of the 37th Western Snow Conference, pp: 19-28.

22. Leaf, C. F., and A. D. Haeffner, 1971. "A Model for Updating Streamflow Forecasts Based on Areal Snow Cover and Precipitation Index", Proceedings of the 39th Western Snow Conference, pp: 9-16.

23. Leudke, R. G., and S. W. Burbank, 1968. "Volcanism and Cauldron Development in the Western San Juan Mountains, Colorado in Cenozoic Volcanism in the Southern Rocky Mountains". Epis, R. C., editor, pp. 195-208.

24. McLeish, W., 1964. "The Use of Infrared Maps in the Study of Small Scale Ocean Circulations", Proceedings

of the Third Symposium on Remote Sensing of Environment, University of Michigan, Ann Arbor, Michigan, pp. 717-735.

25. McLerran, J. H., and J. O. Morgan, 1966. "Thermal Mapping of Yellowstone National Park", Selected Papers On Remote Sensing of the Environment. Reprinted by the American Society of Photogrammetry in cooperation with Willow Run Laboratories, the University of Michigan, Ann Arbor, Michigan, pp. v-xi.
26. McLerran, J. H., 1964. "Airborne Cravasse Detection", Proceedings of the Third Symposium on Remote Sensing of Environment, University of Michigan, Ann Arbor, Michigan, pp: 801-802.
27. Meier, M. F., 1973. "Evaluation of ERTS Imagery for Mapping and Detection of Changes of Snow Cover on Land and on Glaciers", NASA SP-327, pp: 863-875.
28. Noma, A. A., 1974. "Toward Creation of a Digital Terrain Data Base", presented at American Society of Photogrammetry Convention, St. Louis, Missouri (paper available from the author at Defense Mapping Agency, Topographic Center, Washington, D. C. 20315).
29. O'Brien, H. W., and R. M. Munis, 1975. "Red and Near Infrared Spectral Reflectance of Snow", Cold Regions Research and Engineering Laboratory, Research Report 332, Hanover, New Hampshire, 18 pp.
30. Parker, D. C., and M. F. Wolff, 1966. "Remote Sensing", Selected Papers on Remote Sensing of Environ-

ment, reprinted by the American Society of Photogrammetry in cooperation with Willow Run Laboratories, the University of Michigan, Ann Arbor, Michigan, pp: v - xvi.

31. Parshall, R. L., 1941. "Correlation of Streamflow and Snow Cover in Colorado", Trans Amer. Geophys. Union, Vol. 22, Part 1.

32. Peck, E. L., 1972. "Methods of Measuring Snowcover, Snowmelt, and Streamflow Under Winter Conditions", The Role of Snow and Ice in Hydrology, Proceedings of the Banff Symposium, Vol. 1 UNESCO-WMO-IAHS, pp: 582-597.

33. Potts, H. L., 1944. "A Photographic Snow Survey Method of Forecasting Runoff", Trans. Amer. Geophys. Union, Vol. 25, pp: 149-153.

34. Rowan, R. K., 1972. "An ERTS Multispectral Scanner Experiment for Mapping Iron Compounds", Proceedings of the Eighth International Symposium on Remote Sensing of Environment. Vol. 2, pp: 1239-1247.

35. Sinding-Larson, R., 1974. "A Computer Method for Dividing a Regional Geochemical Survey Area into Homogeneous Subareas prior to Statistical Interpretation", Geological Survey of Norway, Trondheim, Norway.

36. Slaveck, R. J., 1964. "Detection and Location of Subsurface Coal Forest", Proceedings of the third Symposium of Remote Sensing of Environment, University of Michigan, Ann Arbor, Michigan, pp: 537-547.

37. Smedes, H. W., 1968. "Geologic Evaluation of Infra-

red Imagery, Eastern Part of Yellowstone National Park, Wyoming and Montana", Technical Letter NASA-83, Manned Spacecraft Center, Houston, Texas, 27 pp.

38. Smeedes, H. W., K. L. Pierce, M. C. Tanguay, and R. M. Hoffer, 1970. "Digital Computer Terrain Mapping from Multispectral Data", Journal of Spacecraft and Rockets 7(9): 1025-1031.

39. Smith, R. S., and Bailey, R. A., 1968. "Resurgent Cauldrons in Studies in Volcanology (Coates, R. C.; Hay, R. L., and Anderson, C. A., editors) Geol. Soc. of America Memoir 116, pp; 613-662.

40. Society of American Foresters, 1967. "Forest Cover Types of North America", Society of American Foresters, Washington, D.C., p. 2.

41. Swain, P. H., T. V. Robertson, and A. G. Wacker, 1971. "Comparison of the Divergence and B-Distance in Feature Selection", LARS Information Note 020871, Laboratory for Applications of Remote Sensing, Purdue University, W. Lafayette, Indiana, 12 pp.

42. Swain, P. H., and Staff, 1972. "Data Processing I: Advancements in Machine Analysis of Multispectral Data", Laboratory for Applications of Remote Sensing, Purdue University, W. Lafayette, Indiana, 8pp.

43. Swain, P. H., and R. C. King, 1973. "Two Effective Feature Selection Criteria for Multispectral Remote

Sensing", LARS Information Note 042673, Laboratory for Applications of Remote Sensing, Purdue University, W. Lafayette, Indiana, 27 pp.

44. Tweto, O. and Sims, P. K., 1963. "Precambrian Ancestry of the Colorado Mineral Belt", Geol. Soc. Amer. Bulletin, Vol. 74, pp. 991-1014.

45. U. S. Department of Agriculture, 1972. "Natural Vegetation of Colorado", Soil Conservation Service Map M7-E-22390, Portland, Oregon. (19 x 25 inches)

46. Vincent, R. K., 1972. "An ERTS Multispectral Scanner Experiment for Mapping Iron Compounds", Proceedings of the Eighth International Symposium on Remote Sensing of Environment, Vol. 2, pp. 1239-1247.

47. Wiesnet, D. R., 197[illegible]. "The Role of Satellites in Snow and Ice Measurements", Advanced Concepts and Techniques in the Study of Snow and Ice Resources, National Academy of Sciences, Washington, D. C., pp: 447-456.

48. Wu, C. L., D. A. Landgrebe, and P. H. Swain, 1974. "The Decision Tree Approach to Classification", LARS Information Note 090174, Laboratory for Applications of Remote Sensing, Purdue University, W. Lafayette, Indiana, 174 pp.

49. Yost, Edward, R. Kalia, S. Wenderoth, R. Anderson, and R. Hollman, 1972. "The Estuarine and Coastal Oceanography of Block Island Sound and Adjacent

New York Coastal Waters", ERTS-1 Symposium Proceedings, Goddard Space Flight Center, Greenbelt, Maryland.